

**UNDERSTANDING THE ROLE OF EIF4A IN GENE REGULATION IN  
HEALTH AND DISEASE**

**THOMAS EDWARD WEBB B.Sc. (Hons, Warwick) M.Sc. (Oxon)**

**Thesis submitted to The University of Nottingham  
for the degree of Doctor of Philosophy**

**(July 2012)**

# Abstract

## **eIF4A**

Eukaryotic initiation factor 4A (eIF4A) is an ATP-dependent RNA helicase responsible for unwinding the secondary structure of mRNAs. In humans, eIF4A exists as three separate paralogs: eIF4AI and eIF4AII possess a high degree of homology while eIF4AIII is distinct. Knockdown of eIF4AII had no effect on the expression of a reporter construct containing a structured RNA hairpin. Knockdown of eIF4AI and treatment with hippuristanol (an eIF4A inhibitor) caused a dramatic reduction in the hairpin-mediated gene. This reporter system was developed as part of this project to act as a screen for eIF4A activity along with an in vitro screening approach.

## **PDCD4**

The activity of eIF4A is suppressed in vivo by the tumour suppressor PDCD4. The fact that loss of PDCD4 function increases the severity of DNA damage is probably attributable its eIF4A-suppressive activity.

## **Alzheimer's Disease**

Based on previous microarray data, it was supposed that eIF4A inhibition may be therapeutically beneficial in the treatment of Alzheimer's disease. As part of this project, it was demonstrated that eIF4A suppression significantly reduced the expression of reporter genes preceded by the 5' UTRs of genes predicted to play harmful roles in Alzheimer's disease. The expression of reporter genes preceded by the 5' UTR sequences of genes predicted to be beneficial in Alzheimer's were not affected by this suppression.

## **Cancer**

Reporter plasmids containing the 5' UTR sequences of the oncogenes ODC1, EGFR and VEGFA have high requirements for eIF4A as estimated using hippuristanol. eIF4A inhibition did not significantly affect the reporters containing the 5' UTRs of non-pathogenic genes. The EGFR 5' UTR was found to contain an IRES which explains why EGFR is upregulated in response to hypoxia.

# Acknowledgements

I would like to start by thanking my primary supervisor Dr Keith Spriggs. Without his support and knowledge and above all patience I would never have finished this project. I would also like to thank my secondary supervisor Prof. Peter Fischer.

There are too many people to acknowledge individually who have helped me in the lab, either by demonstrating techniques or lending me reagents or equipment. I would therefore like to thank everyone in the RNA Biology and Gene Regulation Groups at The University of Nottingham between 2008 and 2012. I would, however like to extend special thanks to Drs Nicola Phillips and Andrew Bottley, members of the Spriggs lab who have been especially supportive.

Outside of my department, I would like to thank the following people:

- Dr Tyson Sharp (University of Nottingham) for letting me use his hypoxic chamber.
- Dr Sven Lammich (Ludwig Maximilians Universität) for providing the ADAM10 reporter plasmid.
- Prof. Ya-Ching Chen (National Taiwan University) for providing the hippuristanol.

I will finish by thanking my girlfriend Claire Horgan and all my friends and family.

# Contents

# List of Abbreviations

15d-PGJ2	15-deoxy-delta 12,14-prostaglandin J2
4E-BP	eIF4E Binding Protein
A $\beta$	Amyloid Beta
ABL1	Abelson Murine Leukaemia Viral Oncogene Homolog 1
AChE	Acetylcholinesterase
ACTB	$\beta$ Actin
AD	Alzheimer's Disease
ADAM10	$\alpha$ Disintegrin and Metalloproteinase Domain-Containing Protein 10
ADP	Adenosine Diphosphate
AP-1	Activator Protein 1
APH1	Anterior Pharynx-Defective 1
APP	Amyloid Precursor Protein
ARE	AU-Rich Element
ATP	Adenosine Triphosphate
BACE1	Beta Site of APP Cleaving Enzyme 1
BLAST	Basic Local Alignment Search Tool
BSA	Bovine Serum Albumin
CBC	Cap-Binding Complex
cDNA	Complementary Deoxyribonucleic Acid
CIAP	Calf Intestinal Alkaline Phosphatase
Clu	Clusterin
CML	Chronic Myelogenous Leukaemia
CMV	Cytomegalovirus
CR1	Complement Receptor 1
CTP	Cytidine Triphosphate
dCTP	Deoxycytidine Triphosphate
DMSO	Dimethyl Sulfoxide
DMEM	Dulbecco's Modified Eagle Medium
DNA	Deoxyribonucleic Acid
DiFMUP	6,8-Difluoro-4-Methylumbelliferyl Phosphate
dNTPs	Deoxynucleotide Triphosphates
dsRNA	Double Stranded Ribonucleic Acid
EDTA	Ethylenediaminetetraacetic Acid

EGF	Epidermal Growth Factor
EGFR	Epidermal Growth Factor Receptor
Egr-1	Early Growth Response Factor 1
eIF	Eukaryotic Initiation Factor
EJC	Exon Junction Complex
EMCV	Encephalomyocarditis Virus
EtBr	Ethidium Bromide
FDA	Food and Drug Administration
FCS	Foetal Calf Serum
FGF-2	Fibroblast Growth Factor
FMDV	Foot and Mouth Disease Virus
GAPDH	Glyceraldehyde 3-Phosphate Dehydrogenase
GDP	Guanosine Diphosphate
GSK3	Glycogen Synthase Kinase 3
GTP	Guanosine Triphosphate
HIF-1	Hypoxia-Inducible Factor 1
HIF1 $\alpha$	Hypoxia-Inducible Factor 1 $\alpha$
HIF2 $\alpha$	Hypoxia-Inducible Factor 2 $\alpha$
HIV	Human Immunodeficiency Virus
HPV	Human Papillomavirus
Hsp70	Heat Shock Protein 70
IGF-IR	Type I Insulin-Like Growth Factor Receptor
IGFR	Insulin-Like Growth Factor 1 Receptor
IRE	Iron Response Element
IRES	Internal Ribosome Entry Site
ITAF	IRES Trans Acting Factor
JNK	c-Jun N-Terminal Kinase
LB	Luria-Bertani (or liquid broth)
MAP	Mitogen-Activated Protein
MAPK	Mitogen-Activated Protein Kinase
MAPT	Microtubule Associated Protein Tau
MBP	Maltose Binding Protein
Met	Methionine
MgCl <sub>2</sub>	Magnesium Chloride
MGMT	O-6-Methylguanine-DNA Methyltransferase
miR	Micro Ribonucleic Acid
MNK1	MAP Kinase-Activated Protein Kinase

mRNA	Messenger Ribonucleic Acid
mTOR	Mammalian Target of Rapamycin
NCBI	National Center for Biotechnology Information
NEB	New England Biolabs
NF- $\kappa$ B	Nuclear Factor Kappa-Light-Chain-Enhancer of Activated B Cells
NMD	Nonsense Mediated Decay
ODC1	Ornithine Decarboxylase 1
PatA	Pateamine A
PABP	Poly(A)-Binding Protein
PAGE	Polyacrylamide Gel Electrophoresis
PBS	Phosphate Buffered Saline
PCR	Polymerase Chain Reaction
PDCD4	Programmed Cell Death Protein 4
PEN2	Presenilin Enhancer 2
PHAS-1	Phosphorylated Heat-Acid Stabled
PI3K	Phosphatidylinositol 3-Kinase
Poly(A)	Polyadenylate
PPAR $\gamma$	Peroxisome Proliferator Activated Receptor $\gamma$
PS1	Presenilin 1
PS2	Presenilin 2
PTB	Polypyrimidine Tract Binding [Protein]
RNA	Ribonucleic Acid
RNAi	Ribonucleic Acid Interference
RNase	Ribonuclease
ROS	Reactive Oxygen Species
rRNA	Ribosomal Ribonucleic Acid
SAM	S-Adenosylmethionine
SDS	Sodium Dodecyl Sulphate
shRNA	Short Hairpin Ribonucleic Acid
siRNA	Short Interfering Ribonucleic Acid
SOD1	Superoxide Dismutase 1
TAE	Tris Base, Acetic Acid and Ethylenediaminetetraacetic Acid
TK	Tyrosine Kinase
Tm	Salt-Adjusted Melting Temperature
TNF- $\alpha$	Tumour Necrosis Factor $\alpha$
TPP	Techno Plastic Products
TRAF2	TNF Receptor-Associated Factor 2

tRNA	Transfer Ribonucleic Acid
TXN	Thioredoxin
uORF	Upstream Open Reading Frame
UTR	Untranslated Region
UV	Ultraviolet Light
VEGFA	Vascular Endothelial Growth Factor A

# Chapter 1. Introduction

## Part 1.

### An Introduction to Translation

#### 1.1.1. Background

In biology, translation is the process by which the nucleotide sequence of a messenger RNA (mRNA) directs the synthesis of a specific peptide (Reviewed in: (Gray and Wickens, 1998)). The machinery of translation is highly conserved across organisms but there are differences between eukaryotes, prokaryotes and archaea (Noller, 2004). Translation in archaea bears a resemblance to that in eukaryotic organisms, particularly in the structure of the ribosome (Allers and Mevarech, 2005; Dennis, 1997). It is this difference in ribosomal composition that allows a large number of antibiotics (e.g. chloramphenicol) to be specific in their disruption of bacterial translation without damaging eukaryotic cells (Pestka, 1974).

Prokaryotic translation is mechanistically similar to eukaryotic although it only requires the action of three main factors as opposed to the large number (>12) often required by eukaryotes (Kozak, 1999; Myasnikov *et al.*, 2009).

The canonical nature of many of the factors and processes of translation has led to the postulation that it was highly evolved even before the divergence of the three main groups of life (Woese, 2002). The relative simplicity of prokaryotic translation, combined with the fact that bacteria are very easy to culture in the laboratory made prokaryotes the model organism for studying translation in the early years of the discipline (Goldstein, 1970).

Although the study of translation in prokaryotes has had a head start, there is now a large body of information about translation in eukaryotes (Reviewed in: (Jackson *et al.*, 2010)).

### 1.1.2. The Stages of Translation

Translation is divided into four stages: initiation, elongation, termination and recycling (Reviewed in: (Pestova et al., 2001)). The initiation of translation requires a large number of proteins termed initiation factors (Reviewed in: (Kozak, 1999)). These factors act in concert to bind the ribosome to a mRNA and allow it to scan for the translation start codon (usually AUG) (Kozak, 1984a). The ribosome is an organelle consisting of a collection of protein and ribosomal RNA (rRNA) molecules divided into small and large subunits; its function is to facilitate the synthesis of a peptide using the amino acid sequence defined by the mRNA (Figure 1.1.) (Reviewed in: (Ramakrishnan, 2002)).

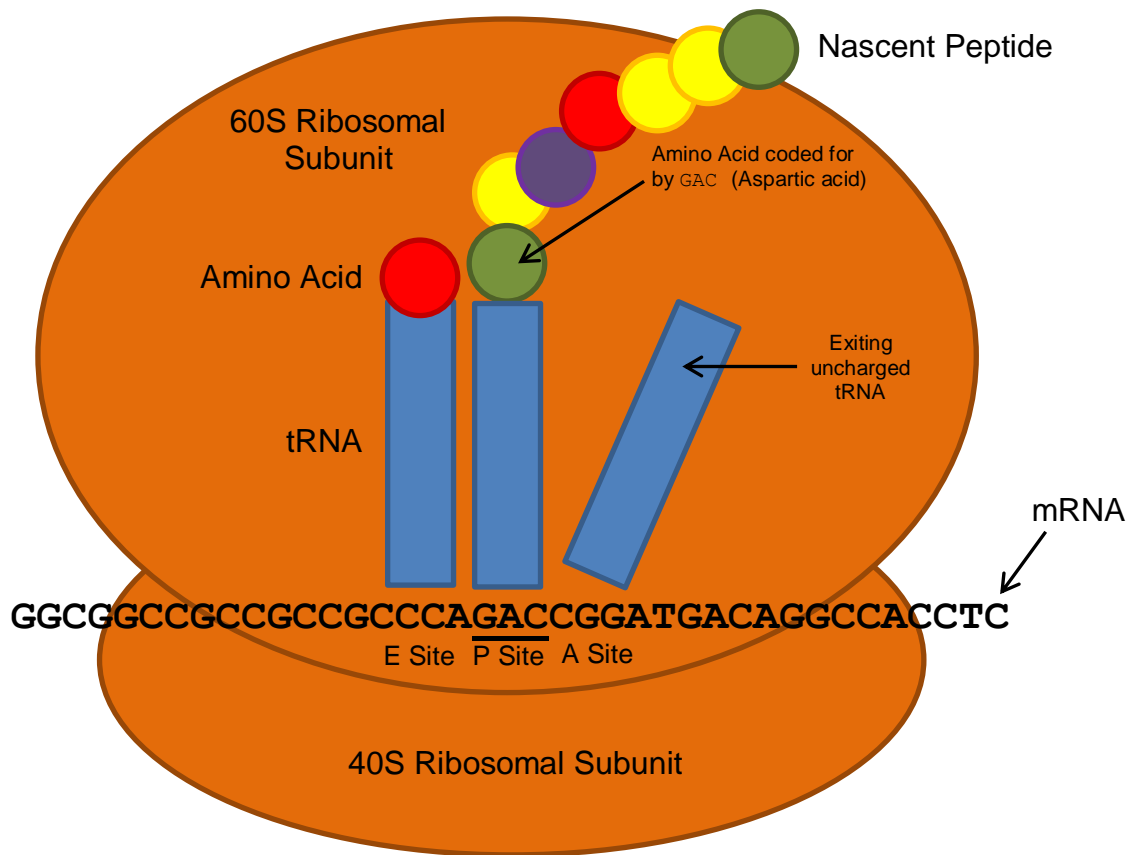


**Figure 1.1. The complete ribosome.** The diagram shows the complete ribosome engaged in the elongation stage of translation.

Translation initiation is a significant regulatory element in the expression of many genes (Reviewed in: (Sonenberg and Hinnebusch, 2009; Thach, 1991)). Regulation occurs at a number of stages of gene expression, for example at the level of transcription, but the regulation of translation is an increasingly interesting field as it has implications in a range of diseases (Gingras et al., 1999; Hollams et al., 2002).

### 1.1.3. Transcription

A pre-mRNA is generated initially when RNA polymerase II transcribes a copy of the relevant section of the cell's genome (Reviewed in: (Nikolov and Burley, 1997)). As the mRNA is synthesised, it is subject to modifications that protect it from exonuclease degradation and allow it to be efficiently translated (Reviewed in: (Erkmann and Kutay, 2004)). The following sections outline these modifications.

### 1.1.4. The 5' Cap

The 5' end of the pre-mRNA is modified by the addition of the 5' cap structure ((Reddy et al., 1974), Reviewed in: (Banerjee, 1980)). The terminal 5' phosphate group of the RNA backbone is removed by hydrolysis performed by a phosphatase, followed by the action of guanosyl transferase which leads to the creation of a diphosphate 5' end. The 5' end then attacks the  $\alpha$ -phosphorous atom of the guanosine triphosphate (GTP) to form the 5'-5' triphosphate bond (Reviewed in: (Kapp and Lorsch, 2004)). The nitrogen atom at position 7 on the guanine cap is methylated by guanine methyltransferase which transfers a methyl group from S-adenosyl methionine (Yamada-Okabe et al., 1999). The methylated guanine triphosphate is referred to as 7-methylguanosine (or simply m<sup>7</sup>G) (Perry and Kelley, 1974).

In addition to protecting the mRNA molecule from degradation by exonuclease enzymes, the cap provides a binding site for factors involved in the initiation of translation.

### 1.1.5. Polyadenylation of an RNA

The 3' terminus is also subject to modification. The RNA strand is cleaved within the 3' untranslated region by an endonuclease that recognises the sequence AAUAAA and cuts the molecule at a site 30 nucleotides downstream (Fitzgerald and Shenk, 1981). The excised fragment is replaced by a polyadenylate (poly(A)) tail consisting of an average of 250 adenylate residues (Wickens, 1990). As it is synthesised, poly(A)-binding proteins (PABPs) become associated with the polyadenylate tail (Sachs et al., 1986). PABP-binding proteins PAIP1 and PAIP2 bind both the RNA-associated domain of PABP and also the carboxy terminus and serve to regulate the level of total protein synthesis (Craig *et al.*, 1998). Binding of PAIP2 to PABP causes PABP to dislocate from the RNA. When PABP levels are depleted E3 ubiquitin ligase degrades PAIP2, this mechanism is believed to even

out fluctuations and maintain consistent protein homeostasis (Khaleghpour *et al.*, 2001; Yoshida *et al.*, 2006).

Like the cap, the poly(A) tail also facilitates the translation of a mRNA as well as stabilising the molecule (Walther *et al.*, 1998). It is believed that mRNA molecules are circularised by the binding of PABP and PAIP1 to 5' cap-associated translation initiation factors, a phenomenon which stimulates translation (Craig *et al.*, 1998; Roy *et al.*, 2002; Yazaki *et al.*, 2000).

#### **1.1.6. mRNA Splicing and Editing**

The non-coding intron sequences are spliced out of an mRNA molecule and the coding exons are ligated together (Berget *et al.*, 1977; Black, 2003). Some introns are self-splicing but the splicing of most introns is mediated by the spliceosome complex (Cech, 1990). The spliceosome consists of small nuclear RNAs (snRNA) and a collection of over 150 polypeptides (Reviewed in: (Kramer, 1996; Zhou *et al.*, 2002)). This complex assembles on the mRNA and recognises the introns by the presence of the splice donor and acceptor sites (Reviewed in: (Robin, 1996)). The donor site at the 5' end of the intron is usually characterised by the presence of the sequence: GU while the acceptor site (at the 3' end) is usually characterised by the sequence: AG (Reviewed in: (Berget, 1995)). Upstream of the acceptor site is a polypyrimidine tract and upstream of this is a conserved adenosine residue known as the branch point (Patton *et al.*, 1991; Smith *et al.*, 1989). The spliceosome brings together and ligates the donor and acceptor sites (Anderson and Moore, 2000). This process causes the RNA to form a loop or 'lariat' which undergoes self-cleavage once the exons have been ligated (Agback *et al.*, 1993; Anderson and Moore, 2000).

Alternative splicing of exons offers a mechanism by which a single mRNA can code for different proteins (Chow *et al.*, 1977). Introns are either spliced out of the mRNA or left in (Black, 2003; Modrek and Lee, 2002). An intron sequence will be translated along with the rest of the mRNA if it is left un-spliced and the protein generated will therefore be different to the one generated by the spliced mRNA (Black, 2003; Modrek and Lee, 2002).

One further method by which mRNA processing may occur is termed RNA editing, this process involves the changing of the nucleotide sequence of the RNA and it confers similar advantages to the cell as alternative splicing (Benne *et al.*, 1986; Covello and Gray, 1993).

### 1.1.7. The Untranslated Regions (UTRs)

The mRNA does not only encode the order in which the amino acids are to be bonded, it also directs the translation machinery as to when to start and stop the process of translation. The start codon is usually AUG while the stop codon is UAG, UAA or UGA (Brenner et al., 1967; Brenner et al., 1965; Hinnebusch, 2011). The mRNA molecule extends beyond the start codon in the 5' direction and beyond the stop codon in the 3' direction. These distal sequences are termed the 5' untranslated region (5' UTR) and the 3' untranslated region (3' UTR) respectively. The best characterised function of the 5' UTR is to regulate the expression of the downstream coding sequence (Kozak, 1987). Some mRNAs possess 'weak' 5' UTRs, these are more difficult to translate due to their length and secondary structure (De Benedetti and Graff, 2004). Many of the genes involved in proliferation are regulated in this way (De Benedetti and Graff, 2004).

### 1.1.8. *Cis*-Acting RNA Elements

#### **The Iron Response Element (IRE)**

The 5' UTR may also may act as an operator, making the expression of the downstream open reading frame (ORF) dependent upon the fulfilment of a certain condition (Aisen et al., 2001). For example, a short RNA stem loop forms in the 5' or 3' UTRs of a number of genes involved in iron metabolism and provides a binding site for iron response proteins (IRPs) (Aisen et al., 2001; Hentze, 1995; Hentze et al., 1987; Hentze and Kuhn, 1996). L ferritin is an example of an IRE-regulated gene involved in the solubilisation and storage of iron (Figure 1.2.) (Reviewed in: (Torti and Torti, 2002)). The 5' UTR of L ferritin contains a single stem loop that acts as a binding site for the iron response proteins (IRPs) (Theil, 1990). Binding of the IRPs in low iron concentrations causes the translational repression of the mRNA (Figure 1.2.) (Reviewed in: (Piccinelli and Samuelsson, 2007; Rouault, 2012)). This system ensures that L ferritin expression varies with cellular iron concentration. Under low iron conditions, resources are not wasted manufacturing this iron storage protein and under high iron conditions the excess iron does not cause toxicity as it is stored by L ferritin (Reviewed in: (Piccinelli and Samuelsson, 2007; Rouault, 2012)).

Transferrin receptor expression is also regulated by an iron response element. The 3' UTR of the transferrin receptor mRNA contains five RNA loops that bind the iron response proteins (Figure 1.3.) (Testa et al., 1993). Unlike the IRE in L

ferritin, the binding of IRPs to the transferrin receptor mRNA causes it to be translationally upregulated as the IRPs stabilise the mRNA allowing it to be translated for longer (Srai and Sharp, 2012). An increase in iron concentration causes the IRPs to dissociate which results in the degradation of the mRNA (Figure 1.3.) (Testa et al., 1993). Upregulation of transferrin receptor expression in response to low iron conditions is consistent with its involvement in the importing of iron into the cell (Testa et al., 1991).

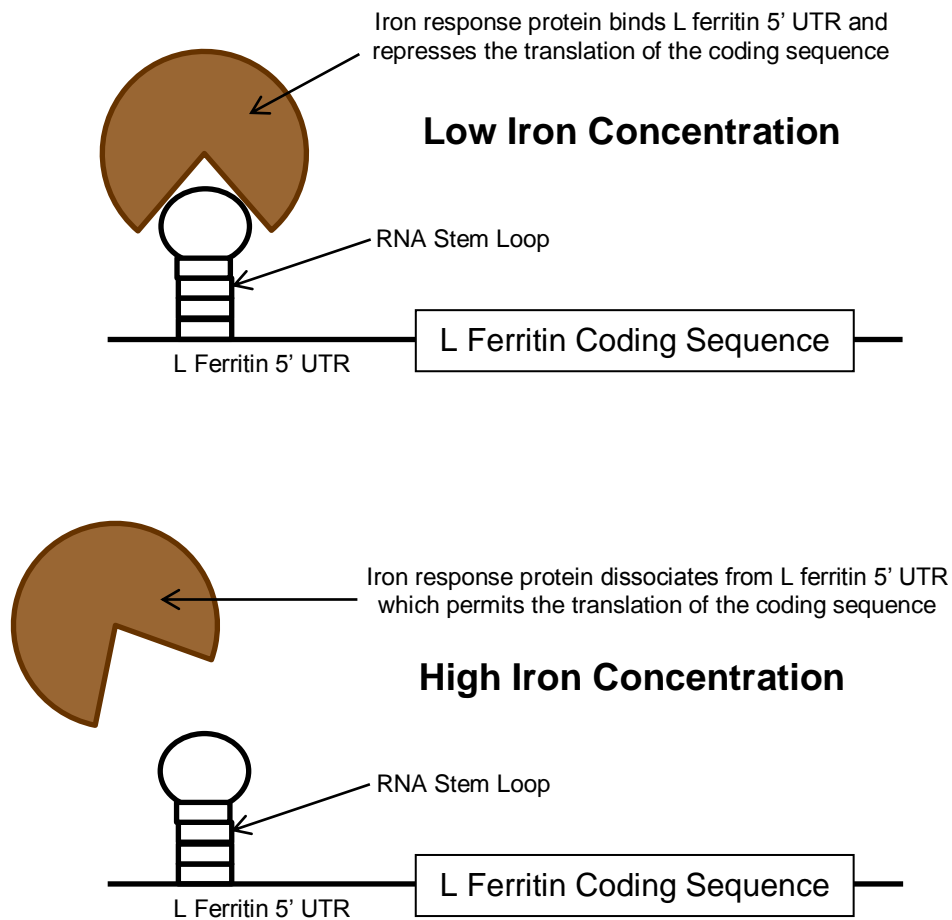


**Figure 1.2. The L ferritin iron response element.** In low-iron conditions, the iron response protein (IRP) represses L ferritin translation by binding the stem loop in its 5' UTR. L ferritin expression is permitted in high-iron conditions by the dissociation of IRP.

## Transferrin Receptor Regulation

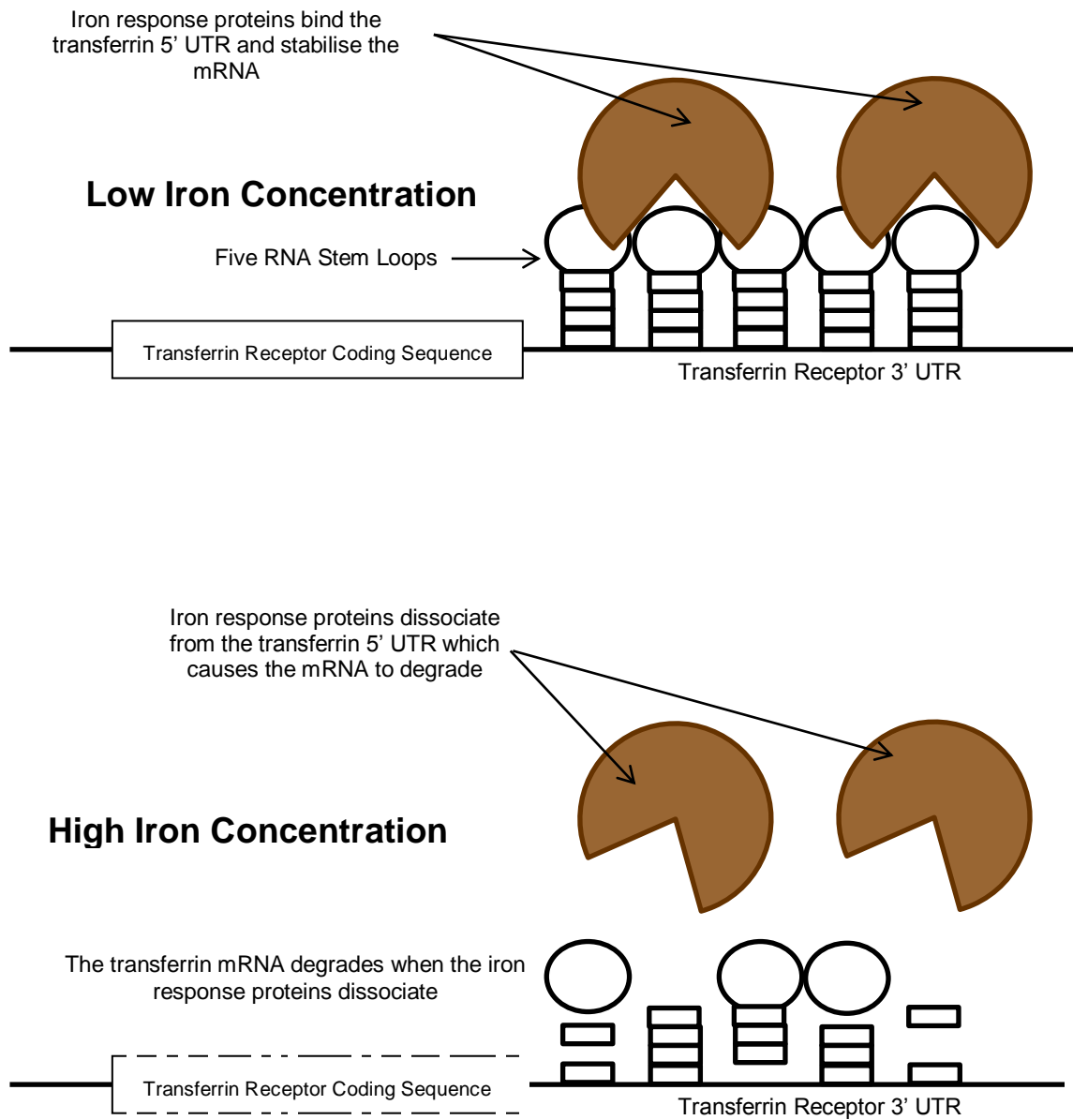


**Figure 1.3. The transferrin receptor iron response element.** In low-iron conditions, the iron response proteins bind to the iron response elements and stabilise the transferrin receptor mRNA. High iron conditions cause the iron response proteins to dissociate and therefore the transferrin receptor mRNA to degrade.

## **Riboswitches**

A riboswitch is a region of an mRNA that directly binds a specific small molecule (Mironov et al., 2002). This binding (which occurs at the aptamer region of the riboswitch) causes the expression platform of the riboswitch to undergo structural changes (Tucker and Breaker, 2005; Wachter, 2010). These changes alter the rate at which the mRNA is expressed (Tucker and Breaker, 2005; Wachter, 2010).

## **uORFs**

The first start codon encountered by the ribosomal subunit complex as it scans the 5' UTR is not always that of the main open reading frame (ORF) of the mRNA (Reviewed in: (Calvo et al., 2009)). Upstream open reading frames (uORFs) generally inhibit the expression of the primary ORF (pORF) as the ribosome may translate the uORF and then stall (Kozak, 1991b). For the pORF to be expressed the ribosome must either reinitiate at the pORF start codon after translating the uORF or it must fail to recognise the uORF start codon (a process called leaky scanning) (Miller and Hinnebusch, 1990; Morris and Geballe, 2000).

The 3' untranslated region also serves to regulate the expression of the gene by providing binding sites for proteins or micro-RNAs that may stabilise or destabilise the mRNA (Lai, 2002; Mazumder *et al.*, 2003).

### **1.1.9. mRNA Export and Pioneer Translation**

The first step in the translation of a mature mRNA molecule is the binding of the nuclear cap-binding complex (CBC) to the 5' cap (Kataoka et al., 1994; Lewis et al., 1996). As transcription occurs in the nucleus and translation does not, the mature mRNA must be exported into the cytoplasm (Kapp and Lorsch, 2004). Although translation does usually occur in the cytoplasm, there is a contested body of evidence that suggests that translation may also occur in the nucleus (Iborra *et al.*, 2004). Normally however, the heterodimeric cap-binding complex facilitates mRNA export from the nucleus via the nuclear pore complex (Bastos et al., 1996). The nuclear cap-binding complex is also believed to play a role in stabilising the poly(A) tail and in the splicing of the mRNA (Flaherty *et al.*, 1997). Once out of the nucleus and in either the cytoplasm or the endoplasmic reticulum (ER), the mRNA undergoes a 'pioneer' round of translation with the cap binding complex still in place (Chiu et al., 2004; Lerner and Nicchitta, 2006). If the mRNA is exported into the ER, the signal recognition particle (SRP) recognises the signal

sequence of the nascent peptide emerging from the ribosome and facilitates the binding of the ribosome to the SRP receptor (Gilmore et al., 1982; Keenan et al., 2001; Walter and Blobel, 1983). The SRP receptor anchors the RNA-ribosome complex to the ER membrane thereby aiding in the secretion of the nascent peptide (Wiedmann et al., 1987).

The pioneer round of translation is believed to facilitate the nonsense mediated decay of mRNAs containing premature translation termination codons which would otherwise lead to the synthesis of potentially harmful truncated peptides (Behm-Ansmant *et al.*, 2007). As part of the mRNA splicing pathway exon junction complexes (EJCs) bind the mRNA upstream of points where exons have been ligated together (Reviewed in: (Chang et al., 2007)). EJCs are displaced from an mRNA by the ribosome as it performs the pioneer round of translation (Figure 1.4.). When the ribosome reaches a stop codon it dissociates from the mRNA. If a mutation causes the introduction of a stop codon upstream of the wild-type stop codon then the ribosome will dissociate at this point. The EJCs downstream of this point will therefore remain attached to the mRNA and provide binding sites for UPFs (regulator of nonsense transcripts) which trigger the decay of the mRNA molecule (Reviewed in: (Chang et al., 2007)).

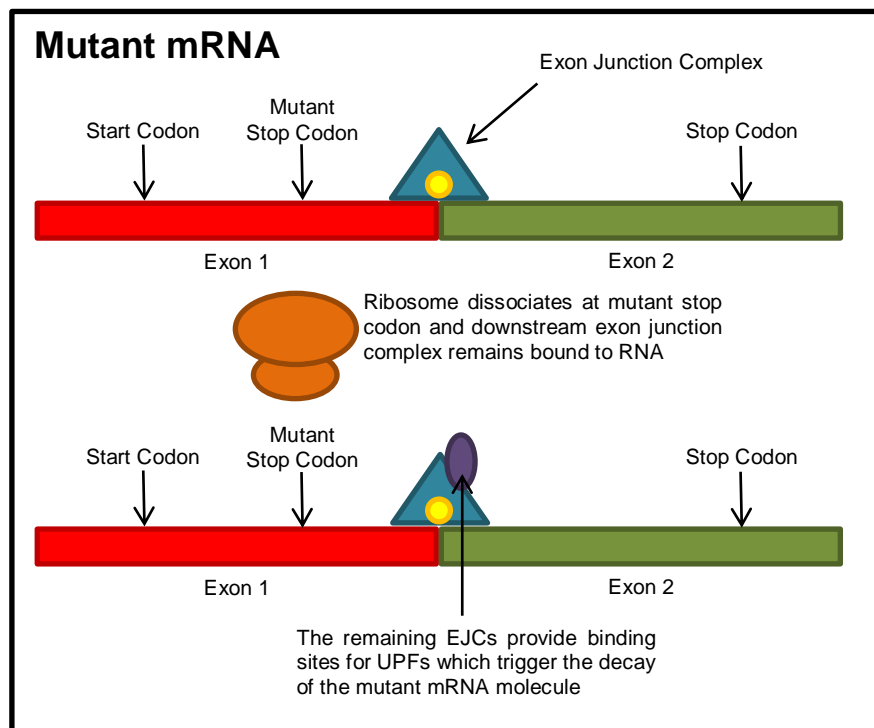
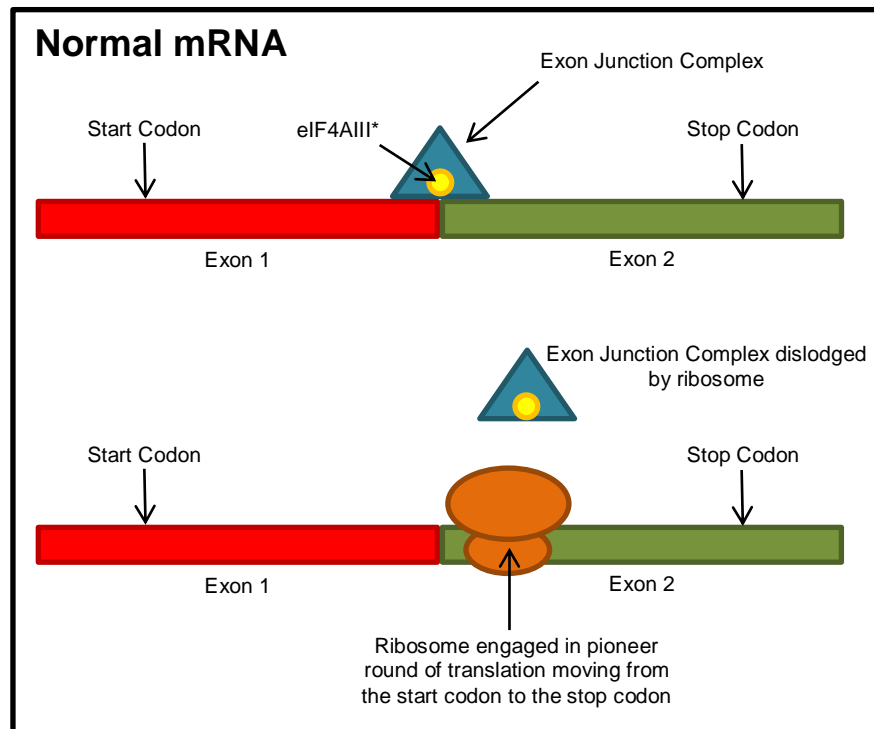


**Figure 1.4. The nonsense mediated decay pathway.** \*eIF4AIII is believed to act as the RNA clamp of the complex (this will be discussed further in the eIF4A Paralogs section).

After the pioneer round of translation, the cap-binding complex is replaced by the eukaryotic initiation factor 4 E (eIF4E) which acts together with a number of other factors to initiate steady-state translation (see next section) (Lee *et al.*, 2008).

#### 1.1.10. Translation Initiation Factors

Factor Name	Size* (kDa)	Function	Reference
eIF2	126	When associated with GTP, eIF2 binds Met-tRNA <sub>i</sub>	(Kimball, 1999)
eIF2B	294	Exchanges eIF2-associated GDP with GTP	(Gomez et al., 2002)
eIF1	12	Facilitate the binding of eIF2-GTP-Met-tRNA <sub>i</sub> to 40S ribosomal subunit and aid in the recognition of the start codon	(Passmore et al., 2007)
eIF1A	17		
eIF5	58		(Chaudhuri et al., 1994)
eIF3	800	Stabilises the above complex and also the cap-binding complex	(LeFebvre et al., 2006)
eIF4E	24	Binds the 5' cap	(Rhoads, 2009)
eIF4A	46	Unwinds the structure of the 5' UTR	(Rogers et al., 2002a)
eIF4B	80	Stimulate eIF4A activity	(Rogers et al., 2001b)
eIF4H	25		
eIF4G	154	Acts as a scaffold for eIF4A and aids in the circularisation of the mRNA	(Lamphear et al., 1995)
eIF5B	139	Facilitates the binding of the 60S ribosomal subunit to the 40S-Met-tRNA <sub>i</sub> -mRNA complex	(Rasheedi et al., 2007)

**Table 1. The main eukaryotic initiation factors.** \* The size refers to the approximate size of the protein in mammals.

### 1.1.11. Translation Initiation

The following figures show how the translation initiation factors (Table 1.) facilitate the binding of the small (40S) ribosomal subunit to the 5' cap of the mRNA and allow the 48S ribosomal subunit complex to scan for and recognise the start codon.

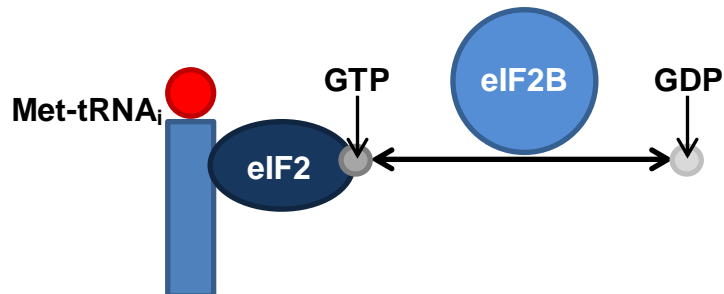


**Figure 1.5. The Formation of the Ternary Complex.** When it is associated with guanosine triphosphate (GTP), eIF2 forms part of the cap-binding complex (Kimball, 1999). The transition from eIF2-GDP (guanosine diphosphate) to eIF2-GTP is catalysed by the heteropentameric translation initiation factor eIF2B (Williams et al., 2001). eIF2-GTP then forms a ternary complex with Met-tRNA<sub>i</sub>. Met-tRNA<sub>i</sub> is the transfer RNA / amino acid complex complementary to the AUG translation start codon (Kimball, 1999).

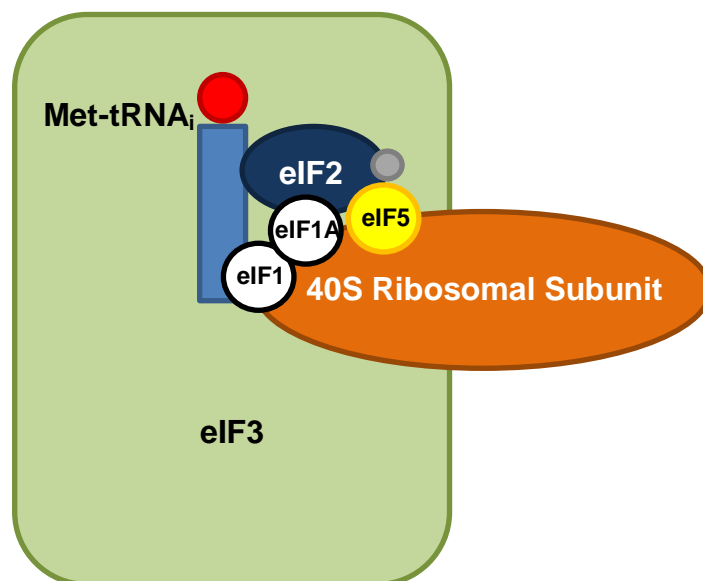


**Figure 1.6. The 43S Complex.** If eIF2 is not phosphorylated and it is associated with triple-phosphorylated guanosine then it is free to become part of the ternary complex (Berg et al., 2002; Kimball, 1999). The attachment of the ternary complex (eIF2-GTP-Met-tRNA<sub>i</sub>) to the 40S ribosomal subunit is facilitated by eIF1, eIF1A, eIF5 and stabilised by eIF3, this leads to the formation of the 43S pre-initiation complex (LeFebvre et al., 2006; Lomakin et al., 2003).

eIF3 is a large multi-subunit initiation factor, it is believed to have a number of regulatory functions that are yet to be explained (Hershey and Merrick, 2000). However, one subunit of eIF3 (p170) is strongly implicated in regulating the cell cycle and proliferation (Dong et al., 2004).

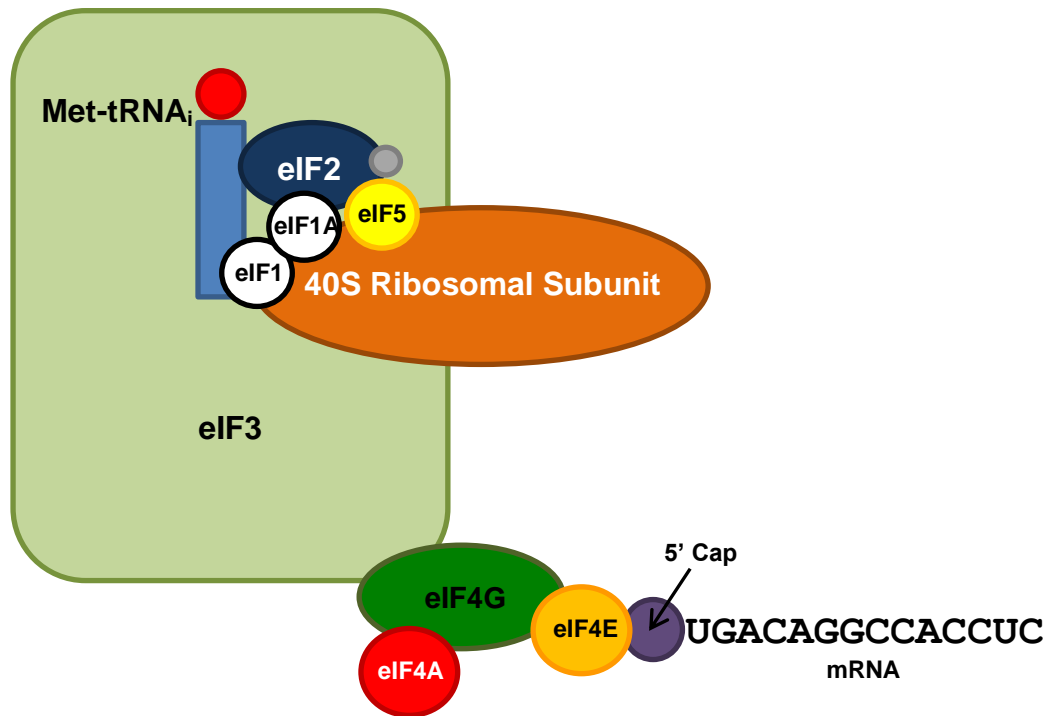


**Figure 1.7. The 48S Complex.** eIF3 and the cap-bound eIF4E are linked by the large scaffold protein eIF4G (Pyronnet et al., 1999). eIF4G binds eIF4E at its N terminal third and binds both eIF3 and eIF4A at its C terminal two thirds (Pyronnet et al., 1999). eIF4A is a bidirectional RNA helicase that binds eIF4G and catalyses the processing of the secondary structure of the mRNA 5' untranslated region in an ATP dependent manner, a process which facilitates ribosome recruitment (Grifo et al., 1984; Ray et al., 1985; Rozen et al., 1990; Svitkin et al., 2001). eIF4A is an abundant cytoplasmic protein, at over three copies per ribosome in HeLa cells it is the most abundant translation initiation factor (Bordeleau et al., 2006; Duncan et al., 1987; Lin et al., 2008).

When complexed together, eIF4A, eIF4E and eIF4G are referred to as eIF4F. Once associated with the cap-bound eIF4F, the 43S pre-initiation complex is now termed the 48S pre-initiation complex. eIF4B and eIF4H both serve to stimulate the helicase activity of eIF4A and make it more processive (Richter-Cook et al., 1998; Richter and Sonenberg, 2005; Richter et al., 1999; Rogers et al., 1999a). eIF4B and eIF4H share a binding site on eIF4A so their activity is likely to be mutually exclusive (Rozovsky et al., 2008). eIF4B (in combination with eIF4G) stimulates the ATPase activity of eIF4A (Nielsen et al., 2011). eIF4H has been proposed to contribute to the RNA affinity of eIF4A (Rozovsky et al., 2008).

eIF4B possesses an RNA recognition motif at its N terminus and an 18S ribosomal RNA (rRNA) binding domain at its C terminus (Methot et al., 1996). eIF4B also binds eIF3, suggesting that it acts as an intermediary between eIF3 and both the ribosome and mRNA (Methot et al., 1996).

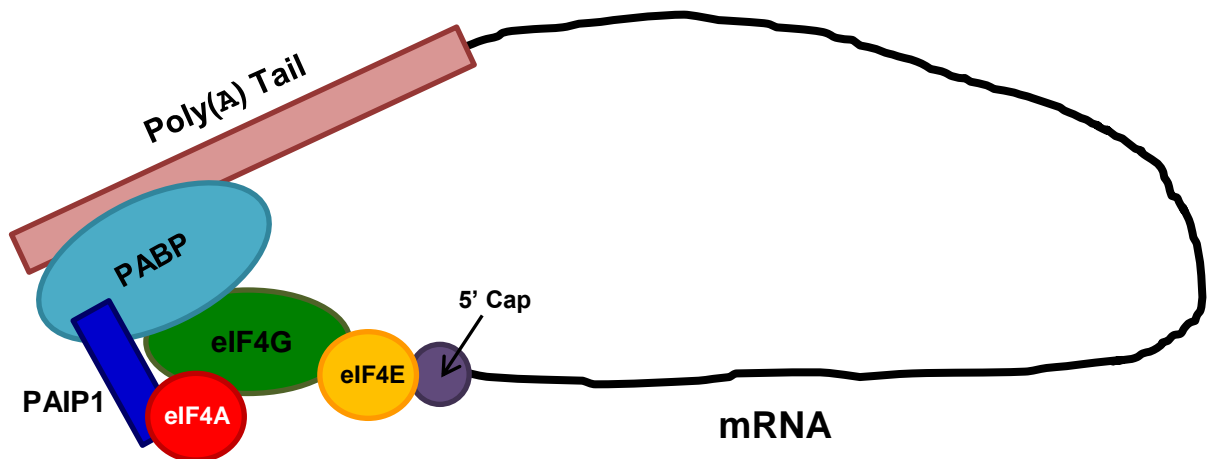


**Figure 1.8. mRNA Circularisation.** The poly(A) tail binding protein (PABP) remains bound to the poly(A) tail while also binding eIF4G thereby creating a mRNA loop that is believed to stimulate translation and also to play a role in the regulation of the expression of certain transcripts (Mazumder et al., 2001; Sachs et al., 1986; Wakiyama et al., 2000). There is also evidence to suggest that the circularised structure may be strengthened by the binding of PABP to eIF4A via PAIP1 (Craig et al., 1998).

It has been proposed that circularisation of the mRNA could serve the same purpose as nonsense mediated decay in that it only allows the expression of intact mRNAs at the expense of the expression of potentially harmful truncated peptides (Searfoss et al., 2001). For example: stop codons introduced into the mRNA upstream of the wild-type stop codon by mutation (nonsense mutations) will lead to the dissociation of the ribosome before it can reach the start codon again thereby repressing the translation of the mutated mRNA (Wilkinson and Shyu, 2002).

#### **Proof of *in vivo* mRNA Circularisation**

The fact that PABP directly binds eIF4G is consistent with the existence of this phenomenon in living cells but alone it is not strong evidence (Tarun, 1996). Stronger evidence comes from the visualisation of cellular mRNAs; polysomes (multiple ribosomes associated with a single mRNA) appear as a ring on electron micrographs and atomic force microscopy of *in vitro* RNA-protein complexes also reveals circular shapes (Tarun and Sachs, 1996; Wells et al., 1998; Yazaki et al., 2000).

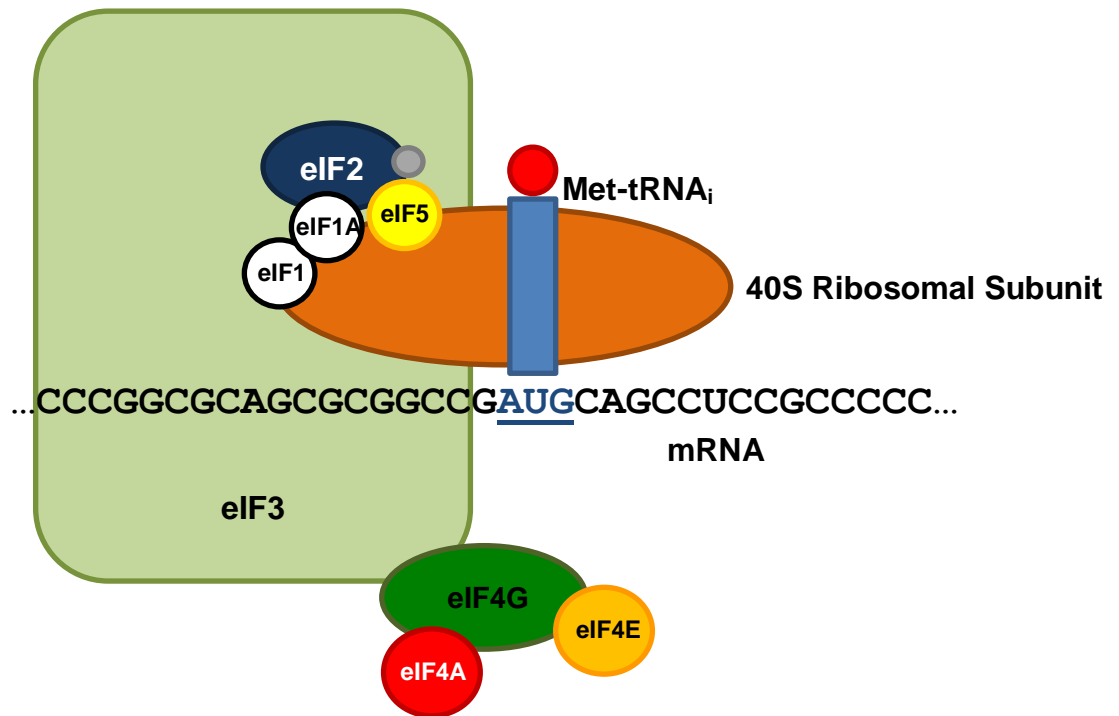


**Figure 1.9.** The next stage is the scanning of the 48S complex along the mRNA in a 5' to 3' direction until it reaches the AUG start codon (Kozak, 1989). The context of the start codon plays an important role in regulating the expression of the downstream open reading frame (Kozak, 1984b). The Kozak consensus sequence is: (gcc)gccRccAUGG (where R is either A or G) (Kozak, 1984b). If the AUG sequence is encountered by the 48S pre-initiation complex in the configuration shown above, the consensus would act as a strong initiator of translation (Kozak, 1984b). Variations in the sequence weaken the ability of the start codon to initiate translation (Kozak, 1984b). This differential confers varying degrees of initiation strength to different genes, thereby regulating the relative amount of their encoded protein produced (Kozak, 1984b). The consensus may even be weak enough that the ribosome does not recognise it as the translation start point at all; this is called leaky scanning (Kozak, 1989). Although the Kozak consensus sequence exhibits variation, the start codon itself is an AUG codon in 99.9% of all eukaryotic genes (prokaryotes use non AUG start codons more commonly) (Sugiharas et al., 1990; Tikole and Sankararamakrishnan, 2006). Once the start codon has been found, the initiator Met-tRNA<sub>i</sub> in the ternary complex is base paired to the RNA. This event triggers eIF5 to facilitate GTP hydrolysis by eIF2 by acting as a GTPase-activating protein (Asano et al., 2001). eIF1 aids in the recognition of the AUG start codon by dissuading base pairing of the Met-tRNA<sub>i</sub> to inappropriate triplets and inhibiting the GTPase activating function of eIF5 in the absence of an AUG triplet (Lomakin et al., 2003; Unbehaun et al., 2004). The 48S subunit contains three sites that function as part of protein synthesis; these are termed: A, P and E (Garrett, 2000). Site A binds tRNA that is aminoacylated (charged with an amino acid), site P binds tRNA attached to the amino acid which is becoming part of the peptide and site E binds the exiting non-bound tRNA (Woodcock et al., 1991). Hydrolysis of eIF2-GTP (to form eIF2-GDP) releases the initiator methionine tRNA into the P site of the ribosomal subunit, the eIF2-GDP then dissociates to be recycled into eIF2-GTP (Campbell et al., 2005). Also believed to dissociate from the ribosome complex at this stage are eIF1, eIF1A, eIF3, eIF4F and eIF5 (Pestova et al., 2001).

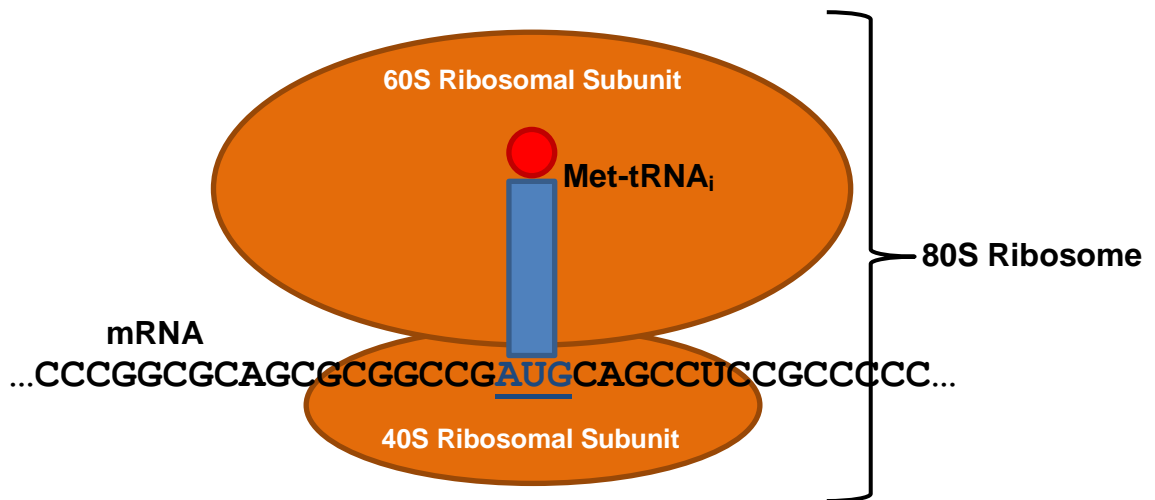


**Figure 1.10.** After the initiation factors dissociate, the ribosome-dependent GTPase activity of eIF5B facilitates the binding of the 60S ribosomal subunit to the 40S-Met-tRNA<sub>i</sub>-mRNA complex (Pestova et al., 2000). With the 80S ribosome now complete and in its correct position on the mRNA, the process of translation initiation is over and elongation can begin.

#### 1.1.12. Examples of the Regulation of Gene Expression at the Level of Translation

##### **Regulation of the rate at which mRNAs are recruited to the endoplasmic reticulum**

Insulin synthesis was found to increase in pancreatic islets with increasing glucose concentration. Despite this increase in insulin expression, the concentration of the insulin mRNA remained constant (Itoh and Okamoto, 1980). It was shown that insulin mRNA molecules localise at the endoplasmic reticulum (where insulin is synthesised) when glucose concentrations are higher (Welsh et al., 1986). The fact that supplemental signal recognition particle introduced into cells exposed to high glucose concentrations increased the rate of insulin mRNA localisation at the ER is consistent with the signal recognition particle being involved in this response (Welsh et al., 1986).

##### **eIF2 and eIF2B Regulation**

Since eIF2-GTP is critical for successful translation (Figure 1.5.), it is logical that the activity of eIF2B is a regulator of translation (Webb and Proud, 1997). Mutations in the gene encoding eIF2B have been strongly linked to the disease 'leukoencephalopathy with vanishing white matter' (VWM) (Li *et al.*, 2004). It is not yet apparent the exact mechanism by which the loss of eIF2B function causes

the pathology but it is known that inhibition of eIF2B causes a decrease in global protein synthesis (Kimball *et al.*, 1998). Despite this general suppression, translation of mRNAs with start codons in the 5' untranslated region increases (Hinnebusch, 2000). Interestingly, one such mRNA encodes CHOP which is a transcription factor responsible for inducing the transcription of a set of stress response genes (Harding *et al.*, 2000; Ubeda and Habener, 2000). This means that loss of either eIF2 or eIF2B function, possibly by natural phosphorylation or pathogenic mutation, will lead to the upregulation of the CHOP-mediated stress response (Harding *et al.*, 2000; Ubeda and Habener, 2000). The relationship between uAUG-mediated gene upregulation in VWM and the disease phenotype is unknown but the fact that prolonged CHOP expression causes apoptosis in astrocytes (as well as other cell types) is consistent with this upregulation being important in the disease (Reviewed in: (Proud, 2011)).

Translation may be suppressed by the phosphorylation of the  $\alpha$  subunit of eIF2 (Kimball, 1999). This phosphorylation converts eIF2 from a substrate of eIF2B to a competitive inhibitor (Kimball, 1999). Downregulation of global protein synthesis by the phosphorylation of eIF2 is induced in response to a range of cellular stresses and performed by a range of different kinases (Kimball, 1999). One example of such a response is the activity of GCN2 (eIF2 kinase general control non-derepressible-2) which is induced by the presence of uncharged tRNA and, as such serves to suppress translation under conditions of amino acid starvation (Wek *et al.*, 2004). Another example is PERK ((RNA-dependent protein kinase)-like endoplasmic reticulum kinase) which phosphorylates eIF2 in response to the presence of misfolded proteins in the endoplasmic reticulum (Kaufman, 2004).

### **eIF4E Regulation**

A number of conditions must be fulfilled for eIF4E to be able to participate in translation initiation (Raught and Gingras, 1999). The fact that eIF4E is generally the least common initiation factor in terms of numbers of molecules per cell (eIF4A is generally the most common (Duncan and Hershey, 1983)) makes it an ideal target for regulation (Hiremath *et al.*, 1985). eIF4E is phosphorylated in response to certain stimuli, one example of which is the hormone insulin (Makkinje *et al.*, 1995). One of the main kinases responsible for phosphorylating eIF4E is 'MAP kinase-activated protein kinase' MNK1 which accesses eIF4E by binding eIF4G (Li *et al.*, 2001). This phosphorylation increases the affinity of eIF4E for the 5' cap and also contributes to a more stable eIF4F complex (Bu *et*

*al.*, 1993; Minich *et al.*, 1994). The binding of eIF4E to eIF4G and hence translation initiation is inhibited by competition for the site on eIF4E by a family of three proteins called eIF4E binding proteins (4E-BPs) which possess a similar 4E-binding domain to eIF4G (Haghighat *et al.*, 1995). The ability of the 4E-BPs to interfere with eIF4E binding is regulated by their phosphorylation state; underphosphorylated forms can bind to eIF4E while hyperphosphorylated forms cannot (Pause *et al.*, 1994a). The 4E-BPs can become hyperphosphorylated in response to growth factors, environmental stimuli or hormones (Fleurent *et al.*, 1997; Lin *et al.*, 1994; Pause *et al.*, 1994a). When the protein PHAS-I (phosphorylated heat-acid stable) is hypophosphorylated it also binds eIF4E but in response to the presence of mitogenic compounds MAP (mitogen activated) kinase rapidly phosphorylates PHAS-I causing it to dissociate from eIF4E (Lin *et al.*, 1994). The released eIF4E can then upregulate translation initiation to meet the increased demands for protein of the process of mitosis (Lin *et al.*, 1994).

### 1.1.13. Cap-Independent Translation Initiation

An internal ribosomal entry site (IRES) is a sequence contained within the 5' untranslated region of a mRNA that recruits the ribosome and initiates translation without the use of the 5' cap and even, in some instances (e.g. the cricket paralysis virus IRES) without the use of translation initiation factors (Fraser *et al.*, 2004; Jang *et al.*, 1988; Kaminski *et al.*, 1995). Originally identified in picornavirus mRNA in 1988, insight into the properties of IRESs was provided when the poliovirus 5' UTR was cloned into a dicistronic plasmid and found to allow the expression of the downstream cistron (Pelletier and Sonenberg, 1988). It became apparent that an IRES could facilitate translation initiation in the absence of either a 5' or 3' end when it was shown to be able to recruit the ribosome to a circular mRNA (Chen and Sarnow, 1995).

A number of different viruses including poliovirus, coxsackievirus, human rhinovirus and foot and mouth disease virus (FMDV) encode a protease in their genome which cleaves eIF4G rendering it unable to bind eIF4E (Borman *et al.*, 1997). This severely impairs cap-dependent translation initiation and thereby increases the ability of the cell to translate the non-cap-dependent IRES-mediated viral genes (Borman *et al.*, 1997). While the cap-associated eIF4E is redundant in IRES-mediated translation initiation, a significant role for eIF4A has become apparent (see next section) (Pause *et al.*, 1994b).

The first eukaryotic mRNA that was found to contain an IRES was *B<sub>1</sub>P* (HSPA5); an immunoglobulin heavy chain binding protein present in B lymphocytes

(Sarnow, 1989). It was discovered when expression levels of BiP remained consistent in cells infected with poliovirus. This was in contrast to the majority of proteins in the cell, the expression of which was inhibited by the cleavage of eIF4G by the virus (Sarnow, 1989). This technique was used to identify more cellular mRNAs that contained IRES elements (Johannes *et al.*, 1999). 68 viral and 115 eukaryotic cellular IRESs have been identified and catalogued in a repository (<http://iresite.org/>, 2012). Despite the increasing numbers of IRESs discovered, a common sequence motif that may be used to accurately predict the presence of an IRES within a sequence has proved elusive (Le and Maizel, 1997). This fact points to the importance of RNA secondary and tertiary structure in the function of an IRES (Xia and Holcik, 2009). Also in support of the idea that the precise three dimensional composition of an IRES is critical to its function is the idea that a single nucleotide change to its sequence can have significant impact on its ability to initiate translation (Fernandez *et al.*, 2005). Where structure is important, for example in ribosomal RNA (rRNA), if a mutation occurs that changes the structure, often a compensatory mutation will arise that will restore the original configuration of the molecule (Hancock *et al.*, 1988).

The fact that IRESs exhibit such variation has been used in support of the hypothesis that they have emerged independently over the course of evolutionary time (Martinez-Salas *et al.*, 2001). Contrary to this idea is the theory that cap-independent translation initiation evolved first and was superseded by cap-dependent initiation (Hernández, 2008). The main argument in favour of extant IRES elements being very ancient sequences is the fact that eIF4E and eIF4G were among the last translation initiation factors to evolve (Hernández, 2008).

IRES-mediated translation initiation combined with eIF4G cleavage is a useful mechanism for viral attack, it is also well established that the cellular IRES elements are used in a regulatory capacity (Borman *et al.*, 1997; Stoneley and Willis, 2004). An example of an IRES-regulated gene is ‘*type I insulin-like growth factor receptor*’ (*IGF-IR*) (Meng *et al.*, 2008).

Cap-independent translation initiation has been thoroughly studied in the *myc* transcription factors with *c-myc*, *L-myc* and *N-myc* mRNAs all demonstrated to contain IRESs (Jopling *et al.*, 2004; Jopling and Willis, 2001; Stoneley *et al.*, 1998). Despite the similar functions of these genes, their IRES elements have differing requirements for the translation initiation factors (Spriggs *et al.*, 2009). For example, the *L-myc* IRES requires PABP and eIF3 in association with eIF4G while the *N-* and *c-myc* IRESs only require the C-terminal domain of eIF4GI and eIF3 but not necessarily complexed (Spriggs *et al.*, 2009). As part of the same

study, hippuristanol treatment of cells transfected with reporter plasmids containing the IRESs revealed that they all have a significant requirement for eIF4A (Spriggs *et al.*, 2009). The IRES element belonging to *N-myc* was shown to have a differential expression pattern in laboratory cell lines of different origins with higher expression in neuronally-derived SH-SY5Y cells (Jopling and Willis, 2001).

IRES *trans* acting factors (ITAFs) may also be responsible for the differing strengths, initiation factor requirements and cell-type specific effects of different IRESs (Lewis and Holcik, 2007). ITAFs are proteins that act as accessories to cellular IRESs, facilitating their association with the ribosome (Mitchell *et al.*, 2005). The mechanism of action of the recently discovered ITAFs is not yet clear but it has been suggested that they may act as a physical bridge between ribosome and RNA or that they enable the RNA to form the structural conformation necessary for ribosomal entry (Mitchell *et al.*, 2005; Yaman *et al.*, 2003). Some ITAFs are associated with most cellular IRESs, for example polypyrimidine tract binding protein (PTB) which is particularly active during apoptosis (Bushell *et al.*, 2006; Mitchell *et al.*, 2005; Spriggs *et al.*, 2005). In general however, IRESs have varying requirements for different ITAFs (Cobbold *et al.*, 2008).

### **The IRES families and their requirements**

IRESs are organised into four families (or 'groups' or 'types') based on the conservation of their structure (Reviewed in: (Pacheco and Martinez-Salas, 2010)). *Picornaviridae* are divided into two main types. Type I includes enterovirus (e.g. poliovirus) and rhinovirus (e.g. human rhinovirus) and type II includes aphthovirus (e.g. foot and mouth disease virus) and cardiovirus (e.g. encephalomyocarditis virus) (Beales *et al.*, 2003; Jackson *et al.*, 1990).

IRES type III contains hepatitis A virus (a member of the *Flaviviridae* family) and type IV contains hepatitis C virus (also a member of the *Flaviviridae* family).

Types I and II require eIF4A, eIF4G (the central domain), eIF4B, eIF2, ATP and eIF3 but not eIF1, eIF1A or eIF4E (de Breyne *et al.*, 2009; Kolupaeva *et al.*, 1998; Pestova *et al.*, 1996a; Pestova *et al.*, 1996b).

The requirement for the activity of eIF4A in the expression of one of the (type II) IRES-mediated genes from encephalomyocarditis virus has been demonstrated (Pause *et al.*, 1994b). Mutant eIF4A with a non-functional HRIGRXXXR domain (believed to be required for RNA binding and ATP hydrolysis) failed to initiate the

translation of the gene encoding the EMC virion in rabbit reticulocyte lysate, unlike the addition of functional eIF4A (Pause et al., 1993; Pause et al., 1994b).

The role of eIF4A in the expression of EMCV IRES-mediated genes may also be structural (Lomakin et al., 2000). It was found that the interaction between eIF4A and eIF4G was able to increase the expression of an EMCV IRES-mediated gene even in the absence of ATP. It was proposed that eIF4A may provide binding sites that induce the IRES to form a structure that is better able to initiate translation (Kolupaeva et al., 2003; Lomakin et al., 2000).

The type III IRES belonging to hepatitis A virus (HAV) is unusual as it has been shown to require eIF4E and eIF4G (Ali et al., 2001). However, like the picornavirus IRESs, the HAV IRES also has a strong requirement for functional eIF4A (Fletcher et al., 2002).

The type IV IRES of hepatitis C virus (HCV) only requires eIF3 and the ternary complex to form a successful 48S complex (Otto and Puglisi, 2004; Tsukiyama-Kohara et al., 1992).

#### **1.1.14. Elongation and Termination**

Whether initiation occurs in a cap-dependent or cap-independent manner, the next step in the translation of a mRNA is elongation. This process is assisted by just two (elongation) factors which facilitate the reciprocating action of the ribosome by positioning an aminoacyl-tRNA at the ribosomal A site, catalysing the condensation reaction that forms the peptide bond between amino acids and shifting the mRNA on by three nucleotides (Reviewed in: (Greganova et al., 2011; Riis et al., 1990)). There may be more than one ribosome engaged in translation of a single mRNA at any one time in order to increase the amount of protein produced per mRNA, multiple ribosomes are collectively referred to as a polysome (Warner *et al.*, 1963).

The process of elongation continues until the ribosome encounters a stop codon, at which point, release factors associate with the large ribosomal subunit and cleave the ester bond between the final amino acid residue and the tRNA (Kisselev *et al.*, 2003). Both the ribosomal subunits dissociate from the mRNA and translation is terminated. The poly(A) tail serves to stimulate the increased translation rate of a mRNA (Munroe and Jacobson, 1990). Circularisation of a mRNA by the joining of eIF4G to the PABPs as part of translation initiation means that a ribosome that has reached the stop codon will be physically closer to the start codon and therefore readily available for reinitiation should it be required (Asselbergs *et al.*, 1978; Craig *et al.*, 1998).

#### 1.1.14. mRNA Recycling

Factors that influence the rate at which the mRNA degrades (such as miRNAs) are used as a mechanism to control the level of the protein that the mRNA encodes (Valencia-Sanchez *et al.*, 2006). The fact that mRNAs encoding different proteins have different half-lives naturally introduces a further differential between the length of time over which their products are expressed (Tucker and Parker, 2003). Genes that are regulated in this manner tend to be involved in critical cellular functions that require rapid adjustment in response to dynamic environmental conditions (McCarthy, 1998). The main contributor to mRNA stability and longevity is the poly(A) tail, mRNAs do not degrade readily with the tail in place (Decker and Parker, 1993). The activity of deadenylases, which cleave adenine residues from the tail, may be enhanced by sequences in the 3' UTR of the mRNA, for example, the AU-rich element (ARE) (Schiavi *et al.*, 1992). These sequences are notably found to be mutated in oncogenic alleles of the 3' UTR of *c-fos* (Schiavi *et al.*, 1992).

Complete deadenylation of a mRNA leaves the molecule vulnerable to 3' exonucleolytic digestion by the exosome complex (Wilusz *et al.*, 2001). More commonly, once deadenylation has occurred, degradation progresses in a 5' to 3' direction following the removal of the 5' cap (Badis *et al.*, 2004).

## Part 2.

# Eukaryotic Initiation Factor 4 A (eIF4A)

### 1.2.1. The helicase families

eIF4A belongs to a larger family of helicases (Rogers *et al.*, 2002a). The DEAD box helicases are named after their conserved Aspartic acid, Glutamic Acid, Alanine, Aspartic acid (DEAD) motif (Rogers *et al.*, 2002a). Also conserved between family members are nine general motifs: the Q-motif, motif I, motif 1a, motif 1b, motif II, motif III, motif IV, motif V, and motif VI (Linder *et al.*, 1989). The DEAD sequence is contained within motif II (also called the 'Walker B' motif, motif I is also sometimes called the 'Walker A' motif) (Linder *et al.*, 1989). Motifs I, II, Q and VI are involved in ATP hydrolysis, while motifs, 1a, 1b, III, IV, and V are responsible for RNA interaction (Figure 1.11.) (Tanner *et al.*, 2003).

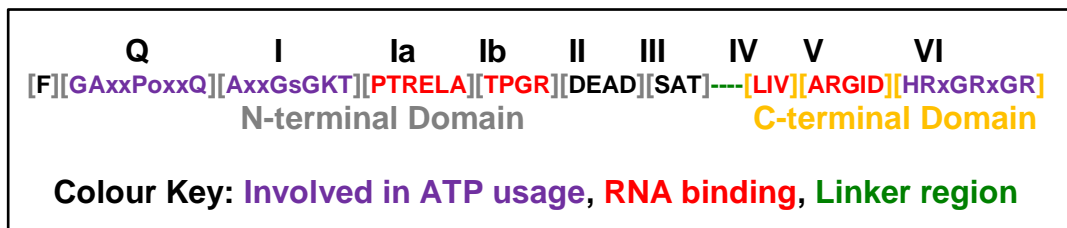


Figure 1.11. The conserved sequence motifs of the DEAD-box helicase family

The DEAD box helicases are closely related to the DEAH and the Ski2 helicases (Wang *et al.*, 2005; Xu *et al.*, 2002). Together these three families are referred to as DExD/H (Rocak and Linder, 2004). The DExD/H family fits into the classification of all helicase proteins as part of superfamily II (Rocak and Linder, 2004). There exist three large super-families (I-III) and two smaller families, they are divided along parameters of structure, such as the conserved DEAD motif, rather than function e.g. DNA or RNA specificity (Gorbalenya and Koonin, 1993). The substrate for all DExD/H helicases is RNA (Rocak and Linder, 2004). The 36 DEAD box helicases predicted to occur in humans are believed to function as part of the processes of: transcription, translation initiation, ribosome biogenesis, mitochondrial gene expression, RNA splicing, RNA transport and mRNA degradation (Abdelhaleem *et al.*, 2003; Cordin *et al.*, 2006; Rocak and Linder, 2004). It has also been proposed that the RNA binding activity of the DEAD box

helicases could be used in the disruption of unfavourable RNA-protein interactions (Rocak and Linder, 2004).

eIF4A is often described as the ‘prototypical’ or ‘archetypical’ DEAD box RNA helicase, this is due to the fact that it was the first to be discovered and it does not contain the C terminal and N terminal extensions seen in many helicases (Rogers *et al.*, 2002a; Sonenberg *et al.*, 1988).

Although DEAD box helicases are found in a large number of species, both prokaryotic and eukaryotic, they are not entirely ubiquitous (Rocak and Linder, 2004). Notable for their total lack of DEAD box helicases are the bacterial species *Chlamydia* and *Borrelia* and the archaea *Pyrococcus* and *Halobacterium* (Rocak and Linder, 2004). The reason for the absence of DEAD box helicases in these organisms is not known.

The conservation of DEAD box helicases across archaea, bacteria and eukaryotes indicates that eIF4A may be the most ancient translation initiation factor (Hernández, 2008; Kyrpides and Woese, 1998).

### 1.2.2. Paralogs

In humans, there exist three paralogs of eIF4A termed eIF4AI (eIF4A1), eIF4AII (eIF4A2) and eIF4AIII (eIF4A3) (Li *et al.*, 1999). eIF4AI and II are structurally similar, with 90-95% homology at the amino acid level (Bordeleau *et al.*, 2005; Conroy *et al.*, 1990). In an early study of translation initiation factors in rabbit reticulocyte lysate, separation of the eIF4F complex revealed the presence of proteins with Dalton masses of: 220,000, 24,000 and 46,000. The 220 kDa protein was eIF4G and the 24 kDa protein eIF4E (Conroy *et al.*, 1990). The 46 kDa protein consisted of both eIF4AI and eIF4AII, present in a 4:1 ratio respectively (Conroy *et al.*, 1990).

As part of the eIF4F complex, eIF4A I and II are referred to as eIF4Ac (‘complexed’) as opposed to eIF4Ar (‘freeform’) (Yang *et al.*, 2003). When not complexed, eIF4AI and II are present in the cytoplasm with no particular localisation (Yang *et al.*, 2003).

eIF4AI and eIF4AII were found to exhibit the same level of RNA processing activity *in vitro* (Conroy *et al.*, 1990; Yoder-Hill *et al.*, 1993). The coding sequences of *eIF4AI* and *II* (from NCBI, RefSeq IDs NM\_001416 for *eIF4AI* and NM\_001967 for *eIF4AII*) have 77% homology (based on the Smith-Waterman algorithm). Until fairly recently, it was supposed that the amino acid similarity of eIF4AI and II, combined with the fact that they both form part of the eIF4F complex meant that they were functionally identical (Bordeleau *et al.*, 2006).

Foot and Mouth Disease Virus (FMDV) 3C protease cleaves eIF4AI but not eIF4AII, this suggests the possibility of a functional difference between the paralogs (Li *et al.*, 2001). It remains to be explained why FMDV should cleave one paralog and not the other (Li *et al.*, 2001). The use of this example as an argument *for* the functional distinction of the two paralogs must be treated sceptically as it may be coincidence that the site of viral cleavage is unique to paralog I (Belsham, 2000).

Also consistent with the theory that paralogs I and II are functionally distinct is the finding that the mRNA levels of the two genes vary between tissues with the highest amounts of *III* recorded in the kidney and the lowest in the thymus in mouse (Nielsen and Trachsel, 1988).

In support of the idea that eIF4AII is functionally important in humans is the fact that there often exist more than one paralog in other species, although this multiplicity is conserved, the reason for the presence of the second paralog in any organism remains to be satisfactorily explained (Kato *et al.*, 2001). This argument relies upon the paradigm that evolutionary conservation across species is often associated with functional importance (Boffelli *et al.*, 2004; Dermitzakis *et al.*, 2005). Contrary to the argument that the presence of a biological structure within an extant organism must mean that it is important is the existence of vestigial features (e.g. junk DNA) which serve no known purpose but do not represent a significant evolutionary disadvantage (Reviewed in: (Biemont and Vieira, 2006)).

As well as eIF4AI and eIF4AII, a third variant of eIF4A exists, eIF4AIII (Li *et al.*, 1999). eIF4AIII shares only 65% amino acid similarity with eIF4AI, the main difference occurring in the N terminal 30 amino acid residues (Li *et al.*, 1999). Despite this difference, eIF4AIII can also act as an ATP-dependent RNA helicase and, like eIF4AI, an RNA-dependent ATPase, the activity of which may be enhanced by eIF4B (Li *et al.*, 1999). Although eIF4AIII is able to perform the same RNA processing function as eIF4AI, it was found to be unable to bind to the ribosome (via eIF4G) and to have an inhibitory effect on translation in general in rabbit reticulocyte lysate (Li *et al.*, 1999). It was concluded that eIF4AIII inhibited translation by competing for the eIF4A binding site on eIF4G but only partially associating with eIF4G when it did bind, eIF4AI binds the central *and* the C terminus of eIF4G while eIF4AIII only binds the central (Li *et al.*, 1999).

While eIF4AI and eIF4AII are located in the cytoplasm, eIF4AIII localises in the nucleus in 'speckle domains' (Holzmann *et al.*, 2000).

The role of eIF4AIII in translation (if any) is unclear, although it has been strongly implicated in both nonsense mediated decay (NMD) and mRNA splicing,

both of which are consistent with the fact that eIF4AIII is found in the nucleus (Ferraiuolo *et al.*, 2004; Holzmann *et al.*, 2000). It was proposed that the helicase activity of eIF4AIII could aid in the process of splicing (Ballut *et al.*, 2005; Ferraiuolo *et al.*, 2004). RNA interference knockdown of eIF4AIII, but not eIF4AI or eIF4AII was found to inhibit nonsense mediated decay in HeLa cells (Ferraiuolo *et al.*, 2004). Within the EJC the ATP binding activity of eIF4AIII is stimulated by the protein MLN51 (Noble and Song, 2007). The ATPase activity of eIF4AIII in the EJC is inhibited by MAGOH (protein mago nashi homolog) and Y14 (Shibuya *et al.*, 2004). This causes eIF4AIII to act as an RNA clamp, anchoring the EJC to the mRNA (Shibuya *et al.*, 2004).

EJC-associated eIF4AIII also provides a binding site for UPF3, one of the factors responsible for triggering the degradation of the mRNA (Ballut *et al.*, 2005).

As part of the function of eIF4AIII in the EJC and in NMD, it is a key regulatory element in suppressing the translation of dendritic mRNAs (Giorgi *et al.*, 2007). Knockdown of eIF4AIII in HeLa and PC-12 cells caused an increase in the product of the neuronal gene *ARC* which encodes a protein that mediates neuronal plasticity and is also involved in the consolidation of long-term memory (Giorgi *et al.*, 2007).

In *Drosophila*, eIF4AIII is involved in the localisation of mRNAs in the development phase of the organism; this phenomenon has yet to be observed in mammalian cells however (Palacios *et al.*, 2004).

Neatly combining the hypotheses that eIF4AIII is involved in both development and the regulation of elements of the nervous system, it was found that knockdown of eIF4AIII in *Xenopus laevis* embryos resulted in full body paralysis with phenotypic abnormalities in sensory neurons, pigment cells and the heart (Haremaki *et al.*, 2010). The mechanism by which loss of eIF4AIII function caused such significant phenotypic defects became clearer when it was found that knockdown of other critical components of the exon junction complex also caused such effects (Haremaki *et al.*, 2010).

### 1.2.3. Structure

eIF4AI is a protein of 406 amino acid residues with a predicted relative molecular mass of 46,153 (Belsham, 2000; Chang *et al.*, 2009).

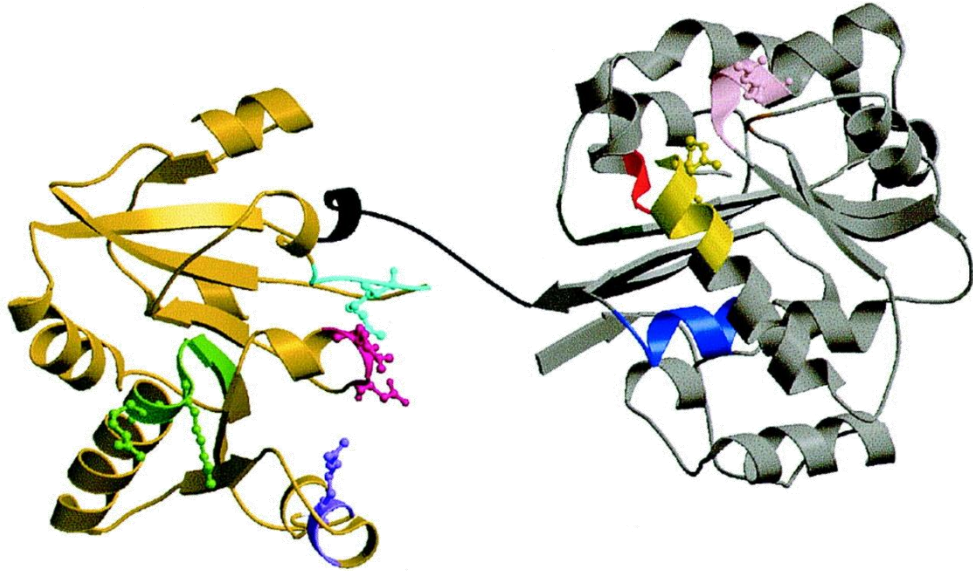


**Figure 1.12. Ribbon diagram of the structure of both domains of yeast eIF4A (Caruthers *et al.*, 2000).** The structure of eIF4A in yeast has been approximated using X-ray crystallographic analysis, (Caruthers *et al.*, 2000). To the left, coloured gold is the carboxyl terminal domain and to the right, coloured silver, is the amino terminus. The proximal linker, coloured black, consists of 11 amino acid residues. The blue regions of the diagram represent motif I (the Walker A motif), amino acid sequence: ASQSGTGKT, residues number 65-72. The yellow region is motif Ia, amino acid sequence: PIRELA, residues 97-102. The red region within the silver carboxyl terminal domain represents the Walker B motif (motif II) which contains the DEAD sequence, residues 169-172. The green region is motif III, amino acid sequence SAT, residues 200-202.

eIF4A has a 'dumbbell' shape (Figure 1.12.) (Caruthers *et al.*, 2000). X-ray crystallographic analysis revealed that the molecule has a total length of 80Å while the proximal linker section is 18Å (Caruthers *et al.*, 2000). Although the conserved motifs are identified in the diagram, their arrangement does not seem to corroborate their known function (Caruthers *et al.*, 2000). As part of the analysis, it was concluded that this meant that eIF4A can be distended in solution and that the linker must possess a degree of flexibility (Caruthers *et al.*, 2000). It was also concluded that ATP binding must cause a conformational change in the shape of the molecule (Caruthers *et al.*, 2000).

#### 1.2.4. Function

The ability of a mRNA to recruit and bind the ribosome is in inverse proportion to the extent and stability of the secondary structure of its 5' UTR (Kozak, 1980; Svitkin *et al.*, 2001). This secondary structure was proposed to aid the ribosome in the recognition of the AUG start codon (Kozak, 1980). This was largely disproven when the study presented data demonstrating that reovirus mRNA which was irreversibly unfolded (by bisulfite treatment in denaturing conditions) retained the ability to bind to wheat germ ribosomes (Kozak, 1980). The same study proposed that the secondary structure may, instead, modulate gene expression; a large number of subsequent studies support this hypothesis (Kozak, 1980; Takimoto and Kuramoto, 1994).

In many instances, it is energetically more favourable for a mRNA molecule, which is single stranded, to form secondary structure than to remain linear due to the hydrogen bond forming tendency of the hydroxyl groups in the ribose sugar (Doty *et al.*, 1959; Higgs, 2000). The nucleotides of an RNA molecule determine its structural conformation by base pairing in a number of different ways. (Mathews, 2006a). Watson-Crick pairing refers to the interaction between adenine and thymine (uracil in RNA) or the interaction between cytosine and guanine (Watson and Crick, 1953). Wobble base pairing is a type of non-Watson-Crick interaction, in mRNA wobble pairing can occur between guanine and uracil or between guanine and adenine (Crick, 1966; Gautheret *et al.*, 1994). Inosine is a modified adenine residue that can form non Watson-Crick hydrogen bonds with cytosine, guanine and uracil (Crick, 1966). The presence of this residue in tRNA has been well documented, it is only more recently that it has been proposed to be present in mRNA (Grosjean *et al.*, 1996; Paul and Bass, 1998). The effect of these interactions on the structure of the RNA molecule is approximately the same as if they were Watson-Crick (Sugimoto *et al.*, 1986).

Hydrogen bonds can form between any of the edges of the nucleotides in a mRNA molecule (Figure 1.13., left panel) (Hoogsteen, 1963). Since the interactions may form in *cis* or *trans* orientations (Figure 1.13..., right panel), there is the potential for the nucleotides to form 10 non-Watson-Crick configurations (e.g. *cis* Hoogsteen-Sugar Edge, *trans* Hoogsteen-Hoogsteen etc.) (Reviewed in: (Leontis et al., 2002)). Each of these interactions is comparable in strength to Watson-Crick pairings (Nikolova et al., 2011).

Another factor that contributes to the stability of the structure of an RNA molecule is the non-covalent interaction between the aromatic rings of the nucleotides, a phenomenon known as stacking (Reviewed in: (Šponer et al., 1996)).

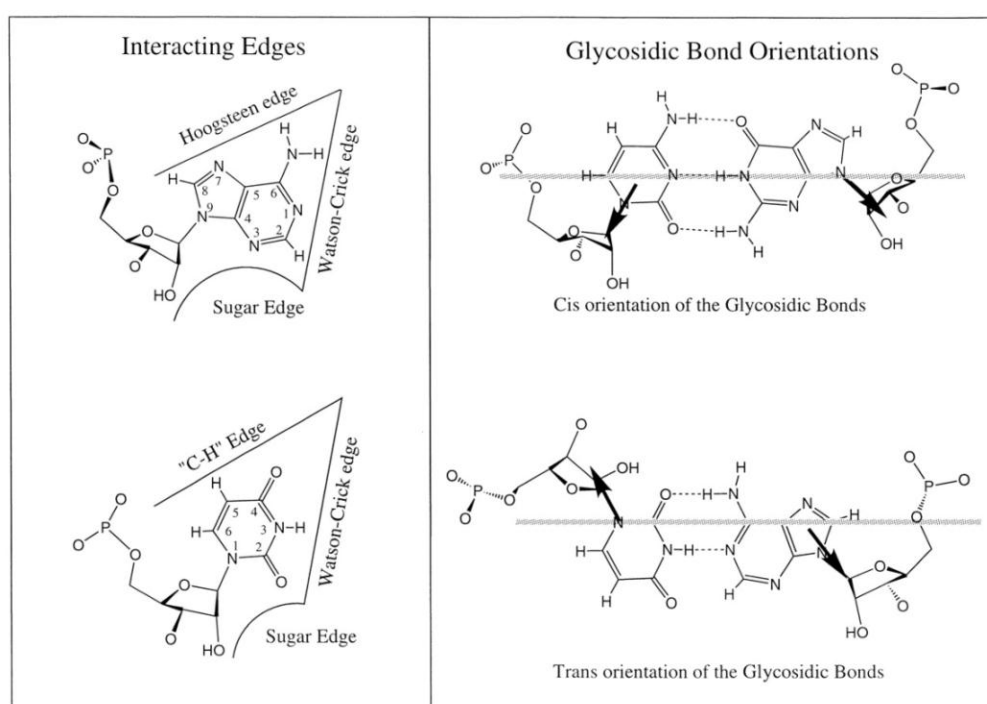


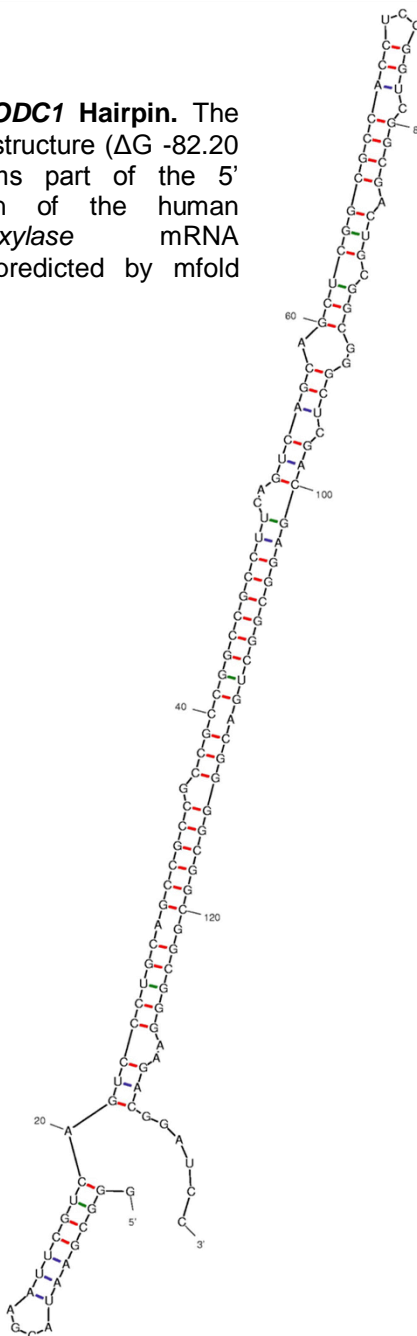
**Figure 1.13.** From: (Leontis et al., 2002). Left Panel: the names of the edges of the RNA nucleotides according to the pairings they form. Right Panel: The orientation of the pairings may be either *cis* or *trans*

Due to the complexity of the process of predicting RNA folding patterns *in silico*, the role of the tertiary structure of a mRNA in the process of translation initiation largely remains to be explored (Westhof and Auffinger, 2006). Tertiary structure has been identified as important in the function of the internal ribosome entry site (IRES) of the hepatitis C virus, although, as was discussed in the background section, this IRES has no requirement for eIF4A (Fraser et al., 2004; Kieft et al., 2002).

Although RNA tertiary structure is difficult to predict, secondary structure can be approximated with a degree of confidence *in silico* (Mathews, 2006b).

The secondary structure formed by an RNA hairpin used as part of this project to investigate the activity of eIF4A was predicted (Figure 1.14.).

**Figure 1.14. The *ODC1* Hairpin.** The stable hairpin RNA structure ( $\Delta G$  -82.20 Kcal/mol) that forms part of the 5' untranslated region of the human *ornithine decarboxylase* mRNA (NM\_002539), as predicted by mfold (Zuker, 2003).



Gibbs free energy ( $\Delta G$ ) is defined as the ability of a thermodynamic system to do work (Gibbs, 1873). The fact that programs like mfold ascribe a negative  $\Delta G$  to RNA structures is consistent with the fact that energy input is required to break the hydrogen bonds and other interactions that stabilise the molecule (Deng and

Cieplak, 2010; Zuker, 2003). In performing this reaction in living cells, ATP is the source of energy and an RNA helicase enzyme is the catalyst (Rocak and Linder, 2004). As early as 1982, it was demonstrated that mammalian eIF4A bound RNA in an ATP-dependent manner (Grifo *et al.*, 1982).

The fact that eIF4A can function *in vitro* means that RNA strand separation assays may be performed (Rozen *et al.*, 1990). One such assay involved the *in vitro* transcription of RNA molecules of varying lengths in which the cytosine residues were radiolabelled with  $^{32}\text{P}$  (Rogers *et al.*, 2001a). These radiolabelled strands were hybridised to unlabelled equivalents (Rogers *et al.*, 2001a). The addition of purified eIF4A to the reaction, along with the relevant buffers and ATP, was found to cause the strands to separate when visualised using polyacrylamide gel electrophoresis followed by autoradiogram detection (Figure 1.15.) (Rogers *et al.*, 2001a).

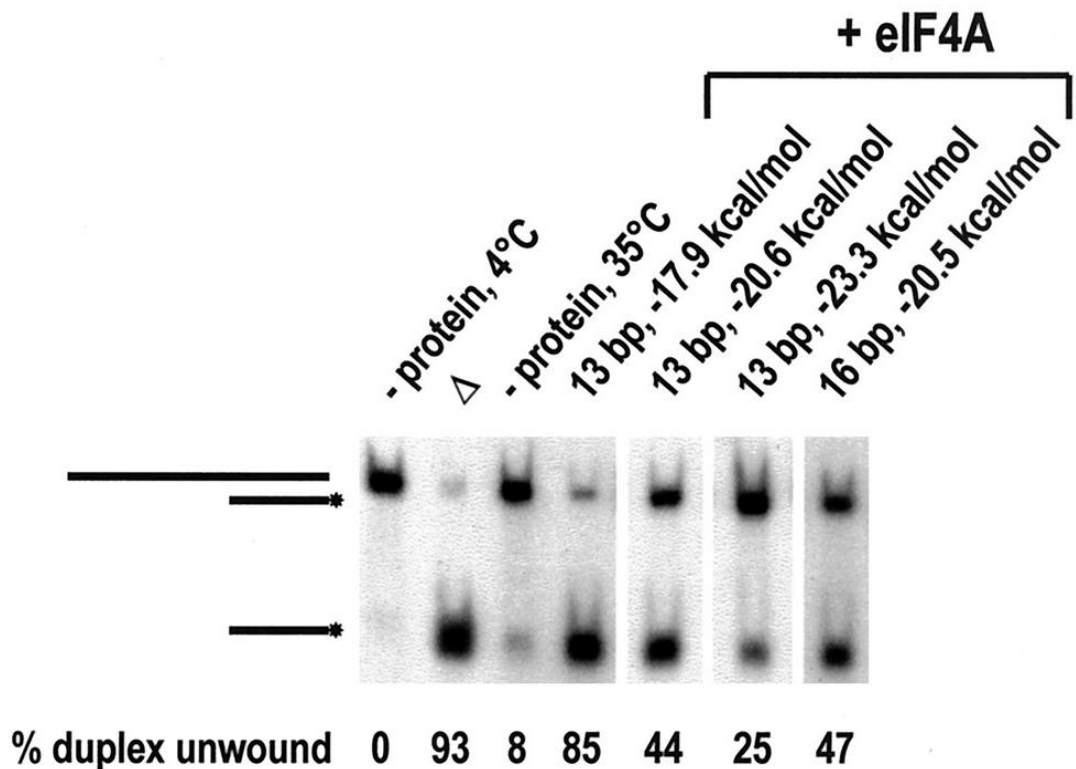


**Figure 1.15. From: (Rogers *et al.*, 2001a). Helicase assay results showing the separation of a partially radiolabelled RNA duplex.** The lanes third and fourth from the left show the difference in the state of the RNA duplex in the absence and presence of eIF4A respectively. Without eIF4A, the duplex remains 92% annealed but with eIF4A, after the same length of time it is only 15% annealed. The four lanes furthest to the right indicate that the predicted free energy of the duplex, ranging from 17.9 kcal/mol to 23.3 kcal/mol, dictates the rate at which it is unwound by eIF4A (Rogers *et al.*, 2001a). Although this study was not the first to demonstrate the functional properties of eIF4A *in vitro*; it is included here because it is replicated as part of this project using similar conditions. The results also show that eIF4A can unwind an RNA duplex *in vitro* (Rogers *et al.*, 2001a).

With regard to the *in vivo* function of eIF4A, the RNA substrate i.e. the messenger RNA molecule may be more than two orders of magnitude larger than the 13 nucleotide duplex and therefore able to form much more stable structures (Figure 1.15.) (Davuluri *et al.*, 2000). Although the entirety of the mRNA has the potential to form secondary structure, including the coding sequence, eIF4A is believed only to be involved in processing the 5' untranslated region as it dissociates when the 80S ribosome is formed, an event which occurs at the start codon at the end of the 5' UTR (Favre *et al.*, 1975; Kapp and Lorsch, 2004).

It was discovered, in bacteria that structure within the coding region of a mRNA did not inhibit the elongation phase of translation because the ribosome itself has RNA helicase activity (Lingelbach and Dobberstein, 1988; Takyar *et al.*, 2005). This activity was found to be ATP-independent, therefore differing from the way in which eIF4A functions (Takyar *et al.*, 2005). It was also found that this activity was not observable until after the process of translation initiation had occurred (Takyar *et al.*, 2005).

The hypothesis is that eIF4A is responsible for processing the secondary structure of the 5' untranslated region in an ATP dependent manner to allow the 40S ribosomal subunit to bind and scan for the start codon (Takyar *et al.*, 2005). At this point the 60S ribosomal subunit binds and the helicase activity of the completed ribosome is used to process the secondary structure of the coding sequence (Takyar *et al.*, 2005).

As discussed in the background section, there is a large degree of variation between the 5' untranslated regions of different genes and the distribution of this variation across the transcriptome is not random, it is used as a regulatory mechanism (Day and Tuite, 1998). An analysis of 699 vertebrate mRNAs found that the average length of the 5' UTR was between 20 and 100 nucleotides for three quarters of the cohort while the remaining quarter possessed 5' UTRs longer than 100 nucleotides (Kozak, 1991a). A more recent bioinformatics approach determined that the median length of 5' UTRs in humans is 150 nucleotides (Pesole *et al.*, 2000).

A 5' UTR that is very short (<10) nucleotides is inhibitory to the expression of the downstream coding sequence as it does not provide adequate room for the ribosome to bind at the cap and recognise the start codon (Kozak, 1987). Conversely, a long 5' UTR does not necessarily mean that it will be inhibitory to translation initiation (Kozak, 1987). This idea is supported by the fact that a 13 nucleotide duplex is unwound at almost the same rate as one that is 16

nucleotides as they both have roughly the same predicted free energy stability (Figure 1.15.) (Rogers *et al.*, 2001a).

Apparent from the study of the 699 vertebrate sequences was the fact that proto-oncogenes tended to possess atypically long 5' UTRs (Kozak, 1987). Proto-oncogenes also tended to differ in their number of upstream open reading frames (uORFs), with an average of two in three containing at least one AUG codon within the 5' UTR (usually more than one) (Kozak, 1987). This is consistent with examples like Her2, the expression of which is normally suppressed by a uORF but under certain conditions in cancer cells, this suppression is bypassed (Mehta *et al.*, 2006).

### 1.2.5. Genes

In *Homo sapiens*, the gene encoding eIF4AI is located on chromosome 17 (p13) (GenBank, 2010). It has a mRNA 1844 nucleotides in length which is divided into a 103 nucleotide 5' UTR (Table 2.), 1221 nucleotide coding sequence and a 520 nucleotide 3' UTR (GenBank, 2010).

*eIF4AII* differs in that it is located on chromosome 3 (q28) and has a slightly longer mRNA at 1905 nucleotides (GenBank, 2010). Also in contrast to *eIF4AI* is the fact that the 5' UTR of *eIF4AII* is only 39 nucleotides in length (Table 2.). The 3' UTR is similar to *eIF4AI*, being 642 nucleotides in length (GenBank, 2010).

The gene encoding eIF4AIII also belongs to chromosome 17 (q25.3), it has a 1734 nucleotide mRNA with a 222 nucleotide long 5' UTR (Table 2.) and a 276 nucleotide 3' UTR (GenBank, 2010).

Name	Length (nucleotides)	GC Content (%)	Predicted Free Energy (kcal/mol)	Accession #
<i>eIF4AI</i>	103	66	-39.20	NM_001416.2
<i>eIF4AII</i>	39	53	-7.00	NM_001967
<i>eIF4AIII</i>	222	74	-75.90	NM_014740
Hairpin	137	74	-82.20	NM_002539 (ODC1)

**Table 2. Details of the 5' UTRs of the eIF4A paralogs and the hairpin**

## 1.2.6. Small Molecule Inhibitors of eIF4A

### Pateamine A

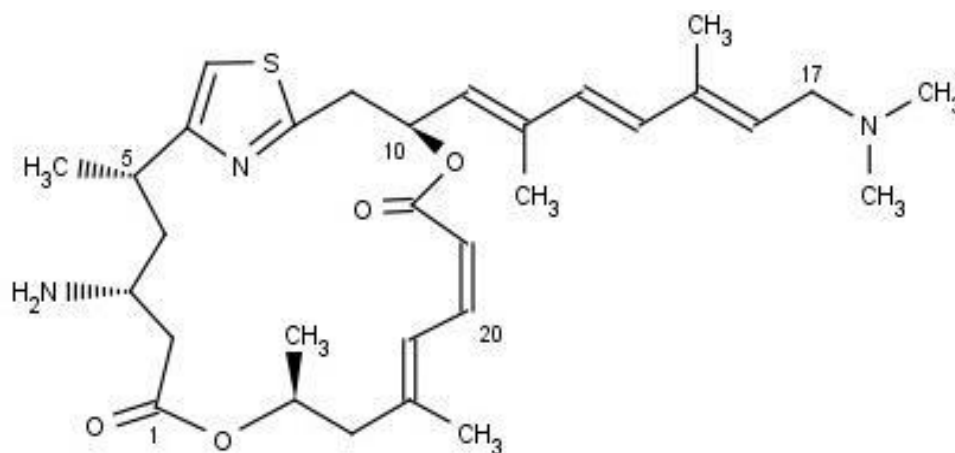


Figure 1.16. The structure of Pateamine A. (Website Reference 1.)

A high-throughput screen of over 90,000 natural products for inhibitors of eukaryotic translation initiation resulted in a single positive hit (Bordeleau *et al.*, 2005). The thiazole-containing polyene bis-lactone pateamine A (PatA) was originally isolated from the marine sponge *Mycale* found off the coast of New Zealand (Romo *et al.*, 1998). Pateamine A enhances the ability of eIF4A to bind to ATP and mRNA, stimulates RNA-dependent ATP hydrolysis and also acts as an agonist of the helicase activity of eIF4A (Bordeleau *et al.*, 2005). Pateamine does not affect the complexed eIF4A (eIF4A<sub>c</sub>) but overstimulation of the free cytosolic eIF4A (eIF4A<sub>f</sub>) causes impromptu, non-specific unwinding of mRNA templates resulting in interference of translation initiation and elongation (Bordeleau *et al.*, 2005). Alongside this activity, pateamine also causes eIF4A<sub>f</sub> to become tightly bound to the RNA template so that the helicase is eventually sequestered away from its cytosolic reservoir and therefore unavailable to form the eIF4F complex necessary for effective translation initiation (Bordeleau *et al.*, 2005). Pateamine A has a high specificity for eIF4A even among the DEAD box helicase family; it was found to have no affinity for the Ded1p helicase, a close relative of eIF4A (Bordeleau *et al.*, 2005).

## Hippuristanol

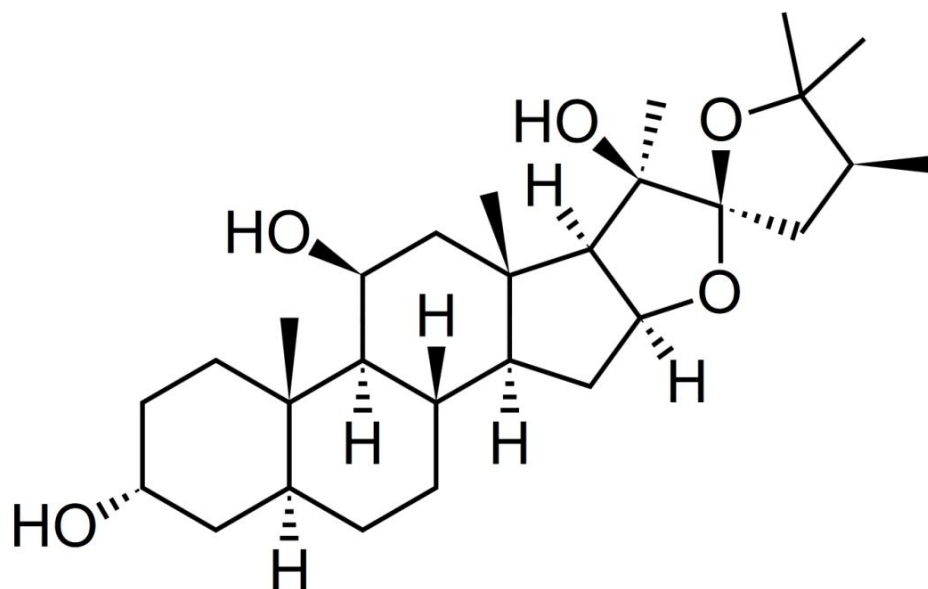
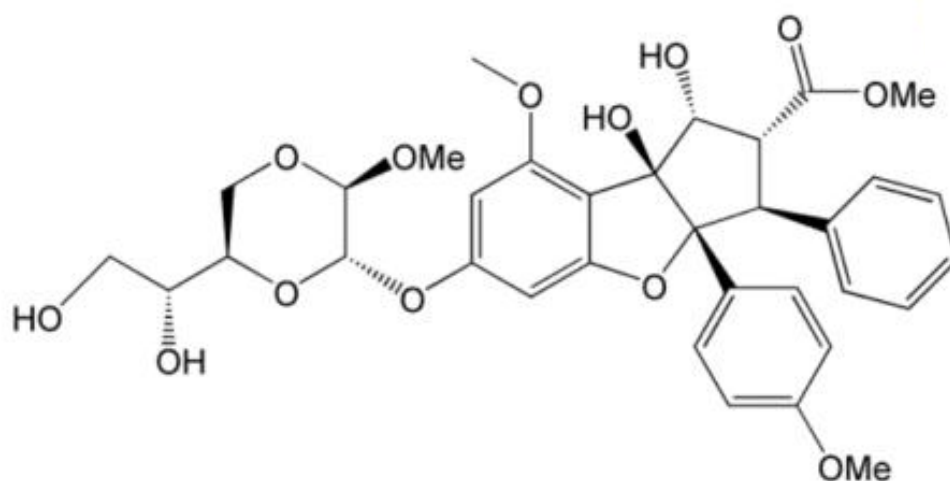


Figure 1.17. The structure of Hippuristanol (Website Reference 2.)

Hippuristanol was identified initially as an *in vitro* inhibitor of eIF4A as part of a high-throughput screen of small molecules (Bordeleau *et al.*, 2006). The molecule itself is a 462.66 g mol<sup>-1</sup> cytotoxic polyoxygenated steroid which was originally isolated from the gorgonian coral *Isis hippuris* found off the coast of Okinawa, Japan (Bordeleau *et al.*, 2006). It was flagged by the screen as a potent and highly specific inhibitor of cap-dependent translation; it was found that a dose of 1 μM was sufficient to reduce translation by 60% in Krebs-2 extracts (Bordeleau *et al.*, 2006). Hippuristanol acts by weakening the ability of eIF4A to bind to RNA by binding in a reversible manner to a number of conserved motifs (IV – VI) within the C terminus of eIF4A (Bordeleau *et al.*, 2006). ATP hydrolysis and mRNA binding are believed to be the responsibility of motif IV while V and VI form the active closed conformation of eIF4A (Bordeleau *et al.*, 2006).

## Silvestrol



**Figure 1.18. The structure of Silvestrol (Website Reference 3.)**

A further small molecule inhibitor of eIF4A was discovered more recently. The cyclopenta benzofuran flavagline silvestrol was originally isolated from the fruits and twigs of *Aglaia silvestris*, a species of plant belonging to the mahogany family (Meliaceae) (Hwang et al., 2004). It was identified as an inhibitor of eIF4A as part of another high-throughput screen of natural products (Bordeleau et al., 2008b). It was established, as part of the same study, that silvestrol acts as a chemical inducer of dimerization causing eIF4A<sub>f</sub> (free-form) to bind strongly to RNA upon contact negating its subsequent use as eIF4A<sub>c</sub> (complexed-form) (Bordeleau et al., 2008b). Silvestrol and its synthetic analogue episilvestrol were previously tested for chemotherapeutic effects against a number of human cancer cell lines before their specific function as translation inhibitors was established (Hwang et al., 2004). These studies generated promising results including an apparent 63.2% reduction in human KB (carcinoma) cell numbers implanted into mouse peritoneum (Kim *et al.*, 2006).

### 1.2.10. Cellular molecules that interact with eIF4A

#### Programmed cell death protein 4 (PDCD4)

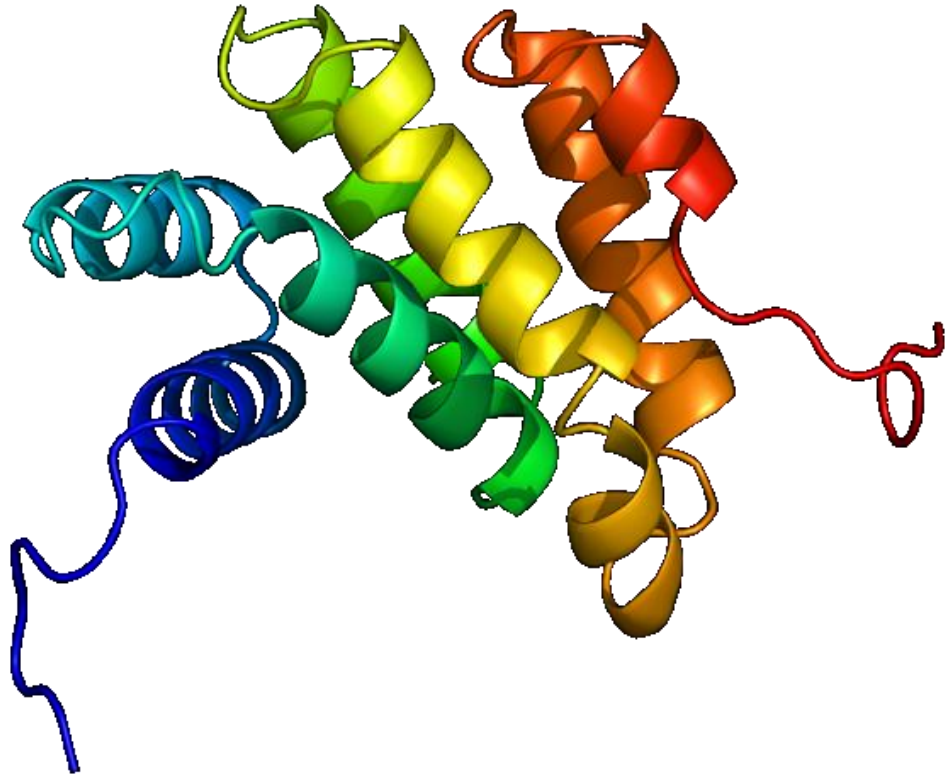


**Figure 1.19. Ribbon diagram of PDCD4 (Website Reference 12.).**

As discussed in the background section, the processive helicase activity of eIF4A is stimulated by eIF4B and eIF4H (Richter-Cook *et al.*, 1998; Richter *et al.*, 1999; Rogers *et al.*, 2001b). Contrary to this action is the activity of PDCD4 which suppresses the function of eIF4A (Yang *et al.*, 2003).

PDCD4 was first discovered as part of a study into the proteins expressed as part of apoptosis (Shibahara *et al.*, 1995). The mRNA of what was then termed simply MA-3 was found to be expressed in a number of cell lines belonging to different species in which apoptosis can be induced (Shibahara *et al.*, 1995).

In general, PDCD4 is a 485 amino acid, 64 kDa protein that is expressed in the nucleus of primarily liver cells during the G<sub>0</sub> phase of the cell cycle and during apoptosis (Goke *et al.*, 2002; Onishi *et al.*, 1998; Yoshinaga *et al.*, 1999).

The link between PDCD4 and eIF4A was discovered when it was found that PDCD4 shared a significant degree of homology with both isoforms of eIF4G (Goke *et al.*, 2002). PDCD4 inhibits the helicase activity of eIF4A and its ability to bind to the C terminal region of eIF4G by forming a complex itself with eIF4G (Goke *et al.*, 2002; Yang *et al.*, 2003). The fact that PDCD4 acts by interfering with eIF4G may explain why it inhibits the translational activity of eIF4A paralogs I and II but not III (Yang *et al.*, 2003).

The JB6 paired mouse cell lines are commonly used in the study of PDCD4, these are individually susceptible and resistant to neoplastic transformation (Cmarik *et al.*, 1999). Knockdown of the constitutively expressed PDCD4 in JB6 P- cells rendered them susceptible to transformation; this revealed that PDCD4 plays some role in tumour-suppression (Cmarik *et al.*, 1999). PDCD4 was found to be 8-10 times *less* highly expressed in the transformation-susceptible JB6 variant (termed P+) (Cmarik *et al.*, 1999). The hypothesis that PDCD4 is an effective tumour suppressor gains further support in light of the fact that artificially elevated levels of PDCD4 in P+ JB6 induces resistance to transformation as induced by 12-O-tetradecanoylphorbol-13-acetate treatment (Bernstein *et al.*, 1992; Yang *et al.*, 2001). This carcinogen works by increasing the binding of the transcription factor AP-1 (activator protein 1) to its target sequences which occur in gene promoters and also by inducing the activation of AP-1-regulated proteins in a posttranslational manner (Bernstein *et al.*, 1992; Yang *et al.*, 2001). The large array of proteins regulated by AP-1 tend to be involved in proliferation, differentiation and apoptosis (Ameyar *et al.*, 2003).

The regulation of the expression of PDCD4 is complex, involving both transcriptional and translational elements (Vikhreva *et al.*, 2010). An example of the latter is the fact that PDCD4 expression is downregulated in response to microRNA-21 (miR-21) which binds to its 3' UTR (Asangani *et al.*, 2007; Davis *et al.*, 2008). This is consistent with the finding that miR-21 is typically overexpressed in solid tumours, wherein it induces invasion and metastasis (Frankel *et al.*, 2008).

It has recently been shown that PDCD4 is involved in the cellular response to DNA damage in chicken DT40 cells as knockout of PDCD4 impaired the recovery response by an unknown mechanism (Singh *et al.*, 2009). The opposite effect was observed in human cells, with suppression of PDCD4 causing a reduction in apoptosis and an increase in survival (Bitomsky *et al.*, 2008). However, when p53 was also suppressed, the same effect as for chicken cells was observed (Bitomsky *et al.*, 2008).

## 15d-PGJ2

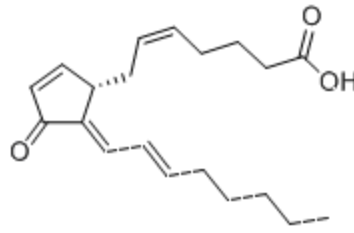


**Figure 1.20. Diagram of 15d-PGJ2 (Website Reference 13.).**

15d-PGJ2 (15-deoxy-delta 12,14-prostaglandin J2) is a cyclopentenone prostaglandin that endogenously inhibits inflammatory responses (Lawrence *et al.*, 2002; Straus and Glass, 2001). 15d-PGJ2 acts as an agonist of the pro-inflammatory transcription factors NF- $\kappa$ B and PPAR $\gamma$  (peroxisome proliferator activated receptor  $\gamma$ ) (Straus *et al.*, 2000). The link between 15d-PGJ2 and eIF4A was first discovered when it was noticed that 15d-PGJ2 causes stress granule formation in un-stressed cells (Kim *et al.*, 2007). Stress granules consist of proteins from the translation pre-initiation complex along with various other proteins that bind RNA; they form in response to stresses such as heat and amino acid starvation (Anderson and Kedersha, 2006). Stress granules also incorporate TRAF2 (TNF receptor-associated factor 2) which binds eIF4GI in such situations (Kim *et al.*, 2005). The normal role of TRAF2 is to stimulate TNF- $\alpha$  (tumour necrosis factor  $\alpha$ ) which is a pro-inflammatory cytokine (Kim *et al.*, 2007). Therefore stress granule formation contributes to the suppression of inflammation (Kim *et al.*, 2007). Pull-down experiments in HeLa cells revealed that eIF4AI was a binding target of 15d-PGJ2, this effect was corroborated by *in vitro* experiments conducted as part of the same study (Kim *et al.*, 2007). 15d-PGJ2 was found to enhance the RNA-binding activity of eIF4A and also, by binding the cysteine residue at position 264 on eIF4A, 15d-PGJ2 interferes with the formation of the eIF4G-eIF4A complex (Kim *et al.*, 2007).

15d-PGJ2 has been proposed as a potential therapeutic anti-metastatic agent due to the fact that it modifies cytoskeletal structure, a property that was found to attenuate the migration of adenocarcinoma cells (Diers *et al.*, 2010). The study outlined above presents strong evidence that 15d-PGJ2 binds and inhibits eIF4A, however the biological relevance of these findings, although consistent with what is known about translation suppression during inflammation, must be questioned (Ma and Hendershot, 2003). Intracellular prostaglandin concentration is difficult to measure as it requires the molecules to be conjugated to proteins but 15d-PGJ2

is believed to have an  $EC_{50}$  (effective concentration) in the low nM range (Powell, 2003). As part of the study, HeLa cells were treated with 50 $\mu$ M 15d-PGJ2, it is unknown whether this reflects the concentration normally found in HeLa cells however (Kim et al., 2007). Therefore, the biological relevance of the interaction between 15d-PGJ2 and eIF4A remains to be established (Powell, 2003).

## HuD

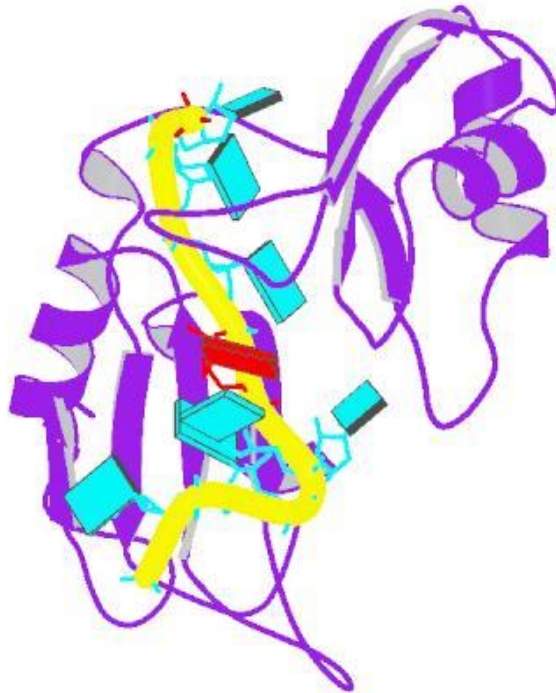


**Figure 1.21. Ribbon diagram of HuD**

HuD (ELAV4) belongs to the Hu family of RNA-binding proteins, the function of which is to stabilise mRNAs containing adenine / uridine rich elements (Deschênes-Furry *et al.*, 2006). It was recently shown, initially using co-immunoprecipitation, then by mutagenesis that HuD directly binds eIF4A (Fukao *et al.*, 2009). This study found that HuD stimulated translation but only when the cap and poly(A) structures were present (Fukao *et al.*, 2009). It was concluded that this effect may be due to HuD attaching the poly(A) tail of a mRNA to the cap (via eIF4A), thereby contributing to the circularisation of the mRNA (a phenomenon known to stimulate translation) (Fukao *et al.*, 2009; Wells *et al.*, 1998). It was also suggested that HuD may act by stimulating the activity of eIF4A (Fukao *et al.*, 2009). It is not known whether HuD stimulates translation indiscriminately or only acts on a certain population of mRNAs, for example, those with adenine / uridine rich elements (to which HuD binds) or those with high eIF4A requirements (Chen and Shyu, 2009; Fukao *et al.*, 2009).

### 1.2.11. Aims of the eIF4A section of the project

#### **New high throughput screens for small molecule inhibitors of eIF4A**

Pateamine A, hippuristanol and silvestrol were all identified as inhibitors of translation by high throughput screens of large libraries of small molecules. One of the aims of this project is to develop new screening strategies to be used in the search for new inhibitors of eIF4A. The current range of eIF4A inhibitors has been used to reveal much about the biology of translation initiation. In addition to this, due to the involvement of eIF4A in cancer, all of the known inhibitors are being considered for use in a chemotherapeutic context. Discovery of another inhibitor that potentially functions in a different way could be useful in future studies of eIF4A and may ultimately form the basis of a treatment for cancer and other diseases.

Two different screens were created as part of this project, one cell-based (*in vivo*) and the other *in vitro*.

#### **Investigating the properties of the three paralogs of eIF4A**

The cell-based screen was used to distinguish more clearly the function of the distinct paralogs of eIF4A. RNA interference was used to suppress the expression of each paralog independently and the effect on the screen was recorded.

The 5' UTRs of the three paralogs are different in terms of length and structure (Table 2.). In order to determine whether these sequences are involved in feedback regulation of the expression of the genes they precede, they were cloned into a reporter system.

#### **PDCD4**

Previous studies have implicated PDCD4 as being involved in the cellular response to DNA damage. One of the aims of this project is to determine the extent to which the role of PDCD4 as a suppressor of eIF4A activity contributes to this response.

# Part 3.

## Alzheimer's Disease

### 1.3.1. Background

Alzheimer's disease (AD) is a neurodegenerative disease characterised by the aggregation of protein plaques and tangles in the neurons of the brain, together with an increase in oxidative stress and neuronal apoptosis (Shimohama, 2000).

Although the pathophysiology of AD has been extensively studied, there is considerable disagreement among experts in the field regarding the importance of certain characteristics of the disease.

### 1.3.2. The molecular basis of Alzheimer's disease

The trigger for the onset of AD is unknown but age is the most significant risk factor with only a small percentage of people developing the early onset (<65 years) form of the disease (Campion *et al.*, 1999).

In either form, there is strong evidence implicating the transmembrane amyloid precursor protein (APP) as being important in the establishment of the pathology (Bayer *et al.*, 1999). The exact function of APP is not known but it is believed to be involved in iron metabolism, synaptic formation, neuronal repair and plasticity (Duce *et al.*, 2010; Priller *et al.*, 2006; Turner *et al.*, 2003). Aberrant cleavage of APP leads to the generation of peptides between 39-43 amino acids in length known as amyloid beta (A $\beta$ ) (Small and Duff, 2008). These peptides aggregate in the intracellular environment to form amyloid plaques (or 'senile plaques') (Perry *et al.*, 1978). The way in which these plaques damage cells is not yet known but it has been suggested that they cause apoptosis by disrupting calcium homeostasis and also that they increase oxidative stress within mitochondria (Chen and Yan, 2006; Yankner *et al.*, 1990). APP is strongly implicated in AD by the fact that sufferers of Down's syndrome generally develop the disease by the age of 40 or 50 (Mann *et al.*, 1984). This correlation is believed to be caused by the fact that *APP* is located on chromosome 21, which is present in triplicate in Down's syndrome patients (Burt *et al.*, 1998; Heyman *et al.*, 1984; Suchowersky and Hayden, 1984). Mutations affecting the gene encoding APP were found to be strong risk factors

for AD in a study of Alzheimer's in a Swedish family (Citron *et al.*, 1994). This collection of missense mutations was subsequently termed the 'Swedish mutation' – although this is a singular term, it is commonly used in the literature to refer to all the mutations identified by the original study (e.g. (Haass *et al.*, 1995)). It was determined that the Swedish mutation caused a disruption in the cellular localisation of recycled APP, making it more susceptible to pathological cleavage leading to the formation of the amyloid beta peptides (Citron *et al.*, 1994; Haass *et al.*, 1995).

The aberrant cleavage of APP is mediated by a number of enzymes and cofactors (Nunan and Small, 2000). 'Beta site of APP cleaving enzyme 1' (BACE1) is a  $\beta$  secretase that cleaves the transmembrane APP, leaving a membrane bound protein (C99) and an extracellular peptide (Hussain *et al.*, 1999; Lin *et al.*, 2000; Sinha *et al.*, 1999; Yan *et al.*, 1999). This initial cleavage step may also be performed by the  $\alpha$  secretase 'disintegrin and metalloproteinase domain-containing protein 10' (ADAM10), which cleaves closer to the cell membrane than BACE1 (Figure 1.22.) (Lammich *et al.*, 1999; Sisodia, 1992). The next stage involves the cleavage of the transmembrane section of APP by a large complex of proteins including a  $\gamma$  secretase (Figure 1.22.) (Edbauer *et al.*, 2003). If the APP molecule was previously cleaved by ADAM10 (or another  $\alpha$  secretase) then cleavage by the  $\gamma$  secretase will result in the generation of harmless protein fragments (Lammich *et al.*, 1999). However, if the APP was cleaved by BACE1 initially then cleavage by the  $\gamma$  secretase will generate A $\beta$  (Figure 1.22.) (Hussain *et al.*, 1999; Lin *et al.*, 2000; Sinha *et al.*, 1999; Yan *et al.*, 1999).

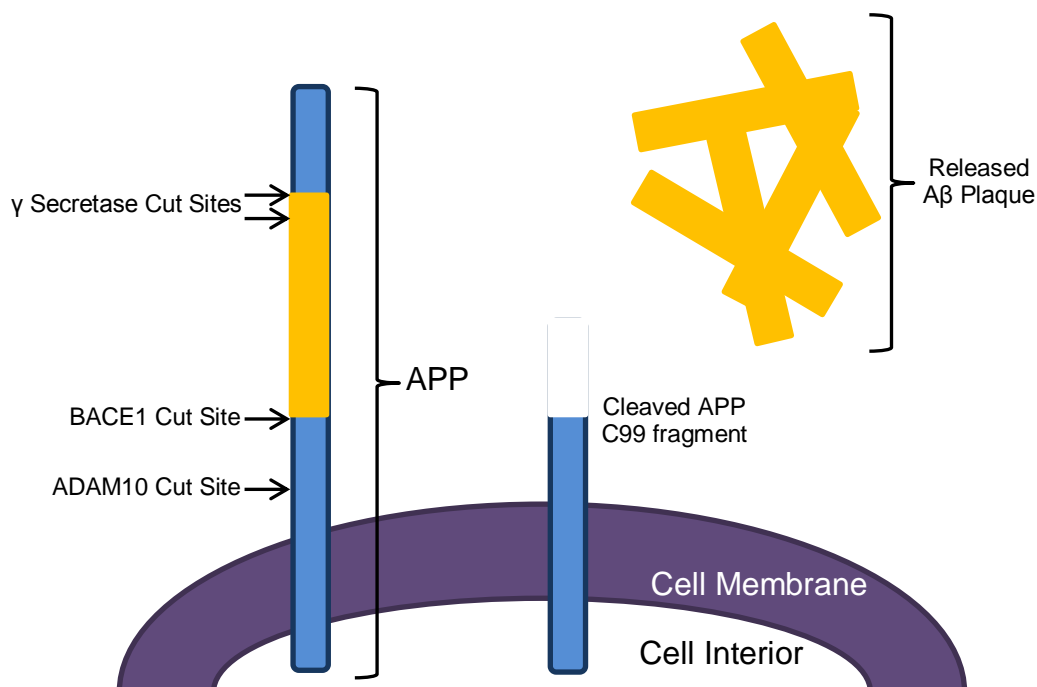


**Figure 1.22. The cleavage of APP.** It takes the combined action of BACE1 and  $\gamma$  secretase to release the  $A\beta$  peptide which then aggregates and forms the pathogenic plaques.

The imprecision of the  $\gamma$  secretase enzyme is responsible for the variation in  $A\beta$  peptide length between 39-43 amino acids (Figure 1.22.) (Hardy, 1997). The  $\gamma$  secretase complex contains the proteins: nicastrin, 'anterior pharynx-defective 1' (APH1), the two presenilin proteins and presenilin enhancer 2 (PEN2) (Kaether *et al.*, 2006). The presenilins PS1 (PSEN1) and PS2 (PSEN2) were implicated in AD when it was discovered that mutations in their encoding genes were a significant risk factor (Sherrington *et al.*, 1995). The mutant presenilin proteins increase the amount of the more pathogenic 42 amino acid form of the  $A\beta$  peptide relative to the 39, 40 and 41 amino acid forms without affecting the total amount of  $A\beta$  produced (Citron *et al.*, 1997).

The proteins clusterin (Clu) and complement receptor 1 (CR1) were first identified as potentially involved in Alzheimer's disease by a Genome-Wide Association Study (GWAS) that screened almost 4000 sufferers and 4000 control individuals from Belgium, Finland, Italy and Spain (Lambert *et al.*, 2009). High levels of Clu in the blood correlated with increased disease severity but did not act as a predictor for AD (Schrijvers *et al.*, 2011). It was suggested that Clu may act as a molecular chaperone for  $A\beta$ , allowing it to form more efficiently (Thambisetty *et al.*, 2010). The GWAS mutant search identified CR1 as implicated in AD possibly

due to its function as part of the immune system, with it potentially having a role in the immunological clearance of aggregated A $\beta$  (Lambert *et al.*, 2009).

Like APP, the 'microtubule associated protein tau' (MAPT) also acts as a precursor for a protein aggregate that causes damage as part of Alzheimer's disease (Tolnay and Probst, 1999). The normal function of MAPT is to stabilise microtubules, particularly those belonging to cells of the nervous system (Goedert *et al.*, 1988). In AD, MAPT becomes hyperphosphorylated by a largely unknown mechanism, causing it to leave the microtubules which degrade in its absence (Hampel *et al.*, 2010). It is believed that over-activity of glycogen synthase kinase 3 (GSK3) may be partially responsible for this hyperphosphorylation (Hooper *et al.*, 2008). A $\beta$  directly stimulates the hyperphosphorylation and therefore release of MAPT (Busciglio *et al.*, 1995). Free MAPT is insoluble and aggregates together to form structures called 'tau tangles' (Hampel *et al.*, 2010).

Oxidative stress in the tissues of the brain, which increases with age, causes an increase in the production of amyloid plaques and tau tangles (Christen, 2000). The increased concentration of these aggregates stimulates further oxidative stress (Christen, 2000; Markesbery, 1997). This stress causes severe damage to neuronal protein and fats and mitochondrial DNA (Hensley *et al.*, 1995; Mecocci *et al.*, 1994; Palmer and Burns, 1994). Superoxide dismutase 1 (SOD1) is frequently found associated with amyloid plaques and tau tangles (Pappolla, 1992). SOD1 forms part of the cellular defence against oxidative stress by converting the superoxide radical to molecular oxygen and hydrogen peroxide (Pappolla *et al.*, 1992). One mechanism by which amyloid plaques perpetuate oxidative stress is by blocking the activity of SOD1 (Yoon *et al.*, 2009). Another antioxidative process involves the expression of the protein thioredoxin (TXN), which is oxidised in preference to other cellular components (e.g. mitochondrial DNA), then subsequently reduced by the enzyme thioredoxin reductase (Wollman *et al.*, 1988). The thioredoxin pathway is particularly important in AD as it is impaired in the neuronal tissues of sufferers of the disease (Lovell *et al.*, 2000).

Studies into the brains of sufferers of Alzheimer's disease taken from biopsy and autopsy revealed that the neurotransmitter acetylcholine consistently depleted compared to control samples (Davies and Verth, 1977; Muir, 1997).

The cholinergic deficit in Alzheimer's disease is consistent with the fact that GSK3 reduces acetylcholine synthesis (Hooper *et al.*, 2008; Hooper *et al.*, 2007). This reduction in acetylcholine may be responsible for a number of the symptoms of Alzheimer's disease as acetylcholine has a definite role in the consolidation of new memory (Hasselmo, 2006).

As part of normal neurotransmission, acetylcholine is broken down by acetylcholinesterase (AChE) (Muir, 1997). In order to maintain levels of acetylcholine in the brains of Alzheimer's sufferers, acetylcholinesterase is pharmaceutically inhibited in the treatment of the disease (see next section).

### 1.3.3. Treatments

Unsurprisingly, given that little is known and less still agreed upon regarding the causes and progression of AD, at present there is no cure and few chemotherapeutic treatments that are beneficial. There are currently three main drugs licensed for the treatment of AD in the UK. All of these inhibit the action of acetylcholinesterase (AChE) which normally catalyses the degradation of the neurotransmitter acetylcholine (Shen *et al.*, 2002). Inhibition of this degradation is intended to slow mental decay as the disease progresses but the effectiveness of drugs that act in this way is disappointing with a slight improvement observed in only half of the patients treated with them (Website Reference 5.).

Many of the therapies currently in development focus on reducing the production of the amyloid plaques and the tau tangles or else on reducing oxidative stress (Godemann *et al.*, 2009; Mancuso *et al.*, 2007; Su *et al.*, 2003).

### 1.3.4. Translational control in Alzheimer's disease via 5' UTRs

The 5' UTR of the mRNA encoding APP contains an iron response element (IRE) that causes its upregulation in response to increased concentrations of cellular iron (Rogers *et al.*, 1999b; Rogers *et al.*, 2002b). The function of this response is unknown but it is consistent with the fact that free iron in the brain increases with age and that iron is particularly concentrated in the brains of AD sufferers (Bartzokis *et al.*, 1997; Lovell *et al.*, 1998; Smith *et al.*, 1998). The *APP* 5' UTR also contains an internal ribosome entry site (IRES) (Beaudoin *et al.*, 2008). Like the IRE, the reason for the presence of the IRES cannot be currently explained (Beaudoin *et al.*, 2008). The IRES contributes to the severity of the pathology by upregulating the expression of APP in response to the ischemic conditions often associated with Alzheimer's disease (Kalaria, 2000).

The 5' UTR of the mRNA encoding BACE1 is important in the translational control of its expression, one of the functions of the highly structured 461 nucleotide sequence is to suppress the translation of the protein (Lammich *et al.*, 2004). The inhibitory effect of the *BACE1* 5' UTR is enhanced by the presence of four upstream open reading frames (uORFs) (Mihailovich *et al.*, 2007; Zhou and Song, 2006). There is currently debate as to the relative importance of the uORFs

verses the secondary structure of the *BACE1* 5' UTR in its suppressive function, with different studies arriving at different conclusions (Mihailovich *et al.*, 2007). The majority of the data support the idea that the uORFs are more inhibitory than the structure, with the second AUG being particularly inhibitory (Mihailovich *et al.*, 2007). It is unclear how the ribosome ultimately bypasses the uORFs in this context, whether it is by reinitiation or leaky scanning (De Pietri Tonelli *et al.*, 2004). Stresses such as hypoxia (e.g. caused by ischemia following a stroke) or viral infections that cause eIF2 $\alpha$  phosphorylation increase the relative translation rate of *BACE1* as repression of eIF2 $\alpha$  weakens the inhibitory ability of the uORFs (Ill-Raga *et al.*, 2011; Sun *et al.*, 2006). The *BACE1* 5' UTR was also found to be able to undergo alternative splicing under certain conditions with the removal of three of the four uORFs (De Pietri Tonelli *et al.*, 2004). Like the majority of the sequence, the uORFs in the *BACE1* 5' UTR are highly conserved across species (Figure 1.23.). The importance of translational control in the expression of *BACE1* is consistent with the finding that it is often upregulated in AD without an increase in its mRNA level (Marcinkiewicz and Seidah, 2000; Preece *et al.*, 2003).

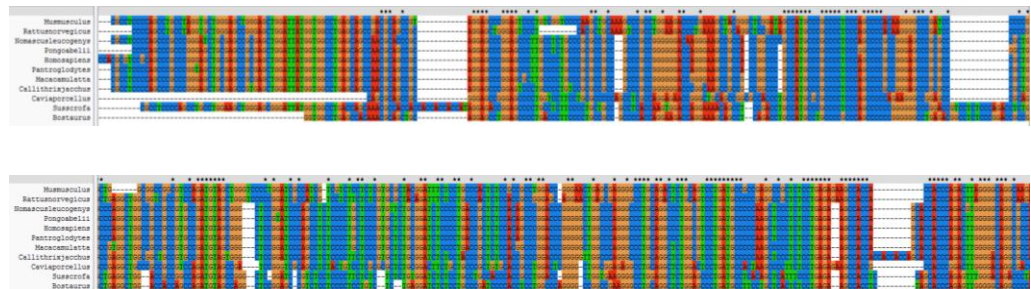


**Figure 1.23. The *BACE1* 5' UTR from 11 different species was aligned using ClustalX 2.1. Canonical bases are indicated by asterisks. The top panel shows the 5' region of the sequences and the bottom panel shown the 3' region.**

The 5' UTR of the mRNA encoding *ADAM10* is similar to the *BACE1* 5' UTR in terms of length, GC content and predicted free energy (Table 3.) but not in terms of sequence (Lammich *et al.*, 2010; Lammich *et al.*, 2004). Also like the *BACE1* sequence, the *ADAM10* 5' UTR represses the expression of the downstream open reading frame (Lammich *et al.*, 2010). The highly structured 5' section and the two uORFs are important in this function (Lammich *et al.*, 2010). For *BACE1* and *ADAM10*, removal of their 5' UTRs results in significant increases in their expression levels *in vivo*, and inclusion of the sequences into luciferase reporter constructs significantly decreases the level of reporter activity observed (Lammich *et al.*, 2010; Lammich *et al.*, 2004). In contrast to *BACE1*, the suppressive nature

of the *ADAM10* 5' UTR was mostly attributed to its predicted secondary structure and less to its uORFs, which are in unfavourable contexts (Lammich *et al.*, 2010). The uORFs of *ADAM10* are highly conserved but unlike those belonging to *BACE1* which are all conserved, one is unique to humans among the species referenced (Figure 1.24).

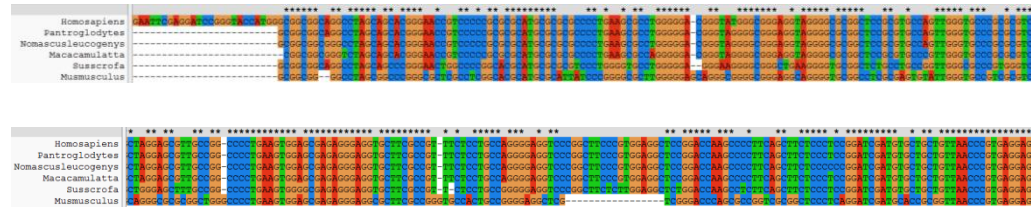


**Figure 1.24. The ADAM10 5' UTR from 11 different species was aligned using ClustalX 2.1. Canonical bases are indicated by asterisks. The top panel shows the 5' region of the sequences and the bottom panel shown the 3' region.**

Name	Length (nucleotides)	GC Content (%)	Predicted Free Energy (kcal/mol)	Predicted Consequence if Overexpressed	uORF(s)	IRES(s)
<i>APP</i>	194	76	-101.10	Harmful	0	1
<i>BACE1</i>	461	76	-226.70	Harmful	4	0
<i>ADAM10</i>	444	68	-215.90	Beneficial	3	0
<i>PS1</i>	284	56	-99.60	Harmful	0	0
<i>PS2</i>	427	57	-157.50	Harmful	0	0
<i>Clu2</i>	305	59	-128.60	?	0	0
<i>CR1</i>	140	50	-35.10	?	0	0
<i>MAPT</i>	320	74	-132.50	Harmful	0	1
<i>SOD1</i>	148	64	-58.70	Beneficial	0	0
<i>TXN</i>	80	54	-24.50	Beneficial	0	0
<i>AChE</i>	139	81	-78.50	Harmful	0	0

**Table 3. Details of the 5' UTRs of the AD-associated genes studied as part of this project**

### **1.3.5. Aims of the Alzheimer's disease section of this project**

The aim of this section is to investigate further the translational control of a number of the genes involved in Alzheimer's disease. The 5' UTRs of a selection of such genes were cloned into luciferase reporter plasmids (Table 3.). This collection of reporters was used to estimate the inhibitory or stimulatory nature of the sequences on the expression of the downstream reporter gene. The eIF4A requirement of each of the 5' UTRs was determined by treating cells transfected with the reporter plasmids with hippuristanol.

# Part 4.

## Oncogenes

### 1.4.1. Background

Cancer results from abnormal or uncontrolled cellular proliferation (Reviewed in: (Hanahan and Weinberg, 2011)). A mutation arising in one or more of a specific cohort of genes may trigger this process. These genes are termed proto-oncogenes in their pre-mutated state and simply oncogenes post-mutation. Another mechanism by which a proto-oncogene may become oncogenic is by its overexpression. The fact that there are a number of proto-oncogenes means that there are a number of different pathways by which a cancer may arise.

### 1.4.2. Causes of Cancer

Once a cancer has developed, more often than not, the original cause of the mutation(s) that led to its establishment will never be discovered. There are several known factors capable of causing neoplastic mutations, including environmental risk factors that increase the probability of such a mutation occurring (Lichtenstein *et al.*, 2000).

It is possible that an error may occur in the cell cycle. For example, during mitosis, translocation of portions of chromosomes may occur (Hartwell and Kastan, 1994). A t(11;14)(q13;q32) translocation event causes part of the enhancer region of IgH to become adjacent to the gene encoding cyclin D1, a protein involved in the progression of the cell cycle (Chesi *et al.*, 1996; Gabrea *et al.*, 1999). This drives higher levels of cyclin D1 expression than normal which results in mantle-cell lymphoma or multiple myeloma (Chesi *et al.*, 1996; Gabrea *et al.*, 1999).

Part of the reason why 'mistakes' only occur relatively infrequently is the presence of 'proof reading' and checking mechanisms that serve to increase the fidelity of DNA replication, repair genetic faults and initiate the programmed death of the cell if the damage is deemed irreversible (Enoch and Norbury, 1995).

p53 (TP53) upregulates the expression of p21 which binds and inactivates cyclin-dependent kinase 2 (CDK2) (J. et al., 1993). CDK2 is involved in the progression of the cell cycle from G<sub>1</sub> to S phase (Levkau et al., 1998).

Genetic susceptibility is a strong contributing factor in some types of cancer, for example Li-Fraumeni syndrome is the name given to the predisposition towards a range of cancers caused by a familial mutation in the gene encoding p53 (Li and Fraumeni, 1969; Malkin, 2011).

The example of Li-Fraumeni syndrome also highlights the importance of tumour suppressors (of which p53 is a well-studied example). On average, p53 is believed to be mutated in half of all human cancers (Hollstein et al., 1991).

Radiation is another risk factor for cancer, the most commonly experienced example of radiation is ultraviolet (UV) light, a component of sunlight that has a wavelength between 295 and 400 nm (English *et al.*, 1997). UV exposure causes damage to the chromosomal DNA of skin cells by inducing the formation of cyclobutyl pyrimidine dimers (Roza *et al.*, 1991). Although there are mechanisms designed to repair these lesions, namely photoreactivation or enzymatic excision, these do not prevent all the mutations from causing eventual harm (Yarosh *et al.*, 1992).

Diet and physical activity contribute to a person's risk of developing cancer in a number of different ways, for example excessive ethanol consumption in alcoholic drinks increases the concentration of its carcinogenic breakdown product acetaldehyde in the liver (Homann *et al.*, 2006; Lambert and He, 1988). The link between obesity and cancer has been thoroughly established although the underlying biology of this relationship remains unclear (Pischon *et al.*, 2008).

Whilst cancer is not generally transmissible horizontally in humans (there is evidence that certain animal tumours are however (Bostanci, 2005)), situations in which an infection causes cancer may make its epidemiological profile resemble that of a transmissible disease (Perz *et al.*, 2006). It may be argued that cancer may be transmitted horizontally between humans by organ transplantation (Buell et al., 2001). An example of a potentially carcinogenic infectious agent is Human Papillomavirus (HPV) which can cause cancer of the cervix (Munoz *et al.*, 1992). Similar to other viruses, persistent HPV infection (usually >10 years) results in inflammation which involves a high rate of cell division, thereby increasing the chances of an oncogenic mutation occurring (Ohshima and Bartsch, 1994). Inflammation is frequently associated with increased oxidative stress within the affected tissue, this is characterised by the formation of reactive oxygen species (ROS) which interfere with enzyme function and gene expression and also cause

damage to proteins, membranes and DNA, potentially inducing mutations (Ohshima and Bartsch, 1994). In addition to causing inflammation, HPV directs the synthesis of proteins E6 and E7 which inactivate the tumour suppressors p53 and pRb (Retinoblastoma protein) respectively (Thomas et al., 1996). This may benefit the virus by suppressing the ability of its host cell to undergo apoptosis (Munger et al., 1992).

Like p53, pRb stalls the cell cycle at G<sub>1</sub> phase before it can progress to S phase (Reviewed in: (Munro et al., 2012)). pRb inactivates transcription factors belonging to the E2F family, the targets of which are involved in inducing the cell to leave the G<sub>1</sub> phase of the cell cycle and enter S phase (Reviewed in: (Munro et al., 2012)). If pRb function was lost by mutation rather than by viral-protease degradation, it was shown that both alleles of pRb have to be mutated (Knudson, 1971). This paradigm represents an interesting distinction between oncogenes and tumour suppressors; oncogenes are frequently activated by mutations occurring in a single allele (i.e. a dominant) whereas tumour suppressors generally need to be defective at both alleles (i.e. recessive) (Reviewed in: (Berger et al., 2011)). This is because the amount of protein expressed as a result of the wild-type allele is sufficient to perform the function of the diploid amount of protein (Reviewed in: (Berger et al., 2011)). Haploinsufficiency does occur in some cases however, for example the level of the tumour suppressor *PTCH* resulting from a single functional allele is not enough to prevent the formation of medulloblastoma in mice (Zurawel et al., 2000).

The precise mechanisms by which the immune system contributes to cancer prophylaxis are yet to be determined (de Visser *et al.*, 2006). However, the fact that HIV infection increases the risk of many different cancers developing is consistent with the immune system being an important line of defence against cancer (Reiche *et al.*, 2004). While very common cancers among HIV carriers such as Kaposi's sarcoma and cervical cancer are most commonly of viral origin (a strain of herpesvirus and HPV respectively for the examples here); non-viral cancers are also more prevalent, for example lung cancer is 2.5 to 7.5 times more frequent (Bower *et al.*, 2003).

#### **1.4.3. The mechanisms by which cancer causes harm**

Regardless of its conception, if the cellular proliferation is allowed to progress unchecked, a tumour may develop (Hanahan and Weinberg, 2011). Cancer is not always associated with the presence of a solid tumour, for example leukaemia

consists of neoplastic white blood cells spread throughout the blood (Teitell and Pandolfi, 2009).

Tumours may be either benign or malignant. A benign tumour is one which does not have the potential to metastasise (Kwee et al., 1982; Russell, 1940). Metastasis is the budding of the primary tumour and the spread of single or groups of cells around the body (Liotta et al., 1991; Prall, 2007). Benign tumours can also be harmful, for example, a uterine fibroid can interrupt reproductive system function and cause pelvic pressure or pain (Stewart, 2001).

Whether benign or malignant, a tumour may cause harm by its 'mass effect'; this is the physical influence of the tumour's presence on nearby organs and tissues, for example, compression of blood vessels causing ischemia (Duncan *et al.*, 2005).

A cancer becomes more harmful if it metastasises, Such satellite cells can be transported by the circulatory or lymphatic system and each has the potential to form a new tumour (Bostick *et al.*, 1998). If metastatic secondary tumours form in the liver, their bulk can cause the severe disruption of hepatic function which may lead to death (Andreas *et al.*, 2005). Frequently, the only treatment for this consequence is a liver transplant which is not often deemed appropriate as there is a strong chance that the new liver may be also populated by secondary tumours (Andreas *et al.*, 2005).

It is possible for neoplastic cells to permeate the blood-brain barrier, so primary tumours derived in any part of the body may spread to the brain and vice-versa (Deeken and Löscher, 2007). The spread of tumours from the brain to the body is only rarely documented (Sanerkin, 1962). Perhaps contrary to expectations, it was found that clumps of neoplastic cells were able to pass through the barrier more readily than individual cells; possibly because these clumps cause damage to the barrier (Zhang et al., 1992).

Once in the brain, the mass effect can easily prove fatal as there is only a finite space for the tumour to grow within the skull (Behin *et al.*, 2003).

#### **1.4.4. Treatments for Cancer**

There are currently four categories of intervention used in the management of cancer, these are: radiotherapy, surgery, chemotherapy and biological therapy (Edwards *et al.*, 2005). Chemotherapy is further divided by the mechanism of action of the chemotherapeutic agent; traditional drugs may be broadly divided into either: anthracyclines antimetabolites, alkaloid-derived compounds, topoisomerase inhibitors or alkylating agents (DeVita and Chu, 2008). All of these primarily work by damaging actively growing cells, for example; alkylating agents

(e.g. treosulfan, topotecan and melphalan) work by crosslinking guanine nucleobases thereby making DNA unable to separate and therefore unable to replicate (Meier *et al.*, 2009). The non-specificity of alkylating agents represents a serious limitation to their use, the fact that they target any dividing cell means that the immune system, hair follicles, the gastrointestinal tract, the skin and elements of the reproductive system are severely compromised (Batchelor, 2001; Hall *et al.*, 1991; Jain *et al.*, 2011; Rezvanfar *et al.*, 2008).

Unlike the majority of cancer-chemotherapeutics which target the cell cycle, usually by damaging the cell's DNA in some way, vincristine (a vinca alkaloid) binds to tubulin, rendering it unable to act as a component of the cytoskeleton which eventually causes the death of the cell (Lobert *et al.*, 1996). Despite this differing mechanism, vinca alkaloids are also associated with debilitating side effects including: seizures, orthostatic hypotension, secretion of antidiuretic hormone and exacerbation of pre-existing neurological disease (Rosenthal and Kaufman, 1974).

Biological therapies target cancer cells specifically by interfering with molecules involved in carcinogenesis (Reviewed in: (Sawyers, 2004)). Biological therapy may be in the form of an antibody against a specific oncoprotein or a small molecule. Cetuximab is an example of an antibody that is used to treat cancer (Baselga, 2001; Pahl *et al.*, 2012). It works by binding the extracellular domain of EGFR (epidermal growth factor receptor) thereby blocking its activation (Baselga, 2001). Some cancer cells express higher levels of EGFR than non-cancerous cells; this contributes to their abnormal proliferative capacity (Bigner *et al.*, 1990; Ekstrand *et al.*, 1991; Humphrey *et al.*, 1990; Schlegel *et al.*, 1994; Schwechheimer *et al.*, 1995; Wikstrand *et al.*, 1998; Yamazaki *et al.*, 1990). Attenuation of EGFR signalling in this way therefore has a more inhibitory effect on the growth of some cancer cells than normal cells (Tsuchihashi *et al.*, 2005).

The drug Imatinib represents a new class of targeted therapy; it acts by inhibiting the activity of ABL1 (Abelson murine leukaemia viral oncogene homolog 1) (van Oosterom *et al.*, 2001). The normal function of this tyrosine kinase is to induce cell differentiation, division and adhesion in response to Cyclin dependent kinase 1 signalling (Bueno *et al.*, 2008). A translocation mutation event between chromosomes 9 and 22 leads to the creation of the 'Philadelphia Chromosome' which encodes a mutant version of *ABL1* which is constitutively activated and therefore induces excessive cell division (Kurzrock *et al.*, 2003). This increased proliferation leads to chronic myelogenous leukaemia (CML), a cancer of the blood originating in the myeloid cells of the bone marrow (Druker, 2008).

Imatinib binds competitively to the active (TK) site of ABL1 thereby reducing its ability to phosphorylate its targets (one of which is 'growth factor receptor-bound protein 2') (Warmuth *et al.*, 1997). The introduction of this drug in 2001 turned CML from a terminal disease into a true chronic condition. Before 2000, the seven year survival rate of patients with CML was less than 50%, it is now nearly 90% (Website Reference 6.).

#### 1.4.5. eIF4A and cancer

While there has been only a moderate amount of research specifically focusing on the role of eIF4A in cancer and its potential as a drug target, there is much in the literature to implicate it as an important factor in neoplasia (Silvera *et al.*, 2010). mRNAs with long or highly-structured 5' UTRs are not as readily translated as those with short or unstructured 5' UTRs (Kozak, 1980; Pickering and Willis, 2005). Genes involved in cancer often possess more inhibitory 5' UTRs (Kozak, 1987; Kozak, 1989; Pickering and Willis, 2005; Willis, 1999).

The importance of the 5' UTR in the regulation of the expression of genes involved in cancer is exemplified by *BRCA1* (breast cancer type 1 susceptibility protein). *BRCA1* is a tumour suppressor (Bishop, 1999). A mutation in the 5' UTR of *BRCA1* that often occurs in breast cancers changes the context of the start codon putting it in a weaker Kozak consensus (Signori et al., 2001). This causes the downregulation of the expression of *BRCA1* which results in the cancer becoming resistant to apoptosis (Signori et al., 2001).

It is reasonable to assume that oncogenes and hence cancer will have a higher dependency on eIF4A than non-cancerous cells since it is known that the requirement for eIF4A in translation is in direct proportion to the extent of mRNA 5' secondary structure (Svitkin *et al.*, 2001).

Although this paradigm is often discussed in the literature, there has been little statistical and structural analysis into the relationship between gene function (e.g. oncogene, housekeeping gene etc.) and 5' UTR length and structure. Less still is known about the role of eIF4A in the expression of tumour suppressor genes. As outlined in the Cancer section, a mutation that deactivates a tumour suppressor is more likely to occur than a mutation that activates an oncogene (Reviewed in: (Hanahan and Weinberg, 2011)). If the expression of tumour suppressor genes is reduced by inhibition of eIF4A then this may mean that targeting of eIF4A could promoter rather than inhibit neoplasia.

In order to briefly address this idea as part of this project, a table of the properties of the 5' UTRs of a selection of housekeeping genes, oncogenes and tumour

suppressor genes was compiled (Table 4.). The housekeeping genes chosen were the control genes for this project (*β actin*, *β tubulin* and *GAPDH*). The oncogenes and tumour suppressor genes are those used as examples in (Hanahan and Weinberg, 2000). This review article covers the main hallmarks of cancer; the genes it references are therefore representative of cancer as a whole.

Name	Length (nucleotides)	GC Content (%)	Predicted Free Energy (kcal/mol)
<i>β Actin</i>	84	74	-15.5
<i>β Tubulin</i>	127	47	-30.1
<i>GAPDH</i>	102	61	-21.9
<i>PDGF</i>	990	71	-485.7
<i>TGFα</i>	249	74	-134.0
<i>EGFR</i>	246	78	-107.5
<i>Her2/neu</i>	239	71	-103.5
<i>E2F</i>	140	79	-81.8
<i>c-myc</i>	526	66	-234.2
<i>CDK4</i>	293	70	-146.1
<i>Max</i>	171	64	-52.8
<i>IGF1</i>	220	37	-38.9
<i>IGF2</i>	753	68	-235.7
<i>IGF1R</i>	1558	71	-860.9
<i>IL3</i>	53	58	-4.9
<i>IL3R</i>	350	56	-133.4
<i>Bcl-2</i>	494	44	-134.1
<i>Telomerase</i>	59	79	-23.6
<i>VEGFA</i>	491	57	-193.3
<i>FGF1</i>	167	57	-58.8
<i>FGF2</i>	69	75	-23.0
<i>VEGFR</i>	286	79	-148.4
<i>ODC1</i>	334	66	-157.50
<i>pRb</i>	167	69	-81.0
<i>p107</i>	80	73	-38.8
<i>p130</i>	119	78	-62.4
<i>TGFβ</i>	883	72	-407.1
<i>p15<sup>INK4B</sup></i>	261	67	-156.3
<i>p21</i>	126	66	-51.4
<i>Smad4</i>	539	66	-257.7
<i>FAS</i>	158	54	-46.6
<i>FASR</i>	347	63	-140.1
<i>TNFα</i>	170	59	-39.9
<i>TNFαR</i>	304	59	-96.7
<i>p53</i>	203	59	-86.0
<i>Bax</i>	70	86	-35.3
<i>CASP8</i>	236	52	-70.4
<i>CASP9</i>	246	76	-123.9
<i>pTEN</i>	1032	72	-562.2
<i>p16<sup>INK4A</sup></i>	307	69	-149.0
<i>Thrombospondin 1</i>	183	62	-52.1
<i>VHL</i>	214	72	-99.7
<i>E-cadherin</i>	125	72	-46.8

**Table 4. Details of the 5' UTRs of a selection of housekeeping, oncogenes and tumour suppressor genes**

	Average Length	S.D.	Average Predicted Free Energy	S.D.	Median Length	Median Predicted Free Energy
Housekeeping	104.3	7.3	-22.5	21.6	102	-21.9
Onco-	408.1	369.8	-179.3	196.9	286.0	-134.0
Tumour Suppressor	257.2	217.2	-115.6	121.6	203.0	-81.0

**Table 5. Summary of the data presented in Table 4.**

It is apparent from Table 4 and Table 5 that oncogenes tend to possess longer and more highly structured 5' UTRs than tumour suppressor and housekeeping genes and that tumour suppressor gene 5' UTRs are longer and more structured than those belonging to housekeeping genes. It must be acknowledged that this is a very small sample size, considering that the total number of oncogenes is believed to be well over 200 (Chandek and Mooi, 2010). Although the sample size limits the confidence with which conclusions may be made based on these data, they suggest that eIF4A inhibition would decrease the expression of oncogenes to a greater extent than it would tumour suppressor genes and housekeeping genes.

As with eIF4A, it is accepted that inhibition of eIF4E results in the selective suppression of mRNAs with long, highly structured 5' UTRs compared to those with short, unstructured 5' UTRs, a phenomenon once referred to as mRNA discrimination (Graff *et al.*, 2008). eIF4E has been strongly implicated in contributing to the pathology of a number of cancers. It was found that overexpression of eIF4E could induce neoplasia (Graff *et al.*, 2008; Lazaris-Karatzas *et al.*, 1990). Phosphorylation of the 4E-BPs in cancers is often associated with poor patient survival rates (O'Reilly *et al.*, 2009).

Suppression of cancer growth by eIF4E inhibition is achieved without apparent toxicity (Graff *et al.*, 2007). The eIF4E inhibitor ribavirin is currently at the phase I / II stage of clinical trials in the USA for treatment of advanced breast cancer (Pettersson *et al.*, 2011).

Initially, eIF4E seems a better choice of drug target in the treatment of cancer than eIF4A as eIF4E is rate limiting in translation initiation whereas eIF4A is the most abundant translation initiation factor in terms of number of molecules per cell (Lin *et al.*, 2008). However, there is evidence to support the idea that eIF4A suppression could be at least as effective as eIF4E suppression.

The level of mRNA encoding eIF4AI is elevated in primary human hepatocellular carcinoma tissues, along with that of eIF4E (Shuda *et al.*, 2000). Another study

showed that the eIF4AI mRNA was on average 5.6 times more abundant in a panel of melanoma cell lines compared to normal human melanocytes (Eberle *et al.*, 1997). Unlike the hepatocellular carcinoma study, the study into melanoma did not find any increase in the eIF4E (or eIF4AII, eIF4B or eIF4G) mRNAs (Eberle *et al.*, 1997). A further advantage of targeting eIF4A rather than eIF4E is the fact that the expression of many oncogenes is IRES-mediated (review: (Silvera *et al.*, 2010)). In cap-independent translation initiation, eIF4E (which binds the 5' cap) is bypassed, whereas many IRESs have high eIF4A requirements (Bordeleau *et al.*, 2006; Jackson, 1988). This means that eIF4A could be more relied-upon by oncogenes for their expression than eIF4E.

In the paper describing the discovery of silvestrol, it was shown that eIF4A suppression in mice suffering from E $\mu$ -Myc lymphoma was able to render the cancer susceptible to doxorubicin chemotherapy (Bordeleau *et al.*, 2008b). The mice in this study were closely monitored for any potential side effects of the eIF4A inhibition. Eight days of daily injections of silvestrol did not cause the mice to lose weight or exhibit detectible levels of impaired liver function or immunosuppression (Bordeleau *et al.*, 2008b).

In a subsequent study by the same group, it was found that silvestrol treatment could not only sensitise cancers to chemotherapy but also dramatically suppress the growth of both lung and pancreatic cancer xenografts in mice (Cencic *et al.*, 2009). The major difference between these two studies was the type of cancer treated; the first study (Bordeleau *et al.*, 2008a) investigated lymphoma whereas the second (Cencic *et al.*, 2009) focused on a solid tumour lung cancer xenograft model. The increased susceptibility of the solid tumour to eIF4A suppression was attributed to the increased reliance of tumours of this type on angiogenesis (Cencic *et al.*, 2009). Human umbilical vein endothelial cells exposed to silvestrol and pro-angiogenic stimuli simultaneously did not undergo angiogenesis (Cencic *et al.*, 2009). The fact that eIF4A inhibitors suppress angiogenesis is consistent with the fact that many of the genes involved in these pathways are translationally controlled e.g. *VEGF* and *FGF-2* (Cencic *et al.*, 2009).

The fact that PDCD4 is a negative regulator of eIF4A function is consistent with the involvement of eIF4A in cancer (Yang *et al.*, 2003). As outlined in the PDCD4 section (page 42), PDCD4 is upregulated during apoptosis and it has been demonstrated that elevated levels of the protein can suppress the growth of cancer cells (Shibahara *et al.*, 1995).

#### 1.4.6. Control genes for this project: *β actin*, *β tubulin* and *GAPDH*

$\beta$  actin (ACTB) is an important cytoskeletal protein, involved in cell structure and motility (Reviewed in: (Engqvist-Goldstein and Drubin, 2003)).  $\beta$  tubulin (TUBB) forms part of the microtubules which are important in both cell structure and intracellular transport (Reviewed in: (Dutcher, 2001)). Glyceraldehyde 3-phosphate dehydrogenase (GAPDH) is involved in glycolysis, aiding in the production of ATP (Reviewed in: (Barber et al., 2005)).  $\beta$  actin,  $\beta$  tubulin and GAPDH all are often used as loading controls e.g. in western blotting (Stürzenbaum and Kille, 2001). Given the frequency of the use of these genes in this capacity, a number of studies have investigated the possible problems of treating them as simply 'housekeeping' genes. These studies generally support the accepted idea that these genes can be used as relevant controls, particularly when all three are used in combination as they are in this project (Bauer *et al.*, 2009; Ferguson *et al.*, 2005). The 5' UTR sequences of each of these genes (Table 6.) were cloned into reporter vectors as part of this project.

#### 1.4.7. Ornithine Decarboxylase 1 (ODC1)

ODC1 is the rate limiting enzyme in the generation of polyamines (Russell and Snyder, 1968). It is overexpressed in certain human cancers, particularly oesophageal (Yoshida *et al.*, 1992). Polyamines have been implicated as agonists in a large number of pathways that contribute to cancer formation and perpetuation (Gerner and Meyskens, 2004). The 5' UTR of human *ODC1* (Table 6.) contains a uORF, a very stable hairpin structure and an IRES (Danner, 2002). The hairpin structure has been used out of context in a number of studies to investigate structured RNA sequences; it is sometimes referred to as the 'ODCHP' or 'hp1' (Bottley *et al.*, 2010). These studies thoroughly support the accepted idea that a structure such as this represents a significant obstacle to the translation of the downstream coding region and has a high requirement for the activity of eIF4A (Svitkin *et al.*, 2001).

The function of this hairpin is to repress the expression of ODC1 in conditions that are generally unfavourable (Mathews et al., 2007; Sergeevich Spirin, 1999). The uORF is believed to be present in order to contribute to the translational repression of the transcript, this effect is predicted to be minimal, however, as the uAUG is in an unfavourable context (Grens and Scheffler, 1990). Deletion of the uAUG was found to make little difference to the properties of the UTR (Grens and Scheffler, 1990). The *ODC1* uORF is highly conserved across species as is the hairpin sequence (Figure 1.25.).

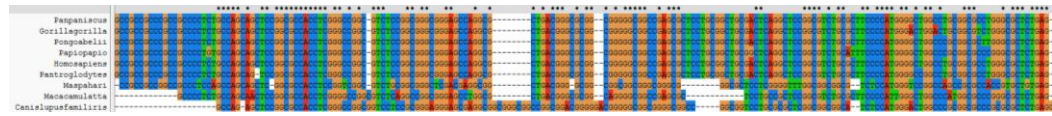


**Figure 1.25. The *ODC1* 5' UTR from nine different species was aligned using ClustalX 2.1. Canonical bases are indicated by asterisks. The top panel shows the 5' region of the sequences and the bottom panel shown the 3' region.**

The 5' UTR of *ODC1* was suspected to contain an IRES following the discovery that the *ODC1* protein was upregulated during the late G2 and mitosis phases of the cell cycle, phases which are typically associated with cap-dependent but not cap-independent translation inhibition (Bonneau and Sonenberg, 1987; Fredlund *et al.*, 1995; Huang and Schneider, 1991). Translation initiation of the mRNA encoding *ODC1* occurs in a cap-dependent manner during the G1 and S phases of the cell cycle, only progressing by cap-independent initiation during G2 and mitosis (Pyronnet *et al.*, 2000). This indicates that the *ODC1* IRES has weak activity since it is out-competed for the translation machinery by the cap which is followed shortly by the unfavourable stable hairpin (Pyronnet *et al.*, 2000). Since polyamines are involved in cellular proliferation and *ODC1* has a very short cellular half-life, it is unsurprising that it is beneficial for the cell to elevate the expression level of *ODC1* during mitosis (Pyronnet *et al.*, 2000; Tabor and Tabor, 1984).

#### 1.4.8. Epidermal Growth Factor Receptor (EGFR)

EGFR is a transmembrane glycoprotein tyrosine kinase (Reviewed in: (Roy S, 2004) and (Herbst, 2004)). Its function is to stimulate, primarily Akt-, MAPK- or JNK-mediated cellular proliferation in response to a range of ligands including transforming growth factor  $\alpha$  (TGF $\alpha$ ) and the family of epidermal growth factors (EGFs) (Oda *et al.*, 2005).

Overexpression of *EGFR* has been strongly linked to poor prognosis in head, neck, ovarian, cervical, bladder and oesophageal cancers and implicated in a large number of other cancers (Nicholson *et al.*, 2001). Mutations in *EGFR* are also important, particularly in instances of glioblastoma multiforme, with ~25% predicted to possess a constitutively active truncated version (EGFRvIII) (Wikstrand *et al.*, 1998). Although there is a strong relationship between the presence of this mutation and poor prognosis, it does not seem to be as significant as the overexpression of *EGFR*, with 40-50% of the glioblastomas assayed for the

presence of the vIII mutant displaying significantly elevated levels of the wild-type receptor (Bigner *et al.*, 1990; Ekstrand *et al.*, 1991; Humphrey *et al.*, 1990; Schlegel *et al.*, 1994; Schwechheimer *et al.*, 1995; Wikstrand *et al.*, 1998; Yamazaki *et al.*, 1990).

The primary mechanism by which *EGFR* is overexpressed is gene amplification, as demonstrated in colorectal, pulmonary, bile duct and soft tissue cancers (Dacic *et al.*, 2006; Dobashi *et al.*, 2004; Nakazawa *et al.*, 2005; Ooi *et al.*, 2004). In each of these instances however, amplification was not the only cause of the overexpression, with a discrepancy between gene dosage and EGFR expression (Kersting *et al.*, 2004). A percentage of this 'extra' overexpression may be attributable to mutations that cause the transcriptional upregulation of the EGFR gene (Chi *et al.*, 1992; Gebhardt *et al.*, 1999; Haley and Waterfield, 1991; Maekawa *et al.*, 1989). The transcription factor 'early growth response factor 1' (Egr-1 or 'EGR1') is responsible for upregulating the expression of *EGFR* in response to stress (Nishi *et al.*, 2002). The existence of this relationship partly explains why *EGFR* expression is upregulated in response to hypoxia (Appl and Klempnauer, 2002; Laderoute *et al.*, 1992; Nishi *et al.*, 2002; Swinson and O'Byrne, 2006).

There has been little research into the possible contribution of translational regulation to *EGFR* overexpression in cancer. One study, however, demonstrated that *EGFR* was upregulated in response to both hypoxia and the activation of hypoxia-inducible factor 2 $\alpha$  (HIF2 $\alpha$  or 'EPAS1') without observing either mutational events or changes in EGFR mRNA levels (Franovic *et al.*, 2007).

Cancer cells overexpressing *EGFR* in hypoxic conditions have a significant survival advantage and tend to be more resistant to chemotherapy (Clarke *et al.*, 2001; Swinson and O'Byrne, 2006; Warburton *et al.*, 2004; Yokoi and Fidler, 2004). This is due to the EGFR signalling via the phosphatidylinositol 3-kinase (PI3K) and MAPK pathways which are associated with cell survival, for example, activation of PI3K leads to the induction of VEGF which stimulates vascularisation (Clarke *et al.*, 2001).

#### **1.4.9. Vascular Endothelial Growth Factor A (VEGFA)**

The normal function of VEGFA is to stimulate angiogenesis as part of embryonic development, wound healing and reproductive functions (Folkman, 1990; Folkman and Klagsbrun, 1987; Plouët *et al.*, 1989). The expression of *VEGFA* is strongly induced by hypoxia which occurs in the tumour microenvironment (Plate *et al.*, 1992; Shweiki *et al.*, 1992). Part of this response was attributed to upregulation

by the transcription factor hypoxia-inducible factor 1 (HIF-1) and also by the hypoxia-induced stabilisation of the normally rapidly degraded VEGFA mRNA (Forsythe *et al.*, 1996; Levy *et al.*, 1996).

Translational control was implicated in the hypoxic stimulation of *VEGFA* expression when it was discovered that its 5' UTR was able to initiate translation in a cap-independent manner (Huez *et al.*, 1998). The very long (491 nucleotide) *VEGFA* 5' UTR contains two independent IRES elements (Huez *et al.*, 1998). It has been proposed that these two IRESs regulate the expression of two different splice variants of VEGFA (Bornes *et al.*, 2004). The *VEGFA* 5' UTR consists of 'IRES B' followed by a CUG initiation codon in frame of the coding region, followed by 'IRES A' (Bornes *et al.*, 2004). The upstream start codon, regulated by IRES B drives the expression of L-VEGF (for 'large' VEGF), a variant which possesses an extra 180 amino acids (Bornes *et al.*, 2004). The function of this larger version is not known, the extra amino acids are proteolytically cleaved off to leave the normal size VEGFA once the protein has been synthesised (Rosenbaum-Dekel *et al.*, 2005). The function of this pathway may be associated with the storage of VEGFA or with the rapid generation of the molecule in response to hypoxic stimuli (Storkebaum *et al.*, 2004).

In general, cells respond to hypoxia by decreasing protein synthesis rates (Pettersen *et al.*, 1986). One mechanism used to accomplish this in the short term, involves the phosphorylation of the translation initiation factor eIF2 $\alpha$  (Koritzinsky *et al.*, 2007). When hypo-phosphorylated, the function of eIF2 $\alpha$  is to assist in the binding of the initiator tRNA to the 40S ribosomal subunit by forming a ternary complex with guanosine triphosphate (GTP). Phosphorylation of eIF2 $\alpha$  inhibits this process, thereby acting as a brake on global translation rates (Koritzinsky *et al.*, 2006; Koumenis *et al.*, 2002).

Exposure to chronic hypoxia causes cells to adopt an additional mechanism of translational suppression (Koritzinsky *et al.*, 2006). The mammalian target of rapamycin (mTOR) becomes attenuated in response to hypoxia by multiple pathways that have yet to be fully described (Brugarolas *et al.*, 2004; Liu *et al.*, 2006; Schneider *et al.*, 2008). When active, mTOR is involved in a number of pathways associated with transcription, proliferation, cell growth and migration (Hay and Sonenberg, 2004). One of its functions is to phosphorylate eukaryotic initiation factor 4E-binding protein 1 (4E-BP1 or 'EIF4EBP1') (Beretta *et al.*, 1996; Brunn *et al.*, 1997; Gingras *et al.*, 2001). eIF4E is the component of the eIF4F complex responsible for recognising and binding the 5' cap of a mRNA in preparation for the formation of the pre-initiation complex (page 16) (Banerjee,

1980; Mathews et al., 2000). Under hypoxic conditions, the mTOR-mediated phosphorylation of 4E-BP1 decreases, thereby permitting it to bind eIF4E which leads to the suppression of cap-dependent translation initiation (Brugarolas *et al.*, 2004; Liu *et al.*, 2006; Schneider, 2008). Since IRES-mediated translation initiation does not involve the binding of the 5' cap, it is favoured under conditions that inhibit eIF4E function (Hellen and Sarnow, 2001; Prevot *et al.*, 2003; Stoneley and Willis, 2004).

**Overview of the 5' UTRs of the genes investigated as part of the oncogenes section of this project**

<b>Name</b>	<b>Length (nucleotides)</b>	<b>GC Content (%)</b>	<b>Predicted Free Energy (kcal/mol)</b>	<b>uORF(s)</b>	<b>IRES(s)</b>
<i><b>β Actin</b></i>	84	74	-15.50	0	0
<i><b>β Tubulin</b></i>	127	47	-30.10	0	0
<i><b>GAPDH</b></i>	102	61	-21.90	0	0
<i><b>ODC1</b></i>	334	66	-157.50	1	1
<i><b>EGFR</b></i>	246	78	-107.50	0	1*
<i><b>VEGFA</b></i>	491	57	-193.30	1	2

**Table 6. Details of the 5' UTRs of the oncogenes and housekeeping genes studied as part of this project.** \* data supporting the existence of an IRES in the *EGFR* 5' UTR are presented in this thesis.

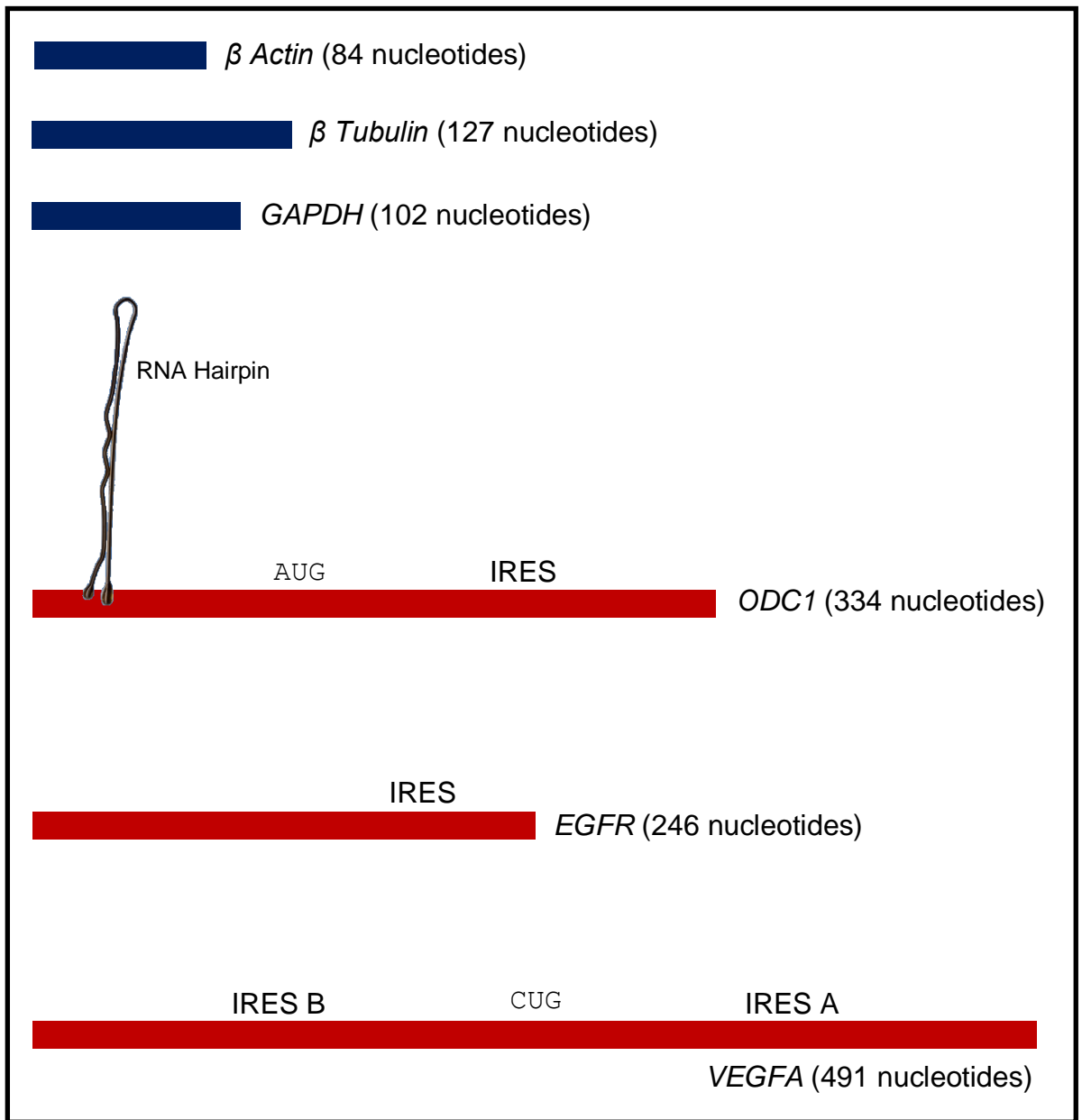


**Figure 1.26. The 5' UTRs of the genes investigated as part of the oncogenes section of this project.** The 5' UTRs of the control housekeeping genes are shown in blue and the 5' UTRs of the proto-oncogenes are shown in red. The sequences are shown to scale.

#### **1.4.10. Aims**

The aim of this section is to investigate further the translational control of a number of the genes involved in cancer. The 5' UTRs of the genes shown on the previous page were cloned into luciferase reporter plasmids. This collection of reporters was used to estimate the inhibitory or stimulatory nature of the sequences on the expression of the downstream reporter gene. The eIF4A requirement of each of the 5' UTRs was determined by treating cells transfected with the reporter plasmids with hippuristanol.

# Chapter 2. Materials and Methods

## 2.1. PCR and Primers

All polymerase chain reactions (PCRs) performed to generate sequences that would eventually be cloned used Phusion Hot Start High Fidelity DNA polymerase (Finnzyme, Cat # F-540S) together with its recommended buffer (20 mM Tris-HCl (pH 7.4 at 25°C), 0.1 mM EDTA, 1 mM DTT, 100 mM KCl, stabilizers and 200 µg/ml BSA) and dNTPs (200 µM). All PCR colony screens used Taq polymerase (Roche, Cat # 11146165001) and its buffer (100 mM Tris-HCl, 15 mM MgCl<sub>2</sub> and 500 mM KCl, pH 8.3 (20°C)). Template concentration was approximately 1 ng for plasmids and 100 ng for cDNA. Primer concentration was 0.5 µM. Components were added to the reaction vessel on ice in the order shown below (Table 7.).

Component	50 µl reaction	20 µl reaction	Final conc.
H <sub>2</sub> O	add to 50 µl	add to 20 µl	-
5x Phusion HF Buffer	10 µl	4 µl	1x
10 mM dNTPs	1 µl	0.4 µl	200 µM each
primer A	x µl	x µl	0.5 µM
primer B	x µl	x µl	0.5 µM
template DNA	x µl	x µl	-
(DMSO, optional)	(1.5 µl)	(0.6 µl)	(3 %)
Phusion DNA Polymerase	0.5 µl	0.2 µl	0.02 U/µl

**Table 7. The components of the PCR reaction, their concentrations and the order in which they were added to the reaction vessel. 20 µl reactions were used for colony screens and 50 µl reactions were used if the product was intended for cloning.**

The reaction vessels were put into a PCR machine (BIOER GenePro). This was programmed with the following parameters (Table 8.).

<b>Cycle Step</b>	<b>Temperature</b>	<b>Time(s)</b>	<b>Cycles</b>
<b>Initial Denaturation</b>	98°C	30	1
<b>Denaturation</b>	98°C	10	35
<b>Annealing</b>	X°C	30	
<b>Extension</b>	72°C	30	
<b>Final Extension</b>	72°C	600	1
<b>Hold</b>	4°C	Hold	1

**Table 8. The program that was run on the PCR machine. X = primer annealing temperature (see below).**

The primer annealing temperatures used were established using the online program ‘Oligo Calc’ (Kibbe, 2007) to determine the salt-adjusted melting temperatures ( $T_m$ ) of the forward and reverse primers for a single reaction, the temperature used was 5°C below the lowest value. Once the PCR machine programme had completed, the products were visualised using agarose gel electrophoresis (see 2.3. DNA agarose gel electrophoresis).

The sequences of the primers used in this project are shown on the following page (Table 9.).

<b>Primer Name</b>	<b>Sequence (5' - 3')</b>
<b>CMV <i>KpnI</i> F</b>	TTTGCGGTACCTCGCGATGTACGGG
<b>CMV <i>HindIII</i> R</b>	CTGGACTAGTGGATCCGAGC
<b>HP <i>HindIII</i> F</b>	GATTACAAAGCTTCTCGAGGGGCGAATACGAATTCGTCA
<b>HP <i>HindIII</i> R</b>	GATTACAAAGCTTTTAATTAAGGATCCGTCTTCCCGCCGCC
<b>HP <i>SpeI</i> F</b>	GATTACAAC TAGTCTCGAGGGGCGAATACGAATTCGTCA
<b>HP <i>NcoI</i> R</b>	GATTACACCATGGTTAATTAAGGATCCGTCTTCCCGCCGCC
<b>eIF4AI <i>XhoI</i> F</b>	TGCGCTCGAGCAGGCGGGGCCGGGGCGGC
<b>eIF4AI <i>PacI</i> R</b>	ACTGATTAATTAAGATCCTTAGAACTAGGGCG
<b>eIF4AII <i>XhoI</i> F</b>	TGCGCTCGATCGGCAGCGGCACAGCGAGG
<b>eIF4AII <i>PacI</i> R</b>	ACTGATTAATTAAGATTCAGAGTCCGCGGAAGA
<b>SOD1 <i>XhoI</i> F</b>	GATACACTCGAGTTTGGGGCCAGAGTGGGCG
<b>SOD1 <i>PacI</i> R</b>	GATACATTAATTA AAACTCGCTAGGCCACGCCGA
<b>TXN <i>XhoI</i> F</b>	GATACACTCGAGTTTGGTGCTTTGGATCCATT
<b>TXN <i>PacI</i> R</b>	GATACATTAATTA ACTTTGGCTGCTGGAGTCTGAC
<b>Ace <i>SpeI</i> F</b>	GATTACAAC TAGTGGGGTGTGTGCGGGGGGCCG
<b>Ace <i>NcoI</i> R</b>	GATTACACCATGGGGCTGCAGGGCAGGCGGCGTC
<b>Tub <i>SpeI</i> F</b>	GATTACAAC TAGTGACCTCGCTGCTCCAGCCTCTGG
<b>Tub <i>NcoI</i> R</b>	GATTACACCATGGGGTTAAAATTTAATTTTTTTTGC
<b>EGFR <i>SpeI</i> F</b>	GATTACAAC TAGTCCCCGGCGCAGCGCGGCCGC
<b>EGFR <i>NcoI</i> R</b>	GATTACACCATGGCGCTGCTCCCCGAAGAGCTCG

**Table 9. Sequences of the PCR primers used in this project**

## 2.2. Restriction digestion

Enzyme Name	Buffer Composition	BSA <sup>1</sup> / SAM <sup>2</sup>	NEB <sup>3</sup> Cat #
<b><i>Bam</i>HI</b>	50 mM Tris-HCl 100 mM NaCl 10 mM MgCl <sub>2</sub> 1 mM Dithiothreitol pH 7.9 @ 25°C	BSA	R0136S
<b><i>Eco</i>RI</b>	100 mM Tris-HCl 50 mM NaCl 10 mM MgCl <sub>2</sub> 0.025 % Triton X-100 pH 7.5 @ 25°C	No	R0101S
<b><i>Hind</i>III</b>	10 mM Tris-HCl 50 mM NaCl 10 mM MgCl <sub>2</sub> 1 mM Dithiothreitol pH 7.9 @ 25°C	No	R0104S
<b><i>Pac</i>I</b>	10 mM Bis-Tris-Propane-HCl 10 mM MgCl <sub>2</sub> 1 mM Dithiothreitol pH 7.0 @ 25°C	BSA	R0547S
<b><i>Xho</i>I</b>	20 mM Tris-acetate 50 mM potassium acetate 10 mM Magnesium Acetate 1 mM Dithiothreitol pH 7.9 @ 25°C	BSA	R0146S
<b><i>Spe</i>I</b>	20 mM Tris-acetate 50 mM potassium acetate 10 mM Magnesium Acetate 1 mM Dithiothreitol pH 7.9 @ 25°C	BSA	R0133S
<b><i>Nco</i>I</b>	50 mM Tris-HCl 100 mM NaCl 10 mM MgCl <sub>2</sub> 1 mM Dithiothreitol pH 7.9 @ 25°C	No	R0193T
<b><i>Kpn</i>I</b>	10 mM Bis-Tris-Propane-HCl 10 mM MgCl <sub>2</sub> 1 mM Dithiothreitol pH 7.0 @ 25°C	BSA	R0142S
<b><i>Ahd</i>I</b>	20 mM Tris-acetate 50 mM potassium acetate 10 mM Magnesium Acetate 1 mM Dithiothreitol pH 7.9 @ 25°C	BSA	R0584S
<b><i>Ase</i>I</b>	50 mM Tris-HCl 100 mM NaCl 10 mM MgCl <sub>2</sub> 1 mM Dithiothreitol pH 7.9 @ 25°C	No	R0526S
<b><i>Bgl</i>III</b>	50 mM Tris-HCl 100 mM NaCl 10 mM MgCl <sub>2</sub> 1 mM Dithiothreitol pH 7.9 @ 25°C	No	R0144S

**Table 10. The restriction endonuclease enzymes used as part of this project.** 1. BSA = bovine serum albumin, SAM = S-adenosylmethionine and NEB = New England Biolabs

<b>Reaction Component</b>	<b>Amount (in a 50 <math>\mu</math>l Reaction)</b>
<b>Buffer</b>	5 $\mu$ l
<b>BSA or SAM</b>	0.5 $\mu$ l
<b>DNA</b>	200 ng (~ 1 $\mu$ l)
<b>Enzyme</b>	1 $\mu$ l
<b>H<sub>2</sub>O</b>	42.5 $\mu$ l (42 $\mu$ l without BSA/SAM)

**Table 11. A typical restriction digestion reaction**

Reactions were assembled as above (Table 11.) and incubated at 37°C. Digestion reactions used for the preparation of cloning vectors were incubated overnight whereas colony screen diagnostics were incubated for approximately two hours. If the digestion product was intended for ligation then the vector was dephosphorylated by adding 1  $\mu$ l Calf Intestinal Alkaline Phosphatase (CIAP NEB Cat# M0290L) to the completed reaction which was then left to incubate at 37°C for a further five minutes.

### **2.3. DNA agarose gel electrophoresis**

The products of PCRs and restriction digests were visualised by horizontal agarose gel electrophoresis. In order to make these gels 1 g agarose (Melford, Cat # MB1200) was added to a Pyrex beaker containing 100 ml 1 $\times$  TAE (Tris base, acetic acid and ethylenediaminetetraacetic acid (EDTA)) to give a final agarose concentration of 1%. This beaker was incubated at full power in a 650 W microwave for two minutes before being placed in a 42 °C water bath to cool for one minute. SYBR Safe (Invitrogen, Cat # S33102) was added to the mixture to give a final volume of 0.04% (4  $\mu$ l). A comb was added to a gel tray and the ends of the tray were sealed using autoclave tape. The gel mixture was poured into the tray and allowed to set at room temperature. Once set, the gel was immersed in a solution of 1 $\times$  TAE running buffer. DNA was mixed in a 10:1 ratio with loading buffer (the master mix of loading buffer consisted of: 6.25 ml of H<sub>2</sub>O, 0.025 g xylene cyanol, 0.025 g bromophenol blue, 1.25 ml 10% SDS and 12.5ml glycerol).

The DNA was added to the submerged wells together with a DNA size-marker ladder. For large bands, such as digested plasmids, a HighRanger DNA ladder (Norgen Biotek, Cat # 11900) was loaded while a 100 bp Ladder (NEB, Cat # N3231L) was used for smaller bands such as PCR products. Gels were usually run for approximately one hour (using a power pack (Bio-Rad Basic) set to 120 V) before visualisation using a ChemiDoc XRS Molecular Imager (Bio-Rad). DNA samples were prepared by the addition of loading buffer which consisted of xylene cyanol and bromophenol blue dyes and glycerol.

#### **2.4. Gel extraction**

All extractions of DNA from agarose gels were performed using the 'Freeze-Squeeze' method. A scalpel was used to excise DNA bands from the gel and transfer them to 1.5 ml microcentrifuge tubes. These were frozen to -80 °C. Tubes were centrifuged at 13, 000 rpm for 10 minutes. The liquid was removed and transferred to new tubes. An equal volume of water to the liquid removed was added to the tubes containing the gel slices, these were then vortexed for 30 seconds before being re-frozen to -80 °C. The tubes were then centrifuged again and the liquid fractions were added to the previous liquid removed from the gel slices. Equal volumes of phenol were added to this liquid. These mixtures were vortexed and centrifuged at 13, 000 rpm for one minute. The upper fractions were transferred to new tubes to which equal volumes of 1:1 phenol : chloroform (containing 4% isoamyl alcohol) were added. These mixtures were vortexed and centrifuged at 13, 000 rpm for one minute. The upper fractions were transferred to new tubes to which equal volumes of chloroform were added. These mixtures were vortexed and centrifuged at 13, 000 rpm for one minute. 2.5 volumes of 100% ethanol and 0.2 volumes of 5M NaAc (sodium acetate) were added to the tubes which were then frozen to -80 °C. The tubes were then centrifuged at 13, 000 rpm for 30 minutes at 4 °C. All the supernatant was removed. The pellets were dried at room temperature and resuspended in 20 µl H<sub>2</sub>O. Yield and purity were quantified by Nanodrop (Thermo Scientific) analysis.

#### **2.5. Ligation**

All ligations used T4 DNA ligase (NEB, Cat # M0202L) with the supplied buffer (50 mM Tris-HCl, 10 mM MgCl<sub>2</sub>, 1 mM ATP, 10 mM Dithiothreitol, pH 7.5 @ 25°C). A typical ligation reaction contained the following components (Table 12.).

Reaction Component	Amount (in a 10 $\mu$ l Reaction)
Buffer	1 $\mu$ l
Vector	100 ng (~ 0.5 $\mu$ l)
Insert	X ng (0 ng in control)
Enzyme	0.5 $\mu$ l
H <sub>2</sub> O	8 $\mu$ l

**Table 12. The components of a standard ligation reaction.** X = insert concentration, this was such that the ratio of vector to insert was 3:1. Reactions containing 0 ng insert were performed in parallel to regular reactions, in order to ascertain the rate of vector self-ligation.

Reactions were assembled as above in 0.5 ml microcentrifuge tubes. Blunt-end or A-tail ligations were incubated overnight at 4°C while sticky-end ligations were incubated at room temperature for at least two hours.

### 2.6 Preparation of Heat-Competent DH5 $\alpha$ *Escherichia coli*

A plate was poured that contained LB with no selective agent. 20  $\mu$ l of one of the aliquots of the previous batch of DH5 $\alpha$  was spread on this plate. Following incubation overnight at 37 °C, a single colony was used to inoculate 2.5 ml liquid LB (also without antibiotic). This starter culture was incubated at 37 °C overnight with agitation before being poured into a 250 ml volume of liquid LB containing 20 mM MgSO<sub>4</sub>. This volume was incubated at 37 °C with agitation for 5 – 6 hours until the A<sub>600</sub> was between 0.4 and 0.6. At this point, the culture was centrifuged at 4000 rpm for ten minutes at 4 °C. In the cold room (maintained at 4 °C), the supernatant was discarded and cell pellets were resuspended in 100 ml ice cold Buffer 1 (30 mM potassium acetate, 10 mM CaCl<sub>2</sub>, 50 mM MnCl<sub>2</sub>, 100 mM RbCl and 15% glycerol, adjusted to pH 5.8 with acetic acid) before being incubated on ice for five minutes and centrifuged as before. The supernatant was discarded and the pellets were resuspended in 10 ml ice cold Buffer 2 (10 mM 3-(N-

morpholino)propanesulfonic acid), 75 mM CaCl<sub>2</sub>, 10 mM RbCl and 15% glycerol, adjusted to pH 6.6 with KOH) and incubated on ice for 45 minutes. This mixture was transferred to 0.5 ml microcentrifuge tubes in 200 µl aliquots. These tubes were flash frozen in liquid nitrogen and stored at -80 °C.

## **2.7. Transformation and plasmid preparation**

Heat-competent DH5α *Escherichia coli* were used to transform plasmids and completed ligations. Cells were incubated with ~ 10 ng DNA on ice before being subject to heat shock at 42°C. The cells were then incubated at 37°C in non-selective liquid media for one hour with agitation. This suspension was spread on Luria-Bertani (LB) plates containing a 100 µg/ml ampicillin. Plates were incubated overnight at 37°C.

Resulting colonies were either screened for successful ligation by PCR (in which a scraping from each colony was used as the template) or screened by diagnostic digest. If the latter, scrapings from a range of colonies were used to inoculate 10 ml liquid LB containing 100 µg/ml ampicillin, these mixtures were grown overnight at 37°C with agitation. The plasmids were purified from the resulting cultures using Promega Wizard® Plus SV Miniprep DNA Purification Columns (Cat# A1460). Briefly, this protocol involves the lysis of cells using a solution of 0.2M NaOH and 1% SDS followed by the addition of resuspension solution (50mM Tris-HCl (pH 7.5), 10mM EDTA and 100µg/ml RNase A). Cellular proteins are degraded by the addition of alkaline phosphatase and the incubation of the reaction for five minutes at room temperature. Neutralisation solution (4.09M guanidine hydrochloride, 0.759M potassium acetate and 2.12M glacial acetic acid (pH 4.2)) was added to stop this reaction. Tubes were centrifuged at 13, 000 rpm for ten minutes before the supernatant was eluted and transferred to one of the DNA binding columns provided with the Miniprep kit. This was centrifuged at 13, 000 rpm for one minute. The supernatant was discarded and 750 µl column wash solution (60% ethanol, 60mM potassium acetate, 8.3mM Tris-HCl, 0.04mM EDTA) was added to the top of the column. The column was then centrifuged again at 13, 000 rpm for one minute. The supernatant was discarded and replaced with 250 µl column wash solution. The column was centrifuged for a further one minute at 13, 000 rpm. The upper part of the column (to which the DNA was bound) was placed in a new 1.5 ml microcentrifuge tube. Nuclease free water (100 µl) was added to the column which was then left for five minutes at room temperature to allow the DNA to dissolve into the water. The tube containing the column was then centrifuged one final time at 13, 000 rpm for one minute to collect the suspended

DNA in the microcentrifuge tube. Yield and purity of DNA were determined by Nanodrop (Thermo Scientific) analysis.

## **2.8. mRNA extraction**

Total RNA was extracted from confluent T75 flasks of SH-SY5Y cells using TRI Reagent® (Sigma-Aldrich, Cat # T9424). The growth medium was removed from flasks and cells were washed twice in PBS solution. 1.5 ml TRI Reagent® was added to the cells and allowed to incubate at room temperature for five minutes. This mixture was then transferred to microcentrifuge tubes and 0.3 ml chloroform was added. Tubes were shaken, left to stand at room temperature for 15 minutes then centrifuged at 13,000 rpm for 15 minutes at 4 °C. The clear, upper phase was carefully transferred to new tubes and 0.75 ml 100% isopropanol was added. The tubes were inverted four times, left to stand at room temperature for ten minutes and then centrifuged at 13,000 rpm for ten minutes at 4 °C. The supernatant was discarded and the RNA pellet was resuspended in 1.5 ml 75% ethanol. Tubes were vortexed then centrifuged at 7,500 rpm for five minutes at 4 °C. The pellet was air-dried then suspended in 50 µl nuclease free water. Yield and purity of RNA were quantified by Nanodrop (Thermo Scientific) analysis.

Polyadenylate RNA was extracted from the total RNA using Oligo-dT Dynabeads® (Invitrogen, Cat # 610-02). 75 µl of the total RNA was made up to 100 µl by the addition of 25 µl nuclease free water. 100 µl Binding Buffer (20 mM Tris-HCl pH 7.5, 1.0 M LiCl and 2 mM EDTA) was added and the mixture was heated to 65 °C for two minutes before being placed on ice. 200 µl of the Dynabeads were washed in Binding Buffer and suspended in a further 100 µl of Binding Buffer. This suspension of beads was added to the RNA mixture. The RNA / Dynabeads suspension was inverted several times before being left on a rotating stand at room temperature for ten minutes to allow the RNA poly(A) tails to anneal to the poly(T) projections on the beads. A magnet was used to separate the Dynabeads (to which the mRNA was bound) from the total mRNA (Figure 2.1.).

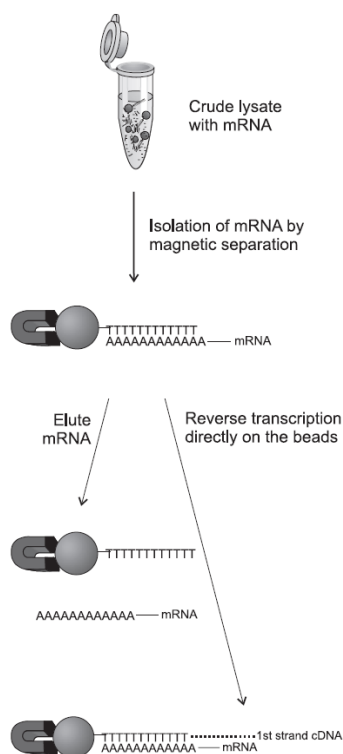


**Figure 2.1. The basic principle of mRNA extraction using Oligo-dT Dynabeads.**

Magnet was removed from the tube and 200  $\mu$ l Washing Buffer B (10 mM Tris HCl pH 7.5, 0.15 M LiCl and 1 mM EDTA) was added. The mixture was pipetted several times before the magnet was placed next to the tube again. This washing procedure was repeated. With the beads attracted to the side of the tube, the supernatant was removed and replaced with 20  $\mu$ l 10 mM Tris-HCl. The magnet was removed and the tube was heated to 80  $^{\circ}$ C for two minutes. The magnet was then placed next to the tube and the eluted mRNA was transferred to a new tube. Yield and purity of mRNA were quantified by Nanodrop (Thermo Scientific) analysis.

## 2.9. Reverse transcription

Extracted poly(A) RNA was used as a template in reverse transcription reactions using SuperScript® III Reverse Transcriptase (Invitrogen, Cat # 11754-050). The following reaction was assembled on ice (Table 13.).

Reaction Component	Amount (in a 20 µl Reaction)
5× VILO™ Reaction Mix*	4 µl
10× SuperScript® Enzyme Mix	2 µl
mRNA	2.5 ng (~ 4 µl)
H <sub>2</sub> O	11.5 µl

**Table 13. A typical SuperScript® III Reverse Transcriptase reaction.** \* VILO Reaction Mix contains random primers, MgCl<sub>2</sub>, and dNTPs.

The reaction was incubated for ten minutes at 25 °C then for 60 minutes at 42 °C then for five minutes at 85 °C. Five units (1 µl) of RNase H (NEB, Cat # M0297S) were then added to degrade the mRNA template and the reaction was incubated for a further 15 minutes at 37 °C. An equal volume of phenol to the reaction volume (20 µl) was added at this point. This mixture was vortexed and centrifuged at 13,000 rpm for one minute. The upper fraction was transferred to a new tube to which 20 µl of 1:1 phenol : chloroform (containing 4% isoamyl alcohol) were added (i.e. 10 µl of each). This mixture was vortexed and centrifuged at 13,000 rpm for one minute. The upper fraction was transferred to a new tube to which an equal volume of chloroform was added. This mixture was vortexed and centrifuged at 13,000 rpm for one minute. 2.5 volumes of 100% ethanol and 0.2 volumes of 5M NaAc (sodium acetate) were added to the tube which was then frozen to -80 °C. The tube was then centrifuged at 13,000 rpm for 30 minutes at 4 °C. All the supernatant was removed. The pellet was dried at room temperature and resuspended in 20 µl H<sub>2</sub>O. The yield and purity of the cDNA were quantified by Nanodrop (Thermo Scientific) analysis.

## 2.10. *In vitro* transcription

The RNA duplexes for the *in vitro* screen and the helicase assay were synthesised using *in vitro* transcription. DNA oligonucleotides were ordered (Table 14.) (Invitrogen).

---

Oligo Name	Sequence (5' - 3')
<b>13 Sense F</b>	TAATACGACTCACTATAGGGAGAGGCTAATGCTATG
<b>13 Sense R</b>	CATAGCATTAGCCTCTCCCTATAGTGAGTCGTATTA
<b>13 Antisense F</b>	GGCTAATGCTATGTCTCCCTATAGTGAGTCGTATTA
<b>13 Antisense R</b>	TAATACGACTCACTATAGGGAGACATAGCATTAGCC
<b>44 F</b>	TAATACGACTCACTATAGGGAGAGGGAGAAAACAAA ACAAAACAAAACACTAGCACCGTAAAGCACGC
<b>44 R</b>	GCGTGCTTTACGGTGCTAGTTTTGTTTTGTTTTGTTT TTCTCCCTCTCCCTATAGTGAGTCGTATTA
<b>11 F</b>	TAATACGACTCACTATAGGGAGAGGGAGAAAACAA
<b>11 R</b>	TTGTTTTTCTCCCTCTCCCTATAGTGAGTCGTATTA

---

**Table 14. The oligonucleotides used as template for the *in vitro* transcription of RNA duplexes used as part of this project. The T7 promoter sequence is shown in red.**

RiboMAX™ Large Scale RNA Production System Kits were used (Promega, Cat # P1300). The following reaction components were assembled on ice (Table 15.).

T7 Reaction Components	Sample Reaction	Control Reaction
T7 Transcription 5X Buffer	20µl	4µl
rNTPs (25mM ATP, CTP, GTP, UTP)	30µl	6µl
linear DNA template (5-10µg total) plus Nuclease-Free Water	40µl	1µl (control DNA) 7µl (water)
Enzyme Mix (T7)	10µl	2µl
<b>final volume</b>	<b>100µl</b>	<b>20µl</b>

**Table 15. The components of a typical *in vitro* transcription**

Reactions were incubated at 37 °C for four hours. At the end of this reaction, 1 µl RQ1 RNase-Free DNase (Promega, Cat # M6101) was added and the reaction was incubated at 37 °C for a further 15 minutes.

An equal volume of phenol to the reaction volume (100 µl) was added at this point. This mixture was vortexed and centrifuged at 13, 000 rpm for one minute. The upper fraction was transferred to a new tube to which 20 µl of 1:1 phenol : chloroform (containing 4% isoamyl alcohol) were added (i.e. 50 µl of each). This mixture was vortexed and centrifuged at 13, 000 rpm for one minute. The upper fraction was transferred to a new tube to which an equal volume of chloroform was added. This mixture was vortexed and centrifuged at 13, 000 rpm for one minute. 2.5 volumes of 100% ethanol and 0.2 volumes of 5M NaAc (sodium acetate) were added to the tube which was then frozen to -80 °C. The tube was then centrifuged at 13, 000 rpm for 30 minutes at 4 °C. All the supernatant was removed. The pellet was dried at room temperature and resuspended in 100 µl H<sub>2</sub>O. The yield and purity of the RNA were quantified by Nanodrop (Thermo Scientific) analysis.

### **2.11. Denaturing gel**

In order to check that the RNA molecules described in the previous section had synthesised successfully, samples of each were run on vertical denaturing gels. 0.5 µg RNA was mixed in a 10:1 ratio with loading buffer (the master mix of loading buffer consisted of: 6.25 ml of H<sub>2</sub>O, 0.025 g xylene cyanol, 0.025 g bromophenol blue, 1.25 ml 10% SDS and 12.5ml glycerol) along with 10× MOPS (1:10), formaldehyde (1.75:10) and formamide (1:1). Gels consisted of 6.36 g Urea, 3 ml 5× TBE, 3.75 ml 40% 19:1 polyacrylamide (made up to 15 ml with H<sub>2</sub>O). This mixture was poured between two glass plates placed 2.5 mm apart and a comb was placed into the unset gel in order to define the wells. The gel was allowed to set and the comb was removed.

Gels were pre-run (in 1× MOPS running buffer) at 200 V at 4°C then for a further 30 minutes following loading, the gel was visualised by ethidium bromide staining and UV excitation using a ChemiDoc™ XRS system (Bio-Rad). RNA size was estimated using a single stranded RNA ladder (NEB, Cat # N0362S).

## 2.12. ATP Usage Quantification 1. 6, 8-difluoro-4-methylumbelliferyl phosphate (DiFMUP)

DiFMUP (Invitrogen, Cat # D6567) was one of the reagents used for quantification of ATP usage by eIF4A *in vitro*. 200  $\mu$ l reactions consisted of 20 mM HEPES (pH 7.2), KCl 70 mM, 2 mM dithiothreitol, 1 mg/ml bovine serum albumin, 1 mM magnesium acetate, 1 mM ATP, 1.8 nM RNA duplex, 0.4 mM eIF4A (0 in control) 100  $\mu$ M DiFMUP and 10  $\mu$ l H<sub>2</sub>O (11  $\mu$ l in control). Reactions were incubated at 37°C for 15 minutes before being cooled to 4°C. Colourimetric analysis was performed using a BioTeK PowerWave XS Microplate Spectrophotometer (Figure 2.2.).

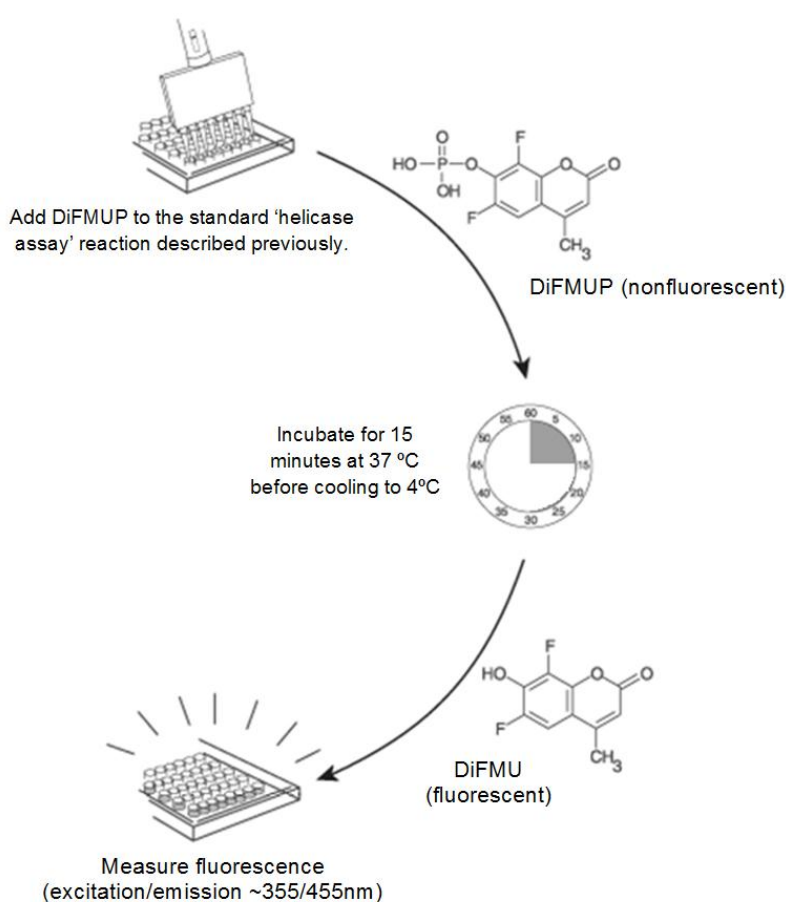
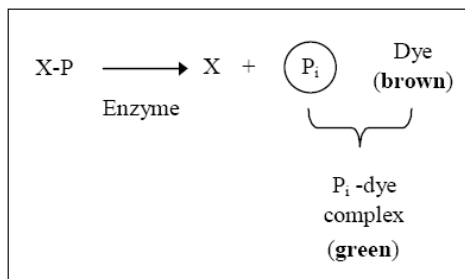


Figure 2.2. The principle of DiFMUP activity

### 2.13. ATP Usage Quantification 2. PiColorlock™

PiColorlock™ (Novus Biologicals, Cat # 303-0030) was the other reagent used for colourimetric ATPase activity assay.



**Figure 2.3. The principle of PiColorlock activity**

The reaction components were the same as for DiFMUP, as were the incubation conditions. After the completion of the reactions, 80 µl of PiColorlock reagent and 1% volume 'Accelerator' (supplied with the PiColorlock™ Kit) were added. The mixtures were incubated for 30 minutes at room temperature before colourimetric analysis was performed using a BioTeK PowerWave XS Microplate Spectrophotometer (Figure 2.3..).

#### 2.14. Western Blot

Two glass plates were placed 2.5 mm apart separated by plastic dividers. A 10% gel was prepared with the following components:

- 1.25 ml resolving buffer (1.5 M Tris pH 8.8 and 1% SDS)
- 2.1 ml H<sub>2</sub>O
- 1.67 ml 19:1 acrylamide
- 50 µl 25% APS (ammonium persulphate)
- 3 µl TEMED (tetramethylethylenediamine)

This mixture was poured between the glass plates and left to set at room temperature for ten minutes. A layer of 100 µl butanol was added to the surface of the set gel. The stacking buffer was prepared as follows:

- 2.5 ml stacking buffer (0.25 M Tris pH 6.8 and 1% SDS)
- 1.8 ml H<sub>2</sub>O
- 0.67 ml 19:1 acrylamide
- 50 µl 25% APS
- 3 µl TEMED

The stacking gel was poured on top of the 10% gel layer and a comb was inserted. The stacking gel was left to set at room temperature for ten minutes. The comb was then removed and the gel was immersed in running buffer (25 mM Tris pH 8.3, 0.192 M glycine and 1% SDS).

Cells were washed twice in PBS before being lysed using sample buffer (100 mM Tris pH 6.8, 20% glycerol, 8% SDS, 20% β-mercaptoethanol, 2 mM EDTA and 0.2 % bromophenol blue). Lysate was transferred to 1.5 ml microcentrifuge tubes, heated to 95 °C for five minutes and loaded into the wells of the immersed gel. A protein ladder (Bio-Rad, Cat # 161-0373) was also loaded. The gel was run at 150 V for two hours.

Six sheets of Whatman filter paper were soaked in blotting buffer (50 mM Tris, 192 mM glycine and 20% methanol). Three of these were placed on the positive electrode of a Semi-Dry Electrophoretic Transfer Cell (BioRad Trans-Blot®, Cat # 170-3940). A piece of PVDF (polyvinylidene fluoride) membrane just larger than the gel (BioRad, Cat # 162-0174) was soaked in 100% methanol then H<sub>2</sub>O then blotting buffer. This was then placed on the three sheets of Whatman paper on the transfer cell. The gel was placed on top of this and another three sheets of blotting buffer-soaked Whatman paper were placed on top of the gel. The negative electrode was placed on top of the stack and the lid was put on top of this. A

voltage of 10 V was applied for one hour. The gel and the Whatman paper were discarded and the membrane was placed in 20 ml TBST (tris-buffered saline and tween) containing 5% Marvel powdered milk (Tesco). This was incubated at room temperature for one hour with agitation. This mixture was removed and replaced with 5 ml primary antibody diluted in TBST and 5% Marvel powdered milk. The primary and secondary antibodies used in this project are shown in Table 16.

Affinity	Raised In	Dilution	Cat #	Secondary Raised In	Secondary Dilution	Secondary Cat#
eIF4AI	Rabbit	1:50	ab31217	Goat	1:1000	ab6012
eIF4AII	Rabbit	1:50	ab31218	Goat	1:1000	ab6012
eIF4AIII	Rabbit	1:250	ab32485	Goat	1:1000	ab6012
PDCD4	Rabbit	1:5000	ab51495	Goat	1:1000	ab6012
p53	Mouse	1:1500	ab26	Goat	1:500	ab9165
EGFR	Rabbit	1:200	ab2430	Goat	1:1000	ab6012
$\beta$ tubulin	Rabbit	1:200	ab6046	Goat	1:1000	ab6012

**Table 16. The antibodies used as part of this project**

The membrane was left exposed to the primary antibody overnight at 4 °C with agitation. The following day, the membrane was washed three times in TBST for five minutes with agitation. The membrane was exposed to the secondary antibody (also dissolved in TBST and 5% Marvel) for one hour at room temperature before being washed in TBST a further three times. 1 ml western blotting reagent (GE Healthcare, Cat # RPN2232) was added to the membrane which was then wrapped in cling film and placed inside a western imaging cassette along with a piece of Kodak X-Omat photographic film (Sigma-Aldrich, Cat # F1274). The membrane was left exposed to the film for approximately 30 seconds before the film was developed.

Completed blots were scanned at a resolution of 600 dpi and bands were quantified using ImageJ (Abramoff et al., 2004). The Rolling Ball algorithm was used to subtract the background of the images and the Watershed algorithm was used to quantify the intensity of the bands (Hanson, 1992; Vincent and Soille, 1991).

At least two replicates were performed for each. Standard deviations are shown as error bars on graphs and p values were generated by Student's T test.

### 2.15. eIF4A Manufacture

The ORF of human *eIF4AI* was cloned into the multi-cloning site of the plasmid pMAL (NEB, Cat # E8200S) by Nicola Phillips, a former member of the RNA Biology Group, University of Nottingham (Figure 2.4.). This plasmid was transformed into heat-competent BL21 *E. coli* which were then grown overnight on an LB plate containing 100 µg/ml ampicillin at 37°C. A single colony was picked and used to inoculate a 10ml volume of liquid LB containing 100 µg/ml kanamycin. This culture was incubated overnight at 37°C with agitation before being decanted into a 1l volume of selective medium.

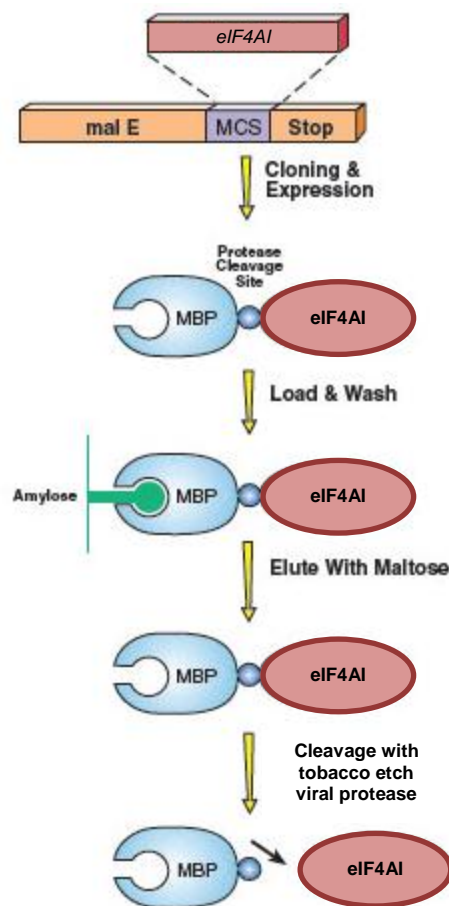
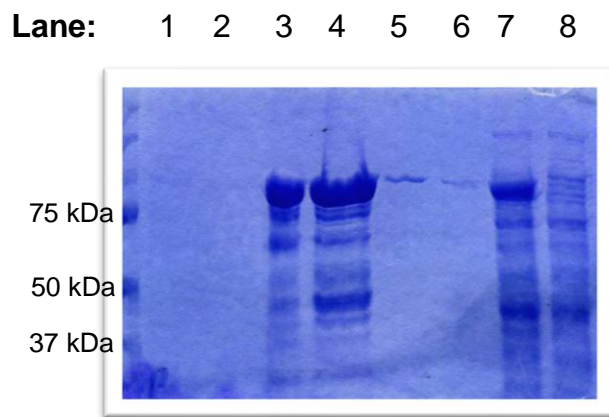


Figure 2.4. The principle of eIF4AI expression and purification.

The 1l culture volume was incubated until  $A_{560}$  reached approximately 0.5 (after 3 – 4 hours). 1mM IPTG (Isopropyl  $\beta$ -D-1-Thiogalactopyranoside) was added at this point to induce protein expression. This volume was incubated for a further 10 hours before being centrifuged at 7000 rpm to pellet the cells. This pellet was resuspended in lysis buffer (20 mM Tris-HCl (pH 7.5), 200 mM NaCl and 1 mM EDTA) and allowed to drip through a 2.5 ml affinity column that was previously prepared by the passage of 50 ml 50% amylose resin and 10 ml lysis buffer. The eIF4AI protein was eluted in six aliquots in elution buffer (20 mM Tris-HCl (pH 7.5), 10 mM maltose, 200 mM NaCl and 1 mM EDTA). The column was washed using wash buffer. Each of the elutions was run on an SDS PAGE gel (see previous section). This gel was visualised using Coomassie brilliant blue.



**Figure 1.5. Elution iterations from the eIF4AI manufacture process.** Lanes 1 – 6 contain the elutions from the binding column followed by the crude lysate in lane 7, and the wash buffer in lane 8. The gel is a 10% western blot gel stained with Coomassie. A protein of the expected size for eIF4A is present in lanes 4 and 5.

Glycerol was added to quantities of solution taken from the tubes containing the elution iterations from lanes four and five at a 1:1 concentration (Figure 1.5.). Nanodrop analysis revealed that the combined protein concentration of tubes four and five was 16 mg/ml.

## **2.16. Cell Culture**

Four different human cell lines were used as part of this project, HeLa (cervical cancer), SH-SY5Y (neuroblastoma), MCF7 (breast cancer) and Huh7 (hepatocyte cellular carcinoma). These were cultured using standard laboratory practice. The growth medium used was High Glucose Dulbecco's modified Eagle medium (DMEM) (Invitrogen, Cat # 10938-025). This was stored at 4°C when not in use. Prior to its addition to the flasks, foetal bovine serum was added to the medium (to a final proportion of 10%), as was L-Glutamine. Foetal calf serum (FCS) was also added to the growth medium for the SH-SY5Y cells.

Cells were grown in T75 (75 cm<sup>2</sup>) TPP cell culture flasks with ventilated lids (Sigma-Aldrich®, Cat # Z707546).

When in use, these flasks were kept in a Thermo Electron HeraCell 150 incubator at 37°C in an atmosphere containing 5% carbon dioxide (CO<sub>2</sub>). Hypoxic incubations were carried out in a ProOx 110 (BioSpherix Ltd.) using an oxygen concentration of 1%.

Numbers of cells within an individual flask were managed by regular 'splitting', i.e. enzymatically dissociating the cells from the surface of the flask, to which they normally adhere, and discarding a proportion of the resulting suspension before replacing the media.

Dissociation of the cells from the flask was achieved by using the serine protease trypsin. The medium was removed from the flask and replaced with 5 ml (in a T75) of phosphate buffered saline (PBS) in order to wash the cells. This would then be replaced with 5 ml trypsin dissolved in PBS (0.25% (w/v)) and the flask incubated for 60 seconds at 37°C (in 5% CO<sub>2</sub>). Dissociation of the cells was confirmed by microscopy.

The procedure outlined above was used in the seeding of 24 well plates. The majority of the experiments performed as part of this project used 24 well plates. These were seeded at a density of 50, 000 cells per well.

Cell viability was estimated using WST-1 reagent (Roche, Cat # 11 644 807 001) following standard protocols.

## **2.17. Cell Preparation**

Before either DNA or RNA transfections, 24 well plates were seeded with cells to a density of 50, 000 cells per well and allowed to settle for at least eight hours, usually overnight.

### **2.18. DNA Transfection**

Plasmid transfection was performed using Fugene 6 (Roche, Cat # 05061377001) using the recommended protocol. For the CMV promoter-based plasmids, 100 ng of DNA was transfected into each 24 well plate well using 0.3  $\mu$ l Fugene and for the SV40-based plasmids, 200 ng was used (suspended in 0.6  $\mu$ l Fugene). DNA was suspended in water and the Fugene in serum free media before being combined and incubated at room temperature for 30 minutes. The combined DNA and Fugene mixture was added to fresh media and vortexed before being used to replace the existing media. Luciferase assays were performed on CMV-based transfections 24 hours after DNA addition unless otherwise stated. 24 hours following SV40 transfections, the medium was changed and the cells incubated for a further 24 hours before luciferase assays were performed.

### **2.19. RNA Transfection**

INTERFERin (Polyplus Transfection, Cat # 409-01) was used to transfect the siRNA molecules targeting the paralogs of eIF4A. 21 ng of siRNA per well was dissolved in 100  $\mu$ l Opti-MEM<sup>®</sup> serum free media (Gentaur, Cat # 31985-070). 4  $\mu$ l INTERFERin was added and the mixture was vortexed for ten seconds and incubated at room temperature for 15 minutes. This volume was added to 200  $\mu$ l growth medium.

eIF4A siRNAs were purchased from Invitrogen, Cat #'s: eIF4AI HSS103141 (sequence: GCCCAAUCUGGGACUGGG), eIF4AII HSS103144 (sequence: TGCCACAATGCCAACTGA) and eIF4AIII HSS103148 (sequence: AGCAGATCATCAAAGGGA), control 12935-300 (sequence: Medium GC). Cells were incubated for 24 hours following initial transfection. Transfections were repeated at this point to add a second hit and make the knockdown more effective. If required, luciferase reporters were co-transfected with the second hit (see DNA Transfection).

### **2.20. Luciferase Assay**

Growth medium was removed from cells and replaced with phosphate buffered saline; this was removed after a few seconds and the dry plates were frozen at -80°C. 40  $\mu$ l of 1 $\times$  passive lysis buffer was added to each well of a 24 well plate and cells were dissociated from the base by scraping with a 1250  $\mu$ l pipette tip. 10  $\mu$ l aliquots of this suspension from each well were transferred to individual wells of a black 96 well plate.

Data were collected using a Promega GloMax Microplate Luminometer and associated GloMax software. The luciferase reagents were LarII and Stop & Glo (Promega, Cat # E1980). The software directed the addition of 25  $\mu$ l of each reagent to each well and the resulting signal was integrated over 10 seconds.

At least three replicates were performed for each. Standard deviations are shown as error bars on graphs and p values were generated by T test.

## 2.21. Northern Blot

Total RNA was extracted from confluent HeLa cells using TRI Reagent® (Ambion, Cat # AM9738). These cells had been transfected with either pRF, pREGFRF or pRtubF 48 hours earlier (Figure 2.6.).

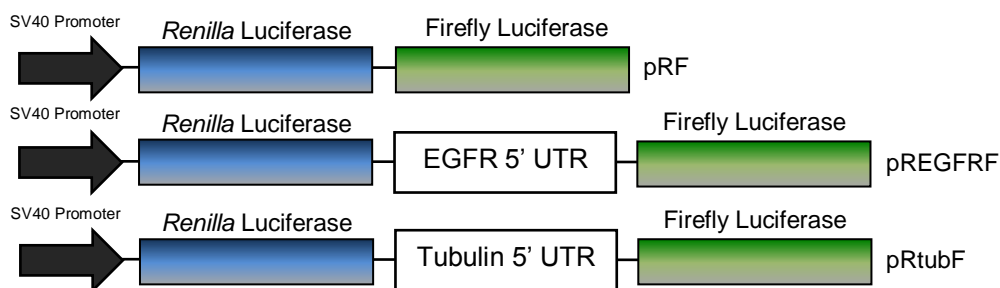


**Figure 2.6. The constructs of the plasmids transfected into HeLa cells and assayed for mRNA integrity by northern blot.**

A horizontal gel tray and a comb were wiped with RNase ZAP (Ambion, Cat # AM9780). A 1% denaturing gel was prepared using the following components:

- 1 g agarose
- 75 ml H<sub>2</sub>O
- 17.5 ml formaldehyde
- 10 ml 10× MOPS (3-(N-morpholino)propanesulfonic acid)

The gel was poured and left to set in a fume hood under a layer of cling film. The mRNA samples were prepared by the addition of the following chemicals:

- 5  $\mu$ l RNA
- 2  $\mu$ l 10× MOPS
- 3.5  $\mu$ l formaldehyde
- 10  $\mu$ l formamide
- 2  $\mu$ l formaldehyde gel-loading buffer

This mixture was incubated at 65 °C for 15 minutes before being centrifuged for five seconds. The gel was submerged in 1× MOPS running buffer and the samples were loaded. A voltage of 100 V was applied to the gel for two hours. The gel was then placed above a tank of 20× SSC (saline-sodium citrate) buffer and below a sheet of Zeta Probe membrane (BioRad, Cat # 162-0159) in the configuration shown below (Figure 2.7.).

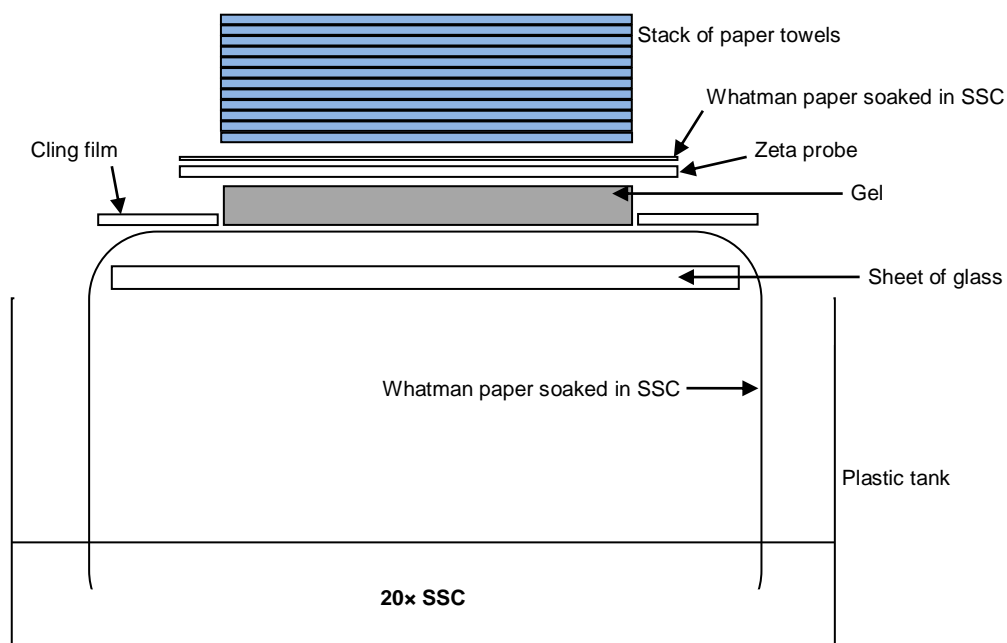


**Figure 2.7. The mechanism by which the RNA was transferred to the Zeta Probe membrane**

The capillary action of the paper towels draws the RNA out of the gel overnight and the RNA becomes bound to the Zeta-Probe membrane. The membrane was subject to UV crosslinking using a Stratalinker (Stratagene, Cat # 400072) set to 1200.

The membrane was then stained with methylene blue (1 ml 1% methylene blue in H<sub>2</sub>O, 0.02% methylene, 5 ml NaAc, 0.3 M acetate pH 5.2 made up to 50 ml with H<sub>2</sub>O) to visualise the RNA. Pencil marks were made to indicate the position of the 18S rRNA and 28S rRNA bands. The dye was washed off using 1× SSC containing 1% SDS.

The template was generated by amplifying a section of the firefly luciferase ORF from pRF using the following primers:

GGAACCGCTGGAGAGCAACTGC; upstream

GCATGCGAGAATCTCACGCAGGC; downstream

The PCR product was used as template for a Klenow fragment reaction with the following components:

- 5 µl 5× labelling buffer (10 mM Tris-HCl pH 7.9, 50 mM NaCl, 10 mM MgCl<sub>2</sub> and 1 mM dithiothreitol)
- 1 µl BSA
- 0.5 µl dNTPs (dATP, dTTP and dGTP)
- 2.5 µl Easy Tides® P<sup>[32]</sup> Deoxycytidine 5' Triphosphate (3000 Ci/mmol)
- 3 µl (30 ng) DNA template
- 12 µl H<sub>2</sub>O
- 1 µl Klenow fragment polymerase (NEB, Cat # M0210S)

The reaction mixture was incubated at 37 °C for one hour before being purified using a Sepharose G50 (GE Healthcare, Cat # 17-0043-01) column. 200 ml Church Gilberts solution (5.1 g Na<sub>2</sub>HPO<sub>4</sub>, 2.19 g NaH<sub>2</sub>PO<sub>4</sub> and 14 g SDS in 200 ml H<sub>2</sub>O) was heated to 65 °C. The membrane was placed inside a hybridisation tube together with 5 ml of the warmed Church Gilberts buffer. The probe was heated to 95 °C for three minutes then cooled on ice for five minutes and added to the hybridisation tube with 5 ml fresh Church Gilberts buffer. The tube was incubated in a rotating incubator at 65 °C overnight. The following day, the blot was washed three times in SSC containing 0.1% SDS. The blot was wrapped in cling film and exposed to a Fujifilm imaging plate (Cat # 2340) that had been blanked by exposure to bright light for 20 minutes. The following day, the probe was discarded and the membrane was washed. The membrane was then exposed to a phosphorimaging screen overnight. The screen was developed using a Storm 825 phosphorimager (GE Healthcare).

## 2.22. T Vector

Since the pGEM®-T Easy cloning vector (Promega, Cat # A3600) is supplied as a linear sequence, it cannot be replicated by molecular cloning. An alternative T cloning vector was designed that could be manufactured in the laboratory as this approach would eliminate the considerable financial outlay in the form of future purchases of pGEM®-T Easy from Promega. The restriction enzyme *AhdI* has the restriction site:

5' GACNNN / NNGTC 3'; if the nucleotides flanking the cut ( / ) are thymine then these will be left as overhanging ends ready to accept the overhanging adenine ends of the insert added by Taq PCR. The chosen plasmid was pBluescript II SK+ (Stratagene); a silent mutation was introduced into the pre-existing *AhdI* site within the ampicillin resistance marker gene of this plasmid. With this *AhdI* site

deleted, another was introduced into the multi cloning region of the pBluescript vector within the lacZ ( $\beta$ -galactosidase) gene by cloning in a construct amplified from pRF containing *XhoI*-*AhdI*-*AhdI*-*EcoRI* restriction sites in that order. The resulting plasmid was digested to completion with *AhdI* and run on an agarose gel with the excision and purification of the larger (~3.0 kbp) fragment. The newly-created T vector, termed pHM-T (for 'Home Made'), was tested by ligating in the A-overhanging CMV promoter fragment used in the cell-based screen.

### 2.23. Helicase Assay

The reaction conditions used in the helicase assay were the same as those used previously (Rogers *et al.*, 1999a). Each 20  $\mu$ l replicate contained the following components:

- 20 mM HEPES (pH 7.2)
- KCl 70 mM
- 2 mM dithiothreitol
- 1 mg/ml bovine serum albumin
- 1 mM magnesium acetate
- 1 mM ATP
- 1.7-1.8 nM RNA duplex
- 0.4 mM eIF4A (0 in control)

The RNA duplex consisted of the same sequence used previously (see section: *In vitro* Transcription) (Rogers *et al.*, 1999a). The 44 bp strand *in vitro* transcription progressed as per the RiboMAX™ protocol, as did the 11 bp transcription but for the replacement of half of the 100 mM CTP input with Easy Tides® P<sup>[32]</sup> Cytidine 5' Triphosphate (3000 Ci/mmol).

Duplexes were annealed by heating a tube containing a 1:1 mixture of both strands to 95 °C in a beaker of water which was then left to slowly cool to room temperature.

The above reactions were incubated at 37 °C for 10 minutes then terminated by the addition of 20  $\mu$ l of stop solution (the master mix consisted of: 5 ml 50% glycerol, 2% SDS, 20 mM EDTA, 0.01% bromophenol blue and 0.01% xylene cyanol). Polyacrylamide gel electrophoresis was used to visualise strand separation (see section: Western Blotting). The protocol was the same as for western blotting with the only exception being that gels were pre-run for 30 minutes at 200 V at 4°C. Samples were loaded and the gels were run at 200 V for one hour. The gels were then desiccated and exposed to Fujifilm phosphorimaging

plates overnight. The following day, the plates were imaged using a Storm 825 phosphorimager (GE Healthcare).

#### siRNA and shRNA Sequences

Target	si / sh	Sequence	Supplier	Cat #
eIF4AI	sh	CCGGGCCGTGTGTTTGATATGCTTACTCG AGTAAGCATATCAAACACACGGCTTTTTG	Sigma-Aldrich	TRCN0000052193
eIF4AI	si	GCCTTCTGATGTGCTTGAGGTGACCAAGA	Invitrogen	HSS103141
eIF4AII	si	CGATGGTGCATCGAGAGCAACTGGAATG	Invitrogen	HSS103144
eIF4AIII	si	TTGCTCTCGGTGACTACATGAATGTCCAG	Invitrogen	HSS103148
PDCD4	sh	CCGGCTGACCTTTGTGGGACAGTAACTCG AGTTACTGTCCCACAAAGGTCAGTTTTTG	Sigma-Aldrich	TRCN0000059081
Control	sh	CCGGCAACAAGATGAAGAGCACCAACTCG AGTTGGTGCTCTTCATCTTGTGTTTTT	Sigma-Aldrich	HSS103148
Control	si	Medium GC	Invitrogen	12935-300

**Table 17. The sequences of the si and sh RNA molecules used to knock down the three paralogs of eIF4A and PDCD4, together with the controls.**

# Chapter 3. Results

## Part 1.

### The Cell-Based Screen

#### 3.1.1. Introduction

In general, high throughput screens use simple, reproducible reactions that generate easily quantifiable results to screen large libraries of molecules for biological activity (Bleicher *et al.*, 2003). It is the aim of this section to develop and optimise a new screening strategy suitable for detecting inhibition of translation initiation *in vivo*. The cell-based and *in vitro* screens were originally intended for a library of 20, 000 small molecules derived from natural sources purchased from ChemBridge (<http://www.chembridge.com/index.php>).

In some ways, the approach was similar to that used by previous studies to identify small molecule inhibitors of eukaryotic translation (Bordeleau *et al.*, 2005; Bordeleau *et al.*, 2006; Hwang *et al.*, 2004; Low *et al.*, 2005; Novac *et al.*, 2004). While the screening strategy described in these papers was able to test for termination inhibition and IRES-mediated translation inhibition, the strategy outlined here should be more sensitive to eIF4A inhibition (Novac *et al.*, 2004). While the construct used to identify hippuristanol and pateamine A contained a hairpin predicted to have a free energy of -38.00 kcal/mol, the *ODC1* hairpin has a predicted free energy of -82.20 kcal/mol (Novac *et al.*, 2004). This means that the *ODC1* hairpin is predicted to require much more input from eIF4A and therefore be more susceptible to a reduction in eIF4A function (Svitkin *et al.*, 2001). It is possible however that the stability of the *ODC1* hairpin may mean that it is refractory to changes in eIF4A activity and display a narrower signal range. The following sections describe the construction of the plasmids that included the CMV promoter and the hairpin (Figure 3.1.).

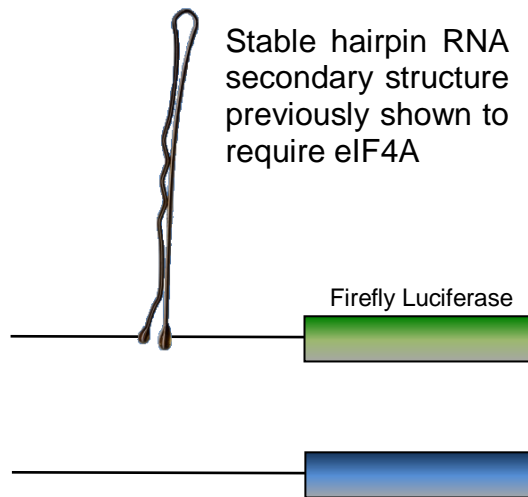


**Figure 3.1. Representations of the mRNA molecules generated by the two plasmids to be used as part of the cell-based screen for eIF4A inhibitors.** The image of the hairpin represents the *ODC1* 5' UTR RNA hairpin, this sequence was cloned upstream of a gene encoding firefly luciferase. Since this structure requires the activity of eIF4A for the efficient expression of the downstream gene, the expression level of the firefly luciferase is proportional to the functionality of eIF4A in cells recipient of these constructs (Svitkin *et al.*, 2001). The *Renilla* luciferase mRNA was co-transfected as a control, it does not contain any 5' sequence predicted to be inhibitory.

Cultured cells were transfected with the plasmids containing these sequences and these cells were subject to treatment with different molecules. If a molecule had specific eIF4A-inhibitory activity, a drop in firefly luciferase expression was observed while the expression of the *Renilla* gene remained constant.

### 3.1.2. Cloning the cytomegalovirus (CMV) promoter

Two plasmids were purchased from Promega (Madison WI), the first was pGL4.15[luc2P/Hygro] and the second pGL4.80[*hRlucP*Neo], Catalogue numbers E6701 and E6981 respectively (Figure 3.2.). Each plasmid contains a different luciferase gene, pGL4.15[luc2P/Hygro] contains the gene derived from *Photinus pyralis*, a species of North American firefly (McDermott, 1911) and pGL4.80[*hRlucP*Neo] encodes a luciferase protein derived from the Sea Pansy *Renilla reniformis* (Milton J, 1960). The reason for the use of these disparate reporter genes is the fact that their products emit light in response to different reagents and as such can be expressed in the same cell and their signals detected individually. Both of the luciferase genes have been modified to include the PEST sequence within their coding regions. Originally identified in the carboxy terminal region of murine ornithine decarboxylase, PEST acts to destabilise the protein giving it a shorter cellular half-life, thereby making the reporter system more sensitive (Loetscher *et al.*, 1991).

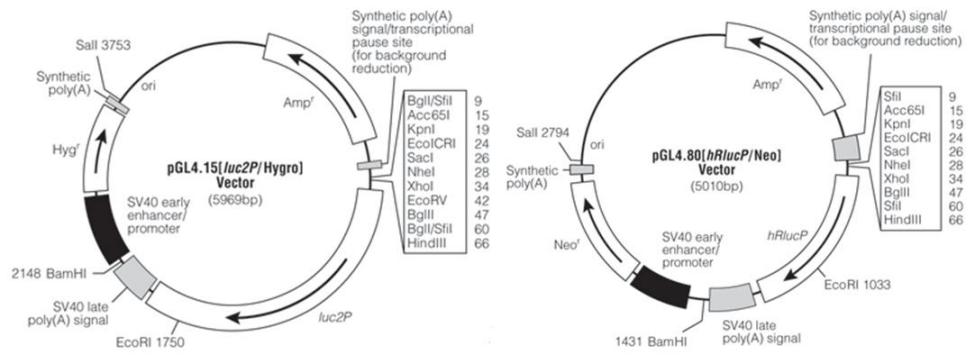


**Figure 3.2. Plasmid maps of pGL4.15 and pGL4.80**

In order to drive the expression of the reporter genes, the cytomegalovirus (CMV) promoter sequence was cloned into both plasmids using *KpnI* and *HindIII* restriction sites (Figure 3.2.).

The CMV promoter sequence was amplified from pcDNA3.1 (Invitrogen, Cat # V385-20) using primers containing a *KpnI* restriction site in the forwards primer and a *HindIII* site in the reverse primer (Table 9.). The PCR was performed using Phusion Hot Start High Fidelity DNA polymerase (Finnzyme, Cat # F-540S) with recommended conditions. Between the final extension and hold stages of the PCR program, 10 units of Taq DNA polymerase (QIAGEN, Cat # 201203) were added to the reaction which was incubated for an extra 15 minutes. This additional step added single adenosine nucleotides to the ends of the PCR product which was purified and ligated into pGEM-T® (Promega, Cat # A3600). The CMV sequence was digested out of this plasmid (termed pGEMTCMV) using *KpnI* and *HindIII* before being cloned into both pGL4.15 and pGL4.80 using these restriction sites. Successful cloning was confirmed by sequencing (Appendix 1. Sequencing) and the completed plasmids, pGL4.15cmv and pGL4.80cmv are referred to in this thesis as p15 and p80 respectively. The plasmids were then tested for activity by transfection into SH-SY5Y cells which were incubated overnight and lysed for luciferase assay the following day, both generated expected signals.

### 3.1.3. Cloning the *ODC1* hairpin into p15 and p80

A version of the plasmid encoding the *Renilla* luciferase (p80) was created in order to demonstrate that any effects of the hairpin were not specific to the firefly luciferase ORF.

The *ODC1* hairpin was previously cloned into the Promega plasmid pGEM®-4Z (by Nicola Phillips, a former member of the RNA Biology Group, University of Nottingham). Standard PCR was used to amplify the sequence; both primers contained *Hind*III restriction sites (Table 9.). The PCR product was digested, purified and cloned into the *Hind*III site immediately downstream of the CMV promoter in both p15 and p80 (Figure 3.4.). Successful cloning was initially confirmed by digestion with *Eco*RI which has a recognition site within the hairpin sequence. This diagnostic digestion revealed that the hairpin had cloned into p15 and p80 successfully and also that some colonies on the p80 ligation plate contained plasmids in which the hairpin had cloned backwards (Figure 3.3.). Sequencing verified that this was the case. Primers including *Spe*I and *Nco*I restriction sites were used to amplify the hairpin (Table 9. Figure 3.3.). The product was digested to completion with *Spe*I and *Nco*I, as was pRF. The hairpin was cloned into pRF between these sites which are located between the two luciferase cistrons. Transcription from the SV40 promoter in the pRF plasmid generates a dicistronic mRNA encoding *Renilla* luciferase and firefly luciferase proteins (Figure 3.3.). This approach has been used for a number of years to test sequences for IRES activity (Stoneley *et al.*, 1998), since the downstream firefly cistron has no cap structure then it will only be expressed if the sequence preceding it is able to initiate translation in a cap-independent manner. It is important to show that the hairpin sequence does not exhibit IRES activity as such activity may interfere with the results and make interpretation more difficult.

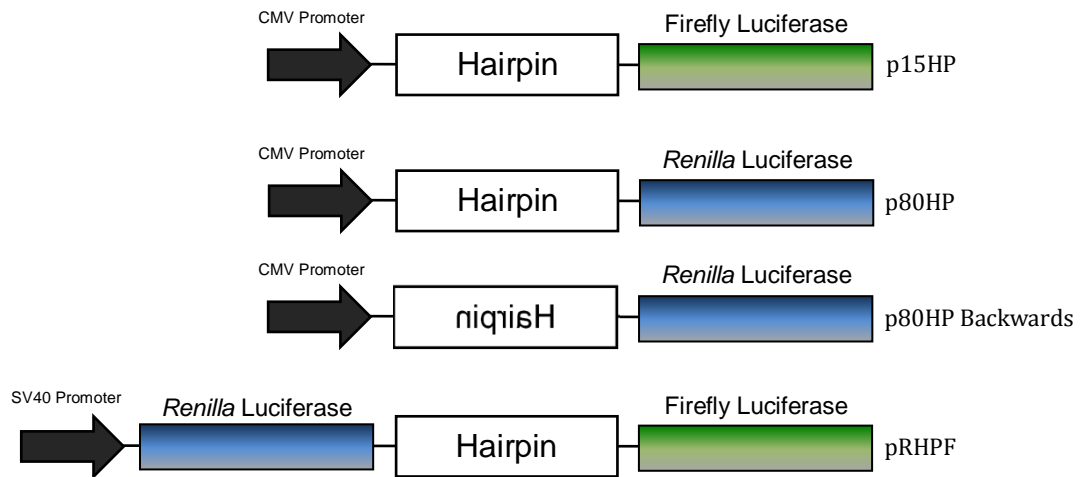


**Figure 3.3. Construct diagrams of p15HP, p80HP, p80HP-Backwards and pRHPF**

*KpnI* CMV Promoter Sequence

GGCCTAACTGGCCGGTACCTCGCGATGTACGGGCCAGATATACGCGTTGACATTGATTATTGACTAGTTATTAAT  
 AGTAATCAATTACGGGGTCATTAGTTTCATAGCCATATATGGAGTTCGCGTTACATAACTACGGTAAATGGCC  
 CGCCTGGCTGACCGCCCAACGACCCCGCCCATTTGACGTCATAATGACGTATGTTCCCATAGTAACGCCAATAG  
 GGACTTTCATTGACGTCAATGGGTGGAGTATTTACGGTAAACTGCCCACTTGGCAGTACATCAAGTGTATCATA  
 TGCCAAGTACGCCCTATTGACGTCAATGACGTAATGGCCCGCTGGCATTATGCCAGTACATGACCTTAT  
 GGGACTTTCCTACTTGGCAGTACATCTACGTATTAGTCATCGCTATTACCATGGTGTATGCGGTTTTGGCAGTACA  
 TCAATGGGCGTGGATAGCGGTTTGACTCACGGGATTTCCAAGTCTCCACCCCATTGACGTCAATGGGAGTTTGT

Sequencing Primer Site pCMVF\_pcDNA3

TTTGGCACAAAATCAACGGGACTTTCCAAAATGTCGTAACAACCTCCGCCCCATTGACGCAAATGGGCGGTAGGC  
 GTGTACGGTGGGAGGCTATATAAGCAGAGCTCTCTGGCTAACTAGAGAACCCTGCTTACTGGCTTATCGAAA

Transcription Start Site

↓ *HindIII* *XhoI*

TTAATACGACTCACTATAGGGAGACCCAAGCTGGCTAGCGTTTTAACTTAAGCTTCTCGAGGGGCGAATACGAAT

ODC Hairpin

TCGTACGTCCCTGCAGCCGCCCGCGCCGCTTCAGTCAGCAGCTCGGGCCACCTCCGGTCGGCGACTGCC

*PacI* *HindIII*

CGGGCTCGACGAGGCGGCTGACGGGGCGCGGGAAGACGGATCCTTAATTAAAAGCTTGGCAATCCGGTAC

Firefly Luciferase

TGTTGGTAAAGCCACCATGGAAGATGCCAAAACATTAAGAAGGGCCAGCGCCATTCTACCCACTCGAAGACGG  
 GACCGCCGGCGAGCAGCTGCACAAAGCCATGAAGCGCTACGCCCTGGTGCCCGGCACCATCGCCTTACCAGCGC  
 ACATATCGAGGTGGACATTACCTACGCCGAGTACTTCGAGATGAGCGTTCCGGTGGCAGAAGCTATGAA.....

**Figure 3.4. The sequence of the CMV promoter and the *ODC1* hairpin in p15**

### 3.1.4. Initial luciferase and transfection reagent test

In order to test that the luciferase was working correctly, p15 was transfected into HeLa and assayed for luciferase activity. Two different transfection reagents, Fugene 6 (Roche, Cat # 05061377001) and Lipofectamine (Invitrogen, Cat # 15338-500) were used to establish which was most effective (Figure 3.5.).

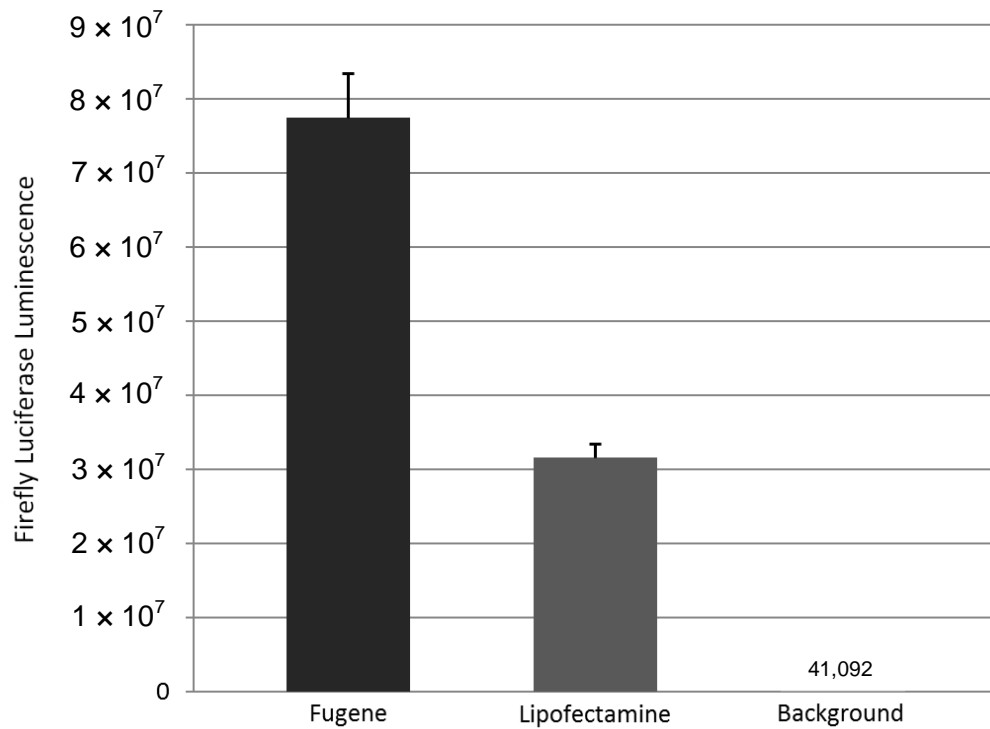


**Figure 3.5. Initial test of p15 activity in HeLa cells.** A 24 well plate was seeded with HeLa cells. The following day, three wells were transfected with p15 at a concentration of 100 ng per well using either Fugene or Lipofectamine. 24 hours later, cells were lysed and luciferase assays were performed. Single experiment, average of three repeats, error bars represent standard deviation. The background signal was generated by luciferase assay reagents in the absence of test sample.

Lipofectamine transfection resulted in a lower luciferase signal (Figure 3.5.). Microscopy revealed that wells treated with this reagent tended to contain an increased number of dissociated cells (data not shown). This indicates that Lipofectamine is not as well tolerated as Fugene and may interfere with the cellular processes under investigation. Based on the results of this experiment, Fugene 6 was used for DNA transfection throughout this project. Regardless of transfection reagent, p15 generates a strong luciferase signal (Figure 3.5.).

### 3.1.5. The hairpin is more inhibitory forwards than backwards

In order to test that the *Renilla* luciferase plasmids were working and that the hairpin had inhibitory activity on the expression of the luciferase, the plasmids p80, p80HP and p80HP-Backwards were transfected into HeLa and assayed for activity 24 hours later. The hairpin caused a decrease in reporter gene expression relative to the control and also the hairpin was more than twice as inhibitory in the forwards orientation (Figure 3.6.).

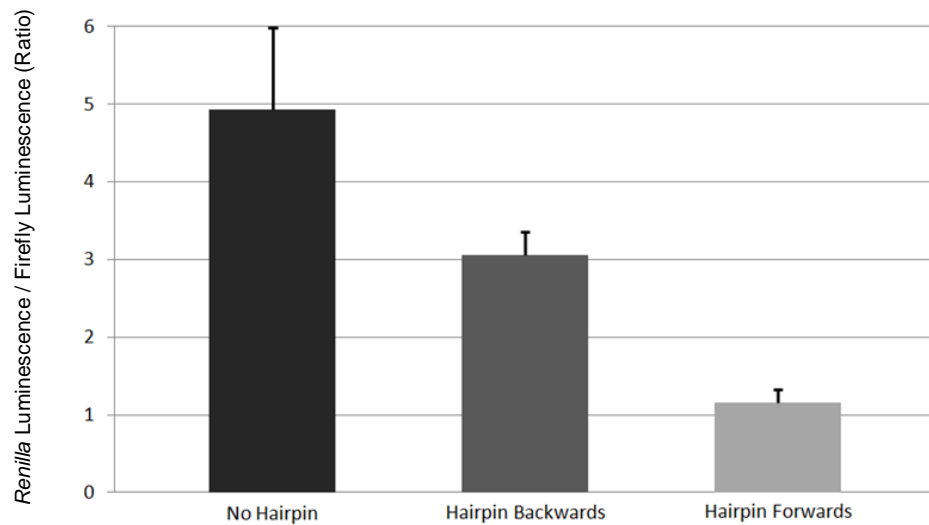


**Figure 3.6. The effect of the hairpin in forwards and reverse orientations on the expression of the downstream *Renilla* luciferase reporter gene in HeLa cells.** A 24 well plate was seeded with HeLa cells. The following day, three wells were transfected with p80 (no hairpin), p80HP and p80HP-Backwards at a concentration of 100 ng of each per well. 24 hours later, cells were lysed and luciferase assays were performed. Single experiment, average of three repeats, error bars represent standard deviation.

This result is unexpected given that the predicted free energy of the hairpin is roughly the same for either orientation.

### 3.1.6. The promoterless reporter

It was important for the interpretation of the subsequent results to demonstrate that the hairpin did not exhibit cryptic promoter activity in this context and behaved as an inhibitory structure.

A promoterless version of p15HP was created by disabling the CMV promoter. The restriction enzyme *AseI* has restriction sites 52 base pairs from the 5' end of the 744 base pair CMV promoter sequence and 48 base pairs from the 3' end, no other *AseI* sites occur in p15HP. p15HP was digested to completion with *AseI*, excising the proximal 644 base pairs of the promoter from the backbone which was then ligated back together.

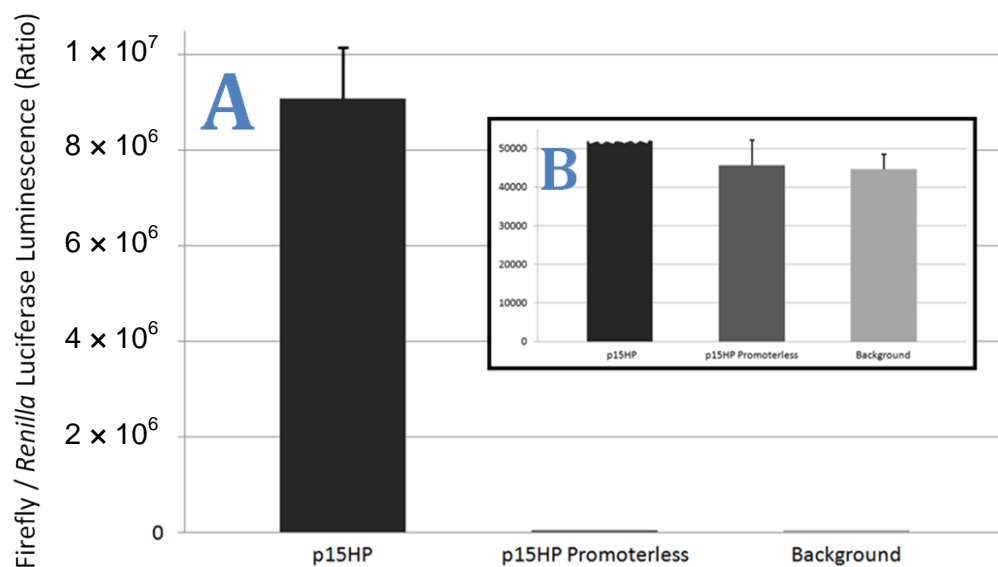


**Figure 3.7. A. – the effect of disabling the CMV promoter on the expression of the firefly luciferase.** A 24 well plate was seeded with HeLa cells. The following day, three wells were transfected with p15HP and p15HP-Promoterless at a concentration of 100 ng per well. 24 hours later, cells were lysed and luciferase assays were performed. Panel B. shows a magnification of the bottom of Panel A. Single experiment, average of three repeats, error bars represent standard deviation. The background luciferase level was determined using lysate from untransfected cells.

Removal of the function of the CMV promoter in p15HP caused a reduction of luciferase expression to background levels (Figure 3.7.). This result confirms that the hairpin does not exhibit promoter activity in this context.

### 3.1.7. shRNA knockdown of eIF4A has an inhibitory effect on the hairpin reporter

The next stage was to test whether the hairpin reporter responded to eIF4A inhibition by suppressing eIF4AI expression in cells transfected with p15HP and p80.

Two pLKO.1-puro plasmids were purchased (Table 18.). One contained a sequence designed to target eIF4AI expression while the other contained a control sequence confirmed to have no target in human cells (Table 18.).

Target	Sequence	Supplier	Cat #
eIF4AI	CCGGGCCGTGTGTTTGATATGCTTACTCG AGTAAGCATATCAAACACACGGCTTTTTG	Sigma-Aldrich	TRCN0000052193
Control	CCGGCAACAAGATGAAGAGCACCAACTCG AGTTGGTGCTCTTCATCTTGTGTTTTT	Sigma-Aldrich	HSS103148

**Table 18. Details of the shRNA plasmids used to test the cell-based screen.**

The sequences shown above (Table 18.) were located within the plasmids downstream of a U6 promoter sequence (Figure 3.8.).

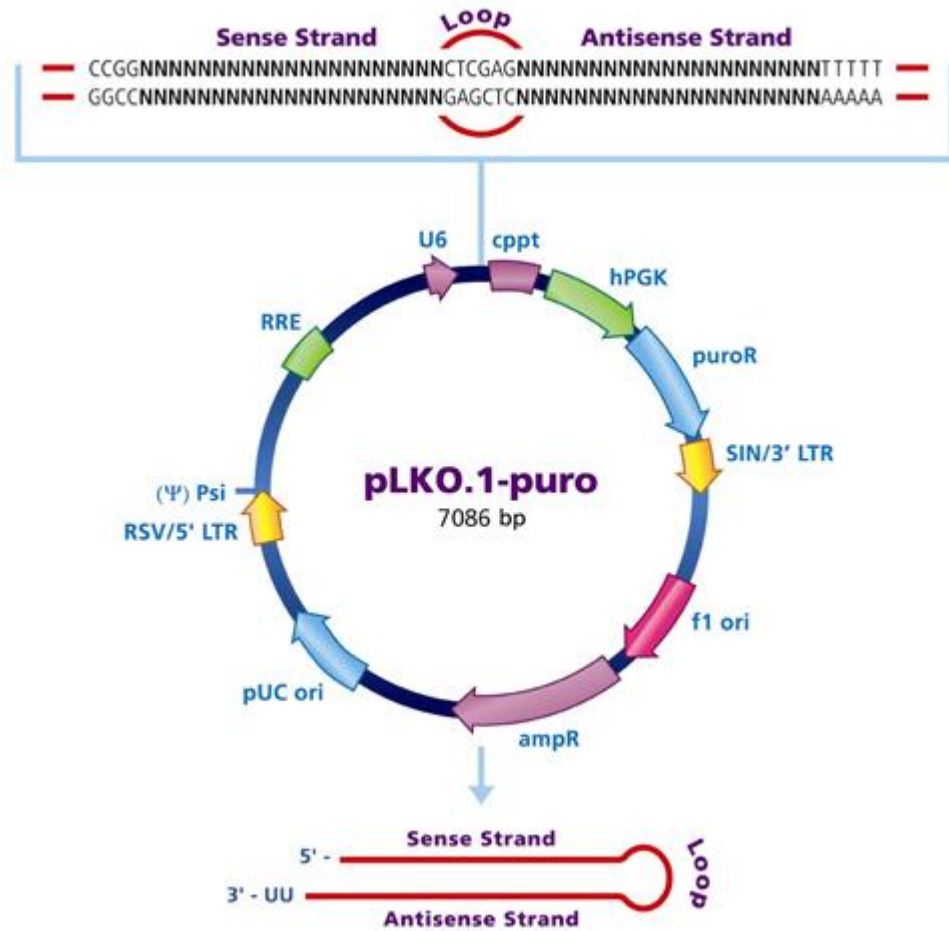
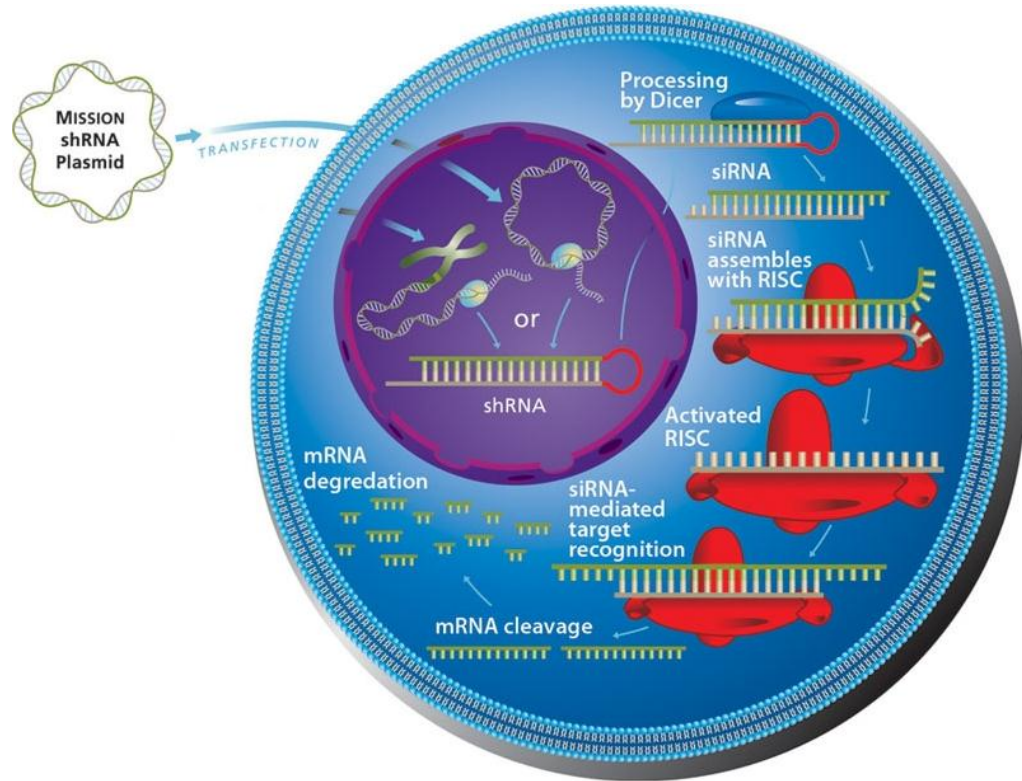


Figure 3.8. Map of the pLKO.1-puro plasmid that contained the eIF4AI and control shRNA sequences.

Following transfection of the shRNA plasmid into cells, the U6 promoter directs RNA polymerase III to generate an uncapped RNA which folds to form the shRNA.

The shRNA is converted to a single strand by Dicer and the RNA-induced silencing complex (RISC) (Reviewed in: (Pratt and MacRae, 2009)). The shRNA is structured so that the strand that remains associated with the RISC is complementary to the coding sequence of eIF4AI (Figure 3.9.).



**Figure 3.9. Mechanism of gene silencing using a MISSION shRNA plasmid.**

Source of diagram: Website Reference 11.

The pairing of the shRNA sequence with the eIF4AI mRNA causes both molecules to be degraded by the cell (Figure 3.9..) (Reviewed in: (Pratt and MacRae, 2009)).

The control and eIF4AI shRNA plasmids were transfected into HeLa cells along with the p80 (control) and p15HP (hairpin-mediated) reporter plasmids.

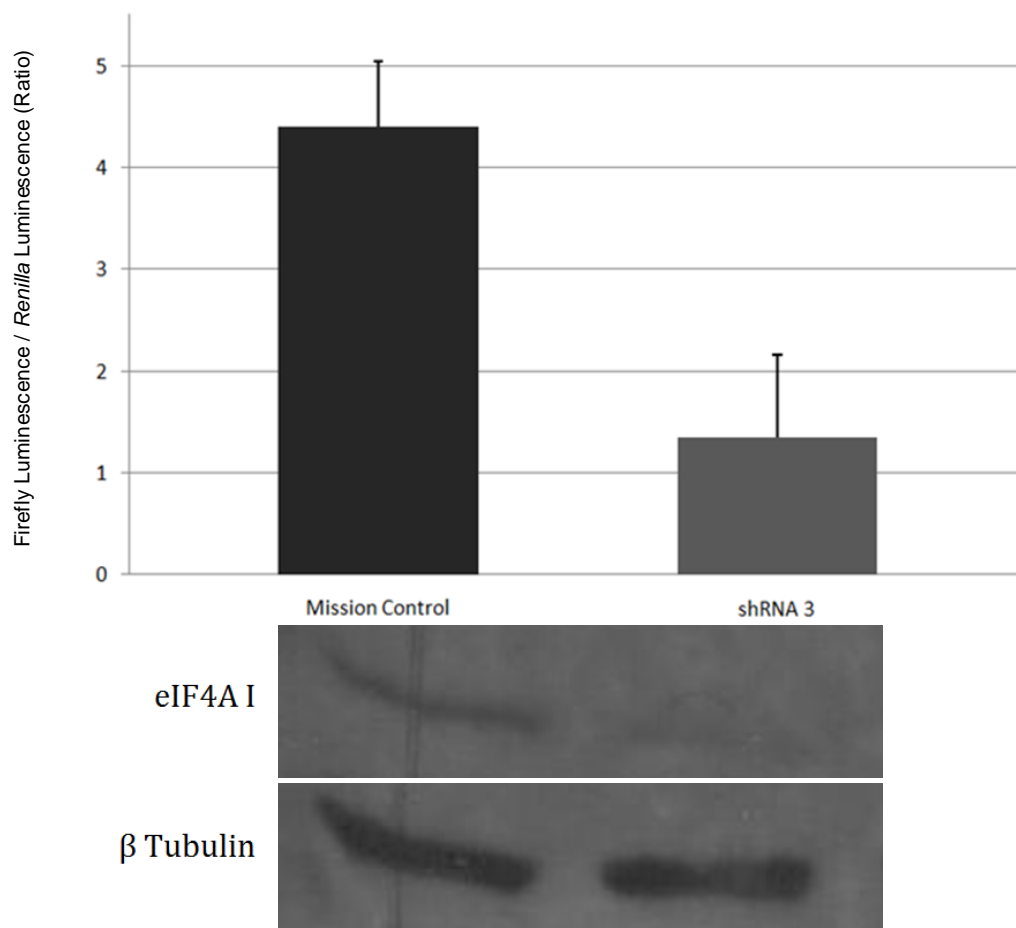


**Figure 3.10. The effect of knockdown of eIF4AI using shRNA.** A 24 well plate was seeded with HeLa cells. The following day, six wells were transfected with p15HP and p80 at a concentration of 100 ng of each per well. Three of these wells were also transfected with the non-target Mission Control plasmid (Sigma-Aldrich MISSION Control, Cat # SHC002) and three with the shRNA plasmid targeting eIF4A. Single experiment, average of three repeats, error bars represent standard deviation. The knockdown plasmid used was: Sigma-Aldrich TRCN0000052193, Clone ID: NM\_001416.1-495s1c1. On the top panel, this plasmid is referred to as shRNA 3, this is because it was the best performing of five knockdown plasmids previously tested for activity. 24 hours later, cells were lysed and luciferase assays were performed. The western blots below the top panel show the protein levels of eIF4AI and  $\beta$  tubulin as part of the initial test of each of the knockdown plasmids. Quantification of the eIF4A bands relative to the  $\beta$  tubulin bands using ImageJ revealed that the eIF4A level in the cells recipient of the knockdown plasmid was approximately 50% lower than those transfected with the control plasmid.

Knockdown of eIF4AI using shRNA caused a significant reduction in the expression of the firefly luciferase reporter plasmids containing the hairpin sequence relative to the control *Renilla* luciferase reporter ( $p = 0.032$ ) (Figure 3.10).

### 3.1.8. Hippuristanol has an inhibitory effect on the hairpin reporter

With eIF4A expression attenuation clearly detectable by the reporter system, cells transfected with the hairpin-reporter and control plasmids were treated with hippuristanol in order to establish whether the system was sensitive enough to identify small molecule inhibition of eIF4A. Based on previous literature, it was predicted that hippuristanol would cause a large drop in the expression of the luciferase preceded by the hairpin (Bordeleau *et al.*, 2006; Svitkin *et al.*, 2001).

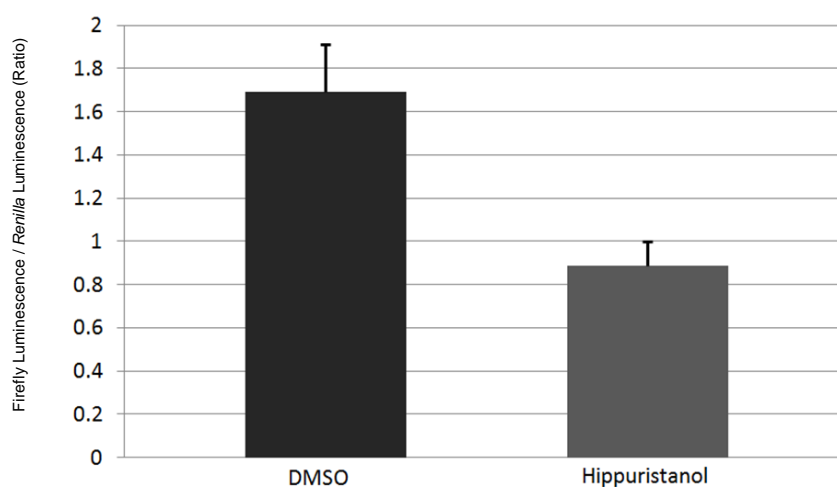


**Figure 3.11. The effect of 10  $\mu$ M hippuristanol treatment on the expression of the firefly luciferase encoded by p15HP.** A 24 well plate was seeded with HeLa cells. The following day, six wells were transfected with p15HP and p80 at a concentration of 100 ng of each per well. 24 hours later, the growth medium was changed for fresh medium (100  $\mu$ l per well) containing 10  $\mu$ M hippuristanol or DMSO (in which the hippuristanol was dissolved), three wells were recipient of each. Following a six hour incubation, cells were lysed and assayed for luciferase activity. Single experiment, average of three repeats, error bars represent standard deviation.

Hippuristanol treatment caused a significant reduction in the expression of the firefly luciferase encoded by p15HP relative to the DMSO control ( $p = 0.0046$ ) (Figure 3.11.). When this experiment was repeated in SH-SY5Y, similar results were generated (data not shown).

### 3.1.9. Optimisation of the hairpin reporter using hippuristanol

10  $\mu$ M hippuristanol treatment causes a ~50% reduction in hairpin-mediated reporter expression (Figure 3.11.). While this result was expected, the magnitude of the effect was disappointing. If the hairpin reporter system were to be used in a high throughput context then it would be advantageous if it were much more sensitive. Like the shRNA directed against eIF4A, hippuristanol treatment represents a positive control for the screen. In order to test whether the assay would be more sensitive with a shorter recovery time, an experiment was performed in which this recovery period was reduced from 24 hours to four hours (Figure 3.12.).

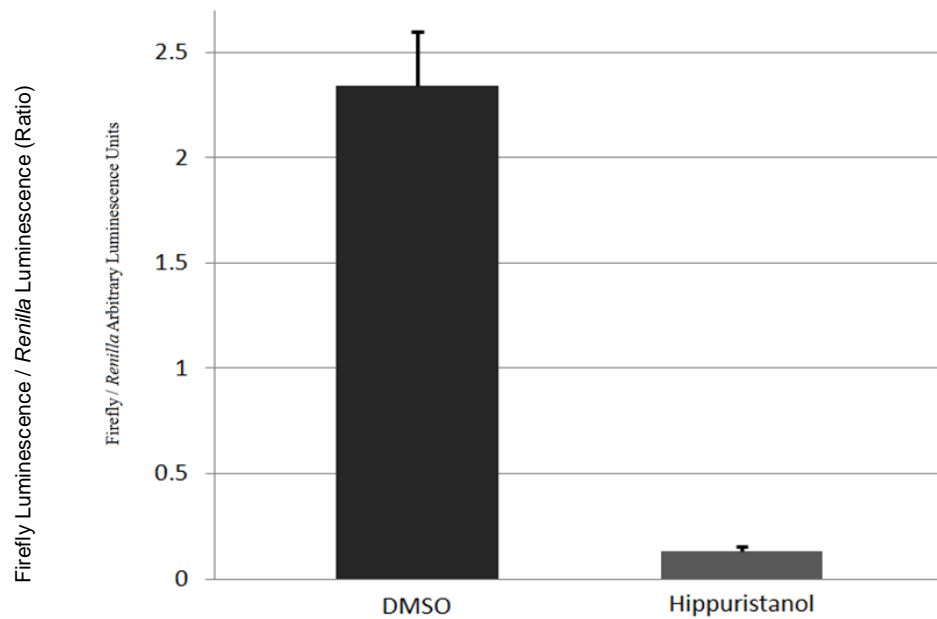


**Figure 3.12. The effect of 10  $\mu$ M hippuristanol treatment on the hairpin reporter in HeLa after allowing cells only four hours to recover from transfection.** The experiment was performed exactly as described in the legend to Figure 3.11.. except that the 24 hour recovery phase was reduced to four hours. Single experiment, average of three repeats, error bars represent standard deviation.

The assay was much more sensitive using this approach (Figure 3.122.), the addition of 10  $\mu$ M hippuristanol caused a 94% reduction in normalised luciferase expression relative to the control ( $p = 0.00028$ ). The magnitude of the effect and the low standard deviations indicate that the hairpin reporter system (or ‘cell-based screen’) would be suitable for use in a high throughput context. It is probable that the four hour recovery from transfection did not allow the firefly luciferase protein to accumulate to the same level as after the 24 hour recovery. There was therefore less of it to degrade following the treatment of the cells with hippuristanol

### 3.1.10. The hairpin reporter system is suitable for screening eIF4E inhibitors

Since structured mRNAs have a greater requirement for eIF4E as well as for eIF4A, it was proposed that the hairpin reporter system may also be suitable for screening for eIF4E inhibitors (Graff *et al.*, 2008; Svitkin *et al.*, 2001). The positive control in this experiment was a 5' cap analogue; these molecules competitively bind eIF4E and prevent it from anchoring the translation initiation complex to the mRNA 5' cap (Cai *et al.*, 1999). In addition to the cap analogue, it was decided that the system should also be used to test 12 small molecules identified as potential inhibitors of eIF4E by an *in silico* screen (undertaken by Francois Meullenet, a former member of the RNA Biology Group, University of Nottingham).

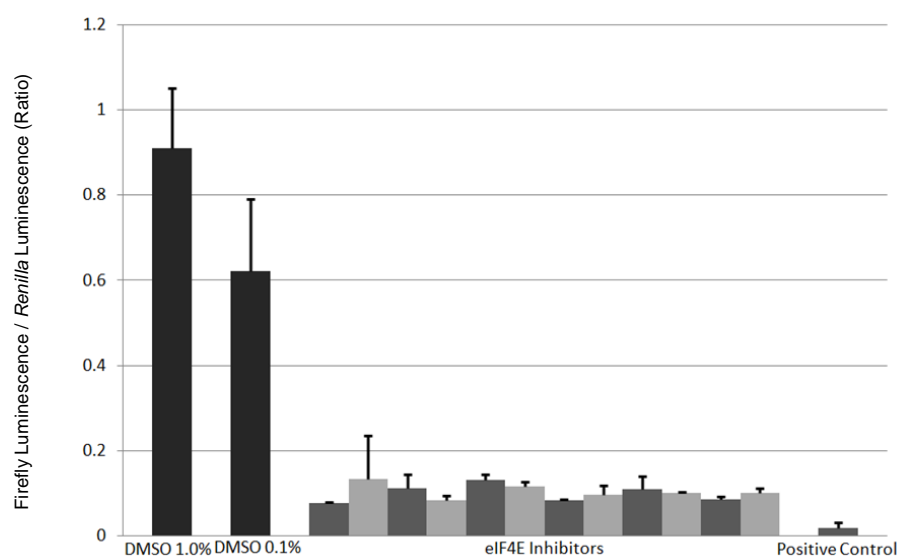


**Figure 3.13. The effect of predicted and actual eIF4E inhibitors on the hairpin reporter.** Four 24 well plates were seeded with HeLa cells. The following day, all of the wells were transfected with p15HP and p80 at a concentration of 100 ng of each per well. Four hours later, the growth medium was changed for 100  $\mu$ l fresh medium per well. Wells were treated in triplicate with either DMSO, one of the unknown molecules predicted to be inhibitory to eIF4E or the positive control (cap analogue). Following a six hour incubation, cells were lysed and assayed for luciferase activity. Single experiment, average of three repeats, error bars represent standard deviation.

All of the compounds, including the positive control, caused a significant reduction in hairpin-mediated firefly luciferase expression relative to both the *Renilla* luciferase and the DMSO controls (Figure 3.13.). This indicates that the cell-based screen is able to detect eIF4E inhibition and that all of the 12 molecules identified by the *in silico* screen have biological activity consistent with their predicted properties.

### 3.1.11. Screening FDA approved drugs

With the cell-based screen demonstrated to be able to detect and quantify eIF4E inhibition (Figure 3.13.), it was proposed that it may also be able to detect mTOR inhibition. Suppression of mTOR activity results in the dephosphorylation of 4E-BP1 which then binds eIF4E and sequesters it away from the eIF4F complex (Wang *et al.*, 2007). The mTOR signalling pathway also results in the phosphorylation, and therefore activation, of eIF4B which is a stimulating co-factor of eIF4A (Shahbazian *et al.*, 2006). If mTOR were to be inhibited and eIF4B became less active then the translation of highly structured mRNAs, like the hairpin reporter, is likely to be reduced to a greater extent than non-structured messages (Shahbazian *et al.*, 2010).

Like the assay of the predicted eIF4E inhibitors, molecules predicted to be inhibitors of mTOR were identified as part of another project (undertaken by Sarah Smalley, a member of the Biochemistry Department, University of Sussex). The predicted function of these molecules was not revealed until after the experiment so no positive control was included. However, it would be interesting to test the effect of rapamycin treatment on the cell-based screen in the future (Brown *et al.*, 1994). The identity of the seven molecules provided for assay was not revealed but they have all been previously approved by the FDA (Food and Drug Administration) and all are able to modulate the expression of the oncogene O-6-methylguanine-DNA methyltransferase (MGMT). Any molecule that suppresses the activity of MGMT will be of clinical interest but especially so if this molecule has already been granted approval for use in humans by the FDA.

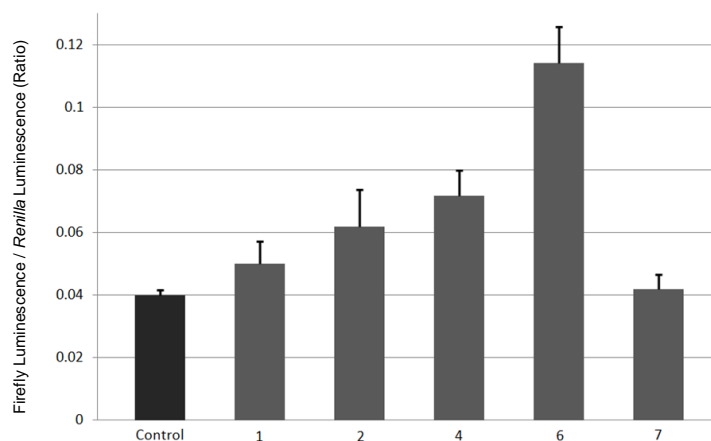


**Figure 3.14.** The effect of the FDA-approved drugs on the expression of the firefly luciferase in p15HP normalised to the *Renilla* luciferase control. The experiment described in the legend to Figure 3.13 was repeated with the only difference being the molecules used to treat the cells. Single experiment, average of three repeats, error bars represent standard deviation.

Three of the molecules caused a significant increase in normalised p15HP luciferase expression relative to the control (Figure 3.14.). The result for compound five is absent due to the fact that treatment with this molecule killed the cells. The concentration of compound five was reduced in a repeat experiment to 0.500×, 0.250× and 0.125× the quantity that killed the cells. Although reduced mortality was observed with reducing concentration, there was no difference between treatment and control (data not shown). Without a positive control, no confident conclusions can be drawn from this experiment and therefore it is not known whether the cell-based screen is able to detect molecules that exhibit this activity.

## Part 2.

### *In Vitro* Screen Results

#### 3.2.1. Introduction

The high throughput screens that led to the discovery of hippuristanol, pateamine A and silvestrol used *in vitro* (reticulocyte lysate-based) approaches (White, 2000). The advantages of *in vitro* assays include their affordability, simplicity, specificity and the fact that they are not subject to inconsistencies arising from cell confluency or passage fluctuations (Masimirembwa *et al.*, 2001). The main disadvantages of the *in vitro* approach compared to the cell-based approach are that shRNA knockdown cannot be used and that *in vitro* assays are inherently more artificial than those using live cells (Masimirembwa *et al.*, 2001). A good example of when the two assays can work in concert in this project is in adjusting for cell membrane permeability and toxicity. A molecule may have strong eIF4A-inhibitory activity but at the concentration used in the cell-based assay, it may not pass through the cell membrane or it may be toxic to the cell and therefore register only as a hit in the *in vitro* screen.

Given the strengths and weaknesses of each, it was decided that both should be designed and optimised as part of this project. The previous section describes the construction and optimisation of the cell-based screen (using the hairpin reporter system) while this section will outline the optimisation stages of the *in vitro* screen.

Compared to the cell-based screen which involved well established principles, the *in vitro* screen was highly experimental. Two main approaches were assessed for their suitability for use in a high throughput context.

##### 3.2.1.A. Ethidium bromide (EtBr) incorporation

Ethidium bromide binds to DNA by intercalating between the bases of the double stranded molecule or to RNA between the nucleotides that are double stranded as part of the secondary structure (Gatti *et al.*, 1975). Although EtBr can bind single stranded DNA and RNA, crucially, this interaction is significantly weaker than its intercalation with double stranded molecules (Cosa *et al.*, 2001). The EtBr-based *in vitro* screen reaction consisted of a short RNA duplex between which, EtBr molecules were intercalated, together with eIF4A and the buffers needed for it to function and ATP. Incubation of this reaction should allow the eIF4A to unwind and separate the duplex, causing a quantifiable drop in EtBr signal proportional

to the activity of the eIF4A. The inclusion of RNase T1, which cleaves only single stranded RNA, may increase the observed effect of strand separation (Figure 3.15.) (Czaja et al., 2004).

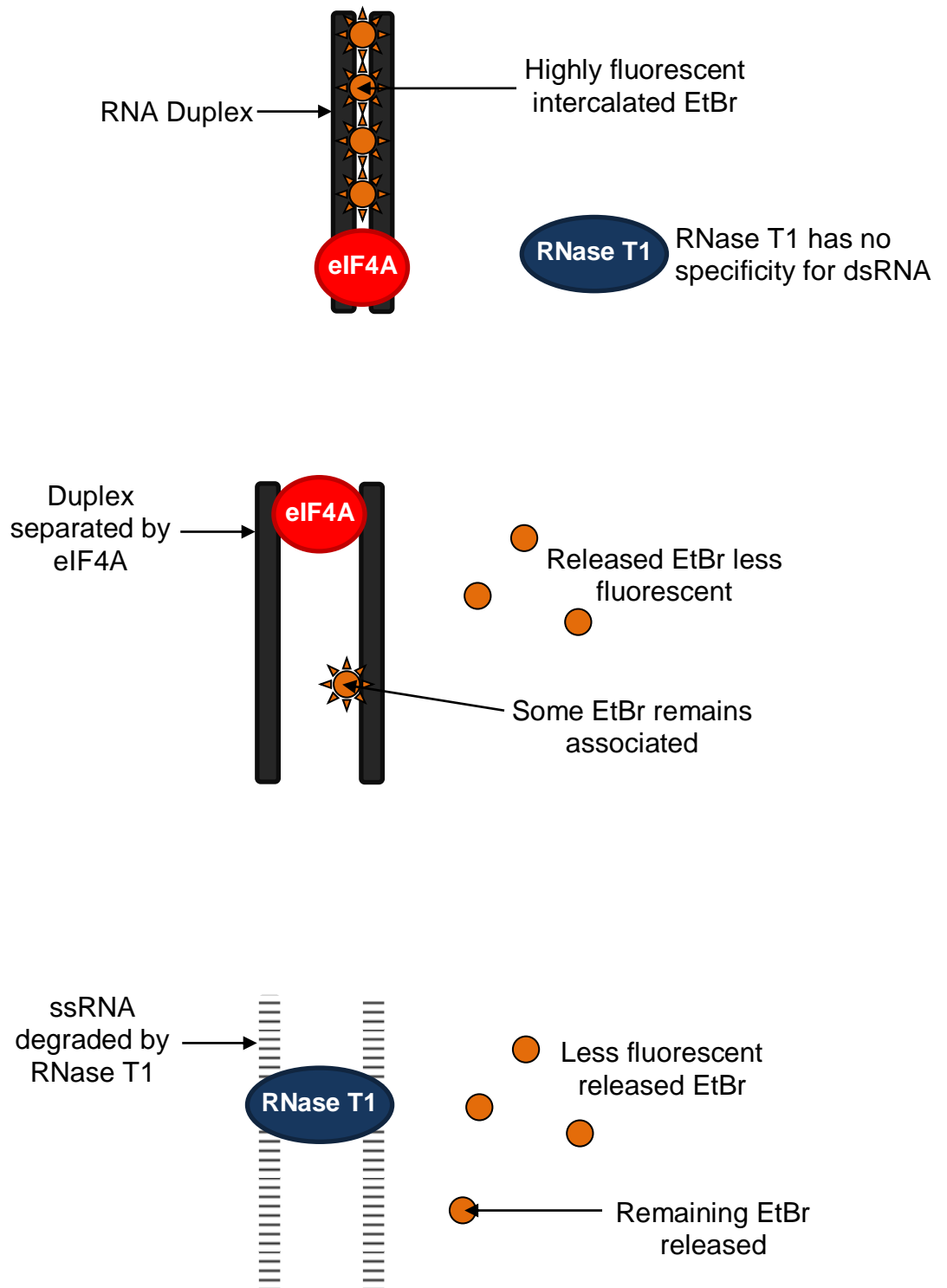


**Figure 3.15. The principle of the *in vitro* screen.** If the eIF4A successfully unwinds the duplex, a drop in EtBr fluorescence should be observable. The bottom panel shows that RNase T1 may increase the dynamic range of this fluorescence change by degrading the single stranded RNA.

The use of ethidium bromide in this way has been documented previously as part of a study that used a similar approach to assay the RNA-cleaving activity of a deoxyribozyme (a catalytic DNA motif) (Ferrari and Peracchi, 2002). This study concluded that the technique is simple, fast and inexpensive and should up-scale easily to multi-well plates (Ferrari and Peracchi, 2002). If the attributes of the assay described above are transferable to an assay for eIF4A activity then it is likely that this may prove to be a very effective high-throughput screening strategy.

#### **3.2.1.B. ATP usage quantification**

Since eIF4A is an ATP-dependent RNA helicase, incubation of the duplex reaction described above will be accompanied by a drop in ATP concentration as eIF4A converts it to ADP in order to process the duplex. The Materials and Methods section outlines the two protocols used to assay ATP availability as part of this project.

### 3.2.2. Helicase Assay

The first stage in the creation of a new *in vitro* screen for eIF4A activity was to check whether the stock of eIF4A was functional. For this purpose, a radioactive helicase assay was performed.

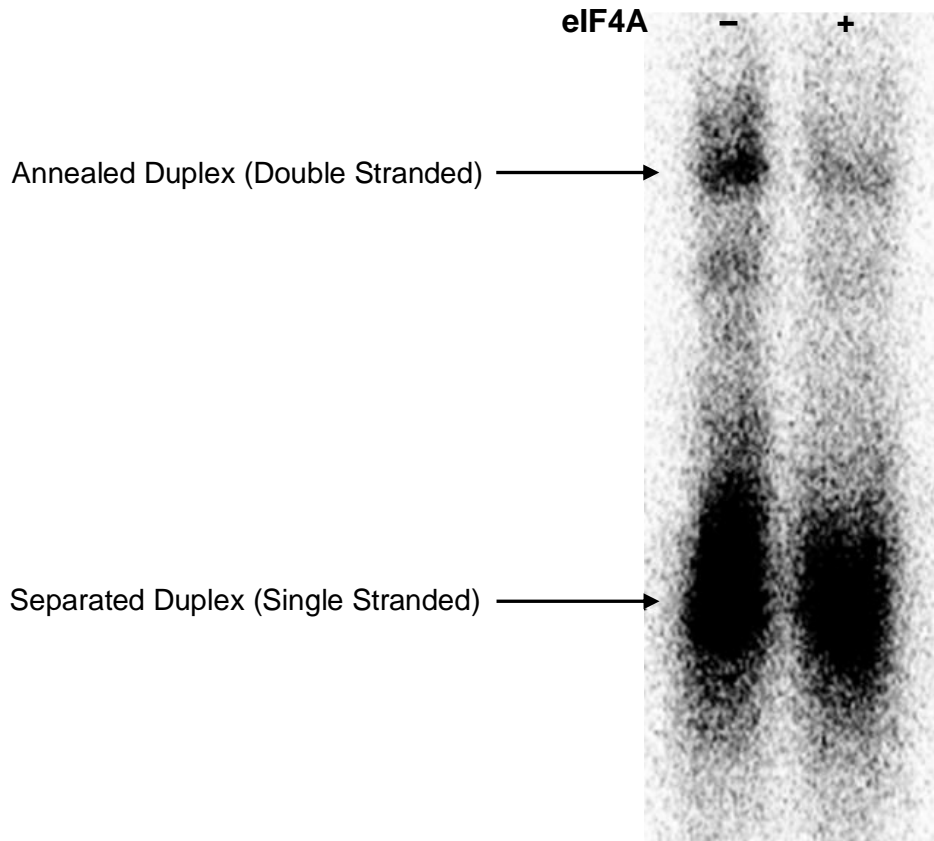


**Figure 3.16. *In vitro* radioactive assay for RNA helicase activity.** The reaction visualised in the left lane did not contain eIF4A while the reaction on the right did contain eIF4A.

Addition of eIF4A caused the separation of a semi-radioactive RNA duplex consisting of an unlabelled 44 nucleotide molecule and a radiolabelled 13 nucleotide molecule (Figure 3.16.). Image quantification using ImageJ (using Rolling Ball and Watershed algorithms) (Abramoff et al., 2004) revealed that the larger nucleotide sized band decreased by approximately 50% between the two treatments indicating that the eIF4A had separated the duplex. The reason for the presence of so much separated duplex in the control lane is unknown. Performing the helicase assay at a lower temperature may reduce the amount of spontaneous duplex separation.

### 3.2.3. Ethidium bromide incorporation.

With a stock of eIF4A confirmed to have activity *in vitro*, the next stage was to test the sensitivity of ethidium bromide at detecting the presence of RNA. If the assay was to work then double stranded RNA would have to stimulate EtBr emission to a level much higher than background. The difference in EtBr signal between the presence and absence of RNA is predicted to be greater than the difference between double- and single-stranded RNA so the maximum effect eIF4A can have on the assay will be less than the difference between plus and minus RNA (Figure 3.17.).

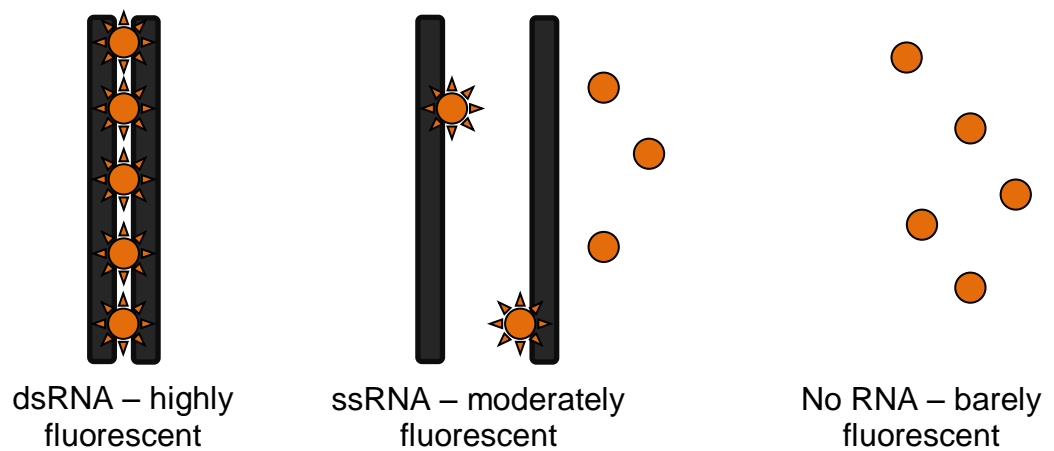


**Figure 3.17. Ethidium bromide is most fluorescent when associated with double stranded RNA**

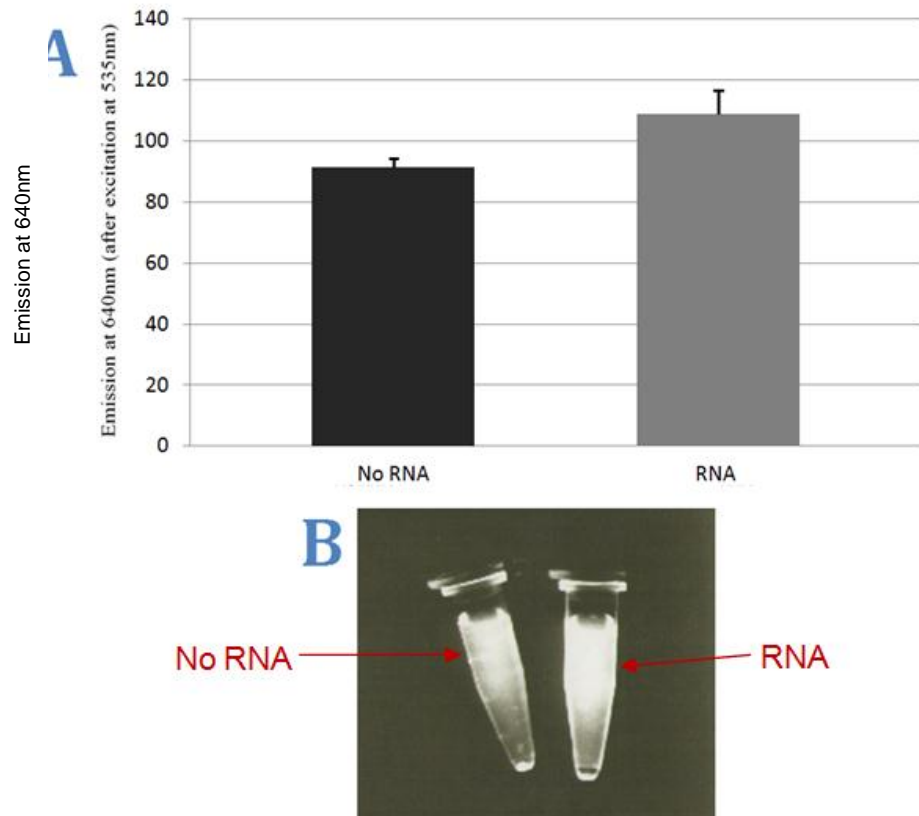


**Figure 3.18. Ethidium bromide solution with and without dsRNA.** 4.5  $\mu\text{g}$  double stranded RNA identical in sequence to the duplex used previously was suspended in 1200  $\mu\text{l}$  of water to give a final concentration of 0.5  $\text{pmol}/\mu\text{l}$  (Rogers *et al.*, 1999a). A final concentration of 0.01  $\mu\text{g}/\mu\text{l}$  ethidium bromide (EtBr) was also added. Part A. shows the effect of the addition of RNA on the emission of the EtBr solution measured at a wavelength of 640 nm following excitation at 535 nm. Single experiment, average of three repeats, error bars represent standard deviation. Part B. shows the tube containing this solution photographed under UV light adjacent to a tube containing only the water and EtBr (no RNA).

The presence of 4.5  $\mu\text{g}$  of double stranded RNA caused an approximate 16% increase in EtBr excitation compared to an RNA concentration of 0  $\mu\text{g}$  ( $p = 0.0279$ ) (Figure 3.18. A.). This proportion is mirrored in the image below Panel A. (Figure 3.18. B.); the tube containing the RNA appears brighter but only marginally.

It would be interesting to investigate the effect of denaturing the duplex or using single stranded RNA.

In a repeat experiment, the concentration of EtBr was reduced from 0.01  $\mu\text{g}/\mu\text{l}$  to 0.001  $\mu\text{g}/\mu\text{l}$ . It was predicted that this would reduce the amount of EtBr that is not associated with the RNA duplex, thereby lowering the background. Disappointingly however, the signal from the replicates containing the RNA decreased by the same proportion as the background. Although EtBr has been used in solution in other studies (Ferrari and Peracchi, 2002), it must be concluded that it is not appropriate for use as part of the *in vitro* screen protocol.

### 3.2.4. SYBR Safe Incorporation 1.

Like EtBr, SYBR Safe is commonly used to visualise DNA and RNA as part of gel electrophoresis (Martineau *et al.*, 2008). With the previous results indicating that EtBr would not be sensitive enough for use in the *in vitro* assay, SYBR Safe was trialled instead.

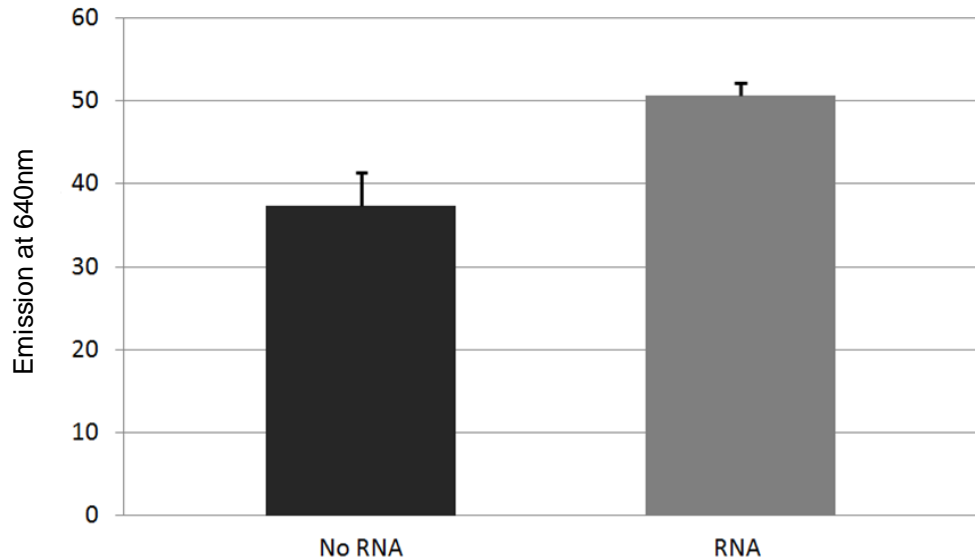


**Figure 3.19. Fluorescence of 1000x SYBR Safe (1  $\mu$ l in 20  $\mu$ l volume) in the presence / absence of 4500 ng dsRNA.** The experiment described in the legend to Figure 3.18. was repeated with SYBR Safe in place of EtBr. Single experiment, average of three repeats, error bars represent standard deviation.

A 28% increase in fluorescence was observed in the tube containing the RNA relative to the tube without ( $p = 0.0262$ ) (Figure 3.19.). This was a bigger difference than that observed using EtBr (which was 16%).

### 3.2.5. SYBR Safe Incorporation 2.

With the results on the previous page showing that SYBR Safe was more sensitive than EtBr at detecting the presence of RNA, it was decided that it could progress to the next stage and it could be added to helicase assay reactions with and without either eIF4A or RNase T1. It is not apparent from the literature whether SYBR Safe is an intercalating agent in the same way as EtBr; it is therefore not possible to predict the effect of the action of eIF4A on an RNA duplex stained with SYBR Safe. RNase T1 was also added to some reactions in order to see whether it increased the magnitude of the observed effect of eIF4A on the emission signal from the reaction. Since RNase T1 only cuts single stranded RNA, it was predicted that it would cleave RNA previously separated by the eIF4A, thereby reducing the signal from the SYBR Safe.

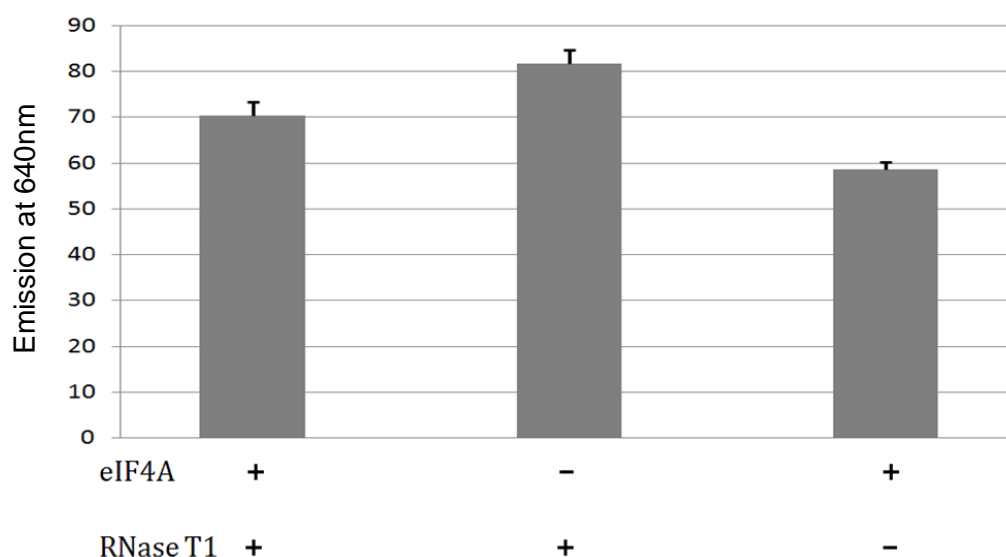


**Figure 3.20. Fluorescence of 1000x SYBR Safe (1  $\mu$ l in 20  $\mu$ l volume) and 4500 ng dsRNA in the presence / absence of eIF4A and RNase T1.** SYBR Safe was added to the standard helicase assay reaction (see Materials and Methods) which contains the RNA duplex, eIF4A and the buffers needed for it to function. Reactions were incubated at 37°C for 15 minutes before the stop solution (see Materials and Methods) was added. Stopped reactions were subject to light with a wavelength of 535 nm and their emission at 640 nm was recorded. Single experiment, average of three repeats, error bars represent standard deviation.

The presence of eIF4A in the helicase assay reaction containing SYBR Safe caused a 28% reduction in fluorescence relative to the non-eIF4A control in the absence of RNase T1 ( $p = 0.0423$ ) and a 15% reduction in the presence of RNase T1 (Figure 3.20). Although the results are as expected for eIF4A, there is not a great deal of difference between the reactions that did and did not contain eIF4A.

### 3.2.6. ATP usage – DiFMUP 1.

Since eIF4A is an ATP-dependent RNA helicase, as the helicase assay reaction progresses ATP will be used (Grifo *et al.*, 1982). DiFMUP is an ATP analogue that becomes fluorescent when it is dephosphorylated (Williams and Scott, 2009). Increased fluorescence resulting from a helicase assay containing DiFMUP indicates a greater rate of ATP usage.

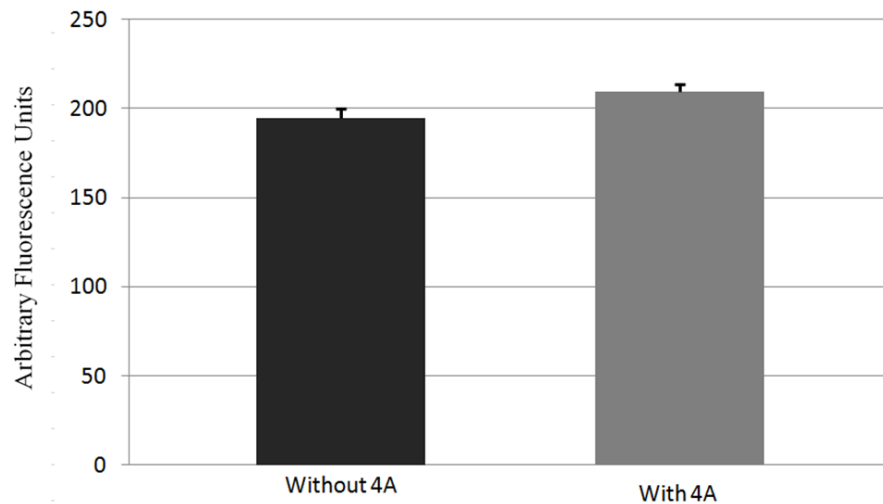


**Figure 3.21. The helicase assay reaction containing DiFMUP with and without eIF4A.** 10 µg/ml DiFMUP was added to the standard helicase assay reaction that either contained or did not contain eIF4A. These reactions were incubated at 37°C for 15 minutes before the stop solution was added. The stopped reactions were excited using light with a wavelength of 365 nm and emission was quantified at 640 nm. Single experiment, average of three repeats, error bars represent standard deviation.

The inclusion of eIF4A in the helicase assay reaction containing DiFMUP caused an 8% increase in quantified ATP usage ( $p = 0.022$ ) (Figure 3.21.). The high background fluorescence from the reaction without eIF4A was a problem.

### 3.2.7. ATP usage – DiFMUP 2.

In order to determine the reaction component responsible for the high background observed in the previous figure, the concentrations of RNA, ATP and eIF4A were varied independently.

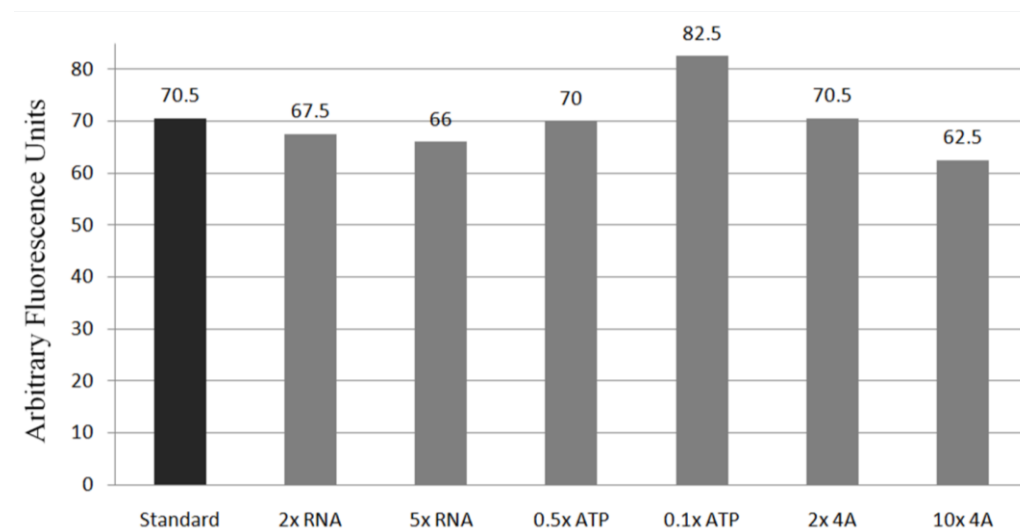


**Figure 3.22. The effect of varying reaction component concentrations on the sensitivity of DiFMUP.** The standard helicase assay reaction containing 10  $\mu\text{g/ml}$  DiFMUP was repeated using different concentrations of RNA, ATP and eIF4A. The standard helicase assay reaction consists of: 20 mM HEPES (pH 7.2), KCl 70 mM, 2 mM dithiothreitol, 1 mg/ml bovine serum albumin, 1 mM magnesium acetate, 1 mM ATP, 1.7-1.8 nM RNA duplex and 0.4 mM eIF4A. Single experiment, one replicate per condition.

The only condition that caused a noticeable difference (a 15% increase) in observed ATP usage relative to the control is the tenfold reduction in ATP concentration (Figure 3.22.). This is expected given that DiFMUP is an ATP analogue, and reduction of the actual ATP is likely to increase the relative concentration of DiFMUP in the reaction meaning that more of it will be converted to its fluorescent breakdown product.

The fact that increasing RNA and eIF4A concentrations cause reduced PiColorlock signals may be contrary to expectations but it must be kept in mind that just one replicate was performed for each condition.

### 3.2.8. ATP usage – DiFMUP 3.

In order to test at which time-point the DiFMUP assay was most sensitive, a timecourse experiment was performed using varying ATP concentrations.

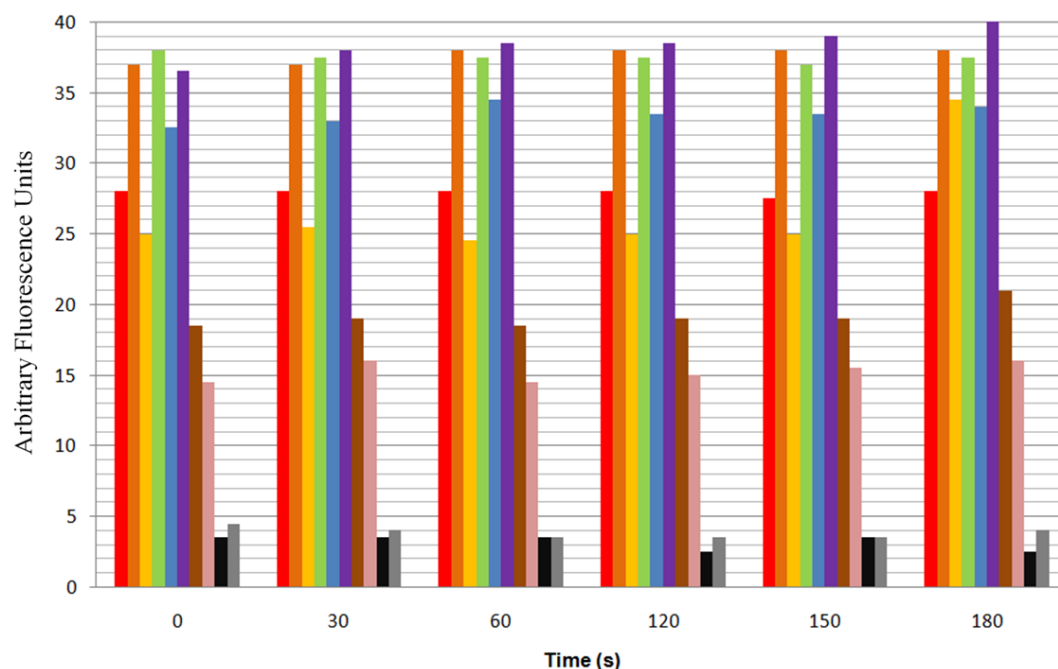


**Figure 3.23. A timecourse of helicase assay reactions containing DiFMUP and varying concentrations of ATP.** The helicase assay including DiFMUP was repeated using varying ATP concentrations, with and without eIF4A over a timecourse of 180 seconds. Colour Key: 0 ATP, 0 ATP + eIF4A, 1% ATP, 1% ATP + eIF4A, 10% ATP, 10% ATP + eIF4A, 100% ATP, 100% ATP + eIF4A, 1000% ATP, 1000% ATP + eIF4A. ATP concentrations are expressed as percentages of the concentration in the standard helicase assay reaction. The standard helicase assay reaction consists of: 20 mM HEPES (pH 7.2), KCl 70 mM, 2 mM dithiothreitol, 1 mg/ml bovine serum albumin, 1 mM magnesium acetate, 1 mM ATP, 1.7-1.8 nM RNA duplex and 0.4 mM eIF4A. Single experiment, one replicate per condition.

The reactions containing lower concentrations of ATP (including 0% ATP) were more sensitive to the presence of eIF4A than those containing higher concentrations of ATP (Figure 3.23.). This result is expected given that lower concentrations of ATP increase the relative concentration of DiFMUP in the reaction. This means that a greater percentage of DiFMUP is likely to be converted to its fluorescent breakdown product.

The time course made little difference to the fluorescence measured for any of the reactions. It would be interesting to repeat this experiment over a range of different temperatures. This may reveal that DiFMUP undergoes spontaneous breakdown and that lower temperatures may reduce the background level of DiFMUP fluorescence.

### 3.2.9. ATP Usage – PiColorlock 1.

Another approach for quantifying ATP usage was tried. PiColorlock increases in absorbance at 635 nm in the presence of inorganic phosphate ( $P_i$ ) which is a break-down product of ATP (Freschauf *et al.*, 2010).

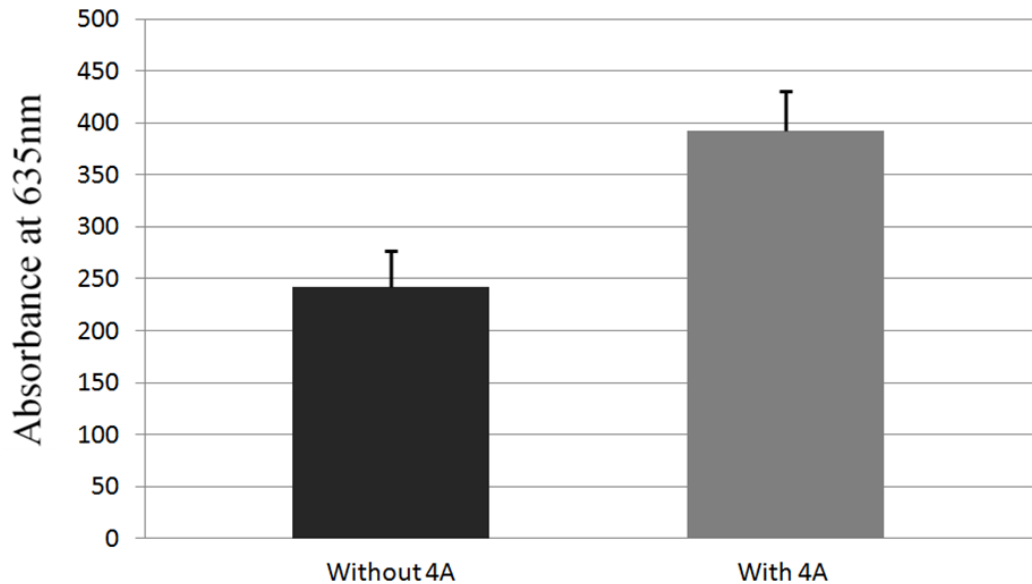


**Figure 3.24.** The standard helicase assay reaction containing PiColorlock was incubated at 37°C for 15 minutes with and without eIF4A before the absorbance of the reaction at 635nm was measured. Single experiment, average of three repeats, error bars represent standard deviation.

The inclusion of eIF4A in the helicase assay reaction caused a 34% increase in  $P_i$  concentration as quantified by the absorbance of PiColorlock at 635 nm ( $p = 0.0036$ ) (Figure 3.24.).

### 3.2.10. ATP Usage – PiColorlock 2.

While the approach shown in the previous figure was the most successful so far, the background signal is still high. The reaction components were incubated with the PiColorlock reagent independently in order to ascertain the cause of the background.

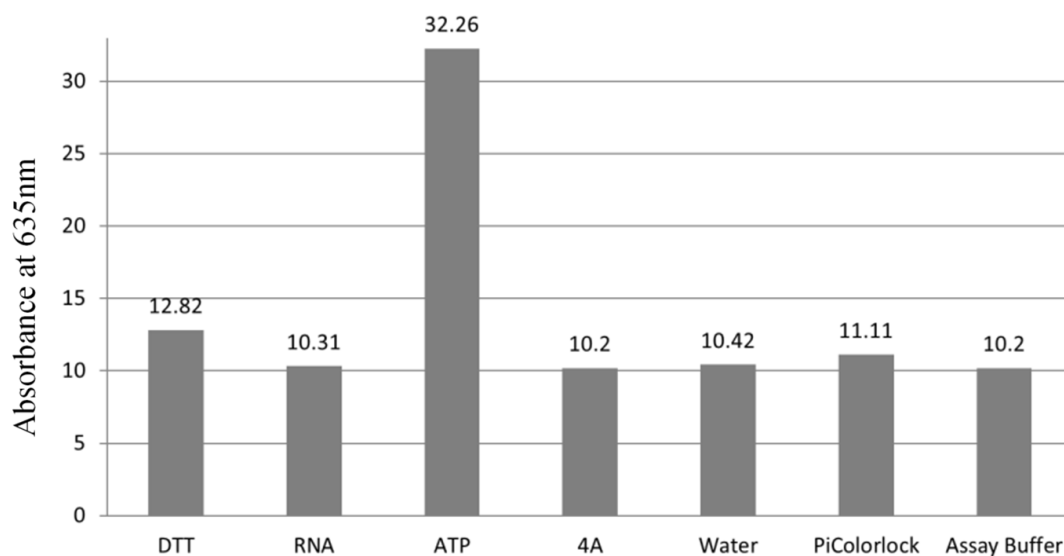


**Figure 3.25. The effect of the helicase assay reaction components on the absorbance of PiColorlock.** All of the individual reaction components of the helicase assay were combined with PiColorlock and incubated at 37°C for 15 minutes before the absorbance at 635 nm of each mixture was quantified. Single experiment, one replicate per condition.

ATP was the only reaction component that caused a noticeable increase in background absorbance when assayed in isolation (Figure 3.25.). This was expected given that ATP can spontaneously hydrolyse (Galán *et al.*, 1999). Although this happens at a low rate below 60°C, it is clearly enough to cause the background signal (Figure 3.24.) (Galán *et al.*, 1999).

### 3.2.11. ATP Usage – PiColorlock 3.

Rather than a high background, it could be that the stock of eIF4A had a low level of ATPase activity in the reaction. In order to test this, a positive control was used. DnaK (also called Hsp70), a protein involved in the cellular response to heat-shock, has been used as a positive control for ATPase activity in previous studies (Agranovsky *et al.*, 1997).

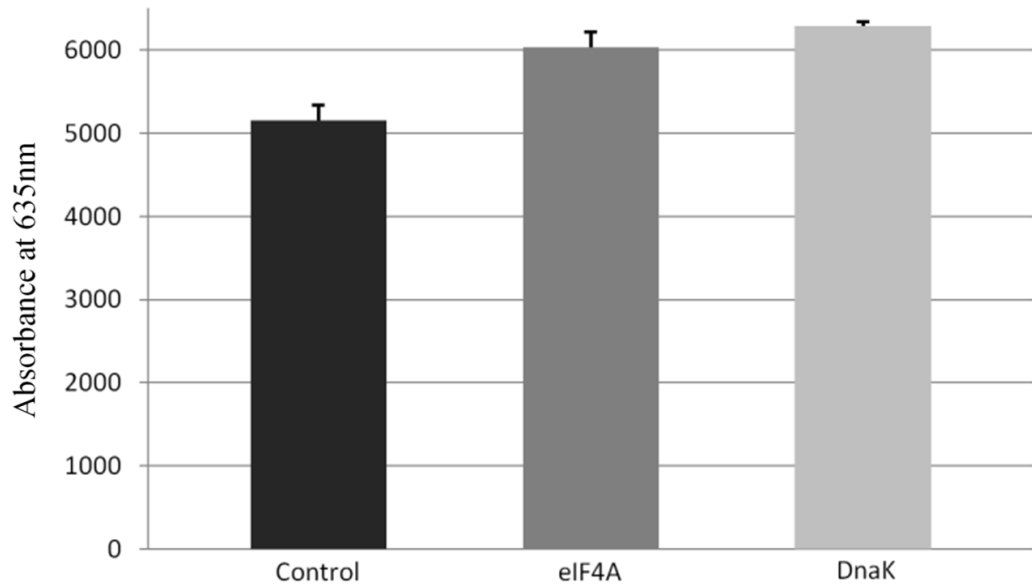


**Figure 3.26. The helicase assay reaction containing PiColorlock and a positive control for ATPase activity.** Nine reactions were incubated for 15 minutes at 37°C, three were without enzyme (control), three contained eIF4A and three contained 0.4 mM DnaK. After the reactions were stopped, their absorbance at 635 nm was quantified. Single experiment, average of three repeats, error bars represent standard deviation.

eIF4A and the positive control ATPase DnaK both caused significant increases in  $P_i$  concentration (Figure 3.26.). If the DnaK had generated a signal significantly higher than the control and eIF4A signals, it may have been assumed that the eIF4A was not very active. The fact that the control signal is similar to that generated by both the eIF4A and the DnaK indicates that it is the background that is high rather than the eIF4A having weak ATPase activity (Figure 3.24.).

## Part 3.

### eIF4A Paralogs Results

There exist three different paralogs of eIF4A in humans. Each mRNA contains a 5' UTR that is different in terms of length, GC content and predicted free energy (Table 19.).

Name	Length (nucleotides)	GC Content (%)	Predicted Free Energy (kcal/mol)	Accession #
<i>eIF4AI</i>	103	66	-39.20	NM_001416.2
<i>eIF4AII</i>	39	53	-7.00	NM_001967
<i>eIF4AIII</i>	222	74	-75.90	NM_014740

**Table 19. Details of the 5' UTRs of each of the paralogs eIF4A**

The purpose of this section is to investigate the effect of individual knockdown of the three eIF4A paralogs on the hairpin reporter system and also the effect of individual knockdown and hippuristanol treatment on reporters containing the 5' UTRs of the paralogs themselves.

### 3.3.1. Cloning the *eIF4A* 5' UTRs

The 5' UTRs of the three human paralogs of eIF4A were cloned into p15 downstream of the CMV promoter and upstream of the firefly luciferase gene.

Primers were designed based on sequences from NCBI, RefSeq IDs NM\_001416 for *eIF4AI*, NM\_001967 for *eIF4AII* and NM\_014740 for *eIF4AIII* (Table 2., Table 9.). The *eIF4AII* 5' UTR was created by annealing oligonucleotides as it is only 39 nucleotides in length. The UTRs for paralogs *I* and *III* were amplified from SH-SY5Y cDNA using standard Phusion PCR. Primers were complementary to the 20 nucleotides closest to the 5' or 3' ends of the sequences and included *PacI* and *XhoI* sites which enabled the sequences to be cloned into p15. Digestion of p15HP with *XhoI* and *PacI* excises the hairpin which can be replaced with any other sequence. Successful cloning was confirmed by sequencing.

Before the *eIF4A* 5' UTR-reporters were used, the effect of individual paralog knockdown on the hairpin reporter system (described in section: 3.1.1. Cell Based Screen Introduction) was established.

3.3.2. The effect of individual siRNA knockdown of each paralog on the hairpin reporter system

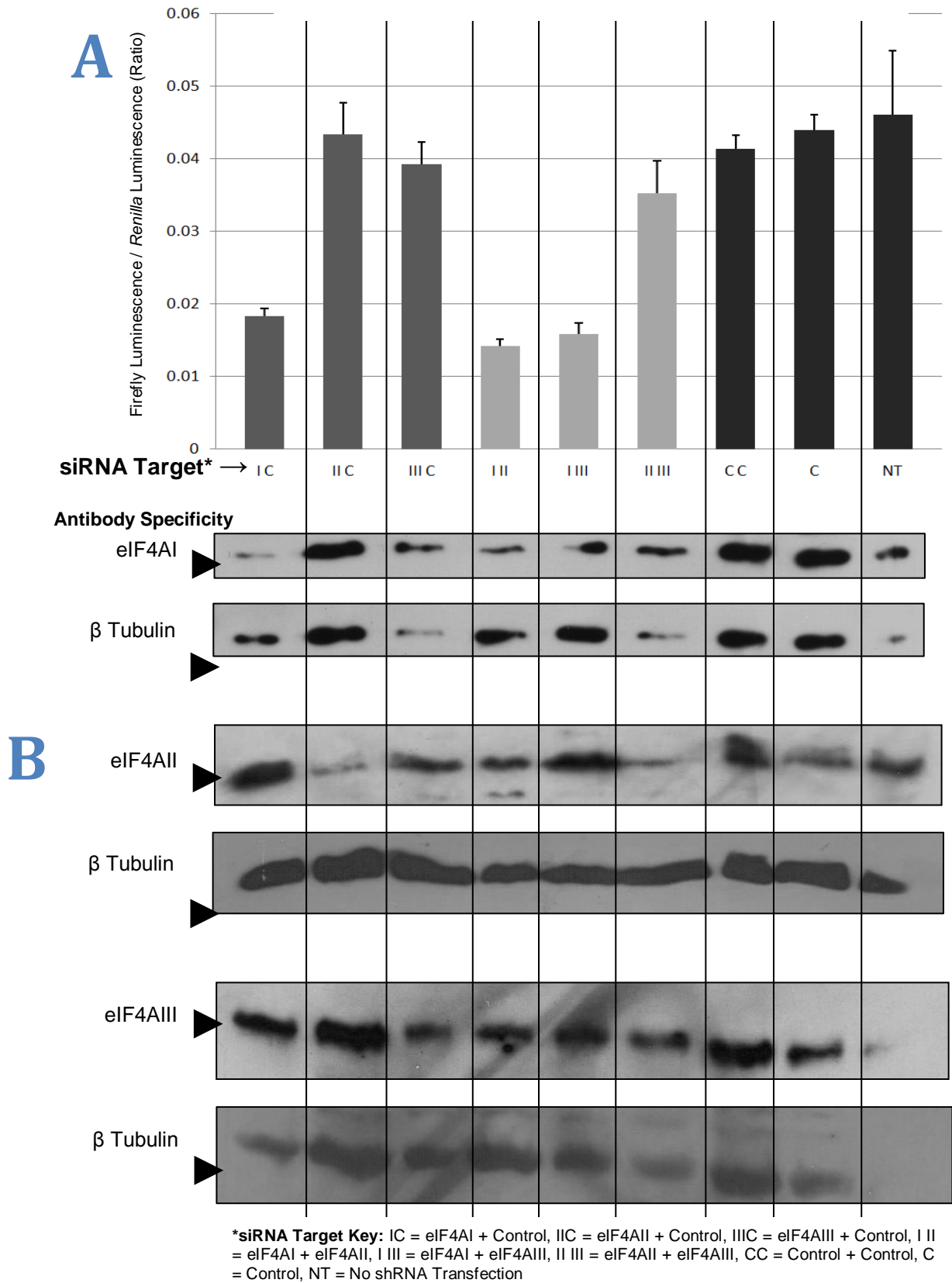


**Figure 3.27. The effect of the individual and combined knockdown of the three paralogs of eIF4A in SH-SY5Y.** The bar graph (A.) shows the luciferase activity of plasmids transfected into cells previously recipient of siRNA knockdown. Single experiment, average of three repeats, error bars represent standard deviation. The lower part (B.) shows the western blots that confirm the knockdown of each paralog with the control  $\beta$  tubulin blot underneath, the order from left to right is the same as on the bar graph. The black arrow to the left of the western blots represents 50 kDa. Westerns were performed in triplicate but only one (representative) blot is shown.

Although knockdown of eIF4AII and eIF4AIII was successful, only knockdown of eIF4AI caused a reduction in the expression of the hairpin reporter (Figure 3.27.).

### 3.3.3. Cell viability in response to individual paralog knockdown as estimated by WST-1 Assay

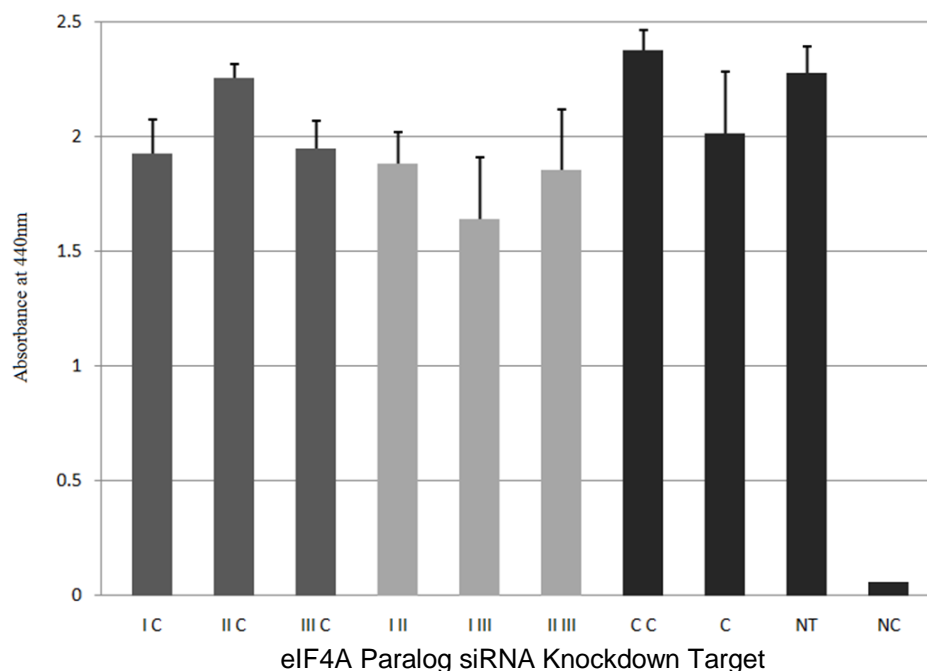


**Figure 3.28. WST-1 viability assays were performed on SH-SY5Y cells recipient of siRNA sequences targeting each of the paralogs of eIF4A in order to quantify cell viability.** Higher values indicate greater viability. (C = control, NT = no siRNA transfection, NC = negative control (empty well)). Single experiment, average of three repeats, error bars represent standard deviation.

Although some of the viability assays performed on the cells previously recipient of targeted siRNAs seem to be slightly lower than the controls (Figure 3.28.), none of the data were statistically significant compared to the CC, C and NT fields (Figure 3.28). Relative to the negative control (NC), there was a strong signal from all of the viability assays performed on the cell-containing wells (Figure 3.28.). There are many other methods for assessing cell viability besides WST-1. These alternatives together with the limitations of the WST-1 will be explored in the Discussion section.

### 3.3.4. eIF4A 5' UTR reporters and paralog knockdown

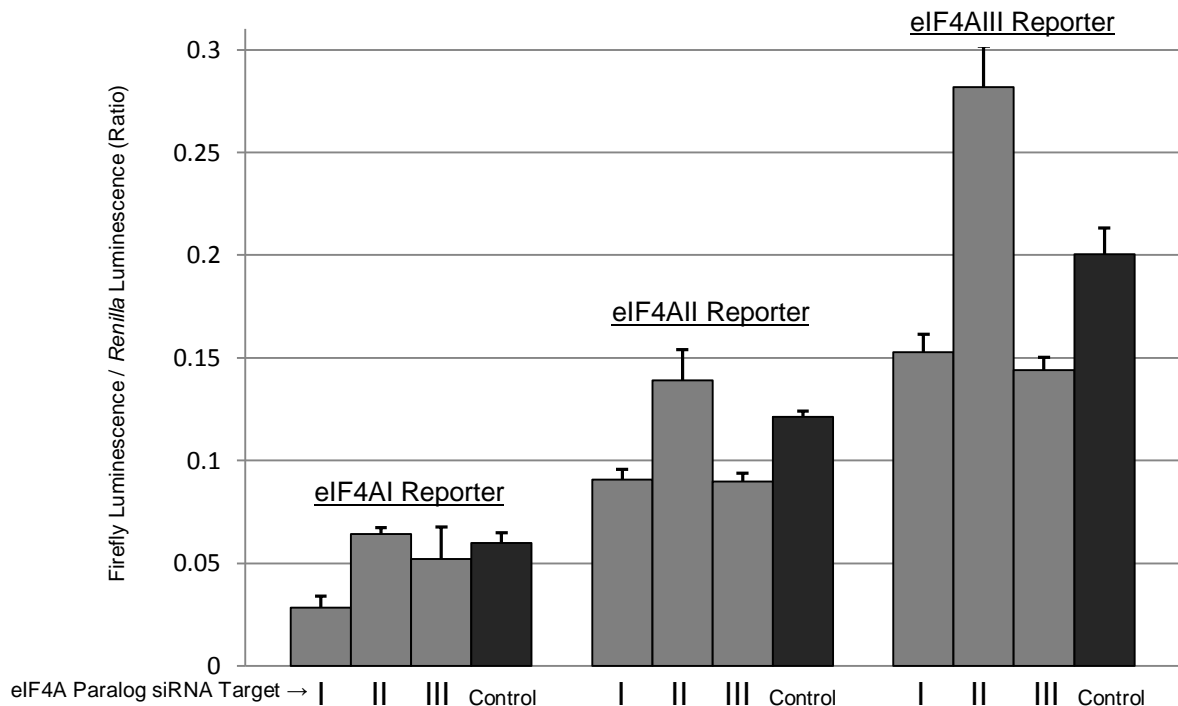


**Figure 3.29. The effect of eIF4A and eIF4B knockdown on reporters containing the 5' UTRs of the three paralogs of eIF4A.** A 24 well plate was seeded with SH-SY5Y cells. The following day, these were transfected simultaneously with siRNAs targeted against each paralog of eIF4A (or eIF4B), one of the reporter plasmids containing the three different 5' UTRs of *eIF4A* and the control p80 plasmid. 24 hours later, the luciferase expression within these cells was quantified. Single experiment, average of three repeats, error bars represent standard deviation.

In general, between paralog reporters *I*, *II* and *III*, normalised luciferase activity increases in a stepwise manner (Figure 3.29.). Knockdown of eIF4AI caused a small decrease in the expression of the *eIF4AI* 5' UTR reporter. Knockdown of eIF4AII and eIF4AIII did not affect the expression of the *eIF4AI* reporter relative to the control. Knockdown of eIF4AI and eIF4AIII and eIF4B had no effect on the expression of the *eIF4AII* 5' UTR reporter. However, knockdown of eIF4AII caused a significant increase in the expression of the *eIF4AII* reporter. For the *eIF4AIII* reporter, knockdown of eIF4AI and eIF4AIII caused a reduction and knockdown of eIF4AII caused an increase.

### 3.3.5. *eIF4A* 5' UTR reporters and hippuristanol treatment

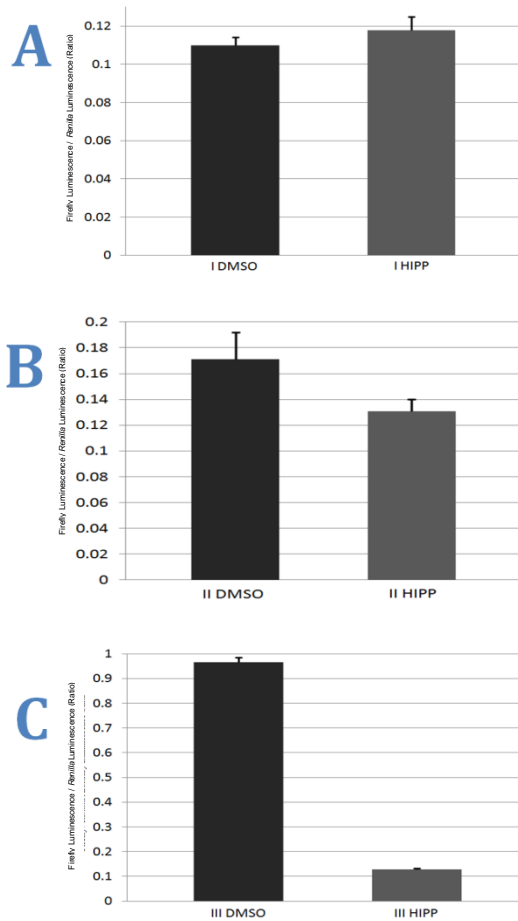


**Figure 3.30. The effect of 10 μM hippuristanol on the *eIF4A* paralog reporters.** A 24 well plate was seeded with SH-SY5Y cells. The following day, cells were transfected with one of the *eIF4A* paralog 5' UTR reporters. Four hours later, 10 μM hippuristanol was added and cells were incubated for a further six hours before being lysed for luciferase assay. Panel A. = *eIF4AI*, Panel B. = *eIF4AII* and Panel C. = *eIF4AIII*. Single experiment, average of three repeats, error bars represent standard deviation.

Hippuristanol had no effect on the *eIF4AI* reporter (Figure 3.30. A.). There was a small decrease in the expression of the *eIF4AII* reporter in response to hippuristanol (B.) and there was a substantial decrease in the *eIF4AIII* reporter (C.). The control levels for paralogs *I*, *II* and *III* are 0.11, 0.17 and 0.95 respectively; this is consistent with previous results (Figure 3.29.).

## Part 4.

### PDCD4 Results

As outlined in the Introduction, PDCD4 is a cellular antagonist of eIF4A that regulates its function (Goke *et al.*, 2002; Onishi *et al.*, 1998; Shibahara *et al.*, 1995; Yoshinaga *et al.*, 1999). Also referred to in the Introduction is the fact that loss of PDCD4 impairs the ability of a cell to respond to DNA damage (Bitomsky *et al.*, 2008; Singh *et al.*, 2009).

As part of this project, the effect of PDCD4 knockdown on the hairpin reporter system was observed. It was predicted that the loss of this eIF4A inhibitor would increase the relative expression of the hairpin-mediated reporter gene relative to the control reporter. This result would not reveal anything new about the biology of translation initiation as the relationship between eIF4A and PDCD4 has been well researched but it would test whether the hairpin reporter system would identify molecules that inhibited PDCD4 as part of a high throughput screen (Yang *et al.*, 2003). It was also necessary to demonstrate that the shRNA knockdown of PDCD4 worked effectively as it would be used to investigate further the role of PDCD4 in the DNA damage response. It was predicted that the interaction between PDCD4 and eIF4A was the cause of the involvement of PDCD4 in this response i.e. eIF4A activity contributes to the severity of DNA damage.

### 3.4.1. PDCD4 knockdown and the hairpin reporter

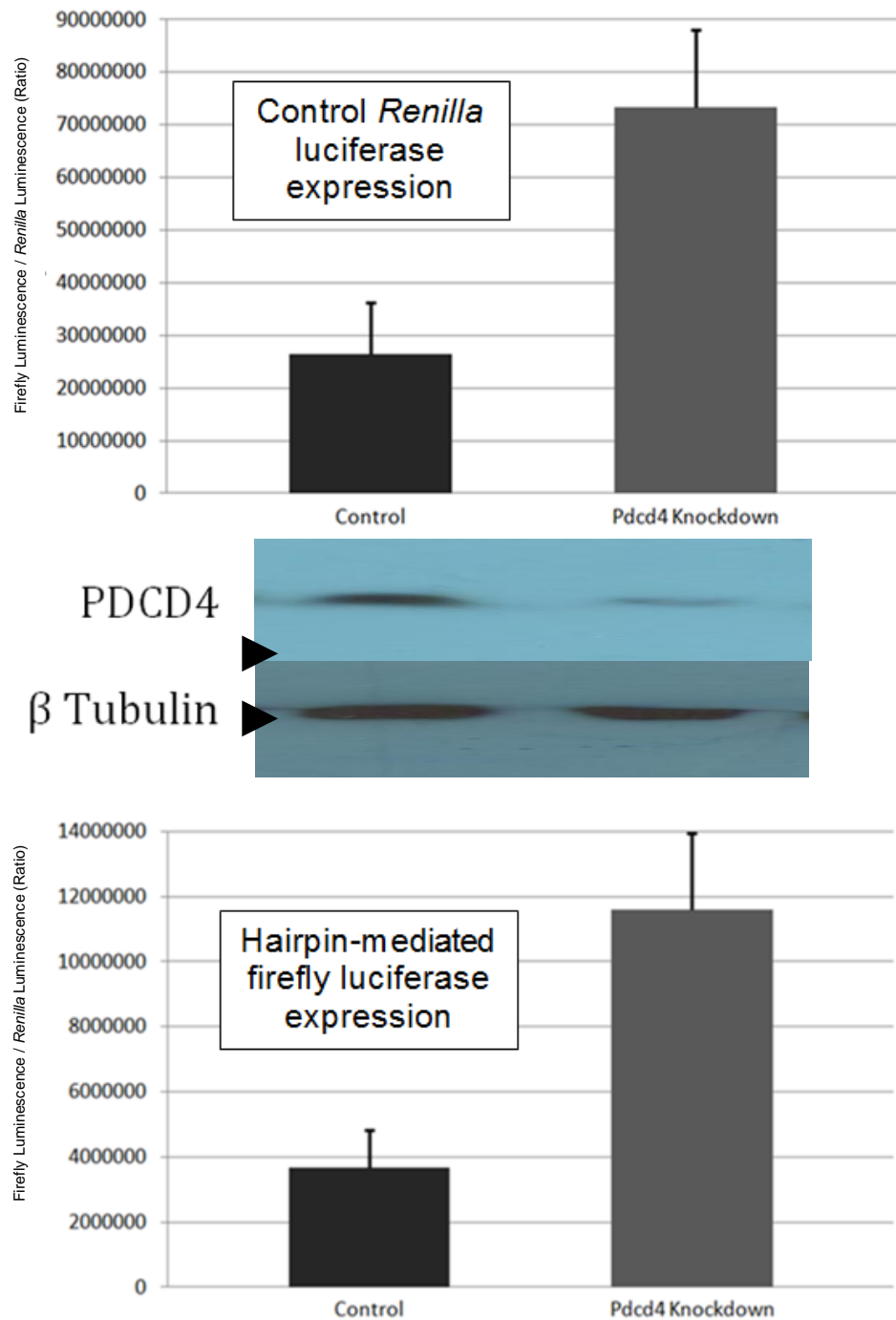


**Figure 3.31. The effect of PDCD4 knockdown on the hairpin reporter system.** A 24 well plate was seeded with SH-SY5Y cells. The following day, six wells were transfected with p15HP and p80, three of these were also transfected with a PDCD4 knockdown plasmid (Sigma-Aldrich, TRCN0000059081, NM\_014456.3-914s1c1) and the other three were also transfected with a control plasmid (Sigma-Aldrich MISSION Control, Cat # SHC001). 24 hours later, cells were lysed for luciferase activity assay and western blot. Single experiment, average of three repeats, error bars represent standard deviation.

PDCD4 knockdown caused a 2.78 fold increase in p80 *Renilla* luciferase activity ( $p = 0.005$ ) but a 3.16 fold increase in p15HP activity ( $p = 0.003$ ) (Figure 3.31.). However, when the response to PDCD4 knockdown of the control (p80) was compared to that of the hairpin-containing reporter (p15HP), the data were found to be statistically non-significant ( $p = 0.180$ ). Western blots for PDCD4 revealed that the knockdown worked successfully. There was a 39% reduction in PDCD4 level in the cells recipient of the shRNA knockdown plasmid relative to the control and relative to the level of  $\beta$  tubulin (Figure 3.31.) (westerns quantified using ImageJ (Abramoff et al., 2004)).

With the knockdown plasmid demonstrated to work (Figure 3.31.), the next stage was to investigate the effect of the reduction of PDCD4 protein level on cell viability and the number of dissociated cells in response to ultraviolet (UV) light. UV treatment is a well characterised stimulator of DNA damage and it is used to study the phenomenon in the laboratory (Sinha and Hader, 2002).

The following section outlines the experiments that were performed to ascertain the tolerance of SH-SY5Y and HeLa to DNA damage when their PDCD4 protein level was reduced. Two cell lines, originating from different human tissues, were used to try to exclude any potential cell line specific effects.

### 3.4.3. SH-SY5Y cell viability following UV exposure and PDCD4 knockdown

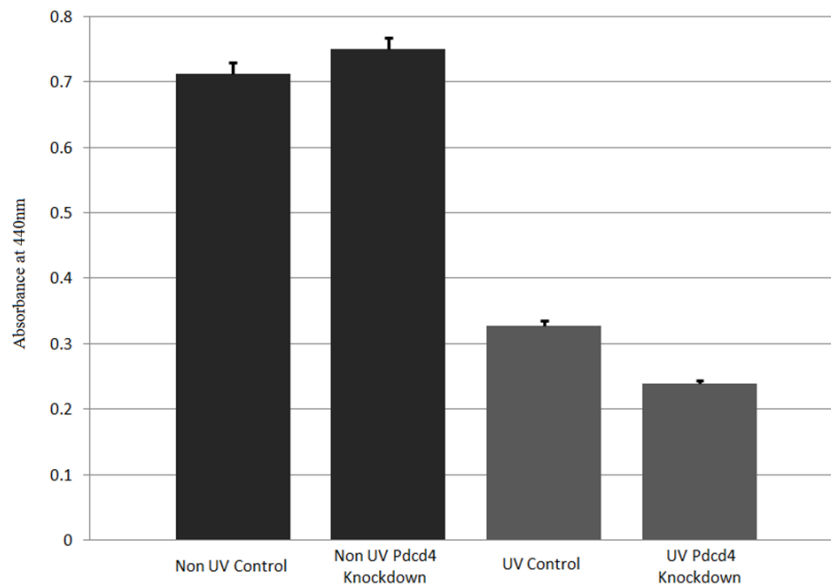


**Figure 3.32. The effect of PDCD4 knockdown on SH-SY5Y viability following UV irradiation.** Two 24 well plates were seeded with SH-SY5Y cells. The following day, six wells of each were transfected with the PDCD4 knockdown plasmid and six with the control plasmid. 24 hours later, one plate was exposed to 275 J/m<sup>2</sup> UV light while the other was mock irradiated. The plates were allowed to recover for a further 24 hours before WST-1 viability assays were performed. Single experiment, average of six repeats, error bars represent standard deviation.

There was a significant increase in SH-SY5Y viability following PDCD4 knockdown under control conditions ( $p = 0.025$ ) (Figure 3.32.). The opposite was true for cells irradiated with UV, PDCD4 knockdown caused a significant decrease in viability ( $p = 0.00003$ ). In general, UV treatment caused viability to reduce by over half.

### 3.4.4. SH-SY5Y dissociated cell count following UV exposure and PDCD4 knockdown

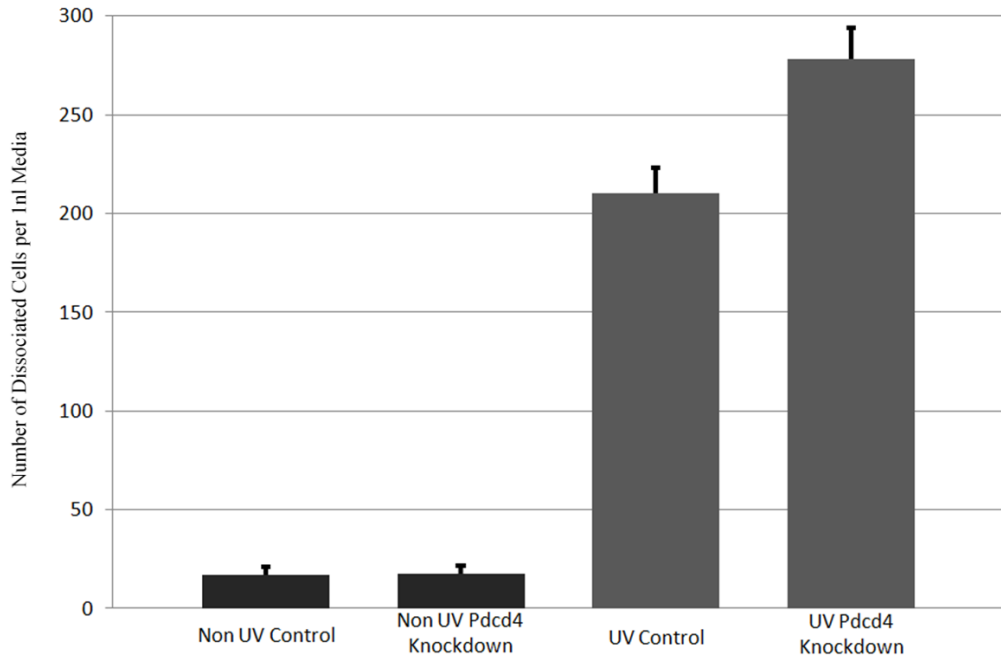


**Figure 3.33. The effect of PDCD4 knockdown on the number of dissociated SH-SY5Y cells following UV irradiation.** Two 24 well plates were seeded with SH-SY5Y cells. The following day, six wells of each were transfected with the PDCD4 knockdown plasmid and six with the control plasmid. 24 hours later, one plate was exposed to 275 J/m<sup>2</sup> UV light while the other was mock irradiated. The plates were allowed to recover for a further 24 hours before the dissociated cells were counted by haemocytometry. Single experiment, average of six repeats, error bars represent standard deviation.

There is no statistical difference between the number of dissociated cells under normal conditions following PDCD4 knockdown ( $p = 0.3785$ ) (Figure 3.33.). This was in contrast to the dissociated cells in UV treated wells which were statistically more prevalent in wells also recipient of PDCD4 knockdown shRNA ( $p = 0.0076$ ). There was also an approximate 15 fold increase in dissociated cells between control and UV-treated wells respectively.

The number of dissociated cells in a tissue culture vessel is often regarded as an unreliable measure of viability as floating cells may not necessarily be dead and dead cells may remain attached or have disintegrated. It is important therefore to interpret these data alongside the WST-1 proliferation assay data. Comparison of these two assays gives a more reliable representation of cell death and health than either alone.

### 3.4.5. Confirmation of knockdown in SH-SY5Y cells

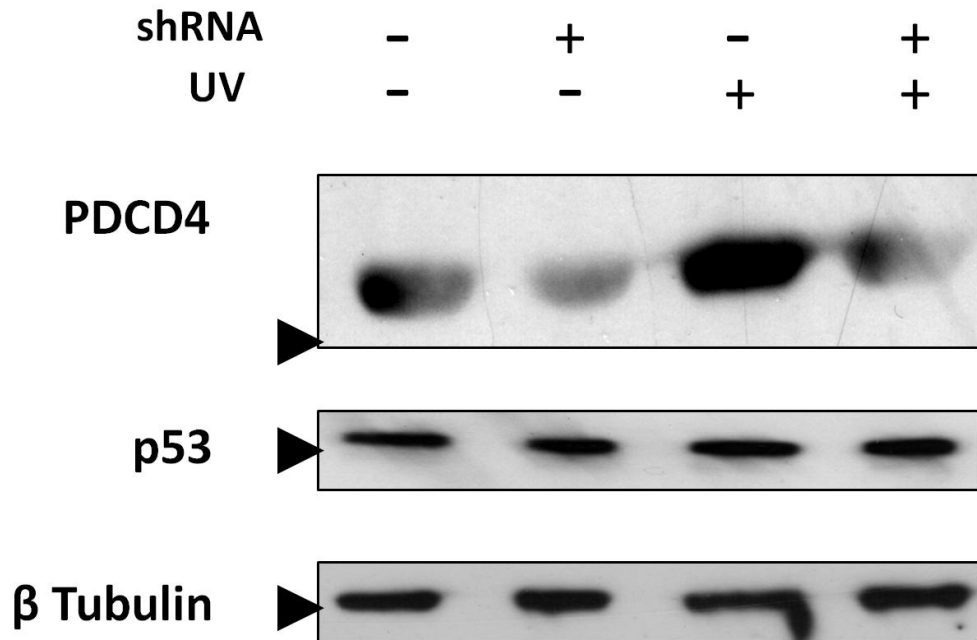


**Figure 3.34. Western blots for PDCD4 that confirm the success of the knockdown.** The SH-SY5Y cells used for the previous two experiments were lysed and the protein levels of PDCD4, p53 and  $\beta$  tubulin were estimated by western blot in order to confirm that the knockdown was successful. The black arrow indicates 50 kDa on the protein ladder.

PDCD4 protein levels fell in response to the transfection of shRNA plasmids targeted against it while they remained constant following treatment with the control, non-target shRNA (Figure 3.34.). PDCD4 protein levels seem to increase in response to UV treatment. Protein levels of p53 and  $\beta$  tubulin did not change in response to UV treatment or PDCD4 knockdown. The p53 blot was performed because it was presumed that this protein is involved in the PDCD4-mediated DNA damage response by a previous study (Bitomsky *et al.*, 2008).

### 3.4.6. HeLa cell viability following UV exposure and PDCD4 knockdown

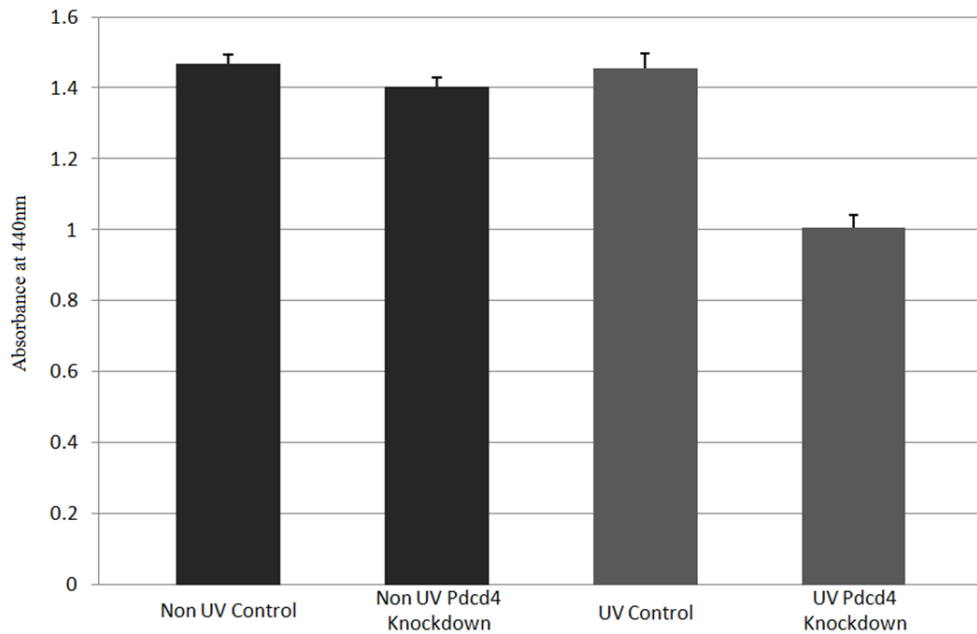


**Figure 3.35. The effect of PDCD4 knockdown on HeLa viability following UV irradiation.** Two 24 well plates were seeded with HeLa cells. The following day, six wells of each were transfected with the PDCD4 knockdown plasmid and six with the control plasmid. 24 hours later, one plate was exposed to 275 J/m<sup>2</sup> UV light while the other was mock irradiated. The plates were allowed to recover for a further 24 hours before WST-1 viability assays were performed. Single experiment, average of six repeats, error bars represent standard deviation.

There was a slight but significant reduction in HeLa viability following PDCD4 knockdown under control conditions ( $p = 0.0176$ ) (Figure 3.35.). This effect was accentuated in cells irradiated with UV, PDCD4 knockdown caused a much greater decrease in viability ( $p = 0.00007$ ). In general, UV treatment caused little reduction in viability in HeLa cells.

### 3.4.7. HeLa dissociated cell count following UV exposure and PDCD4 knockdown

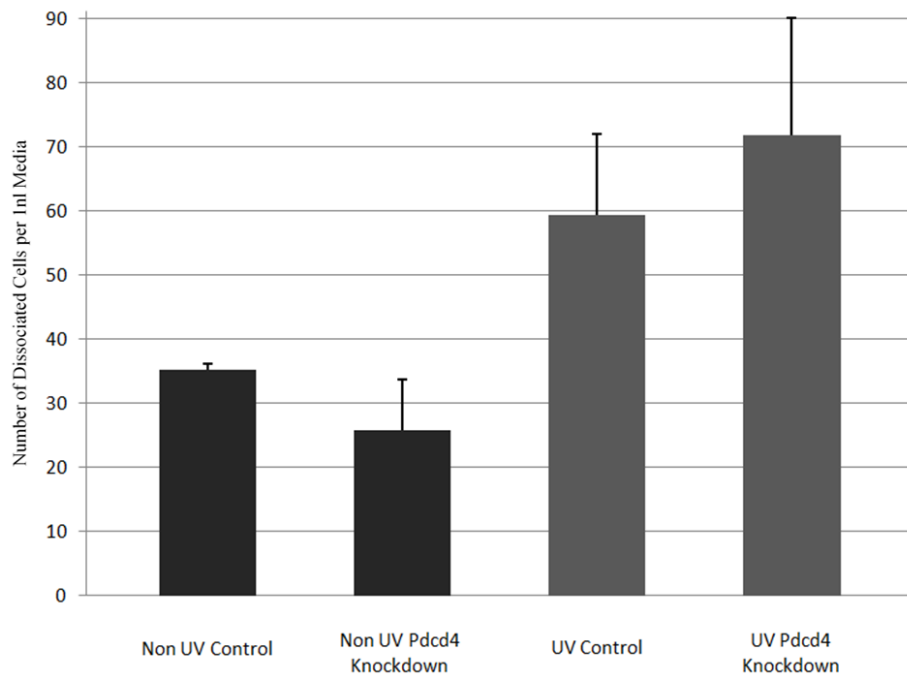


**Figure 3.36. The effect of PDCD4 knockdown on the number of dissociated HeLa cells following UV irradiation.** Two 24 well plates were seeded with HeLa cells. The following day, six wells of each were transfected with the PDCD4 knockdown plasmid and six with the control plasmid. 24 hours later, one plate was exposed to 275 J/m<sup>2</sup> UV light while the other was mock irradiated. The plates were allowed to recover for a further 24 hours before the dissociated cells were counted by haemocytometry. Single experiment, average of six repeats, error bars represent standard deviation.

There was a slight statistical drop between the number of dissociated cells in the control wells and the PDCD4-knockdown wells under normal conditions ( $p = 0.0199$ ) (Figure 3.36.). There was no statistical difference between the data for plus and minus shRNA in UV treated wells ( $p = 0.1027$ ). In general, there was an approximate two-fold increase in the number of dissociated cells between minus and plus UV treatment respectively.

### 3.4.8. Confirmation of knockdown in HeLa

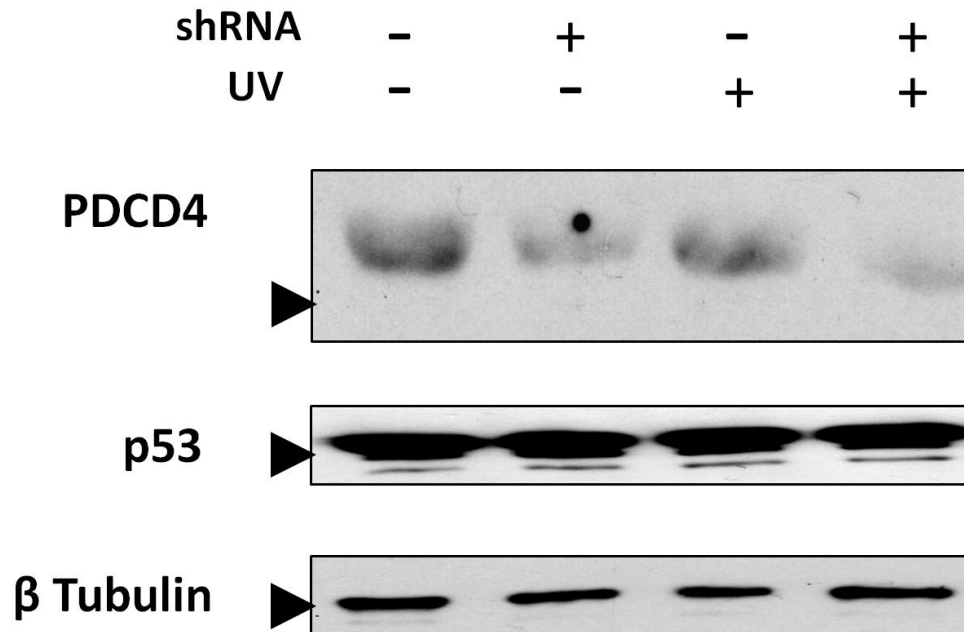


**Figure 3.37. Western blots for PDCD4 that confirm the success of the knockdown.** The HeLa cells used for the previous two experiments were lysed and the protein levels of PDCD4, p53 and  $\beta$  tubulin were estimated by western blot in order to confirm that the knockdown was successful. The black arrow indicates 50 kDa on the protein ladder.

PDCD4 protein levels fell in response to the transfection of shRNA plasmids targeted against it while they remained constant following treatment with the non-target control shRNA (Figure 3.37.). Protein levels of p53 and  $\beta$  tubulin did not change either in response to UV treatment or PDCD4 knockdown.

## **Part 5.**

### **Alzheimer's Disease**

#### **3.5.1. Introduction to the Alzheimer's Disease Results Section**

Prior to the start of this project, a microarray was performed on lysate from HeLa cells previously treated with hippuristanol (by Andrew Bottley). This identified APP, MAPT and acetylcholinesterase expression as being susceptible to eIF4A inhibition. It was confirmed by western blot that hippuristanol treatment reduced the expression of these three genes.

This was the original reason for investigating the relationship between eIF4A activity modulation and Alzheimer's disease. A database of all the genes reported as being involved in Alzheimer's disease in the literature was compiled. A number of these genes were selected and their 5' UTRs were cloned into reporter plasmids. The genes investigated are shown in Table 3 and their properties are discussed in the Introduction.

### 3.5.2. Cloning the Alzheimer's-associated 5' UTRs into p15

The 5' UTRs of *SOD1* and *TXN* were amplified from cDNA using primers shown in the Materials and Methods section (Table 9.). The 5' UTRs of: *PS1*, *PS2*, *BACE1*, *Clu2*, *CR1*, *MAPT*, *AChE* and *APP* were ordered from GenScript based on contemporary data from the NCBI (National Center for Biotechnology Information) website. These sequences were cloned into p15 using *XhoI* and *PacI* (Figure 3.38.).

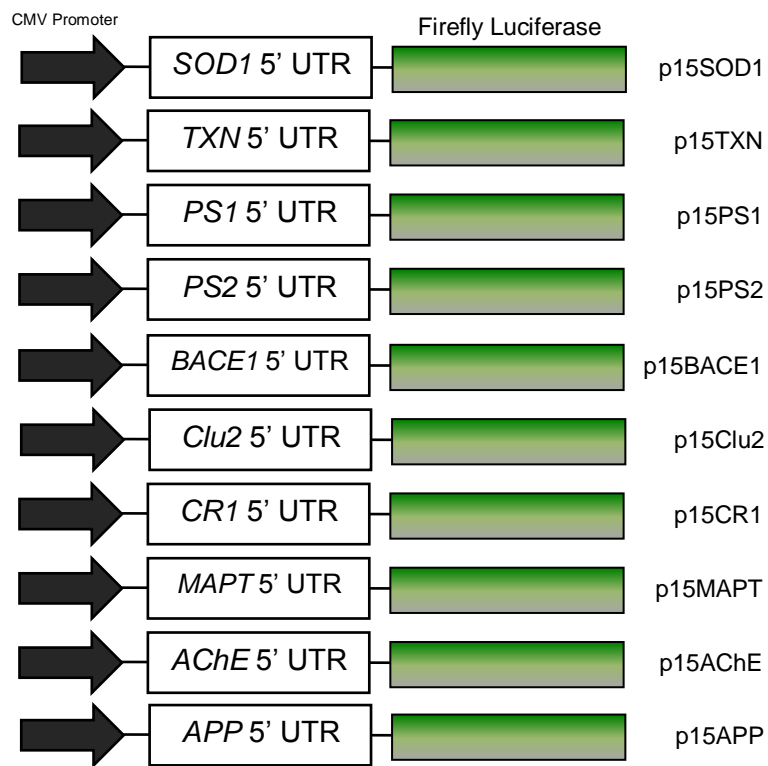


**Figure 3.38. Construct diagrams showing the cloning site in p15 and the 5' UTRs of the Alzheimer's-associated genes**  
*Renilla Luciferase*

### 3.5.3. The 5' UTR sequences of genes predicted to play harmful roles in Alzheimer's disease are inhibitory to reporter expression

It was suspected that eIF4A suppression could be an effective mechanism for treating Alzheimer's disease. Overexpression of certain genes e.g. *APP*, *MAPT* and *BACE1* contributes to the severity of AD; these genes are referred to in this project as 'harmful'. Given that these genes possess longer and potentially more highly structured 5' UTRs than the genes involved in the defence against oxidative stress, it was predicted that they would have a greater eIF4A requirement.

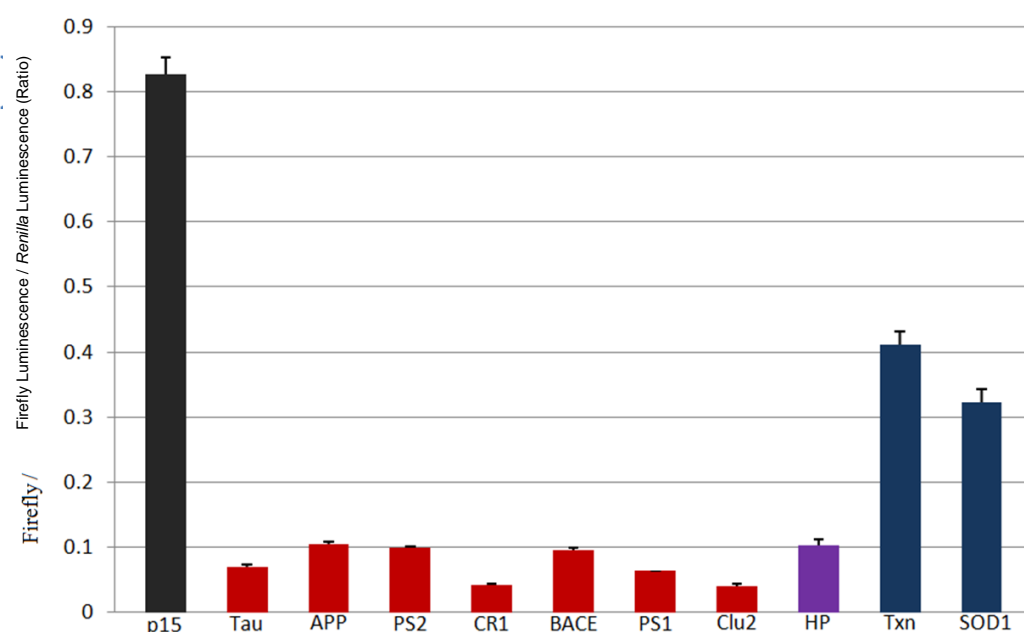


**Figure 3.39. The reporter plasmids containing the Alzheimer's-associated 5' UTRs were transfected into SH-SY5Y cells.** Reporters containing 5' UTRs of genes predicted to play a harmful role in Alzheimer's are shown in red, those predicted to be beneficial are shown in dark blue, the hairpin control is shown in purple and the p15 control is shown in charcoal. Single experiment, average of six repeats, error bars represent standard deviation.

In SH-SY5Y cells, reporters containing 5' UTRs belonging to genes predicted to play harmful roles in Alzheimer's generated much lower signals than those containing the 5' UTRs of genes predicted to be beneficial. The p15 control (B.) generated a much stronger signal than the reporters containing ectopic sequence. The hairpin reporter generated a similar signal to the 'harmful' reporters.

### 3.5.4. Promoterless reporter plasmids generate no signal

In order to test for cryptic promoter activity, the promoterless versions of the reporters were assayed for luciferase activity.

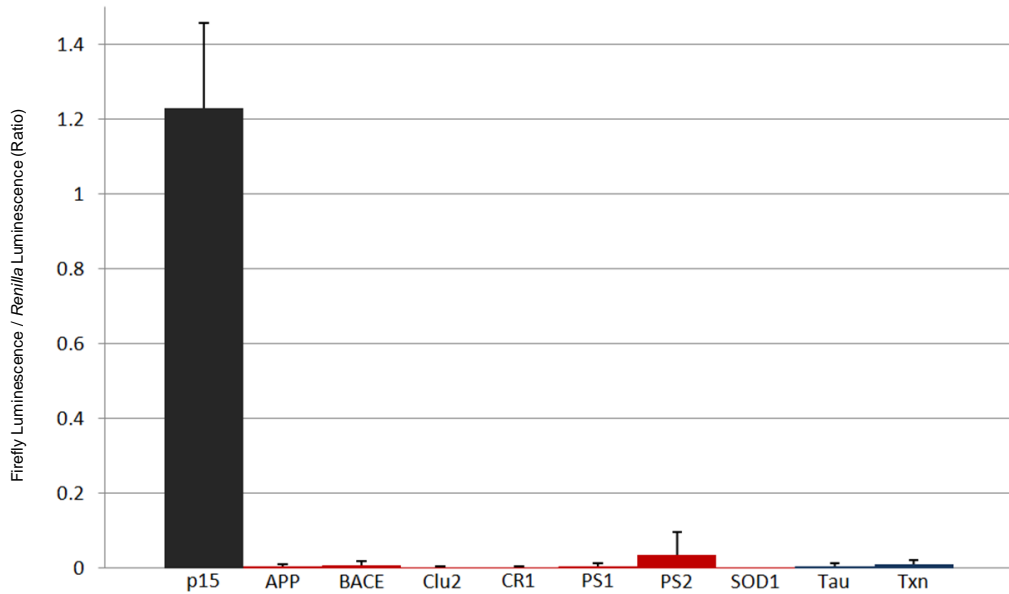


**Figure 3.40. Versions of the Alzheimer's reporters without the CMV promoter were created and assayed for activity in SH-SY5Y cells.** The p15 control included a functional promoter. Single experiment, average of three repeats, error bars represent standard deviation.

Removal of the promoter sequence (by excision using *AseI*) from the reporters reduced their activity to the same level as the activity observable in untransfected cells (Figure 3.40). The slight effect observed from the promoterless *PS2* reporter was generated by a single outlier in the data, the fact that the other replicates generate background signals suggests that this is not cryptic promoter activity or it would be ubiquitous among *PS2* reporters.

### 3.5.5. Hippuristanol reduces the expression of reporters containing 5' UTRs of genes predicted to play harmful roles in AD

To test the eIF4A requirement of each of the reporters, SH-SY5Y cells transfected with one of each were treated with hippuristanol, an inhibitor of eIF4A.

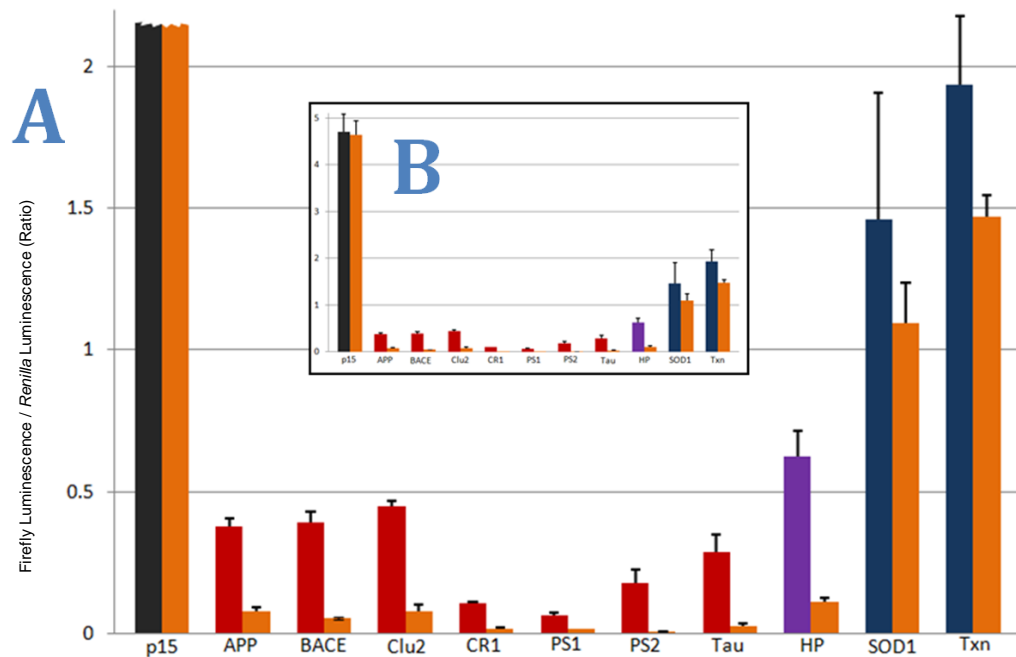


**Figure 3.41. The effect of 10  $\mu$ M hippuristanol on the Alzheimer's-associated 5' UTR-mediated expression of reporters in SH-SY5Y cells.** Three 24 well plates were seeded with SH-SY5Y cells. The following day, six wells were transfected with each of the Alzheimer's reporter plasmids (in addition to p80). Four hours later, three wells of each were treated with either 10  $\mu$ M hippuristanol or DMSO. Six hours later, cells were lysed for luciferase assay. The charcoal, red, purple or dark blue bars were generated from cells recipient of only DMSO while those in orange were generated from cells recipient of 10  $\mu$ M hippuristanol. Panel B shows the full image while the Panel A shows a close up of the lower part of the same image. Single experiment, average of three repeats, error bars represent standard deviation.

Hippuristanol had no effect on the p15 control reporter (Figure 3.41. B.). All of the reporters containing 5' UTRs from genes associated with the harmful effects of Alzheimer's and the hairpin reporter yielded significantly reduced levels of activity in response to hippuristanol treatment (Figure 3.41.. A. and B.). There was no significant effect on the *SOD1* reporter but a slight statistical reduction was observed in the data for the *TXN* reporter ( $p = 0.0168$ ).

### 5.5.6. The effect of hippuristanol on the *ADAM10* reporter

Since the *ADAM10* 5' UTR is currently being investigated by another lab (Sven Lammich (Ludwig Maximilians Universität)), it was not cloned as part of the reporter collection. However, Dr Lammich kindly provided his *ADAM10* reporter plasmid for use in this project.

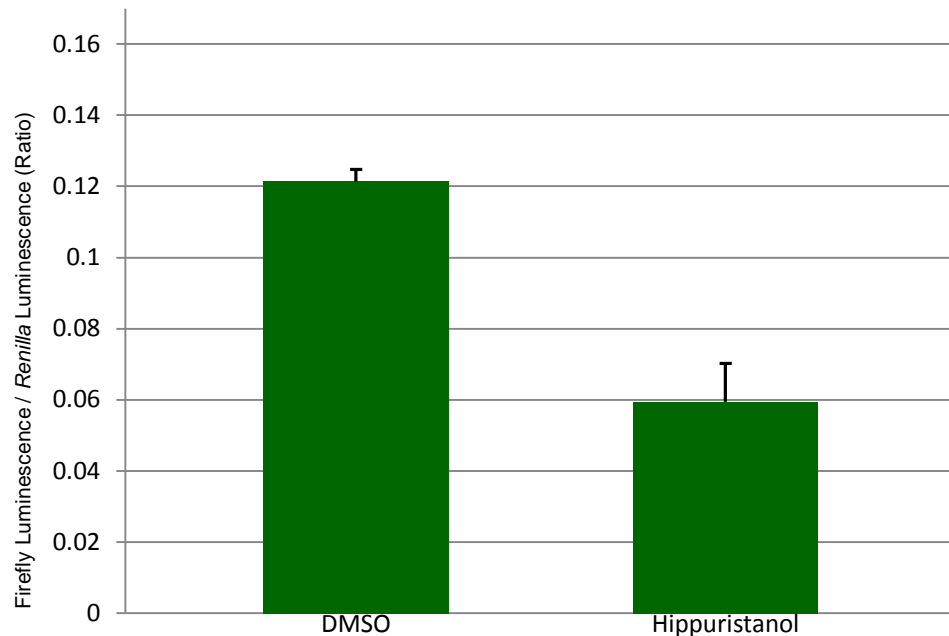


**Figure 3.42. The effect of 10 µM hippuristanol treatment on cells transfected with a reporter plasmid containing the 5' UTR of *ADAM10*.** A 24 well plate was seeded with SH-SY5Y cells. The following day, six wells were transfected with the *ADAM10* 5' UTR reporter and six with its associated control (in addition to p80). Four hours later, three wells of each were treated with either 10 µM hippuristanol or DMSO. Six hours later, cells were lysed for luciferase assay. Firefly luciferase counts were normalised to Renilla luciferase counts. The ratio of firefly luciferase activity to Renilla luciferase activity of the reporter containing the *ADAM10* 5' UTR was normalised to the ratio of the control. Single experiment, average of six repeats, error bars represent standard deviation.

The *ADAM10* reporter was provided cloned into the plasmid pcDNA6/V5-His which had been modified to include the firefly luciferase open reading frame (Figure 3.43). These results could not be directly compared to the rest of the data which were generated using the p15 reporter system created as part of this project.



**Figure 3.43. The *ADAM10* reporter construct**

Hippuristanol caused a statistically significant 31% reduction in the expression of the reporter containing the *ADAM10* 5' UTR (Figure 3.42).

### 5.5.7. Hippuristanol causes a significant reduction in *AChE* reporter expression

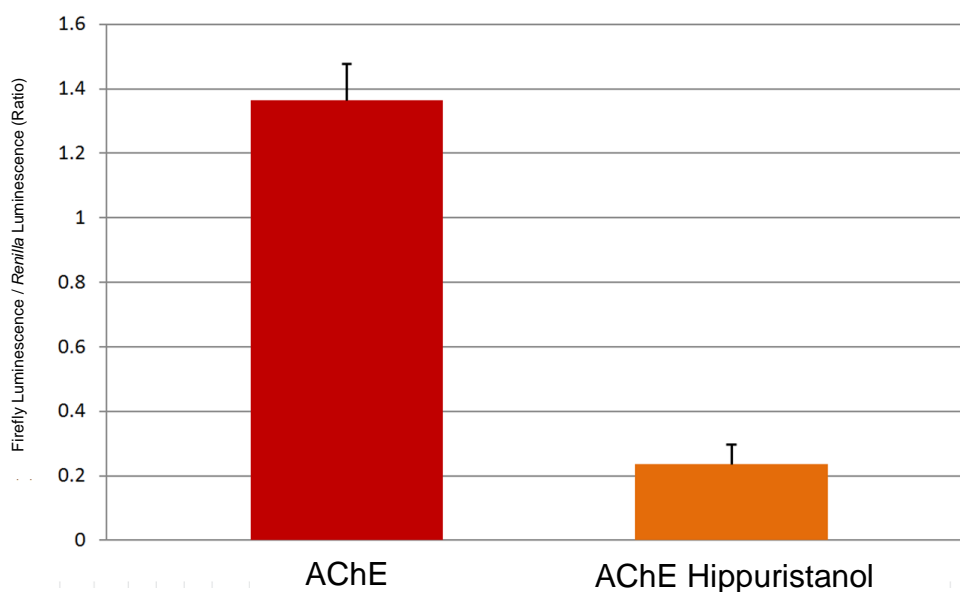


**Figure 3.44. The effect of hippuristanol on the reporter containing the 5' UTR of *acetylcholinesterase*.** A 24 well plate was seeded with SH-SY5Y cells. The following day, six wells were transfected with p15AChE. Four hours later, 10  $\mu$ M hippuristanol (or the equivalent amount of DMSO) was added to the cells. Six hours later, cells were lysed and luciferase assays were performed. Single experiment, average of three repeats, error bars represent standard deviation.

Hippuristanol treatment caused a significant reduction in the expression of the luciferase gene in the reporter containing the *acetylcholinesterase* 5' UTR ( $p = 0.00001$ ) (Figure 3.44.).

### 5.5.8.. The promoterless *AChE* reporter

The result from pRAceF is unexpected given that the *acetylcholinesterase* 5' UTR is predicted to form a hairpin. It was expected that the sequence would suppress reporter expression like the *ODC1* hairpin, rather than stimulate it. In order to establish whether the sequence had promoter activity, the CMV promoter was removed from the reporter and the experiment was repeated.

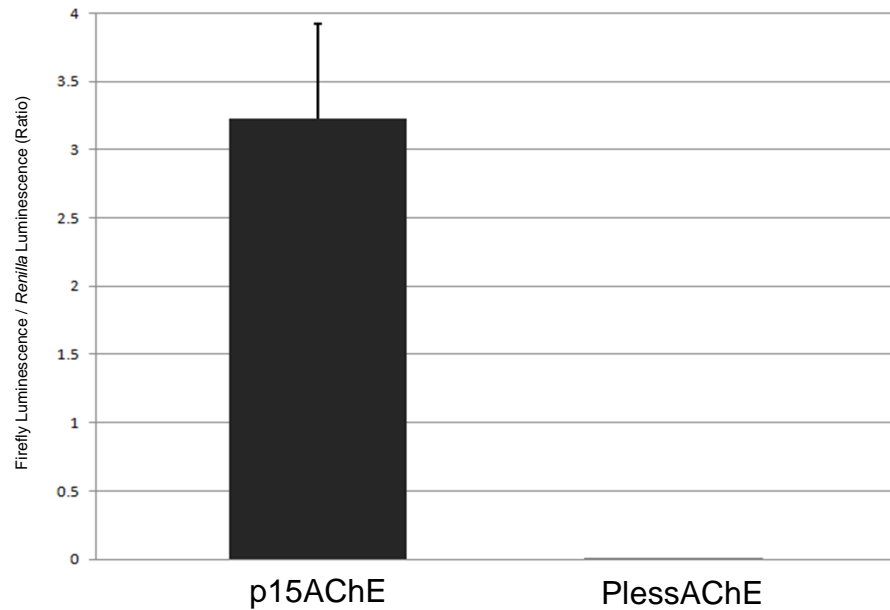


**Figure 3.45. The effect of removing the promoter sequence from the *acetylcholinesterase* (*Ace*) 5' UTR reporter.** A 24 well plate was seeded with SH-SY5Y cells. The following day, three wells were transfected with p15AChE and three with PlessAChE (promoterless). 24 hours later, cells were lysed and luciferase assays were performed. The panel shows the normalised expression levels of the control and promoterless reporters. Single experiment, average of three repeats, error bars represent standard deviation.

Removal of the CMV promoter sequence from the *acetylcholinesterase* reporter (to create the plasmid Plessp15AChE) caused a reduction of luciferase activity to background levels (Figure 3.45.).

## Part 6.

### Cancer Results

#### 3.6.1. Introduction to the Cancer Results Section

Unlike in Alzheimer's disease, there exists a moderate amount of evidence implicating eIF4A in cancer. In order to further investigate this relationship, the 5' UTRs of three oncogenes and three housekeeping genes were cloned into the luciferase reporter system created as part of this project. The 5' UTRs of *ODC1* has been studied extensively and shown to contain a stable hairpin, a uORF and an IRES, as has the *VEGFA* 5' UTR which was shown to contain a uORF and two IRES elements (see Introduction). Although a well studied oncogene, there is little mention of the 5' UTR of *EGFR* in the literature. The housekeeping genes are  *$\beta$  actin*,  *$\beta$  tubulin* and *GAPDH*.

The details of the six 5' UTRs studied as part of this section are shown in Table 20 and each gene is discussed in the Introduction.

---

Name	Length (nucleotides)	GC Content (%)	Predicted Free Energy (kcal/mol)	uORF(s)	IRES(s)
<i><math>\beta</math> Actin</i>	84	74	-15.50	0	0
<i><math>\beta</math> Tubulin</i>	127	47	-30.10	0	0
<i>GAPDH</i>	102	61	-21.90	0	0
<i>ODC1</i>	334	66	-157.50	1	1
<i>EGFR</i>	246	78	-107.50	0	1*
<i>VEGFA</i>	491	57	-193.30	1	2

---

Table 20. The details of the 5' UTRs of the housekeeping genes and oncogenes investigated in this section.

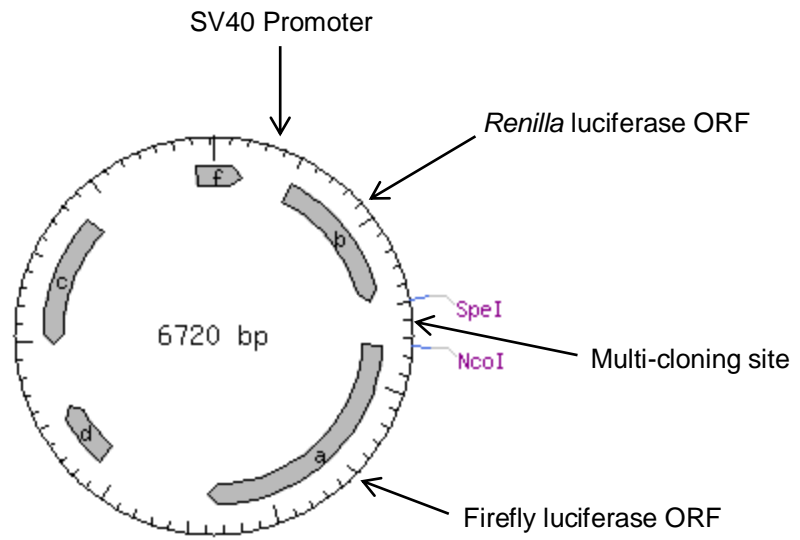


Figure 3.46. Map of the pRF parent vector

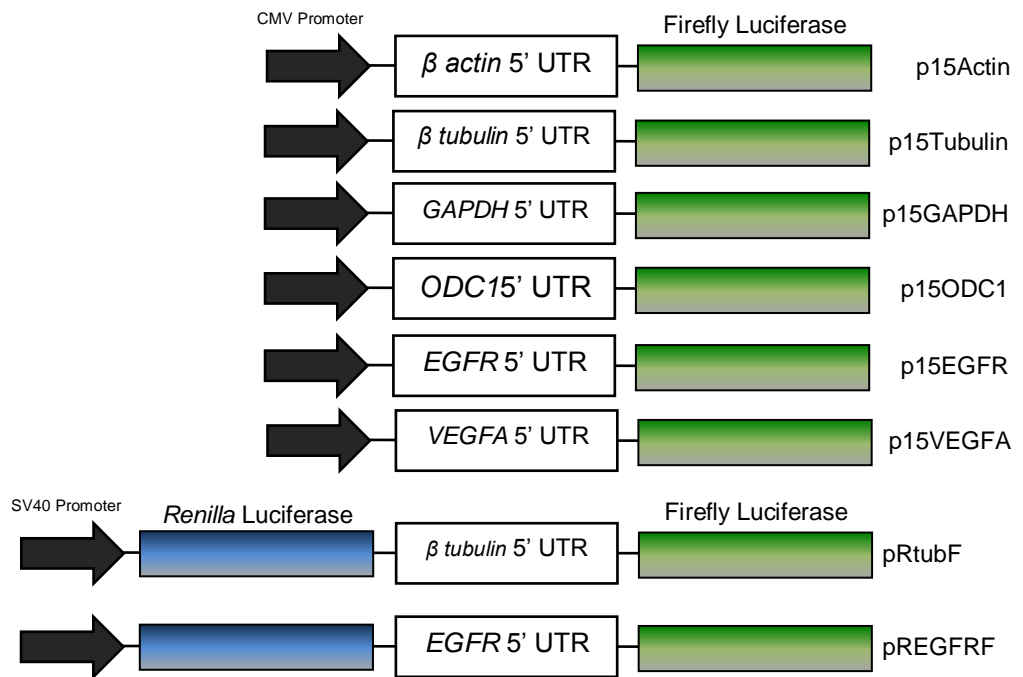


Figure 3.47. Construct diagrams of the cancer-associated 5' UTR reporters

### 3.6.2. Plasmid construction

The sequences of the 5' UTRs of human *β actin*, *β tubulin*, *GAPDH*, *ODC1*, *EGFR* and *VEGFA* as they appeared on the NCBI website (August 2010) were ordered as complete sequences from GenScript and cloned into p15 (Figure 3.47.). Promoterless variants were constructed by excising the proximal 80% of the CMV promoter sequence by *AseI* digest. Primers for the *β tubulin* and *EGFR* 5' UTRs were designed which included *SpeI* (upstream) and *NcoI* (downstream) restriction sites (Table 9.). These sequences were amplified using standard Phusion PCR and cloned into pRF (Figure 3.46.) in between the two luciferase cistrons. A truncated mutant version of the *EGFR* 5' UTR was created by *NotI* digestion. The plasmid that contained this mutant version was termed pREGFRF*NotIMut* (see page 174 for diagram).

### 3.6.3. Hippuristanol causes a greater reduction in oncogene reporter expression than housekeeping gene reporter expression in SH-SY5Y cells.

The effect of the 5' UTR sequences on the luciferase reporters was established by transfecting the collection of reporter into SH-SY5Y cells. The eIF4A requirement of each of the reporters was established using hippuristanol treatment.

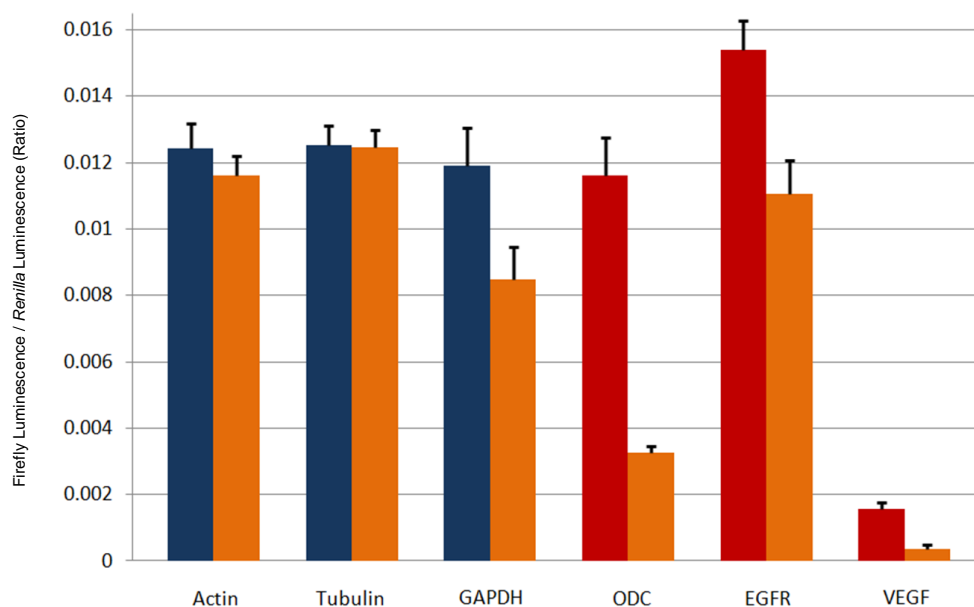


**Figure 3.48. The effect of 10 μM hippuristanol on the oncogene 5' UTR-mediated expression of reporters in SH-SY5Y cells.** Two 24 well plates were seeded with SH-SY5Y cells. The following day, six wells were transfected with each of the oncogene reporter plasmids (in addition to p80). Four hours later, three wells of each were treated with either 10 μM hippuristanol or DMSO. Six hours later, cells were lysed for luciferase assay. The red bars (representing proto-oncogenes) and the dark blue bars (representing housekeeping genes) were generated from cells recipient of only DMSO while those in orange were generated from cells recipient of 10 μM hippuristanol. Single experiment, average of three repeats, error bars represent standard deviation.

Although the *actin*, *tubulin* and *GAPDH* reporters generate similar expression levels, hippuristanol only caused a reduction in the expression of the *GAPDH* reporter ( $p = 0.0018$ ) (Figure 3.48.). There was no statistical difference between the firefly luciferase / *Renilla* luciferase ratios generated by the *ODC1* reporter and the housekeeping controls but hippuristanol caused a 72% reduction in its expression ( $p = 3.41E-06$ ). The firefly luciferase / *Renilla* luciferase ratio generated by the *EGFR* reporter were statistically higher than any of the controls ( $p = 0.0010$ ), hippuristanol also caused a reduction in the expression of the *EGFR* reporter ( $p = 0.0003$ ). The *VEGFA* reporter generated a much weaker signal than the controls, approximately 87% lower ( $p = 2.19E-08$ ). Hippuristanol caused a substantial decrease in the expression of the *VEGFA* reporter ( $p = 3.53E-05$ ).

### 3.6.4. Hippuristanol has no effect on cell viability in SH-SY5Y cells as estimated by WST-1 assay

If eIF4A is to be an effective drug target in the treatment of cancer, suppression of its function must not be overly toxic to the cell. As part of this project, cell viability following eIF4A suppression using hippuristanol was quantified using WST-1 reagent.

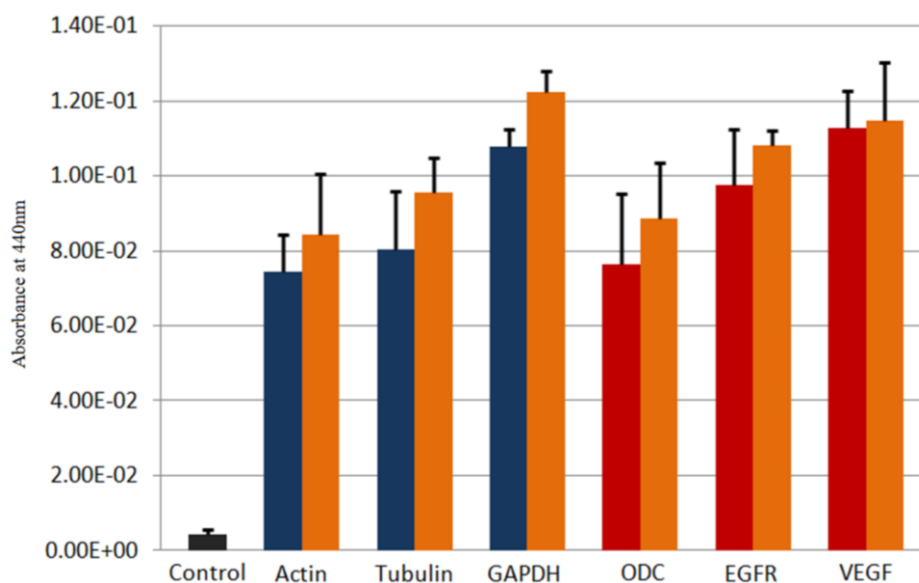


**Figure 3.49. The viability of SH-SY5Y cells treated with hippuristanol.** WST-1 viability assays were performed on SH-SY5Y cells transfected with the oncogene reporters and treated with hippuristanol or DMSO (Figure 3.4.). Before cells were lysed for luciferase assay, WST-1 reagent was added to the media and plates were incubated for a further one hour. After this incubation, 100  $\mu$ l of the media / WST-1 mixture was assessed by spectrophotometry. The interpretation of this graph is the same as for the previous figure with the exception of the y axis which represents arbitrary viability units (absorbance at 440 nm). The control was performed on wells containing no cells. Single experiment, average of three repeats, error bars represent standard deviation.

Relative to the control, all of the cells appeared viable (Figure 3.49.). There is no statistical difference between the data for plus and minus hippuristanol ( $p = 0.051$ ).

### 3.6.5. Hippuristanol causes a greater reduction in oncogene reporter expression than housekeeping gene reporter expression in HeLa cells

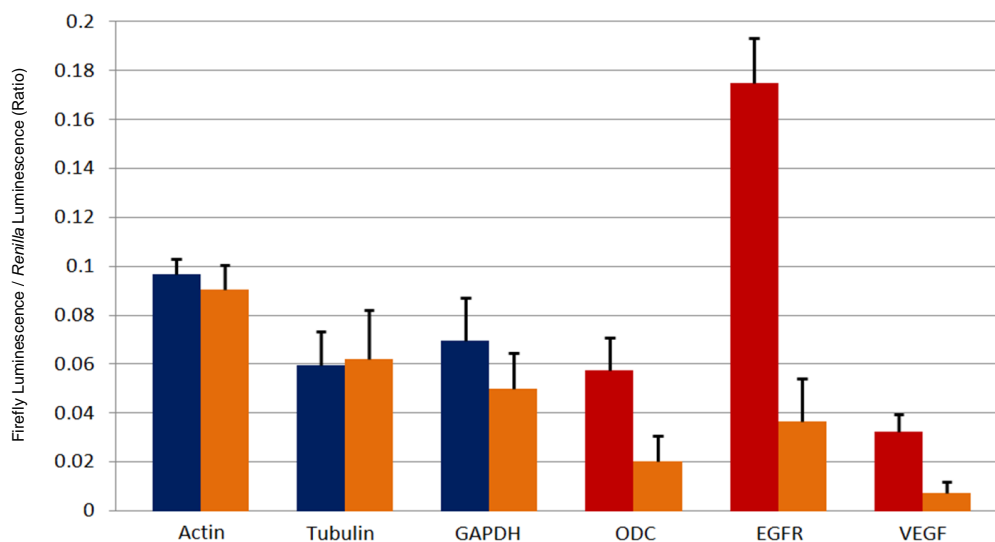


**Figure 3.50. The effect of 10  $\mu$ M hippuristanol on the oncogene reporter collection in HeLa cells.** Two 24 well plates were seeded with HeLa cells. The following day, six wells were transfected with each of the oncogene reporter plasmids (in addition to p80). Four hours later, three wells of each were treated with either 10  $\mu$ M hippuristanol or DMSO. Six hours later, cells were lysed for luciferase assay. The red or dark blue bars were generated from cells recipient of only DMSO while those in orange were generated from cells recipient of 10  $\mu$ M hippuristanol. Single experiment, average of three repeats, error bars represent standard deviation.

The results of the experiment conducted in HeLa (Figure 3.48.) were broadly similar to those generated using SH-SY5Y (Figure 3.50.). The main difference between cell lines is the substantial difference between the *EGFR* reporter and the controls ( $p = 0.0010$ ). In HeLa, the *EGFR* reporter activity also differed in that it responded more strongly to hippuristanol treatment, reducing by 79% ( $p = 0.0003$ ) compared to 28% in SH-SY5Y ( $p = 0.0003$ ).

### 3.6.6. Hippuristanol has no effect on cell viability in HeLa cells

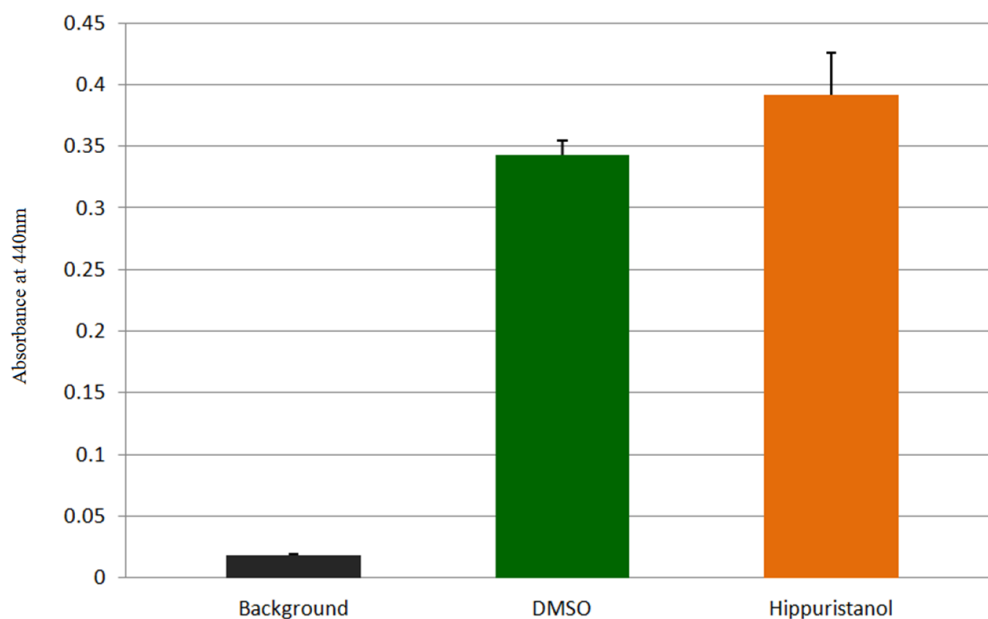


**Figure 3.51. The viability of HeLa cells treated with hippuristanol.** WST-1 viability assays were performed on HeLa cells transfected with the oncogene reporters and treated with hippuristanol or DMSO (Figure 3.50.). Before cells were lysed for luciferase assay, WST-1 reagent was added to the media and plates were incubated for a further one hour. After this incubation, 100  $\mu$ l of the medium / WST-1 mixture was assessed by spectrophotometry. The interpretation of this panel is the same as for the previous figure with the exception of the y axis which represents arbitrary viability units (absorbance at 440 nm). The control was performed on wells containing no cells. The interpretation of this panel is the same as for the previous figure with the exception of the y axis which represents arbitrary viability units (absorbance at 440 nm). The control was performed on wells containing no cells. Single experiment, average of three repeats, error bars represent standard deviation.

Hippuristanol had a similar effect on the viability of HeLa (Figure 3.549.) as it did on SH-SY5Y (Figure 3.51.). There was a slight but non-significant increase in viability in response to hippuristanol treatment ( $p = 0.2581$ ).

### 3.6.7. Hippuristanol causes a reduction in EGFR protein level

In order to ascertain whether the effect of eIF4A inhibition on the *EGFR* reporter is biologically relevant, the protein level of EGFR in HeLa recipient of hippuristanol treatment (or control treatment) was estimated by western blot. Bands were quantified using ImageJ (Abramoff et al., 2004).

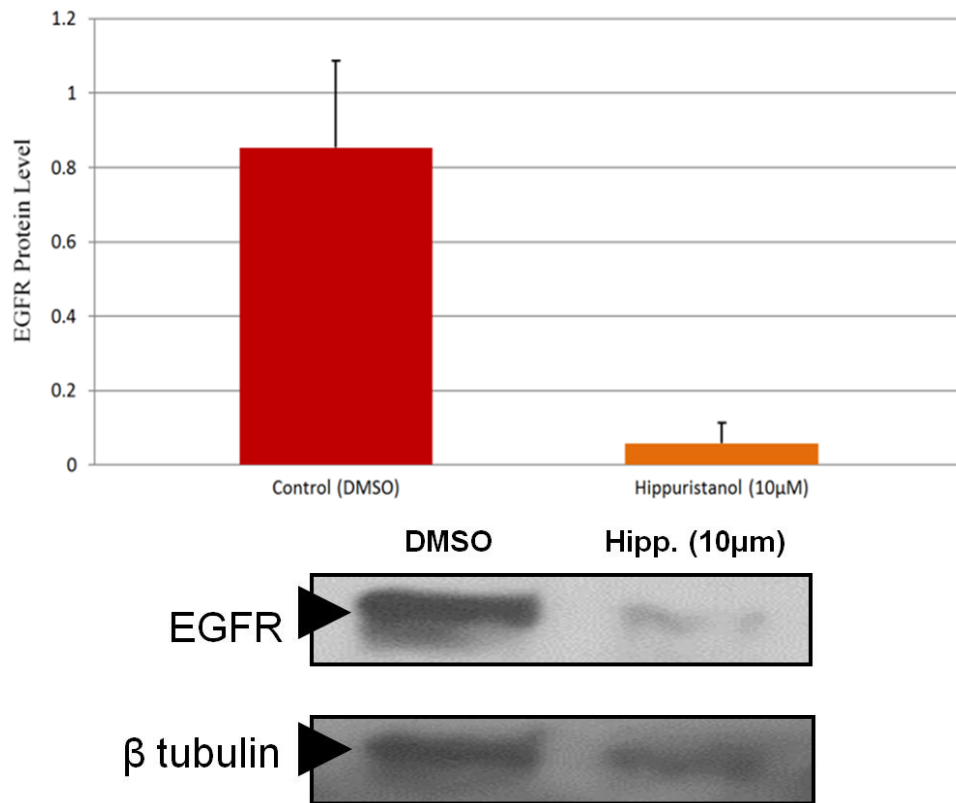


**Figure 3.52. The effect of hippuristanol on EGFR protein level.** HeLa cells were treated for 24 hours with either 10 μM hippuristanol or DMSO, lysates from these cells were western blotted for EGFR. Blots were run in triplicate, quantified relative to a β tubulin loading control and averaged. The size marker on the EGFR blot represents 150 kDa, the marker on the tubulin blot represents 50 kDa. Representative blots are shown, single experiment, average of three repeats, error bars represent standard deviation.

10 μM hippuristanol treatment caused a significant reduction in EGFR protein level in HeLa ( $p = 0.0106$ ) Figure (3.52.).

### 3.6.8. Promoterless oncogene reporters are not functional

Promoterless versions of the oncogene reporters were used to test for cryptic promoter activity.



**Figure 3.53. Versions of the oncogene reporters without the CMV promoter were created and assayed for activity in SH-SY5Y cells.** The p15 control included a functional promoter. Single experiment, average of three repeats, error bars represent standard deviation.

Removal of the CMV promoter from the reporters caused a reduction in luciferase activity to background levels in SH-SY5Y cells (Figure 3.5.). The experiment was repeated in HeLa cells with the same result (data not shown).

### 3.6.9. The *EGFR* 5' UTR in pRF (pREGFRF) allows the expression of the downstream cistron

In order to test for IRES activity, the *EGFR* 5' UTR was cloned into the dicistronic reporter pRF.

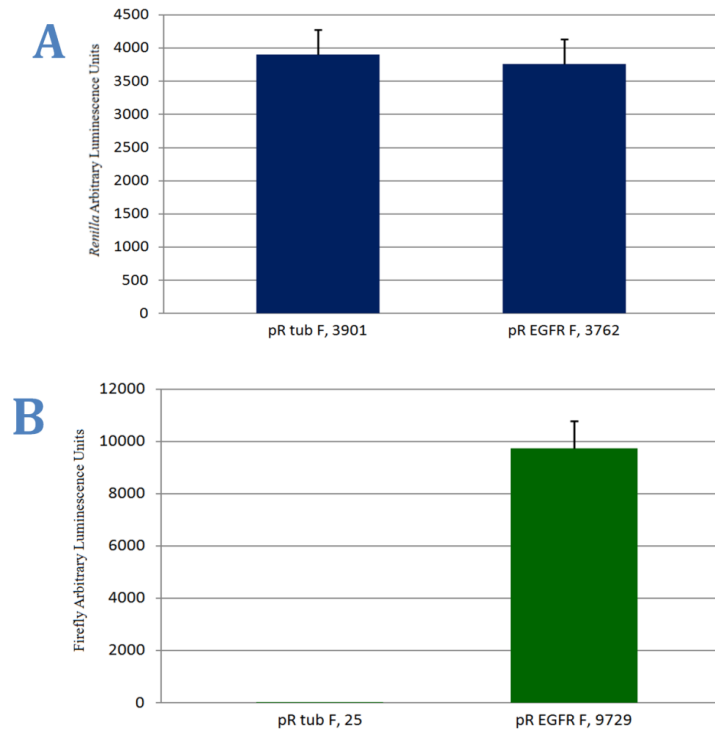


**Figure 3.54. The *EGFR* 5' UTR in a dicistronic context.** A 24 well plate was seeded with SH-SY5Y cells. The following day, eight wells were transfected with pREGFRF and eight with pRtubF. 48 hours later, cells were lysed and luciferase assays were performed. Panel A shows the levels of *Renilla* luciferase activity of pRtubulinF and pREGFRF transfected into SH-SY5Y cells. Panel B shows the firefly luciferase activity of the same constructs. Single experiment, average of eight repeats, error bars represent standard deviation.

There was no significant difference between *Renilla* luciferase expression levels between the two plasmids ( $p = 0.2690$ ) (Figure 3.5. A.). Panel B shows that the  $\beta$  tubulin reporter pRtubF generated only background levels of firefly luciferase expression (25) while the EGFR reporter generated a signal of almost 10,000 (9,729).

### 5.6.10. The *EGFR* 5' UTR in promoterless pRF generates no signal

In order to establish whether the apparent IRES activity of the *EGFR* 5' UTR (Figure 3.5.) was due to cryptic promoter activity in the dicistronic context, the experiment was repeated using a promoterless version of the plasmid.

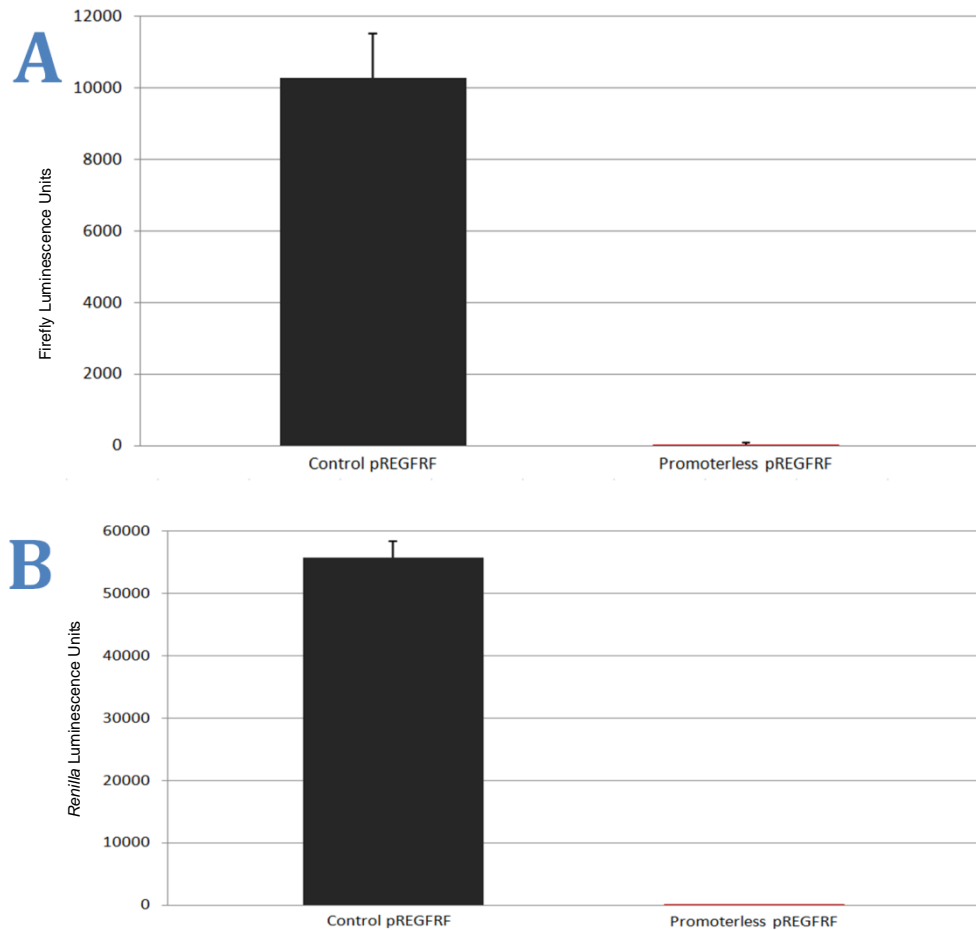


**Figure 3.55. The *EGFR* 5' UTR in a promoterless dicistronic context.** A 24 well plate was seeded with SH-SY5Y cells. The following day, eight wells were transfected with pREGFRF and eight with Promoterless-pREGFRF. 48 hours later, cells were lysed and luciferase assays were performed. Panel A shows the levels of firefly luciferase activity of pREGFRF and Promoterless-pREGFRF transfected into SH-SY5Y cells. Panel B shows the *Renilla* luciferase activity of the same constructs. Single experiment, average of eight repeats, error bars represent standard deviation.

With no promoter sequence driving the transcription of the dicistronic *Renilla*ORF-*EGFR*5'UTR-fireflyORF sequence, there was a reduction in both *Renilla* luciferase and firefly luciferase expression (Figure 3.55..).

### 5.6.11. Northern analysis reveals that the *EGFR* 5' UTR does not induce splicing

The firefly luciferase signal from pREGFRF may be the result of the *EGFR* 5' UTR acting as a splice site for the dicistronic mRNA (Figure 3.5.). This may potentially result in a capped, functional firefly luciferase-encoding mRNA (Figure 3.56.).

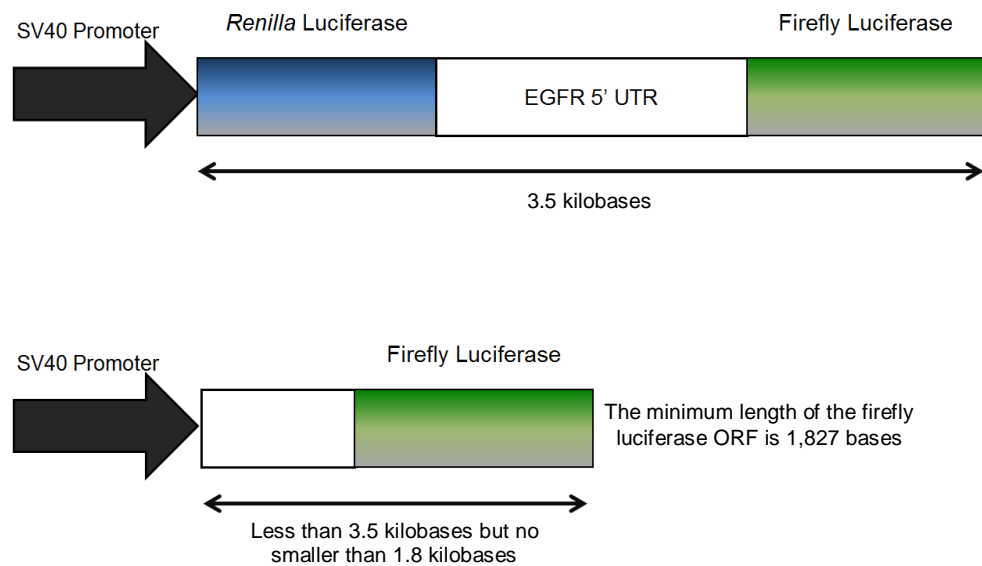


**Figure 3.56. The mRNA that may result from the *EGFR* 5' UTR facilitating the splicing of the mRNA generated by pREGFRF.** The size of the full-length transcript is 3.5 kb (top construct); a spliced variant of this will be shorter in length.

In order to determine whether the luciferase signal from pREGFRF is a result of IRES activity or splicing events, a northern blot was performed (see Materials and Methods). The probe was complementary to the firefly luciferase open reading frame so if the spliced transcript shown above were being generated then an extra band would be apparent on the gel.

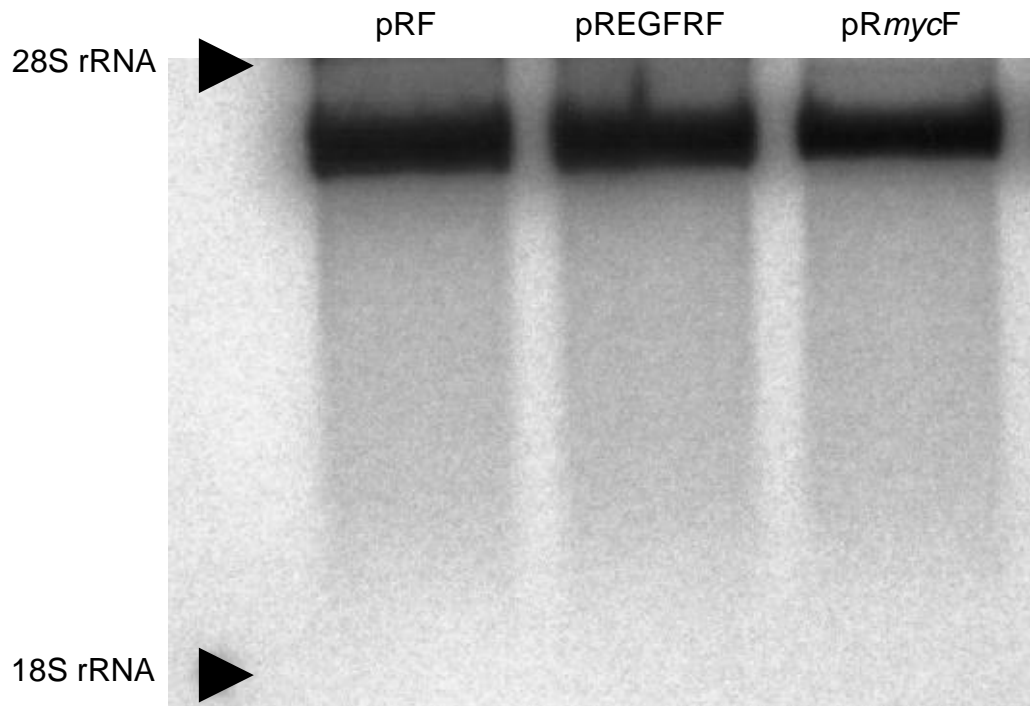


**Figure 3.57. Northern blot using a probe complementary to the firefly luciferase open reading frame.** The 18S rRNA is approximately 1.9 kilobases and the 28S rRNA is approximately 4.9 kilobases. All the lanes contain a transcript of the expected size. Experiment repeated with the same result (data not shown)

The *EGFR* 5' UTR probably does not induce splicing given that the transcript of pREGFRF generates a single mRNA of the expected size.

### 5.6.12. The *EGFR* 5' UTR has IRES activity four in different cell lines

In order to test whether the IRES activity of the *EGFR* 5' UTR observed in SH-SY5Y cells was an artefact unique to these cells, the experiment was repeated in a further three laboratory cancer cell lines.

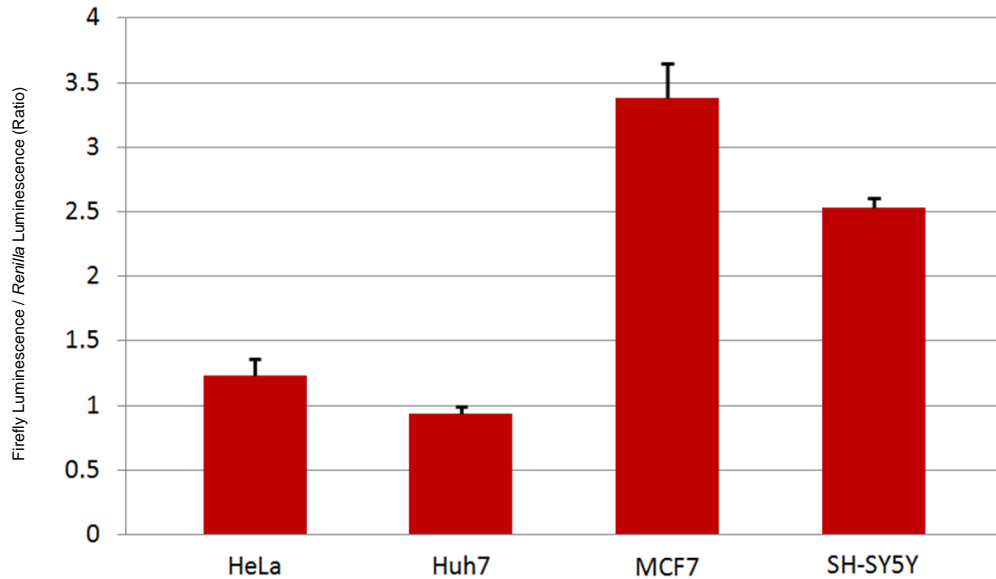


**Figure 3.58. The IRES activity of the *EGFR* 5' UTR in different cell lines.** 24 well plates were seeded with HeLa, Huh7, MCF7 and SH-SY5Y cells. The following day, six wells of each were transfected with pREGFRF. 48 hours later, luciferase assays were performed on the cellular lysates. Single experiment, average of six repeats, error bars represent standard deviation.

IRES activity was apparent in all four cell lines (Figure 3.58.). There was a difference in normalised pREGFRF expression (firefly luciferase activity / *Renilla* luciferase activity) between different cell lines. All differences are statistically significant (HeLa vs Huh7 data  $p = 0.0169$ ).

### 5.6.13. Mapping of the *EGFR* IRES using upstream start codons

In order to establish where the ribosome enters the *EGFR* 5' UTR, mutant versions of the sequence were generated and cloned into pRF. The principle of the out-of-frame upstream AUG mutant mapping is shown below (Figure 3.5.).

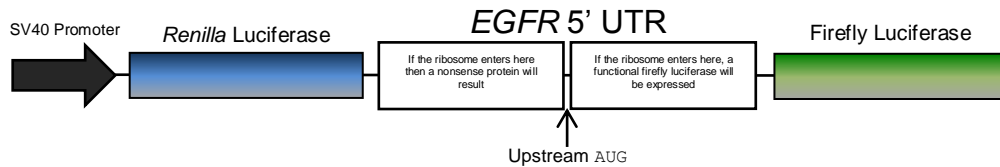


**Figure 3.59. Representation of the mutant *EGFR* sequence containing the introduced upstream AUG sequence (out of frame of the firefly luciferase cistron) and the consequences of the ribosome entering either side.**

If the ribosome enters the 5' UTR upstream of the introduced AUG and initiates translation at this point, it will encounter a stop codon 114 nucleotides downstream and produce a 38 amino acid peptide (Figure 3.). If the ribosome enters downstream of the introduced AUG, the wild-type firefly luciferase protein will be expressed (Figure 3.).

### Mutant Peptide:

GVRPSPRLAANATTTAHGPLTPSSIDRESRSELFGEQR 38

### Wild-type firefly luciferase:

```
MEDAKNIKKGPAPFYPLEDGTAGEQLHKAMKRYALVPGTIAFTDAHIEVDITYAEYFEMS 60
VRLAEAMKRYGLNTNHRIVVCSENSLQFFMPVLGALFIGVAVAPANDIYNERELLNSMGI 120
SQPTVVVFSKKGLQKILNVQKKLP I I Q K I I I M D S K T D Y Q G F Q S M Y T F V T S H L P P G F N E Y D 180
FVPESFDRDKTIALIMNSSGSTGLPKGVALPHRTACVRFSHARDPIFGNQIIPDTAILSV 240
VPFHHGFGMFTTLGYLICGFRVVLMYRFEELFLRSLQDYKIQSALLVPTLFSFFAKSTL 300
IDKYDLNLHEIASGGAPLSKEVGEAVAKRFHLPGIRQGYGLTETTSAILITPEGDDKPG 360
AVGKVVVFFFEAKVVDLDTGKTLGVNQRGELCVRGPMIMSGYVNNPEATNALIDKDGWLHS 420
GDIAYWDEDEHFFIVDRLKSLIKYKGYQVAPAELESILLQHPNIFDAGVAGLPDDDAGEL 480
PAAVVVLEHGKTMTEKEIVDYVASQVTTAKKLRGGVVFVDEVKGLTGKLDARKIREILLI 540
KAKKGGKIAVNSHGFPPEVEEQAAGTLPMSCAQESGMDRHPAACASARINV 591
```

**Figure 3.60. Amino acid sequences of the mutant peptide resulting from the ribosome entering the *EGFR* 5' UTR upstream of the out-of-frame AUG and the wild-type firefly luciferase.**

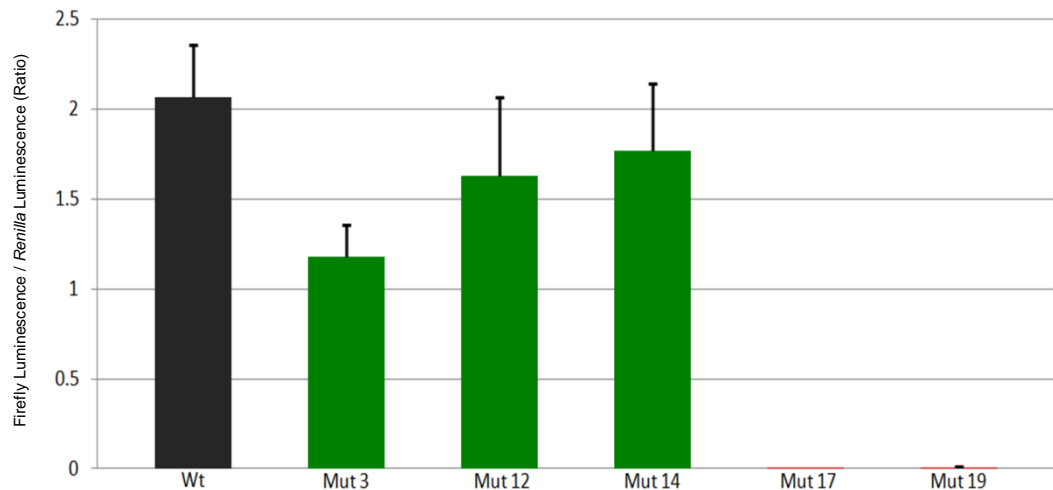


**Figure 3.61. Mutant versions of the *EGFR* 5' UTR containing introduced AUG sequences.** Two 24 well plates were seeded with SH-SY5Y cells. The following day, six wells of each were transfected with mutant versions of the *EGFR* reporter and the wild-type pREGFRF plasmid. 48 hours later, cells were lysed and luciferase assays were performed. The sequences of the mutant versions are shown on the next page. Single experiment, average of six repeats, error bars represent standard deviation.

Mutants 3 – 14 permitted the successful expression of the firefly luciferase gene whereas mutants 17 and 19 did not (Figure 3.61.). This indicates that the ribosome entry site of the IRES is between 61 – 25 nucleotides from the wild-type start codon; this region is highlighted in purple in the wild-type sequence on the following page.

**Wild-type**

CCCCGGCGCAGCGCGGCCGCAGCAGCCTCCGCCCCCGCACGGTGTGAGCGCCCGAC  
GCGGCCGAGGCGGCCGGAGTCCCGAGCTAGCCCCGGCGGCCGCCGCCAGACCG  
GACGACAGGCCACCTCGTCGGCGTCCGCCCCGAGTCCCCGCCTCGCCGCCAACGCCAC  
AACCACCGCGCACGGCCCCCTGACTCCGTCCAGTATTGATCGGGAGAGCCGGAGCGA  
GCTCTTCGGGGAGCAGCG

**Mut 3 (changed base 115 bases from wild type start codon)**

CCCCGGCGCAGCGCGGCCGCAGCAGCCTCCGCCCCCGCACGGTGTGAGCGCCCGAC  
GCGGCCGAGGCGGCCGGAGTCCCGAGCTAGCCCCGGCGGCCGCCGCCAGACCG  
GAtGACAGGCCACCTCGTCGGCGTCCGCCCCGAGTCCCCGCCTCGCCGCCAACGCCAC  
AACCACCGCGCACGGCCCCCTGACTCCGTCCAGTATTGATCGGGAGAGCCGGAGCGA  
GCTCTTCGGGGAGCAGCG

**Mut 12 (130)**

CCCCGGCGCAGCGCGGCCGCAGCAGCCTCCGCCCCCGCACGGTGTGAGCGCCCGAC  
GCGGCCGAGGCGGCCGGAGTCCCGAGCTAGCCCCGGCGGCCGCCGCCAGACCG  
GACGACAGGCCACCTCaTgGGCGTCCGCCCCGAGTCCCCGCCTCGCCGCCAACGCCAC  
AACCACCGCGCACGGCCCCCTGACTCCGTCCAGTATTGATCGGGAGAGCCGGAGCGA  
GCTCTTCGGGGAGCAGCG

**Mut 14 (187)**

CCCCGGCGCAGCGCGGCCGCAGCAGCCTCCGCCCCCGCACGGTGTGAGCGCCCGAC  
GCGGCCGAGGCGGCCGGAGTCCCGAGCTAGCCCCGGCGGCCGCCGCCAGACCG  
GACGACAGGCCACCTCGTCGGCGTCCGCCCCGAGTCCCCGCCTCGCCGCCAACGCCAC  
AACCACCGCGCACGGCatgCTGACTCCGTCCAGTATTGATCGGGAGAGCCGGAGCGA  
GCTCTTCGGGGAGCAGCG

**Mut 17 (223)**

CCCCGGCGCAGCGCGGCCGCAGCAGCCTCCGCCCCCGCACGGTGTGAGCGCCCGAC  
GCGGCCGAGGCGGCCGGAGTCCCGAGCTAGCCCCGGCGGCCGCCGCCAGACCG  
GACGACAGGCCACCTCGTCGGCGTCCGCCCCGAGTCCCCGCCTCGCCGCCAACGCCAC  
AACCACCGCGCACGGCCCCCTGACTCCGTCCAGTATTGATCGGGAGAGCCGGAtgGA  
GCTCTTCGGGGAGCAGCG

**Mut 19 (241)**

CCCCGGCGCAGCGCGGCCGCAGCAGCCTCCGCCCCCGCACGGTGTGAGCGCCCGAC  
GCGGCCGAGGCGGCCGGAGTCCCGAGCTAGCCCCGGCGGCCGCCGCCAGACCG  
GACGACAGGCCACCTCGTCGGCGTCCGCCCCGAGTCCCCGCCTCGCCGCCAACGCCAC  
AACCACCGCGCACGGCCCCCTGACTCCGTCCAGTATTGATCGGGAGAGCCGGAGCGA  
GCTCTTCGGGGAGatGCG

**Figure 3.62. The wild-type and mutant forms of the *EGFR* 5' UTR that were cloned into pRF. The mutant start codons are shown underlined and in green, the bases that were changed are shown in lower case.**

### 3.6.14. An upstream AUG mutant in a monocistronic context

One of the mutant versions of the *EGFR* 5' UTR was cloned into p15 which encodes firefly luciferase in a monocistronic context. This would test whether translation initiation progresses in a cap-dependent or cap-independent manner (Figure 3.63.).

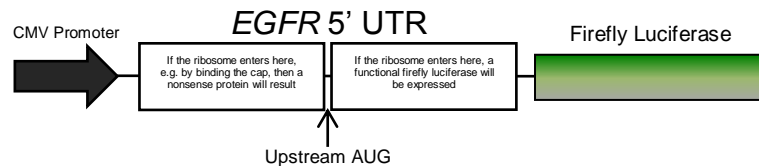


**Figure 3.63. A mutant version of the *EGFR* 5' UTR in the monocistronic p15 reporter plasmid.** If the pre-initiation complex binds to the 5' cap then a non-functional version of the luciferase will result and luciferase activity in cells transfected with this plasmid will be the same as the background. However, if the ribosome enters the sequence using the IRES, which is predicted to be in the 3' section of the sequence (Figure 3.61.), then a functional luciferase protein will result.

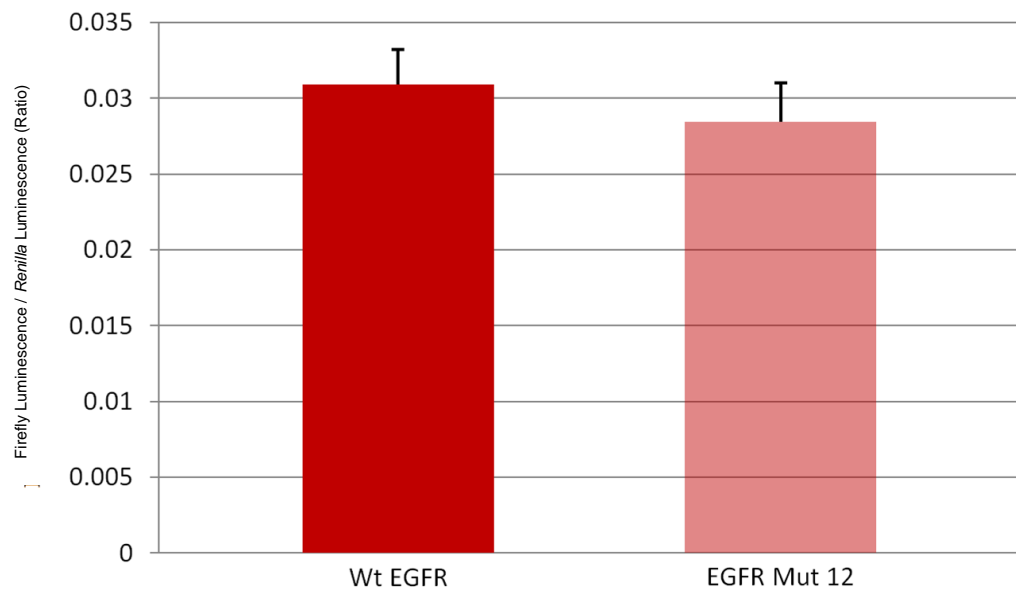


**Figure 3.64. A mutant version of the *EGFR* 5' UTR in a monocistronic reporter.** A 24 well plate was seeded with SH-SY5Y cells. The following day, six wells were transfected with p15EGFRMut12 and six with p15EGFR (wild-type). All 12 wells were transfected with the p80 control. 24 hours later, cells were lysed and luciferase assays were performed. Single experiment, average of four repeats, error bars represent standard deviation.

The introduction of an AUG start codon approximately in the middle of the *EGFR* 5' UTR out of frame of a downstream monocistronic reporter gene had no statistical effect on the data generated by this reporter ( $p = 0.3427$ ) (Figure 3.64.).

### 3.6.15. Truncation of the *EGFR* 5' UTR has no effect on IRES activity

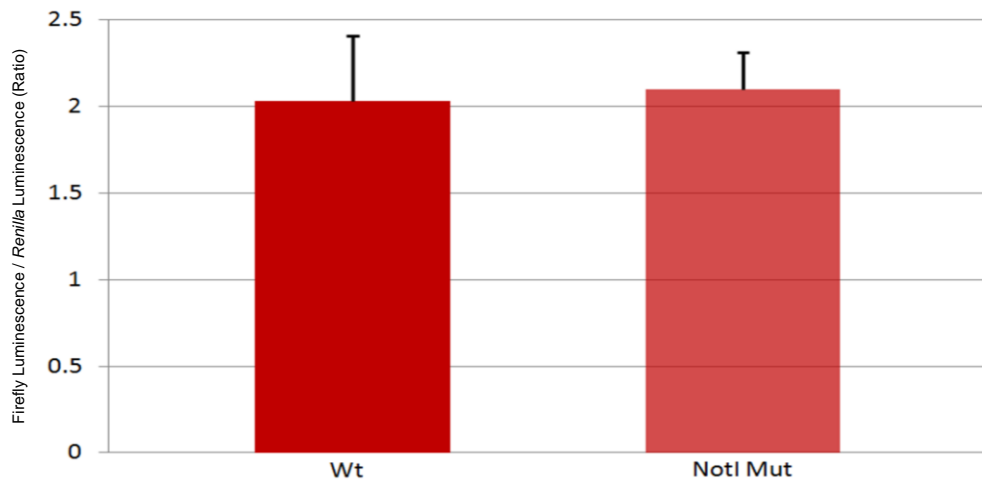


**Figure 3.65. A truncated version of the *EGFR* 5' UTR in a dicistronic reporter.** A 24 well plate was seeded with SH-SY5Y cells. The following day, six wells were transfected with pREGFRF*NotI*Mut and six with p15EGFR (wild-type). All 12 wells were transfected with the p80 control. 24 hours later, cells were lysed and luciferase assays were performed. Single experiment, average of four repeats, error bars represent standard deviation.

The removal of the **red** bases (below) by *NotI* digestion caused no decrease in firefly luciferase expression (Figure 3.65.). This indicates that this region is not involved in the IRES activity of the sequence.

#### Wild-type

```
CCCCGGCGCAGCGCGGCCGAGCAGCCTCCGCCCCCGCACGGTGTGAGCGC  
CCGACGCGGCCGAGGCCGGAGTCCCGAGCTAGCCCCGGCGGCCGCC  
GCCAGACCGGACGACAGGCCACCTCGTCGGCGTCCGCCCGAGTCCCCGCCT  
CGCCGCCAACGCCACAACCACCGCGCACGGCCCCCTGACTCCGTCCAGTATT  
GATCGGGAGAGCCGGAGCGAGCTCTTCGGGGAGCAGCG
```

### 3.6.16. Hippuristanol significantly reduces firefly luciferase expression generated by pREGFRF

The signal from the monocistronic *EGFR* 5' UTR reporter decreases in response to hippuristanol treatment. The following experiment was performed in order to establish whether the same was true if the sequence was in a dicistronic context.

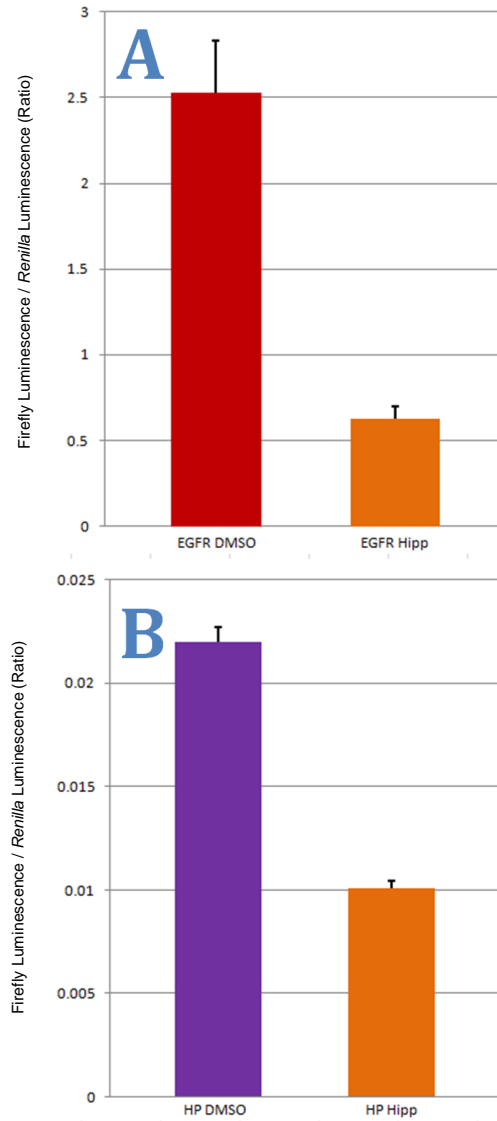


**Figure 3.66. The effect of hippuristanol on pREGFRF.** A 24 well plate was seeded with SH-SY5Y cells. The following day, six wells were transfected with pREGFRF (A.) and another six were transfected with p15HP and p80 (B.). 24 hours later, hippuristanol (or DMSO) was added to the cells. After incubation for a further 24 hours, cells were lysed for luciferase assay. Single experiment, average of three repeats, error bars represent standard deviation.

Hippuristanol treatment caused a significant reduction in firefly luciferase activity in both the pREGFRF reporter ( $p = 0.0002$ ) (Figure 3.66. A.) and the hairpin control ( $p = 6.72689E-06$ ) (Figure 3.66. B.).

### 3.6.17. The *EGFR* IRES maintains reporter expression in hypoxia

In order to establish whether the previously observed upregulation of EGFR in response to hypoxia was translationally controlled, the *EGFR* reporter plasmid was assayed for activity in cells incubated under hypoxic conditions (Franovic *et al.*, 2007).

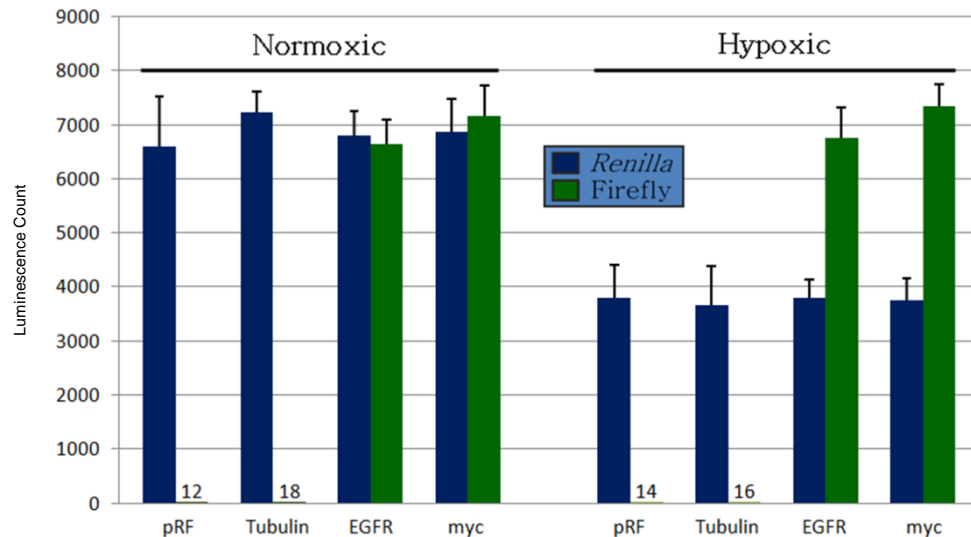


**Figure 3.67. The effect of hypoxia on pREGFRF.** Two 24 well plates were seeded with SH-SY5Y cells. The following day, six wells from each were transfected with pRF, pRtubulinF, pREGFRF or pRmycF. One plate was incubated in a normoxic (atmospheric) oxygen concentration and the other in hypoxic (1% O<sub>2</sub>) conditions. 24 hours later, cells were lysed for luciferase assay. Single experiment, average of six repeats, error bars represent standard deviation.

Hypoxia caused a ~50% reduction in levels of *Renilla* luciferase expression ( $p = 1.18E-22$ ) (Figure 3.6.). In both hypoxic and normoxic conditions, pRF and pRtubulinF generated only background levels of firefly luciferase activity while pREGFRF and pRmycF generated strong firefly luciferase signals which are maintained in hypoxic conditions (Figure 3.6.).

### 3.6.18. Hypoxia has little effect on cell viability

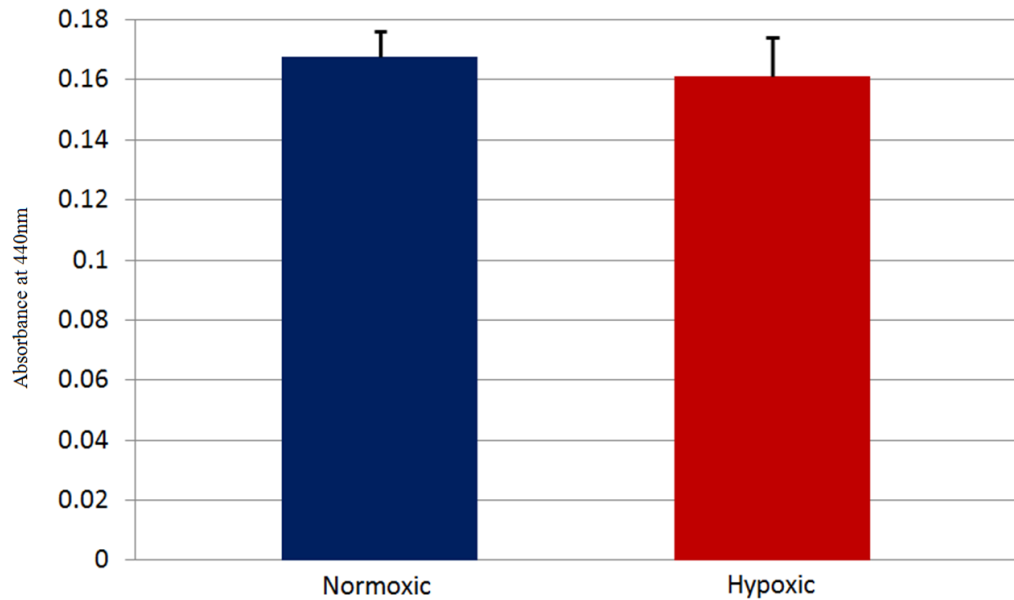


**Figure 3.68. The effect of a 24 hour incubation under hypoxic conditions on the viability of SH-SY5Y cells.** WST-1 assays for cell viability were performed on the cells incubated in hypoxic and normoxic conditions. Single experiment, average of six repeats, error bars represent standard deviation.

Hypoxia had no significant effect on SH-SY5Y cell viability ( $p = 0.1620$ ) when assayed over the 30 minutes immediately following 24 hour incubations in hypoxic and normoxic conditions (Figure 3.68.).

### 3.6.19. Iron response activity in different cell lines and the effect of the truncation mutant

In order to test whether the iron-responsive nature of the *EGFR* reporter was an artifact unique to SH-SY5Y cells, it was repeated in different cell lines. The plasmid containing the truncated version of the *EGFR* sequence (page 174) was also assayed for activity in the three different cell lines.

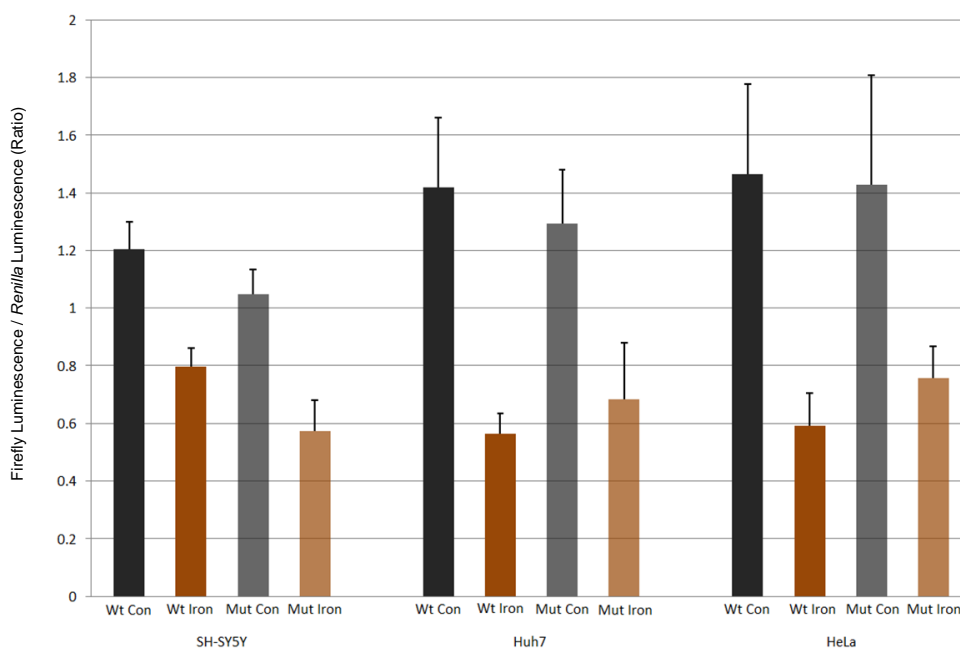


**Figure 3.69. The effect of iron on the wild-type and mutated *EGFR* 5' UTR reporters in three different cell lines.** 24 well plates were seeded with SH-SY5Y, Huh7 or HeLa cells. 12 wells of each plate were transfected with either pREGFRF or pREGFRF~~NotMut~~. Six wells of each of these were either treated with 250  $\mu$ M ammonium iron citrate or an equal volume of H<sub>2</sub>O ('con'). Single experiment, average of six repeats, error bars represent standard deviation.

Removal of the bases shown in red on page 174 did not cause a loss of the iron-responsive property of the sequence in either SH-SY5Y, Huh7 or HeLa cells (Figure 3.69.). Both the wild-type *EGFR* sequence and the mutant had iron-response activity in all three cell lines.

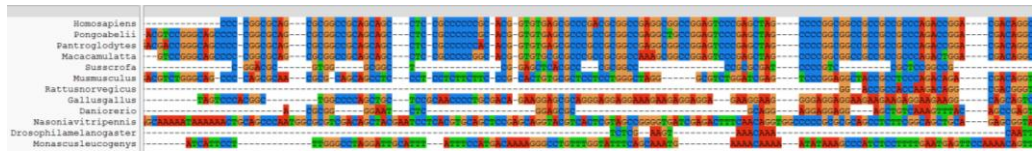
### 3.6.20. The *EGFR* 5' UTR in a phylogenetic context

Common Name	Latin Name	E value	% Homology with Human <i>EGFR</i> 5' UTR
Common chimpanzee	<i>Pan troglodytes</i>	4e-120	99%
Sumatran orang-utan	<i>Pongo abelii</i>	2e-116	98%
Rhesus macaque	<i>Macaca mulatta</i>	3e-103	95%
Common marmoset	<i>Callithrix jacchus</i>	0.002	93%

**Table 21. A BLAST search was performed referencing the human *EGFR* 5' UTR sequence against the non-redundant (nr) database of sequences (29/10/2011) (Altschul *et al.*, 1997)**

In addition to performing a BLAST search for similarity to the human sequence, the term 'egfr' was used to search genome sequences of all species on the NCBI Gene database (<http://www.ncbi.nlm.nih.gov/gene/?term=egfr>, 2/11/2011). This identified matches in species not listed above (Table 21.), these sequences were compiled into a new database in addition to the sequences identified by the BLAST search. A ClustalW2 alignment was performed (using <http://www.ebi.ac.uk/Tools/msa/clustalw2/>, 2/11/2011 with default parameters (Larkin *et al.*, 2007)). This alignment was then visualised using ClustalX v2.1 (Larkin *et al.*, 2007) (Figure 3.70.).

The 5' half of the human *EGFR* 5' UTR sequence aligned to that of ten different species



The 3' half

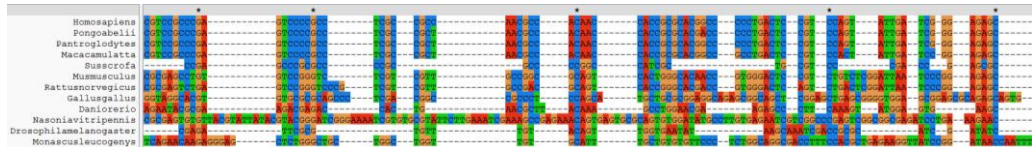
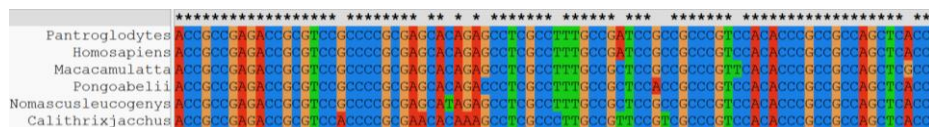


**Figure 3.70. ClustalX v2.1 visualisation of a ClustalW2 alignment of the *EGFR* 5' UTR of 12 different species.** The sequence belonging to the common marmoset (*Calithrix jacchus*) is not included as it is only 40 bases in length and is probably only a fragment of the full-length sequence belonging to this organism. There is a much higher degree of sequence conservation in the 3' half of the sequence. Canonical bases are indicated by asterisks.

The significance of the conservation of the *EGFR* 5' UTR sequence remains to be determined as the  $\beta$  *actin* and  $\beta$  *tubulin* 5' UTR sequences are also highly conserved (Figure 3.71.).

The  $\beta$  *actin* 5' UTR sequence aligned to that of five different species



The  $\beta$  *tubulin* 5' UTR sequence aligned to that of 13 different species

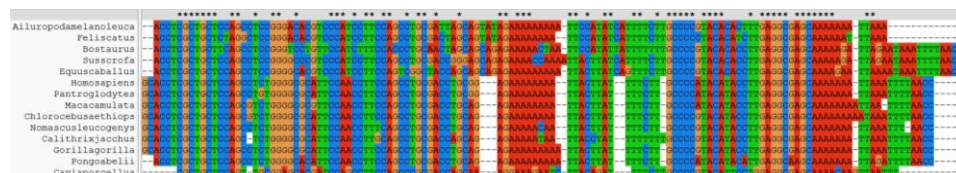


**Figure 3.71. ClustalX v2.1 visualisation of a ClustalW2 alignment of the *EGFR* 5' UTR of 12 different species.**

# Chapter 4. Discussion

## Part 1.

### Screens for eIF4A Activity

#### 4.1.1. Conclusions from the Optimisation of the *In Vitro* and Cell-Based Screens

- The most successful *in vitro* screen approach was only moderately responsive to the activity of eIF4A (Figure 3.24).
- However, the optimised cell-based screen was highly sensitive to a reduction in eIF4A function (using hippuristanol (Figure 3.12.) and RNAi (Figure 3.10., 3.27.)) and eIF4E function (using a cap analogue, Figure 3.13.)).
- It is interesting that eIF4E suppression has a greater effect on the hairpin-mediated reporter than it does on the control reporter. The mRNA discriminatory effect of eIF4E inhibition has been documented (Graff et al., 2008) but it remains to be explained why it occurs.
- Promoterless and dicistronic variants of the hairpin reporter plasmid revealed that the hairpin did not exhibit cryptic promoter or IRES activity (Figure 3.3., Figure 3.7.). It may be possible that the hairpin acts as a cryptic enhancer in the context of the reporter plasmid but this is unlikely as the luciferase expression level from the hairpin-containing plasmid (p15HP) is much lower than that of the control plasmid (p15) (Figure 3.6.).
- This means that the hairpin reporter system could form the basis of a high-throughput screen for new small molecule inhibitors of translation.
- Alongside the radioactive helicase assay (Figure 3.16.), the *in vitro* screen may prove to be useful in the low throughput assessment of eIF4A function *in vitro*. It may be particularly useful in identifying false positive hits generated by the high throughput cell-based screen. For example, if a molecule in the library had activity similar to that of pifithrin- $\alpha$  which inhibits firefly luciferase activity (but not *Renilla* luciferase), this would be registered as a positive for translation initiation inhibition by the cell-

based screen but would be revealed as a negative by the *in vitro* assay (Rocha et al., 2003).

#### 4.1.2. Limitations of the screens

- The optimised cell-based screen approach involved the transfection of the reporter plasmids into the cell using Fugene 6 followed by a short (four hour) recovery period before the eIF4A inhibitor was added to the cells (Figure 3.12.).
- The problem with up-scaling this approach is the cost and inconsistency associated transiently transfecting a large number (potentially >100, 000 wells) of cells.

#### 4.1.3. Future work on the screens

- One solution to the problem of up-scaling the cell-based screen would be to create a stable cell line which constitutively expresses the control *Renilla* luciferase gene and the hairpin-mediated firefly luciferase gene.
- This would be theoretically easy to create as the plasmids contain hygromycin (pGL4.15) and neomycin (pGL4.80) resistance genes.
- The problem with this solution is that there would be a perpetually high concentration of firefly luciferase protein within the cells. An eIF4A inhibitor added to these cells would only curtail *de novo* luciferase expression. The accumulated protein would have to degrade for the effects of the inhibition to be observable.
- An inducible expression vector could be used to combine both these approaches. For example, the hairpin and the luciferase ORF could be cloned into the plasmid below (Figure 4.1., Clontech, Cat # 631168) between the Tet-On 3G sequence and the SV40 polyA signal. Tetracycline would be added along with the candidate molecule. This would mean that all the subsequent firefly luciferase expression would be proportional to the functionality of the eIF4A in the cells.

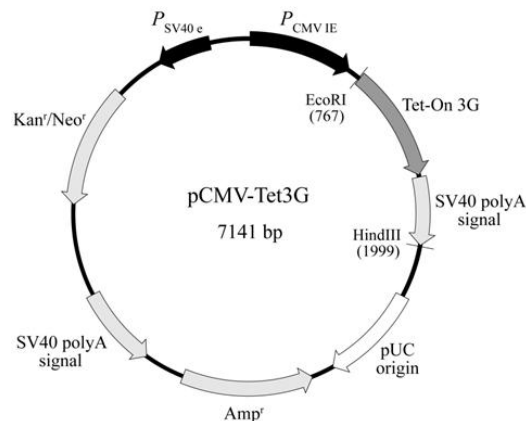


**Figure 4.1. An example of a tetracycline-inducible plasmid that already contains a CMV promoter sequence.**

## Part 2.

### eIF4A Paralogs

#### 4.2.1. The effect of individual siRNA knockdown of each paralog on the hairpin reporter system

- Consistent with the data generated using shRNA, knockdown of eIF4AI using siRNA causes a reduction in hairpin-mediated luciferase expression (Figure 3.27.).
- Interestingly, knockdown of eIF4AII (confirmed to be successful by western blot) does not cause a significant reduction in hairpin-mediated luciferase expression relative to the control (Figure 3.27.).
- The consensus in the literature is that paralogs I and II perform the same function (see 1.2.2. Paralogs). The fact that eIF4AII is not detectibly involved in the unwinding of the secondary structure of the hairpin-containing luciferase mRNA (Figure 3.27.) strongly supports the theory that it is functionally distinct from eIF4AI under these conditions.
- Individual or combined knockdown of each of paralog of eIF4A has little effect on cell viability (estimated using WST-1) or the number of dissociated cells (Figure 3.28.).
- This may be a surprising result given the apparent importance of these proteins in gene expression. Although surprising, cellular tolerance to eIF4A suppression has been documented in the literature (see 1.4.5. eIF4A and Cancer).

#### 4.2.2. Limitation of the data generated by the hairpin reporter in response to eIF4A knockdown

- The western blots confirming the successful knockdown of each of the paralogs of eIF4A (Figure 3.27.) must be repeated if these data are to be published. The unconvincing appearance of some of the knockdowns limits the confidence with which conclusions may be drawn from this experiment.
- In mouse cells, it has been shown that eIF4AII is more highly expressed during quiescent phases of growth whereas eIF4AI is constitutively expressed (Williams-Hill et al., 1997). A confluent flask of cells was used for the experiment in this project that determined that knockdown of eIF4AII had no effect on the expression of the hairpin-mediated firefly

luciferase gene. No general conclusions can therefore be made until the experiment is repeated using a range of different cell densities so that the effect of the differential expression of the two different paralogs can be established.

- WST-1 (Roche, Cat # 11 644 807 001) is a tetrazolium salt that is cleaved by mitochondrial dehydrogenases which generates formazan (which changes the colour of the media). This assay therefore does not measure cell viability directly. As such, care must be taken when making conclusions regarding overall viability based on WST-1 assay alone.
- Alongside WST-1 assay, floating cell counts can give an indication of the health of the population of cells. However, this approach is also flawed if it is used to make general inferences regarding cell viability as dead cells may not float and floating cells may not be dead.

#### **4.2.3. Future work focusing on the effect of knocking down each paralog on the hairpin reporter system**

- The western blots must be repeated.
- The experiment should be repeated using cells at different densities.
- It would be interesting to determine the effect of individual eIF4A paralog knockdown on sequences other than the hairpin. For example, expression from the Alzheimer's disease- or cancer- associated reporter plasmids may be different in response to individual knockdown compared to hippuristanol treatment.

#### **4.2.4. The response of the *eIF4A* 5' UTR reporters to paralog knockdown and hippuristanol treatment**

- In order to establish whether the genes encoding the three paralogs of eIF4A are translationally controlled by a feedback mechanism, cells transfected with reporter plasmids containing the 5' UTRs of the each of the genes were treated with siRNAs directed against the three proteins (Figure 3.29).
- As expected, knockdown of eIF4AI caused reductions in the signals of all three reporters roughly proportional to the amount of predicted secondary structure (Figure 3.29).
- Despite being highly structured, the *eIF4AIII* 5' UTR stimulates reporter gene expression and has a less than expected requirement for eIF4AI function (Figure 3.29). The function of this reduced requirement may be

to preserve eIF4AIII expression under conditions that are inhibitory to eIF4AI (and possibly eIF4E). Since eIF4AIII is involved in mRNA splicing and other processes associated with mRNA turnover, it may be necessary for cell survival (Ferraiuolo et al., 2004; Holzmann et al., 2000). While it has previously been shown that knockout of eIF4AIII is lethal during development, knockdown in mature cells is tolerated (Haremaki et al., 2010). The stimulatory effect of the *eIF4AIII* 5' UTR together with its resistance to eIF4AI suppression and the importance of the gene in development specifically, indicate that translational control of the sequence is likely to be important in immature organisms.

- Somewhat surprisingly, hippuristanol treatment causes a different effect to the knockout of eIF4AI on the reporters containing the *eIF4A* 5' UTR sequences (Figure 3.30.). Hippuristanol is thought to inhibit paralogs I and II but not III (Bordeleau et al., 2006). The *eIF4AIII* reporter behaves like the hairpin reporter following hippuristanol treatment, a significant drop in reporter gene expression is observed (Figure 3.30.). The similarity of the data generated by combined eIF4AI and eIF4AII knockdown and hippuristanol treatment is consistent with the idea that hippuristanol inhibits eIF4AII in addition to eIF4AI (Figure 3.29., Figure 3.27., Figure 3.30.).

#### **4.2.5. Limitations of the data generated by the *eIF4A* 5' UTR reporters**

- The main difficulty in interpreting these findings is that fact that eIF4AIII has multiple roles, none of which is fully understood (see 1.2.2. Paralogs).

#### **4.2.6. Future work inhibiting each paralog of eIF4A in cells transfected with reporter plasmids containing the 5' UTRs of each paralog**

- As with the previous experiment, it would be interesting to establish whether there are any cell-growth dependent effects on the expression of the *eIF4A* 5' UTR reporters.

## Part 3.

### PDCD4

#### 4.3.1. Conclusions from the response of the hairpin reporter to PDCD4 knockdown

- PDCD4 knockdown causes an increase in the expression of the control *Renilla* luciferase protein but a more significant increase in the expression of the hairpin-mediated firefly luciferase protein (Figure 3.31.). This differential is expected given the previously demonstrated requirement of the hairpin reporter for eIF4A activity.
- Although there is no statistical difference between the control and the PDCD4 knockdown-treated hairpin reporters (Figure 3.31.), optimisation of the knockdown and the reporter system may eventually lead this difference to become significant.

#### 4.3.2. The limitations of the experiment in which the response of the hairpin reporter to PDCD4 knockdown was observed

- The fact that PDCD4 knockdown is not statistically detectible (Figure 3.31.) is a major limitation to the use of the cell-based screen to identify new small molecule inhibitors of PDCD4.

#### 4.3.3. Future work on the detection of PDCD4 activity using the hairpin reporter

- A reporter plasmid containing a much more highly structured sequence preceding the luciferase ORF may be more sensitive to changes in PDCD4 activity.
- Ideally this sequence would require the maximum eIF4A activity of the cell. Inhibition of PDCD4 would be predicted to cause an increase in this activity.

#### 4.3.4. PDCD4 knockdown and the response to DNA damage by UV light

- Under normal conditions, PDCD4 knockdown does not significantly affect viability or the number of dissociated SH-SY5Y cells or HeLa cells UV treatment decreases cell viability and increases the number of dissociated cells, knockdown of PDCD4 in combination with UV exposure further decreases viability and further increases the number of dissociated cells in SH-SY5Y and in HeLa (Figure 3.32., Figure 3.33., Figure 3.34., Figure 3.35., Figure 3.36., Figure 3.37.).

- These data support the idea that PDCD4 is important in the DNA damage response in human cells as well as in chicken cells, as has been previously demonstrated (Bitomsky et al., 2008; Singh et al., 2009).
- Experiments performed by other members of our laboratory (mainly Andrew Bottley and Alexander Kondrashov) involved the treatment of cells with hippuristanol prior to UV exposure or chemically-induced DNA damage. It was found that eIF4A inhibition caused a significant increase in viability in HeLa and SH-SY5Y cells in both these cases. In JB6+ cells, which lack PDCD4, a marked increase in viability was observed in response to DNA damage when eIF4A was suppressed.
- These data suggest that the involvement of PDCD4 in the response to DNA damage may be due to its inhibitory relationship with eIF4A.

#### **4.3.5. Limitations of the experiments ascertaining the effect of PDCD4 knockdown on the DNA response**

- The limitations of using WST-1 assay and floating cell counts to estimate cell viability are discussed previously.

#### **4.3.6. Future work investigating the relationship between PDCD4 and DNA damage**

- In order to get a more complete picture of cell viability following DNA damage and PDCD4 knockdown, other techniques could be applied alongside the WST-1 assay and the floating cell counts. For example, bromodeoxyuridine (BrdU) labelling which is used to quantify the rate at which DNA is synthesised in a cell or a cytolysis assay which is used to estimate cell membrane stability.
- It would also be interesting to investigate the response of PDCD4-impaired cells to a range of different UV intensities and durations of exposure.

## Part 4.

### Alzheimer's Disease

#### 4.4.1. Conclusions from the Alzheimer's disease-associated reporter collection

- It has been previously shown that the expression of a luciferase gene is suppressed when its mRNA contains the 5' UTRs belonging to: *APP*, *BACE1*, *ADAM10* or *MAPT*. The data presented in this thesis corroborate these findings (Figure 3.39.).
- The 5' UTRs of *Clu1*, *CRI*, the *presenilins*, *SOD1* and *TXN* also suppress reporter gene expression (Figure 3.39.).
- Interestingly, the 5' UTRs of *SOD1* and *TXN* are less inhibitory than the rest (Figure 3.39.). This indicates that suppression of eIF4A would not impair the cellular defence against oxidative stress (Pappolla et al., 1992; Wollman et al., 1988).
- The reporters containing the 5' UTRs of the genes predicted to play harmful roles in Alzheimer's disease had significantly elevated eIF4A requirements relative to the reporters containing the 5' UTRs of *ADAM10*, *SOD1* and *Txn* (Figure 3.41, Figure 3.42.).
- The eIF4A requirement of the 5' UTR of *ADAM10* is much lower than expected based on its length and predicted free energy (Figure 3.42., Figure 5.1.).
- The eIF4A requirement of the *AChE* 5' UTR is much higher than expected based on its length and predicted free energy (Figure 3.44., Figure 5.1.). This is consistent with the fact that the sequence is very (81%) GC rich and predicted to form a hairpin (Figure 4.2.).
- The existence of this hairpin may serve to regulate acetylcholinesterase expression in neuronal cells, in which translational control is heavily relied upon to modulate gene expression away from the nucleus e.g. at the far end of an axon (Costa-Mattioli, 2009).
- It is possible that the high eIF4A requirement of the sequence is overcome in neuronal cells by HuD which stimulates the activity of eIF4A is only expressed in neuronal cells and has previously been shown to bind to the 3' UTR of *acetylcholinesterase* (Deschênes-Furry *et al.*, 2006).

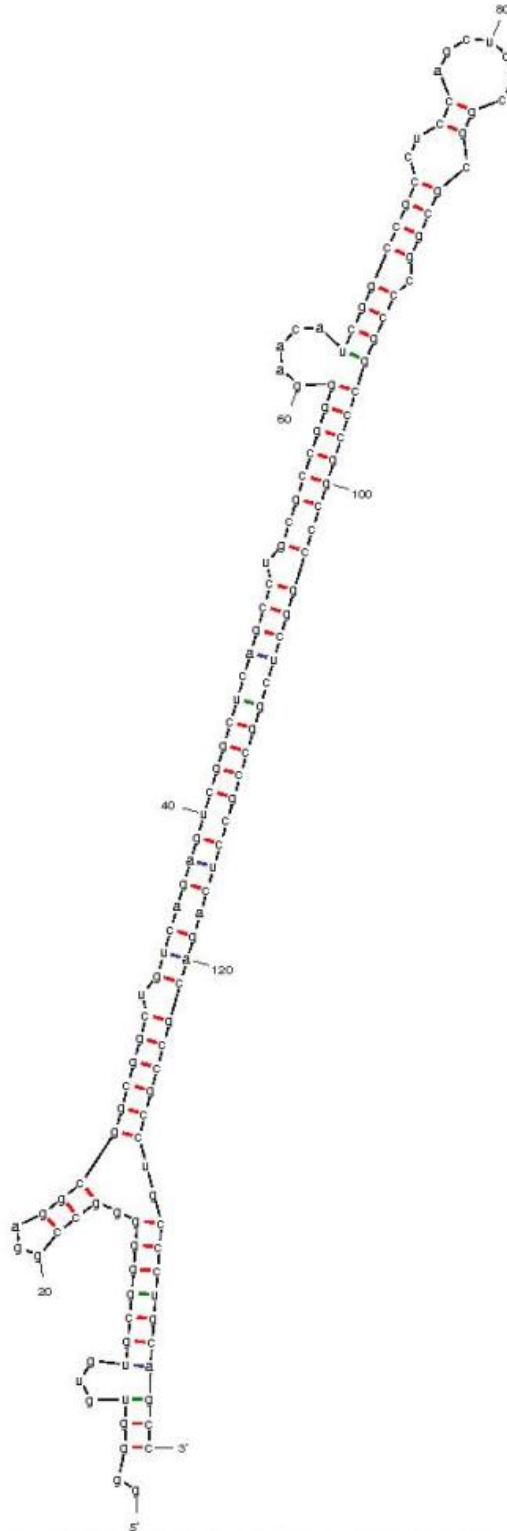


**Figure 4.2.** The predicted secondary structure of the entire *acetylcholinesterase* 5' UTR

#### **4.4.2. Limitations of the data generated by the Alzheimer's disease-associated reporter collection**

- The data from the *ADAM10* reporter cannot be directly compared to the rest as they were generated using a different reporter system (Figure 3.42.).

#### **4.4.3. Future work investigating the effect of Alzheimer's disease-associated 5' UTR sequences on the expression of downstream luciferase genes**

- It is necessary to demonstrate that the *AChE* 5' UTR forms a hairpin structure in reality using *in vitro* structure mapping as it is currently only predicted (by mfold) to do so.
- It would be interesting to expand the collection of Alzheimer's disease-associated reporter plasmids.

#### **4.4.4. eIF4A as a drug target in Alzheimer's disease**

- The dependency of the expression of APP and MAPT on eIF4A function has been demonstrated at the protein level by Andrew Bottley, a member of the RNA Biology Group, University of Nottingham (Bottley *et al.*, 2010).
- The data from the reporter library also support the idea that eIF4A may prove to be a useful drug target for the treatment of Alzheimer's disease (Figure 3.41.).
- WST-1 assays revealed that eIF4A suppression (using hippuristanol) treatment was very well tolerated (Figure 3.49.).

#### **4.4.5. Limitations of using eIF4A as a drug target in Alzheimer's disease**

- The claim that eIF4A could be used as a drug target for the treatment of Alzheimer's disease can only be made with a limited amount of confidence. The potential physiological effects of eIF4A suppression in humans cannot be anticipated based on the data presented in this thesis.

#### **4.4.6. Future work into the involvement of eIF4A in Alzheimer's disease**

- The collection of Alzheimer's disease-associated reporters is currently being used to investigate further the properties of the UTR sequences (e.g. using mutagenesis etc).

## Part 5.

### Cancer

#### 4.5.1. Conclusions from the oncogene reporter collection

- In HeLa and SH-SY5Y cells, the *ODC1* reporter generates a signal similar to the control reporters, the *EGFR* reporter generates a stronger signal than the controls and the *VEGFA* reporter generates a weaker signal (Figure 3.48., Figure 3.50.).
- The signal from the *ODC1* reporter may be regarded as resulting from a balance between the stimulatory effect of the IRES and the inhibitory effects of the hairpin and the uORF (Figure 3.48., Figure 3.50.) (Danner, 2002).
- Although the *VEGFA* 5' UTR contains two IRES elements, it is likely that the combined stimulatory effect of these is not sufficient to overcome the inhibitory effect of the long, highly structured sequence (Figure 3.48., Figure 3.50.) (Huez *et al.*, 1998).
- Like the reporters containing the Alzheimer's-associated sequences, the reporters containing the 5' UTRs of genes involved in cancer generated lower signals in response to hippuristanol treatment than those containing 5' UTRs of housekeeping genes (Figure 3.48., Figure 3.50.). The results for the  *$\beta$  actin*,  *$\beta$  tubulin*, *GAPDH*, *ODC1* and *VEGFA* reporters were as expected based on the predicted secondary structures of the sequences and the current literature (Figure 3.48., Figure 3.50.).

#### 4.5.2. The *EGFR* 5' UTR

- The *EGFR* 5' UTR sequence was found to permit the expression of the downstream cistron in pRF in four different human cell lines without exhibiting cryptic promoter activity or induce splicing (Figure 3.54, Figure 3.55., Figure 3.56., Figure 3.57., Figure 3.58.).
- The ribosome is predicted to enter the sequence close to the start codon (Figure 3.59., Figure 3.60., Figure 3.61., Figure 3.62., Figure 3.63., Figure 3.64., Figure 3.65.). This potentially explains why the 5' UTR is less inhibitory to reporter gene expression than predicted.
- The presence of an IRES in the 5' UTR of *EGFR* is consistent with the translational upregulation of the expression of EGFR expression in hypoxic conditions (in which cap-independent translation initiation is favoured).

- Expression of the downstream firefly cistron within cells transfected with pREGFRF remained constant following exposure to hypoxic conditions (Figure 3.67.). This is consistent with the translational upregulation of EGFR expression being mediated by the 5' UTR.
- Providing very strong evidence for the presence of an IRES in the *EGFR* 5' UTR is the fact that knockdown of a number of IRES *trans* acting factors (ITAFs) reduces EGFR expression (Lindsay Wilson, personal communication, 2011).
- The *EGFR* 5' UTR exhibits a significant requirement for eIF4A in monocistronic and dicistronic contexts in HeLa and SH-SY5Y cells (Figure 3.48., Figure 3.50., Figure 3.66.). The fact that the sequence behaves in almost exactly the same way in response to hippuristanol in a monocistronic context (in which the ribosome has the option of entering at the cap) and a dicistronic context (in which the ribosome must enter at the IRES) supports the idea that the IRES is favoured (Figure 3.66.).
- Since the ribosome appears to enter the sequence between 25 and 61 nucleotides away from the start codon (Figure 3.61.), it would be expected that the *EGFR* 5' UTR should have an eIF4A requirement comparable to that of a much shorter sequence. The predicted secondary structure of the full length *EGFR* 5' UTR and the region identified as the ribosomal entry site is shown on the following page (Figure 4.3.).
- If the region of the *EGFR* 5' UTR upstream of the ribosome entry site was subject to sequence drift, probability suggests that the sequence would contain approximately three AUG codons (Enard *et al.*, 2002; King and Wilson, 1975). The fact that there are no upstream AUGs in the *EGRF* 5' UTR is consistent with the sequence having some function.

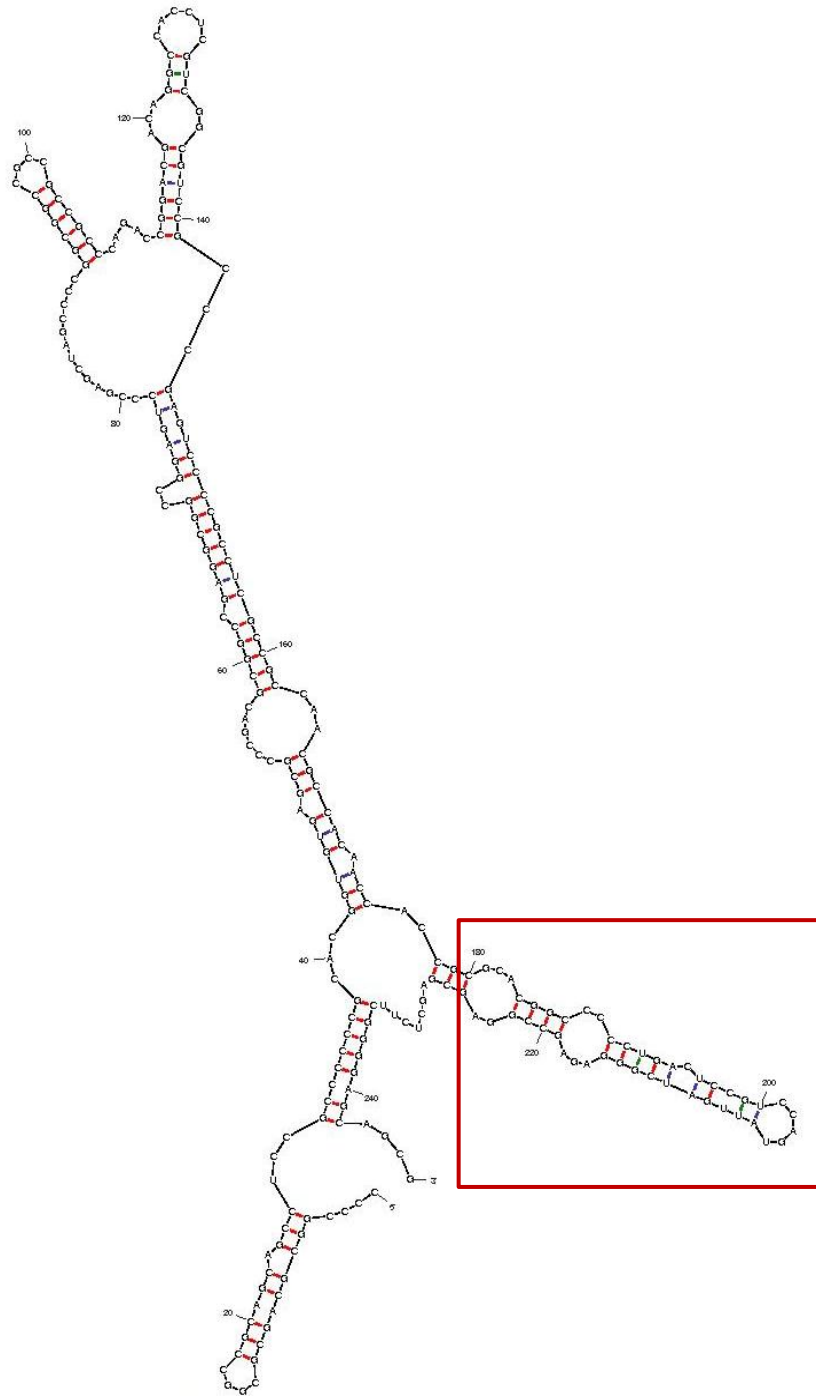


**Figure 4.3. mfold prediction of the full length *EGFR* 5' UTR secondary structure.** The region indicated in red is the **predicted ribosomal entry site**.

- The ribosomal entry site within the *EGFR* 5' UTR is predicted to form a hairpin (Figure 4.3.). This short hairpin only has a free energy of -18.2 kcal/mol (mfold (Zuker, 2003)). This level of structure is similar to that of the  $\beta$  actin 5' UTR, which has a low eIF4A requirement (Figure 3.48., Figure 3.50.). The existence of this hairpin is therefore not sufficient by itself to explain the high eIF4A requirement of the *EGFR* 5' UTR.
- The explanation for the discrepancy between this eIF4A requirement and the fact that that the IRES allows the majority of the sequence to be bypassed is probably the fact that the IRES itself requires eIF4A. The IRESs belonging to the human genes *c-myc*, *N-myc* and *BiP* have a strong requirement for eIF4A (Bordeleau *et al.*, 2006; Spriggs *et al.*, 2009; Thoma *et al.*, 2004). It has been suggested that this requirement indicates that the structure of these IRESs needs 'remodelling' by eIF4A before they are able to function (Kolupaeva *et al.*, 2003; Komar and Hatzoglou, 2011; Pause *et al.*, 1994b; Spriggs *et al.*, 2009). However, experimental confirmation of these predicted structures is required to support this model.
- Across the full length of the human *EGFR* 5' UTR, there is a high degree of conservation in other species (Figure 3.70.). This result is expected given that *EGFR* is functionally important. Functional importance is usually associated with evolutionary conservation (Boffelli *et al.*, 2004; Dermitzakis *et al.*, 2005). However, interestingly, the majority of the variation between species occurs in the 5' region (Figure 3.70.). The 3' region, which is expected to contain ribosomal entry site in humans, exhibits a higher degree of conservation across these 13 varied species with five bases in this region the same for all species (Figure 3.70.). This suggests that the IRES may have an important role in the expression of *EGFR*. Evolutionary conservation is particularly significant in untranslated regions as these sequences are generally freer to diversify than coding regions and still perform the same function (Enard *et al.*, 2002; King and Wilson, 1975).
- Hippuristanol significantly suppressed the expression of the *EGFR* protein, reducing it by 93% compared to the control (Figure 3.52.).
- Expression of the firefly luciferase cistron in three different cell lines transfected with pREGFRF was reduced following treatment of these cells with 250  $\mu$ M iron (Figure 3.69.).

#### 4.5.3. Limitations of the data generated by the oncogene reporter collection

- The dicistronic *EGFR* reporter was assayed for activity in four different cell lines (HeLa, Huh7, MCF7 and SH-SY5Y) but the rest of the reporter plasmids were only tested in two (HeLa and SH-SY5Y) (Figure 3.58., Figure 3.58., Figure 3.60.).
- The mutant monocistronic *EGFR* reporter transcript may be subject to reinitiation i.e. the mutant start codon directs the synthesis of a nonsense peptide that is short enough that the ribosome may reinitiate and translate the luciferase ORF (Figure 3.60.). This is unlikely however as expression levels from the mutant plasmid are statistically indistinguishable from those generated by the non-mutated plasmid (Figure 3.64.). This indicates that, in both cases the ribosome is entering at the IRES in the 3' half of the *EGFR* 5' UTR sequence.
- No firm conclusions can be made regarding the response of the pREGFRF reporter to iron treatment as the concentration of iron added may not be biologically relevant (250  $\mu$ M was added to the  $\sim$ 1.8-3.5  $\mu$ M already present in the medium).

#### 4.5.4. Future work on the oncogene reporter collection

- There is sufficient evidence for the existence of an IRES element within the 5' UTR of human *EGFR* to submit for peer review and (subject to approval) publication.
- It would be interesting to use the monocistronic and dicistronic *EGFR* 5' UTR reporter plasmids to further investigate the relationship between EGFR expression and ITAF knockdown (discovered by Lindsay Wilson).

#### 4.5.5. eIF4A as a drug target in cancer

- EGFR, ODC1 and VEGFA are all being investigated for their feasibility as drug targets, each with a range of candidate drugs at various stages in the clinical trials process (2005; Folkman, 2007; Kobayashi et al., 2005; Seiler, 2003). Clearly, targeting these proteins individually is expected to be therapeutically beneficial in the treatment of cancer. The results presented in this thesis suggest that suppression of eIF4A would reduce the expression and therefore the activity of all three of these oncoproteins (Figure 3.48., Figure 3.50.).

- It may prove that eIF4A inhibition could be useful in curtailing the aberrantly high expression of certain oncogenes (including EGFR) in the hypoxic conditions often associated with the tumour environment.
- A previous study into the effect of silvestrol (another small molecule inhibitor of eIF4A) on healthy and tumour-bearing mice found this treatment to be also well tolerated (Cencic et al., 2009). Levels of aminotransferase toxicity markers in the blood of these mice were measured and found to either remain constant or fall (Cencic et al., 2009). As outlined in the Introduction, the mice used in this study were closely monitored and displayed no noticeable side effects to the eIF4A-suppressive treatment (Cencic et al., 2009). A more recent study into the effects of silvestrol by a different group concluded that the molecule has a favourable pharmacokinetic profile in mice and an excellent level of bioavailability when administered inter-peritoneally (Saradhi et al., 2011).

#### **4.5.6. Limitations of using eIF4A as a drug target in cancer**

- While mutations that directly affect eIF4A in cancer have never been documented, it is possible that cancer cells may become resistant to eIF4A inhibitors.
- Tables 4 and 5 show that tumour suppressor genes often possess 5' UTRs with properties that suggest that they may have a high eIF4A requirement. This may mean that inhibition of eIF4A could result in the reduction of tumour suppressor proteins in the cell, potentially making the cancer more aggressive.
- More general considerations regarding the use of eIF4A as a drug target are discussed in the Alzheimer's disease section.

#### **4.5.7. Future work investigating eIF4A as a drug target in cancer**

- The studies investigating the feasibility of using eIF4A as a drug target are discussed in the Introduction.
- It would be necessary to quantify the levels of the tumour suppressor proteins in cells previously treated with eIF4A inhibitors or subject to eIF4A knockdown. This may be useful in anticipating the potential detrimental effects of therapeutic eIF4A inhibition.

## Part 6.

### Overall Summary

#### 4.6.1. Overall Conclusions from the project

- The hairpin reporter system is suitable for identifying new eIF4A inhibitors by high-throughput screening
- eIF4AII has an apparently distinct function to eIF4AI.
- The cellular DNA damage response is impaired if PDCD4 is lacking. This is possibly due to the interaction of PDCD4 with eIF4A.
- The expression of reporter genes preceded by the 5' UTR sequences of genes predicted to play harmful roles in Alzheimer's disease have a greater requirement for eIF4A function than genes preceded by the 5' UTRs of genes involved in the defence against oxidative stress.
- The expression of reporter genes preceded by the 5' UTR sequences of oncogenes also have a greater requirement for eIF4A function than genes preceded by the 5' UTRs of housekeeping genes.
- The *EGFR* 5' UTR contains an IRES that allows the ribosome to enter near the start codon and maintains the expression of the downstream gene in hypoxic conditions.

#### 4.6.2. Limitations of the project and future work

- The biggest limitation of applying the conclusions generated using the reporters to living cells is that the UTR sequence cloned into the plasmids may not be the same as that found in nature. This is particularly true of highly structured sequences as the reverse transcriptase enzyme (used to make a cDNA copy of the RNA for sequencing) may detach from the RNA at regions of very stable structure (Buell et al., 1978; Bustin, 2000).
- To address this potential inaccuracy, 5' RACE (rapid amplification of cDNA ends) primers for the 5' UTR sequences of a number of the genes studied as part of this project are currently being used by members of the RNA Biology Group.
- The Alzheimer's disease reporter collection was only transfected into SH-SY5Y; it would be interesting to investigate the expression pattern of the luciferase genes in different neuronal cell lines.

- Only EGFR and  $\beta$  tubulin protein levels were estimated following hippuristanol treatment. It would be interesting to ascertain whether the levels of ODC1 and VEGFA protein fall in response to eIF4A suppression to the same extent as the luciferase genes preceded by their 5' UTR sequences.

# Chapter 5. Overall Analysis

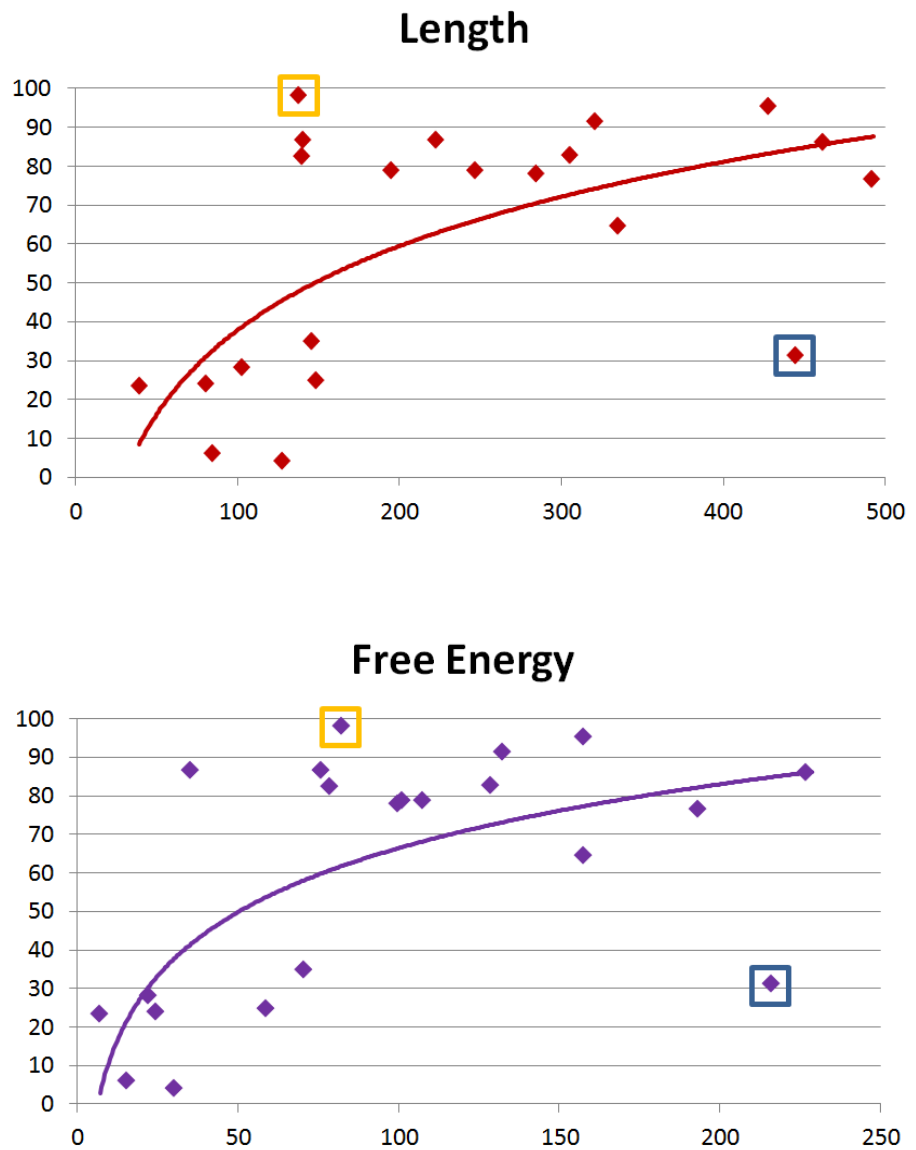


**Figure 5.1.** The length and predicted free energy of the sequences cloned into the reporter plasmids were compared to their eIF4A requirement. This requirement is defined as the percentage drop in reporter expression following treatment of the cells transfected with the reporter with 10  $\mu$ M hippuristanol. The data-points indicated in yellow represent *acetylcholinesterase* and the data-points indicated in blue represent *ADAM10*.

Name	Length (bases)	GC Content (%)	Predicted Free Energy (kcal/mol)	% Drop (eIF4A requirement)
<i>eIF4AI</i>	103	66	-39.20	-7.40688
<i>eIF4AII</i>	39	53	-7.000	23.47715
<i>eIF4AIII</i>	222	74	-75.90	86.78376
<i>Hairpin</i>	137	74	-82.20	98.19891
<i>APP</i>	194	76	-101.1	78.88428
<i>BACE1</i>	461	76	-226.7	86.26154
<i>Clu</i>	305	59	-128.6	82.83702
<i>CR1</i>	140	50	-35.10	86.859
<i>PS1</i>	284	56	-99.60	78.13176
<i>PS2</i>	427	57	-157.5	95.60934
<i>MAPT</i>	320	74	-132.5	91.65273
<i>SOD1</i>	148	64	-58.70	25.02442
<i>TXN</i>	80	54	-24.50	24.03096
<i>ADAM10</i>	444	68	-215.9	31.41395
<i>AChE</i>	139	81	-78.50	82.7139
<i>HTT</i>	145	73	-70.60	34.99489
<i>β Actin</i>	84	74	-15.50	6.14119
<i>β Tubulin</i>	127	47	-30.10	4.409291
<i>GAPDH</i>	102	61	-21.90	28.248
<i>ODC1</i>	334	66	-157.5	64.72523
<i>EGFR</i>	246	78	-107.5	79.08524
<i>VEGFA</i>	491	57	-193.3	76.85123

**Table 22.** The characteristics of each 5' UTR cloned into the reporter system were compiled, together with the percentage drop in their expression following hippuristanol treatment (10  $\mu$ M) in SH-SY5Y cells. This percentage drop may be regarded as proportional to the requirement of the sequence for eIF4A function.

# References

- Abdelhaleem, M., L. Maltais, and H. Wain. 2003. The human DDX and DHX gene families of putative RNA helicases. *Genomics*. 81:618-622.
- Abramoff, M.D., P.J. Magalhaes, and S.J. Ram. 2004. Image Processing with ImageJ. *Biophotonics International*. 11:36-42.
- Agback, P., C. Glemarec, L. Yin, A. Sandström, J. Plavec, C. Sund, S.-i. Yamakage, G. Viswanadham, B. Rouse, N. Puri, and J. Chattopadhyaya. 1993. The self-cleavage of lariat-RNA. *Tetrahedron Letters*. 34:3929-3932.
- Agranovsky, A.A., S.Y. Folimonova, A.S. Folimonov, O.N. Denisenko, and R.A. Zinovkin. 1997. The beet yellows closterovirus p65 homologue of HSP70 chaperones has ATPase activity associated with its conserved N-terminal domain but does not interact with unfolded protein chains. *Journal of General Virology*. 78:535-542.
- Aisen, P., C. Enns, and M. Wessling-Resnick. 2001. Chemistry and biology of eukaryotic iron metabolism. *The International Journal of Biochemistry & Cell Biology*. 33:940-959.
- Ali, I.K., L. McKendrick, S.J. Morley, and R.J. Jackson. 2001. Activity of the Hepatitis A Virus IRES Requires Association between the Cap-Binding Translation Initiation Factor (eIF4E) and eIF4G. *Journal of Virology*. 75:7854-7863.
- Allers, T., and M. Mevarech. 2005. Archaeal genetics - the third way. *National Review of Genetics*. 6:58-73.
- Altschul, S.F., T.L. Madden, A.A. Schäffer, J. Zhang, Z. Zhang, W. Miller, and D.J. Lipman. 1997. Gapped BLAST and PSI-BLAST: a new generation of protein database search programs. *Nucleic Acids Research*. 25:3389-3402.
- Ameyar, M., M. Wisniewska, and J.B. Weitzman. 2003. A role for AP-1 in apoptosis: the case for and against. *Biochimie*. 85:747-752.
- Anderson, K., and M.J. Moore. 2000. Bimolecular exon ligation by the human spliceosome bypasses early 3' splice site AG recognition and requires NTP hydrolysis. *RNA*. 6:16-25.
- Anderson, P., and N. Kedersha. 2006. RNA granules. *The Journal of Cell Biology*. 172:803-808.
- Andreas, P., K. Jochen, and N. Peter. 2005. Transplantation in the management of metastatic endocrine tumours. *Best practice & research. Clinical gastroenterology*. 19:637-648.
- Appl, H., and K.H. Klempnauer. 2002. Targeted disruption of c-myc in the chicken pre B-cell line DT40. *Oncogene*. 21:3076-3081.
- Asangani, I.A., S.A.K. Rasheed, D.A. Nikolova, J.H. Leupold, N.H. Colburn, S. Post, and H. Allgayer. 2007. MicroRNA-21 (miR-21) post-transcriptionally downregulates tumor suppressor Pcd4 and stimulates invasion, intravasation and metastasis in colorectal cancer. *Oncogene*. 27:2128-2136.
- Asano, K., A. Shalev, L. Phan, K. Nielsen, J. Clayton, L. Valášek, T.F. Donahue, and A.G. Hinnebusch. 2001. Multiple roles for the C-terminal domain of eIF5 in translation initiation complex assembly and GTPase activation. *EMBO Journal*. 20:2326-2337.
- Asselbergs, F.A.M., W. Peters, W.J. van Venrooij, and H. Bloemendal. 1978. Diminished Sensitivity of Re-initiation of Translation to Inhibition by Cap Analogues in Reticulocyte Lysates. *European Journal of Biochemistry*. 88:483-488.
- Badis, G., C. Saveanu, M. Fromont-Racine, and A. Jacquier. 2004. Targeted mRNA Degradation by Deadenylation-Independent Decapping. *Molecular Cell*. 15:5-15.
- Ballut, L., B. Marchadier, A. Baguet, C. Tomasetto, B. Seraphin, and H. Le Hir. 2005. The exon junction core complex is locked onto RNA by inhibition of eIF4AIII ATPase activity. *Nature Structural & Molecular Biology*. 12:861-869.
- Banerjee, A.K. 1980. 5'-terminal cap structure in eucaryotic messenger ribonucleic acids. *Microbiology Review*. 44:175-205.
- Barber, R.D., D.W. Harmer, R.A. Coleman, and B.J. Clark. 2005. GAPDH as a housekeeping gene: analysis of GAPDH mRNA expression in a panel of 72 human tissues. *Physiological Genomics*. 21:389-395.

- Bartzokis, G., M. Beckson, D.B. Hance, P. Marx, J.A. Foster, and S.R. Marder. 1997. MR evaluation of age-related increase of brain iron in young adult and older normal males. *Magnetic Resonance Imaging*. 15:29-35.
- Baselga, J. 2001. The EGFR as a target for anticancer therapy—focus on cetuximab. *European journal of cancer*. 37:16-22.
- Bastos, R., A. Lin, M. Enarson, and B. Burke. 1996. Targeting and Function in mRNA Export of Nuclear Pore Complex Protein Nup153. *The Journal of Cell Biology*. 5:1141-1156.
- Batchelor, D. 2001. Hair and cancer chemotherapy: consequences and nursing care – a literature study. *European Journal of Cancer Care*. 10:147-163.
- Bauer, D., V. Haroutunian, R. McCullumsmith, and J. Meador-Woodruff. 2009. Expression of four housekeeping proteins in elderly patients with schizophrenia. *Journal of Neural Transmission*. 116:487-491.
- Bayer, T.A., R. Cappai, C.L. Masters, K. Beyreuther, and G. Multhaup. 1999. It all sticks together--the APP-related family of proteins and Alzheimer's disease. *Molecular psychiatry*. 4:524-528.
- Beales, L.P., A. Holzenburg, and D.J. Rowlands. 2003. Viral Internal Ribosome Entry Site Structures Segregate into Two Distinct Morphologies. *Journal of Virology*. 77:6574-6579.
- Beaudoin, M.E., V.-J. Poirer, and L.A. Krushel. 2008. Regulating amyloid precursor protein synthesis through an internal ribosomal entry site. *Nucleic Acids Research*. 36:6835-6847.
- Behin, A., K. Hoang-Xuan, A.F. Carpentier, and J.-Y. Delattre. 2003. Primary brain tumours in adults. *The Lancet*. 361:323-331.
- Behm-Ansmant, I., I. Kashima, J. Rehwinkel, J. Saulière, N. Wittkopp, and E. Izaurralde. 2007. mRNA quality control: An ancient machinery recognizes and degrades mRNAs with nonsense codons. *Federation of European Biochemical Societies Letters*. 581:2845-2853.
- Belsham, G.J., McInerney, G. M. & Ross-Smith, N. 2000. Foot-and-Mouth Disease Virus 3C Protease Induces Cleavage of Translation Initiation Factors eIF4A and eIF4G within Infected Cells. *Journal of Virology* 74:272-280
- Benne, R., J. Van Den Burg, P.J. Brakenhoff, P. Sloof, J.H. Van Boom, and M.C. Tromp. 1986. Major transcript of the frameshifted coxII gene from trypanosome mitochondria contains four nucleotides that are not encoded in the DNA. *Cell*. 46:819-826.
- Beretta, L., A.C. Gingras, Y.V. Svitkin, M.N. Hall, and N. Sonenberg. 1996. Rapamycin blocks the phosphorylation of 4E-BP1 and inhibits cap-dependent initiation of translation. *EMBO Journal*. 15:658–664.
- Berg, J.M., J.L. Tymoczko, and L. Stryer. 2002. *Biochemistry*. W. H. Freeman, New York.
- Berger, A.H., A.G. Knudson, and P.P. Pandolfi. 2011. A continuum model for tumour suppression. *Nature*. 476:163-169.
- Berget, S.M. 1995. Exon Recognition in Vertebrate Splicing. *Journal of Biological Chemistry*. 270:2411-2414.
- Berget, S.M., C. Moore, and P.A. Sharp. 1977. Spliced segments at the 5' terminus of adenovirus 2 late mRNA. *Proceedings of the National Academy of Sciences*. 74:3171-3175.
- Bernstein, L.R., R. Bravo, and N.H. Colburn. 1992. 12-O-tetradecanoylphorbol-13-acetate—induced levels of ap-1 proteins: a 46-kda protein immunoprecipitated by anti-fra-1 and induced in promotion-resistant but not promotion-sensitive JB6 cells. *Molecular Carcinogenesis*. 6:221-229.
- Biemont, C., and C. Vieira. 2006. Genetics: Junk DNA as an evolutionary force. *Nature*. 443:521-524.
- Bigner, S.H., P.A. Humphrey, A.J. Wong, B. Vogelstein, J. Mark, H.S. Friedman, and D.D. Bigner. 1990. Characterization of the Epidermal Growth Factor Receptor in Human Glioma Cell Lines and Xenografts. *Cancer Research*. 50:8017-8022.
- Bishop, D.T. 1999. BRCA1 and BRCA2 and breast cancer incidence: A review. *Annals of Oncology*. 10:S113-S119.

- Bitomsky, N., N. Wethkamp, R. Marikkannu, and K.H. Klempnauer. 2008. siRNA-mediated knockdown of Pdc4 expression causes upregulation of p21(Waf1/Cip1) expression. *Oncogene*.
- Black, D.L. 2003. Mechanisms of alternative pre-messenger RNA splicing. *Annual Reviews of Biochemistry*. 72:291-336.
- Bleicher, K.H., H.-J. Bohm, K. Muller, and A.I. Alanine. 2003. Hit and lead generation: beyond high-throughput screening. *National Review of Drug Discovery*. 2:369-378.
- Boffelli, D., M.A. Nobrega, and E.M. Rubin. 2004. Comparative genomics at the vertebrate extremes. *National Review of Genetics*. 5:456-465.
- Bonneau, A.M., and N. Sonenberg. 1987. Involvement of the 24-kDa cap-binding protein in regulation of protein synthesis in mitosis. *Journal of Biological Chemistry*. 262:11134-11139.
- Bordeleau, M., J. Matthews, J.M. Wojnar, L. Lindqvist, O. Novac, E. Jankowsky, N. Sonenberg, P. Northcote, P. Teesdale-Spittle, and J. Pelletier. 2008a. Therapeutic suppression of translation initiation modulates chemosensitivity in a mouse lymphoma model. *Journal of Clinical Investigation*. 118:2651-2660.
- Bordeleau, M.E., J. Matthews, J.M. Wojnar, L. Lindqvist, O. Novac, E. Jankowsky, N. Sonenberg, P. Northcote, P. Teesdale-Spittle, and J. Pelletier. 2005. Stimulation of mammalian translation initiation factor eIF4A activity by a small molecule inhibitor of eukaryotic translation. *Proceedings of the National Academy of Science USA*. 102:10460-10465.
- Bordeleau, M.E., A. Mori, M. Oberer, L. Lindqvist, L.S. Chard, T. Higa, G.J. Belsham, G. Wagner, J. Tanaka, and J. Pelletier. 2006. Functional characterization of IRESes by an inhibitor of the RNA helicase eIF4A. *National Journal of Chemical Biology*. 2:213-220.
- Bordeleau, M.E., F. Robert, B. Gerard, L. Lindqvist, S.M. Chen, H.G. Wendel, B. Brem, H. Greger, S.W. Lowe, J.A. Porco, and J. Pelletier. 2008b. Therapeutic suppression of translation initiation modulates chemosensitivity in a mouse lymphoma model. *Journal of Clinical Investigation*. 118:2651-2660.
- Borman, A.M., R. Kirchweger, E. Ziegler, R.E. Rhoads, T. Skern, and K.M. Kean. 1997. eIF4G and its proteolytic cleavage products: Effect on initiation of protein synthesis from capped, uncapped, and IRES-containing mRNAs. *RNA*. 3:186-196.
- Bornes, S., M. Boulard, C. Hieblot, C. Zanibellato, J.S. Iacovoni, H. Prats, and C. Touriol. 2004. Control of the vascular endothelial growth factor internal ribosome entry site (IRES) activity and translation initiation by alternatively spliced coding sequences. *Journal of Biological Chemistry*. 279:18717-18726.
- Bostanci, A. 2005. A Devil of a Disease. *Science*. 307:1035-1035.
- Bostick, P.J., S. Chatterjee, D.D. Chi, K.T. Huynh, A.E. Giuliano, R. Cote, and D.S. Hoon. 1998. Limitations of specific reverse-transcriptase polymerase chain reaction markers in the detection of metastases in the lymph nodes and blood of breast cancer patients. *Journal of Clinical Oncology*. 16:2632-2640.
- Bottley, A., N.M. Phillips, T.E. Webb, A.E. Willis, and K.A. Spriggs. 2010. eIF4A Inhibition Allows Translational Regulation of mRNAs Encoding Proteins Involved in Alzheimer's Disease. *PLoS ONE*. 5:e13030.
- Bower, M., T. Powles, M. Nelson, P. Shah, S. Cox, S. Mandelia, and B. Gazzard. 2003. HIV-related lung cancer in the era of highly active antiretroviral therapy. *AIDS*. 17:371-375.
- Brenner, S., L. Barnett, E.R. Katz, and F.H.C. Crick. 1967. UGA: A Third Nonsense Triplet in the Genetic Code. *Nature*. 213:449-450.
- Brenner, S., A.O.W. Stretton, and S. Kaplan. 1965. Genetic Code: The 'Nonsense' Triplets for Chain Termination and their Suppression. *Nature*. 206:994-998.
- Brown, E.J., M.W. Albers, T. Bum Shin, K. Ichikawa, C.T. Keith, W.S. Lane, and S.L. Schreiber. 1994. A mammalian protein targeted by G1-arresting rapamycin-receptor complex. *Nature*. 369:756-758.
- Brugarolas, J., K. Lei, R.L. Hurley, B.D. Manning, J.H. Reiling, E. Hafen, L.A. Witters, L.W. Ellisen, and W.G. Kaelin. 2004. Regulation of mTOR function in response to hypoxia by REDD1 and the TSC1/TSC2 tumor suppressor complex. *Genes & Development*. 18:2893-2904.

- Brunn, G.J., C.C. Hudson, A. Sekulić, J.M. Williams, H. Hosoi, P.J. Houghton, J.C. Lawrence, and R.T. Abraham. 1997. Phosphorylation of the Translational Repressor PHAS-I by the Mammalian Target of Rapamycin. *Science*. 277:99-101.
- Bu, X., D.W. Haas, and C.H. Hagedorn. 1993. Novel phosphorylation sites of eukaryotic initiation factor-4F and evidence that phosphorylation stabilizes interactions of the p25 and p220 subunits. *Journal of Biological Chemistry*. 268:4975-4978.
- Buell, G.N., M.P. Wickens, F. Payvar, and R.T. Schimke. 1978. Synthesis of full length cDNAs from four partially purified oviduct mRNAs. *Journal of Biological Chemistry*. 253:2471-2482.
- Buell, J.F., J. Trofe, M.J. Hanaway, A. Lo, B. Rosengard, H. Rilo, R. Alloway, T. Beebe, M.R. First, and E.S. Woodle. 2001. Transmission of donor cancer into cardi thoracic transplant recipients. *Surgery*. 130:660-668.
- Bueno, M.J., I. Pérez de Castro, M. Gómez de Cedrón, J. Santos, G.A. Calin, J.C. Cigudosa, C.M. Croce, J. Fernández-Piqueras, and M. Malumbres. 2008. Genetic and Epigenetic Silencing of MicroRNA-203 Enhances ABL1 and BCR-ABL1 Oncogene Expression. *Cancer cell*. 13:496-506.
- Burt, D.B., K.A. Loveland, S. Primeaux-Hart, Y.-W. Chen, N.B. Phillips, L.A. Cleveland, K.R. Lewis, J. Lesser, and E. Cummings. 1998. Dementia in Adults With Down Syndrome: Diagnostic Challenges. *American Journal on Mental Retardation*. 103:130-145.
- Busciglio, J., A. Lorenzo, J. Yeh, and B.A. Yankner. 1995.  $\beta$ -Amyloid fibrils induce tau phosphorylation and loss of microtubule binding. *Neuron*. 14:879-888.
- Bushell, M., M. Stoneley, Y.W. Kong, T.L. Hamilton, K.A. Spriggs, H.C. Dobbyn, X. Qin, P. Sarnow, and A.E. Willis. 2006. Polypyrimidine tract binding protein regulates IRES-mediated gene expression during apoptosis. *Molecular Cell*. 23:401-412.
- Bustin, S. 2000. Absolute quantification of mRNA using real-time reverse transcription polymerase chain reaction assays. *Journal of Molecular Endocrinology*. 25:169-193.
- Cai, A., M. Jankowska-Anyszka, A. Centers, L. Chlebicka, J. Stepinski, R. Stolarski, E. Darzynkiewicz, and R.E. Rhoads. 1999. Quantitative assessment of mRNA cap analogues as inhibitors of in vitro translation. *Biochemistry*. 38:8538-8547.
- Calvo, S.E., D.J. Pagliarini, and V.K. Mootha. 2009. Upstream open reading frames cause widespread reduction of protein expression and are polymorphic among humans. *Proceedings of the National Academy of Sciences*. 106:7507-7512.
- Campbell, S.G., N.P. Hoyle, and M.P. Ashe. 2005. Dynamic cycling of eIF2 through a large eIF2B-containing cytoplasmic body: implications for translation control. *The Journal of Cell Biology*. 170:925-934.
- Campion, D., C. Dumanchin, D. Hannequin, B. Dubois, S. Belliard, M. Puel, C. Thomas-Anterion, A. Michon, C. Martin, F. Charbonnier, G. Raux, A. Camuzat, C. Penet, V. Mesnage, M. Martinez, F. Clerget-Darpoux, A. Brice, and T. Frebourg. 1999. Early-Onset Autosomal Dominant Alzheimer Disease: Prevalence, Genetic Heterogeneity, and Mutation Spectrum. *The American Journal of Human Genetics*. 65:664-670.
- Caruthers, J.M., E.R. Johnson, and D.B. McKay. 2000. Crystal structure of yeast initiation factor 4A, a DEAD-box RNA helicase. *Proceedings of the National Academy of Science USA*. 97:13080-13085.
- Cech, T.R. 1990. Self-Splicing of Group I Introns. *Annual Review of Biochemistry*. 59:543-568.
- Cencic, R., M. Carrier, G. Galicia-Vazquez, M.E. Bordeleau, R. Sukarieh, A. Bourdeau, B. Brem, J.G. Teodoro, H. Greger, M.L. Tremblay, J.A. Porco, and J. Pelletier. 2009. Antitumor activity and mechanism of action of the cyclopentabenzofuran, silvestrol. *PLoS ONE*. 4:e5223.
- Chandek, C., and W.J. Mooi. 2010. Oncogene-induced Cellular Senescence. *Advances in Anatomic Pathology*. 17:42-48 10.1097/PAP.1090b1013e3181c1066f1094e.
- Chang, J.H., Y.H. Cho, S.Y. Sohn, J.M. Choi, A. Kim, Y.C. Kim, S.K. Jang, and Y. Cho. 2009. Crystal structure of the eIF4A-PDCD4 complex. *Proceedings of the National Academy of Sciences*. 106:3148-3153.
- Chang, Y.F., J.S. Imam, and M.F. Wilkinson. 2007. The nonsense-mediated decay RNA surveillance pathway. *Annual Review of Biochemistry*. 76:51-74.

- Chaudhuri, J., K. Das, and U. Maitra. 1994. Purification and Characterization of Bacterially Expressed Mammalian Translation Initiation Factor 5 (eIF-5): Demonstration That eIF-5 Forms a Specific Complex with eIF-2. *Biochemistry*. 33:4794-4799.
- Chen, C.-Y.A., and A.-B. Shyu. 2009. HuD Stimulates Translation via eIF4A. *Molecular Cell*. 36:920-921.
- Chen, C.Y., and P. Sarnow. 1995. Initiation of protein synthesis by the eukaryotic translational apparatus on circular RNAs. *Science*. 268:415-417.
- Chen, X., and S.D. Yan. 2006. Mitochondrial A $\beta$  A potential cause of metabolic dysfunction in Alzheimer's disease. *IUBMB Life*. 58:686-694.
- Chesi, M., P.L. Bergsagel, L.A. Brents, C.M. Smith, D.S. Gerhard, and W.M. Kuehl. 1996. Dysregulation of cyclin D1 by translocation into an IgH gamma switch region in two multiple myeloma cell lines. *Blood*. 88:674-681.
- Chi, D.D., A.V. Hing, C. Helms, T. Steinbrueck, S.K. Mishra, and H. Donis-Keller. 1992. Two chromosome 7 dinucleotide repeat polymorphisms at gene loci epidermal growth factor receptor (EGFR) and pro $\alpha$ 2 (1) collagen (COL1A2). *Human Molecular Genetics*. 1:135.
- Chiu, S.Y., F. Lejeune, A.C. Ranganathan, and L.E. Maquat. 2004. The pioneer translation initiation complex is functionally distinct from but structurally overlaps with the steady-state translation initiation complex. *Genes and Development*. 18:745.
- Chow, L.T., R.E. Gelinas, T.R. Broker, and R.J. Roberts. 1977. An amazing sequence arrangement at the 5' ends of adenovirus 2 messenger RNA. *Cell*. 12:1-8.
- Christen, Y. 2000. Oxidative stress and Alzheimer disease. *The American Journal of Clinical Nutrition*. 71:621s-629s.
- Citron, M., C. Vigo-Pelfrey, D.B. Teplow, C. Miller, D. Schenk, J. Johnston, B. Winblad, N. Venizelos, L. Lannfelt, and D.J. Selkoe. 1994. Excessive production of amyloid beta-protein by peripheral cells of symptomatic and presymptomatic patients carrying the Swedish familial Alzheimer disease mutation. *Proceedings of the National Academy of Sciences*. 91:11993-11997.
- Citron, M., D. Westaway, and D.J. Selkoe. 1997. Mutant presenilins of Alzheimer's disease increase production of 42-residue amyloid beta-protein in both transfected cells and transgenic mice. *Nature Medicine*. 3:67-72.
- Clarke, K., K. Smith, W.J. Gullick, and A.L. Harris. 2001. Mutant epidermal growth factor receptor enhances induction of vascular endothelial growth factor by hypoxia and insulin-like growth factor-1 via a PI3 kinase dependent pathway. *Br J Cancer*. 84:1322-1329.
- Cmarik, J.L., H. Min, G. Hegamyer, S. Zhan, M. Kulesz-Martin, H. Yoshinaga, S. Matsushashi, and N.H. Colburn. 1999. Differentially expressed protein Pcd4 inhibits tumor promoter-induced neoplastic transformation. *Proceedings of the National Academy of Science USA*. 96:14037-14042.
- Cobbold, L.C., K.A. Spriggs, S.J. Haines, H.C. Dobbyn, C. Hayes, C.H. de Moor, K.S. Lilley, M. Bushell, and A.E. Willis. 2008. Identification of internal ribosome entry segment (IRES)-trans-acting factors for the Myc family of IRESs. *Molecular Cell Biology*. 28:40-49.
- Conroy, S.C., T.E. Dever, C.L. Owens, and W.C. Merrick. 1990. Characterization of the 46,000-dalton subunit of eIF-4F. *Archives of Biochemistry and Biophysics*. 282:363-371.
- Cordin, O., J. Banroques, N.K. Tanner, and P. Linder. 2006. The DEAD-box protein family of RNA helicases. *Gene*. 367:17-37.
- Cosa, G., K.S. Focsaneanu, J.R.N. McLean, J.P. McNamee, and J.C. Scaiano. 2001. Photophysical Properties of Fluorescent DNA-dyes Bound to Single- and Double-stranded DNA in Aqueous Buffered Solution. *Photochemistry and Photobiology*. 73:585-599.
- Costa-Mattioli, M., Sossin, W. S., Klann, E. & Sonenberg, N. 2009. Translational Control of Long-Lasting Synaptic Plasticity and Memory. *Neuron*. 61:10-26.
- Covello, P.S., and M.W. Gray. 1993. On the evolution of RNA editing. *Trends in Genetics*. 9:265-268.

- Craig, A.W., A. Haghighat, A.T. Yu, and N. Sonenberg. 1998. Interaction of polyadenylate-binding protein with the eIF4G homologue PAIP enhances translation. *Nature*. 392:520-523.
- Crick, F.H.C. 1966. Codon-anticodon pairing: The wobble hypothesis. *Journal of Molecular Biology*. 19:548-555.
- Czaja, R., M. Struhalla, K. Höschler, W. Saenger, N. Sträter, and U. Hahn. 2004. RNase T1 Variant RV Cleaves Single-Stranded RNA after Purines Due to Specific Recognition by the Asn46 Side Chain Amide. *Biochemistry*. 43:2854-2862.
- Dacic, S., M. Flanagan, K. Cieply, S. Ramalingam, J. Luketich, C. Belani, and S.A. Yousem. 2006. Significance of EGFR Protein Expression and Gene Amplification in Non-Small Cell Lung Carcinoma. *American Journal of Clinical Pathology*. 125:860-865.
- Danner, D.J. 2002. RNA Binding Proteins: New Concepts in Gene Regulation. *American Journal of Human Genetics*. 71:1255-1255.
- Davies, P., and A.H. Verth. 1977. Regional distribution of muscarinic acetylcholine receptor in normal and Alzheimer's-type dementia brains. *Brain Research*. 138:385-392.
- Davis, B.N., A.C. Hilyard, G. Lagna, and A. Hata. 2008. SMAD proteins control DROSHA-mediated microRNA maturation. *Nature*. 454:56-61.
- Davuluri, R.V., Y. Suzuki, S. Sugano, and M.Q. Zhang. 2000. CART classification of human 5' UTR sequences. *Genome Research*. 10:1807-1816.
- Day, D.A., and M.F. Tuite. 1998. Post-transcriptional gene regulatory mechanisms in eukaryotes: an overview. *Journal of Endocrinology*. 157:361-371.
- De Benedetti, A., and J.R. Graff. 2004. eIF-4E expression and its role in malignancies and metastases. *Oncogene*. 23:3189-3199.
- de Breyne, S., Y. Yu, A. Unbehaun, T.V. Pestova, and C.U.T. Hellen. 2009. Direct functional interaction of initiation factor eIF4G with type 1 internal ribosomal entry sites. *Proceedings of the National Academy of Sciences*. 106:9197-9202.
- De Pietri Tonelli, D., M. Mihailovich, A. Di Cesare, F. Codazzi, F. Grohovaz, and D. Zacchetti. 2004. Translational regulation of BACE-1 expression in neuronal and non-neuronal cells. *Nucleic Acids Research*. 32:1808-1817.
- de Visser, K.E., A. Eichten, and L.M. Coussens. 2006. Paradoxical roles of the immune system during cancer development. *Nat Rev Cancer*. 6:24-37.
- Decker, C.J., and R. Parker. 1993. A turnover pathway for both stable and unstable mRNAs in yeast : evidence for a requirement for deadenylation. *Genes and Development*. 7:1632-1643.
- Deeken, J.F., and W. Löscher. 2007. The Blood-Brain Barrier and Cancer: Transporters, Treatment, and Trojan Horses. *Clinical Cancer Research*. 13:1663-1674.
- Deng, N.-J., and P. Cieplak. 2010. Free Energy Profile of RNA Hairpins: A Molecular Dynamics Simulation Study. *Biophysical Journal*. 98:627-636.
- Dennis, P. 1997. Ancient ciphers: translation in Archaea. *Cell*. 89:1007-1010.
- Dermitzakis, E.T., A. Reymond, and S.E. Antonarakis. 2005. Conserved non-genic sequences - an unexpected feature of mammalian genomes. *National Review of Genetics*. 6:151-157.
- Deschênes-Furry, J., N. Perrone-Bizzozero, and B.J. Jasmin. 2006. The RNA-binding protein HuD: a regulator of neuronal differentiation, maintenance and plasticity. *BioEssays*. 28:822-833.
- DeVita, V.T., and E. Chu. 2008. A History of Cancer Chemotherapy. *Cancer Research*. 68:8643-8653.
- Diers, A.R., B.P. Dranka, K.C. Ricart, O.H. Joo Yeun, M.S. Johnson, F. Zhou, M.A. Pallero, T.M. Bodensine, U.J.E. Murphy, D.R. Welch, and A. Landar. 2010. Modulation of mammary cancer cell migration by 15-deoxydelta 12,14-prostaglandin J2: implications for anti-metastatic therapy. *Journal of Biological Chemistry*. 430:10.
- Dobashi, Y., N. Takei, S. Suzuki, H. Yoneyama, M. Hanawa, and A. Ooi. 2004. Aberration of epidermal growth factor receptor expression in bone and soft-tissue tumors: protein overexpression, gene amplification and activation of downstream molecules. *Modern Pathology*. 17:1497-1505.
- Dong, Z., L.H. Liu, B. Han, R. Pincheira, and J.-T. Zhang. 2004. Role of eIF3 p170 in controlling synthesis of ribonucleotide reductase M2 and cell growth. *Oncogene*. 23:3790-3801.

- Doty, P., H. Boedtker, J.R. Fresco, R. Haselkorn, and M. Litt. 1959. Secondary Structure in Ribonucleic Acids. *Proceedings of the National Academy of Sciences*. 45:482-499.
- Druker, B.J. 2008. Translation of the Philadelphia chromosome into therapy for CML. *Blood*. 112:4808-4817.
- Duce, J.A., A. Tsatsanis, M.A. Cater, S.A. James, E. Robb, K. Wikhe, S.L. Leong, K. Perez, T. Johanssen, M.A. Greenough, H.-H. Cho, D. Galatis, R.D. Moir, C.L. Masters, C. McLean, R.E. Tanzi, R. Cappai, K.J. Barnham, G.D. Ciccotosto, J.T. Rogers, and A.I. Bush. 2010. Iron-Export Ferroxidase Activity of Amyloid Precursor Protein Is Inhibited by Zinc in Alzheimer's Disease. *Cell*. 142:857-867.
- Duncan, J.S., G. Gerig, A. Mohamed, and C. Davatzikos. 2005. Finite Element Modeling of Brain Tumor Mass-Effect from 3D Medical Images. In *Medical Image Computing and Computer-Assisted Intervention – MICCAI 2005*. Vol. 3749. Springer Berlin / Heidelberg. 400-408.
- Duncan, R., and J.W. Hershey. 1983. Identification and quantitation of levels of protein synthesis initiation factors in crude HeLa cell lysates by two-dimensional polyacrylamide gel electrophoresis. *Journal of Biological Chemistry*. 258:7228-7235.
- Duncan, R., S.C. Milburn, and J.W. Hershey. 1987. Regulated phosphorylation and low abundance of HeLa cell initiation factor eIF-4F suggest a role in translational control. Heat shock effects on eIF-4F. *Journal of Biological Chemistry*. 262:380-388.
- Dutcher, S.K. 2001. The tubulin fraternity: alpha to eta. *Current Opinion in Cell Biology*. 13:49-54.
- Eberle, J., K. Krasagakis, and C.E. Orfanos. 1997. Translation initiation factor eIF-4A1 mRNA is consistently overexpressed in human melanoma cells in vitro. *International Journal of Cancer*. 71:396-401.
- Edbauer, D., E. Winkler, J.T. Regula, B. Pesold, H. Steiner, and C. Haass. 2003. Reconstitution of [gamma]-secretase activity. *Nat Cell Biol*. 5:486-488.
- Edwards, B.K., M.L. Brown, P.A. Wingo, H.L. Howe, E. Ward, L.A.G. Ries, D. Schrag, P.M. Jamison, A. Jemal, X.C. Wu, C. Friedman, L. Harlan, J. Warren, R.N. Anderson, and L.W. Pickle. 2005. Annual Report to the Nation on the Status of Cancer, 1975–2002, Featuring Population-Based Trends in Cancer Treatment. *Journal of the National Cancer Institute*. 97:1407-1427.
- Ekstrand, A.J., C.D. James, W.K. Cavenee, B. Seliger, R.F. Pettersson, and V.P. Collins. 1991. Genes for Epidermal Growth Factor Receptor, Transforming Growth Factor  $\alpha$ , and Epidermal Growth Factor and Their Expression in Human Gliomas in Vivo. *Cancer Research*. 51:2164-2172.
- Enard, W., P. Khaitovich, J. Klose, S. Zöllner, F. Heissig, P. Giavalisco, K. Nieselt-Struwe, E. Muchmore, A. Varki, R. Ravid, G.M. Doxiadis, R.E. Bontrop, and S. Pääbo. 2002. Intra- and Interspecific Variation in Primate Gene Expression Patterns. *Science*. 296:340-343.
- English, D.R., B.K. Armstrong, A. Kricke, and C. Fleming. 1997. Sunlight and cancer. *Cancer Causes and Control*. 8:271-283.
- Engqvist-Goldstein, Å.E.Y., and D.G. Drubin. 2003. Actin Assembly and Endocytosis: From Yeast to Mammals. *Annual Review of Cell and Developmental Biology*. 19:287-332.
- Enoch, T., and C. Norbury. 1995. Cellular responses to DNA damage: cell-cycle checkpoints, apoptosis and the roles of p53 and ATM. *Trends in Biochemical Sciences*. 20:426-430.
- Erkman, J.A., and U. Kutay. 2004. Nuclear export of mRNA: from the site of transcription to the cytoplasm. *Experimental Cell Research*. 296:12-20.
- Favre, A., C. Morel, and K. Scherrer. 1975. The Secondary Structure and Poly(A) Content of Globin Messenger RNA as a Pure RNA and in Polyribosome-Derived Ribonucleoprotein Complexes. *European Journal of Biochemistry*. 57:147-157.
- Ferguson, R.E., H.P. Carroll, A. Harris, E.R. Maher, P.J. Selby, and R.E. Banks. 2005. Housekeeping proteins: A preliminary study illustrating some limitations as useful references in protein expression studies. *Proteomics*. 5:566-571.
- Fernandez, J., I. Yaman, C. Huang, H. Liu, A.B. Lopez, A.A. Komar, M.G. Caprara, W.C. Merrick, M.D. Snider, R.J. Kaufman, W.H. Lamers, and M. Hatzoglou. 2005. Ribosome stalling regulates IRES-mediated translation in eukaryotes, a parallel to prokaryotic attenuation. *Molecular Cell*. 17:405-416.

- Ferraiuolo, M.A., C.S. Lee, L.W. Ler, J.L. Hsu, M. Costa-Mattioli, M.J. Luo, R. Reed, and N. Sonenberg. 2004. A nuclear translation-like factor eIF4AIII is recruited to the mRNA during splicing and functions in nonsense-mediated decay. *Proceedings of the National Academy of Science USA*. 101:4118-4123.
- Ferrari, D., and A. Peracchi. 2002. A continuous kinetic assay for RNA cleaving deoxyribozymes, exploiting ethidium bromide as an extrinsic fluorescent probe. *Nucleic Acids Research*. 30:e112.
- Fitzgerald, M., and T. Shenk. 1981. The sequence 52-AAUAAA-32 forms part of the recognition site for polyadenylation of late SV40 mRNAs. *Cell*. 24:251-260.
- Flaherty, S.M., P. Fortes, E. Izaurralde, I.W. Mattaj, and G.M. Gilmartin. 1997. Participation of the nuclear cap binding complex in pre-mRNA processing. *Proceedings of the National Academy of Sciences of the United States of America*. 94:11893-11898.
- Fletcher, S.P., I.K. Ali, A. Kaminski, P. Digard, and R.J. Jackson. 2002. The influence of viral coding sequences on pestivirus IRES activity reveals further parallels with translation initiation in prokaryotes. *RNA*. 8:1558-1571.
- Fleurent, M., A.-C. Gingras, N. Sonenberg, and S. Meloche. 1997. Angiotensin II Stimulates Phosphorylation of the Translational Repressor 4E-binding Protein 1 by a Mitogen-activated Protein Kinase-independent Mechanism. *Journal of Biological Chemistry*. 272:4006-4012.
- Folkman, J. 1990. What Is the Evidence That Tumors Are Angiogenesis Dependent? *Journal of the National Cancer Institute*. 82:4-7.
- Folkman, J., and M. Klagsbrun. 1987. Angiogenic factors. *Science*. 235:442-447.
- Forsythe, J.A., B.H. Jiang, N.V. Iyer, F. Agani, S.W. Leung, R.D. Koos, and G.L. Semenza. 1996. Activation of vascular endothelial growth factor gene transcription by hypoxia-inducible factor 1. *Molecular and Cellular Biology*. 16:4604-4613.
- Frankel, L.B., N.R. Christoffersen, A. Jacobsen, M. Lindow, A. Krogh, and A.H. Lund. 2008. Programmed Cell Death 4 (PDCD4) Is an Important Functional Target of the MicroRNA miR-21 in Breast Cancer Cells. *Journal of Biological Chemistry*. 283:1026-1033.
- Franovic, A., L. Gunaratnam, K. Smith, I. Robert, D. Patten, and S. Lee. 2007. Translational up-regulation of the EGFR by tumor hypoxia provides a nonmutational explanation for its overexpression in human cancer. *Proceedings of the National Academy of Sciences*. 104:13092-13097.
- Fraser, C.S., Y.Y. Leary, and D.J. A. 2004. Coordinated assembly of human translation initiation complexes by the hepatitis C virus internal ribosome entry site. *RNA*. 101:16990-16995.
- Fredlund, J.O., M.C. Johansson, E. Dahlberg, and S.M. Oredsson. 1995. Ornithine Decarboxylase and S-Adenosylmethionine Decarboxylase Expression during the Cell Cycle of Chinese Hamster Ovary Cells. *Experimental Cell Research*. 216:86-92.
- Freschauf, G.K., R.S. Mani, T.R. Mereniuk, M. Fanta, C.A. Virgen, G.L. Dianov, J.-M. Grassot, D.G. Hall, and M. Weinfeld. 2010. Mechanism of Action of an Imidopiperidine Inhibitor of Human Polynucleotide Kinase/Phosphatase. *Journal of Biological Chemistry*. 285:2351-2360.
- Fukao, A., Y. Sasano, H. Imataka, K. Inoue, H. Sakamoto, N. Sonenberg, C. Thoma, and T. Fujiwara. 2009. The ELAV protein HuD stimulates cap-dependent translation in a Poly(A)- and eIF4A-dependent manner. *Molecular Cell*. 36:1007-1017.
- Gabrea, A., P.L. Bergsagel, M. Chesi, Y. Shou, and W.M. Kuehl. 1999. Insertion of Excised IgH Switch Sequences Causes Overexpression of Cyclin D1 in a Myeloma Tumor Cell. *Molecular Cell*. 3:119-123.
- Galán, A., O. Llorca, J.M. Valpuesta, J. Pérez-Pérez, J.L. Carrascosa, M. Menéndez, S. Bañuelos, and A. Muga. 1999. ATP hydrolysis induces an intermediate conformational state in GroEL. *European Journal of Biochemistry*. 259:347-355.
- Garrett, R.A., Douthwaite, S. R., Liljas, A., Matheson, A. T., Moore, P. B. & Noller, H. F. 2000. The Ribosome. Structure, Function, Antibiotics and Cellular Interactions. ASM Press, Washington D. C.
- Gatti, C., C. Houssier, and E. Fredericq. 1975. Binding of ethidium bromide to ribosomal RNA: Absorption, fluorescence, circular and electric dichroism study. *Biochimica et Biophysica Acta (BBA) - Nucleic Acids and Protein Synthesis*. 407:308-319.

- Gautheret, D., D. Konings, and R.R. Gutell. 1994. A major family of motifs involving GA mismatches in ribosomal RNA. *Journal of Molecular Biology*. 242:1-8.
- Gebhardt, F., K.S. Zänker, and B. Brandt. 1999. Modulation of Epidermal Growth Factor Receptor Gene Transcription by a Polymorphic Dinucleotide Repeat in Intron 1. *Journal of Biological Chemistry*. 274:13176-13180.
- Gerner, E.W., and F.L. Meyskens. 2004. Polyamines and cancer: old molecules, new understanding. *National Review of Cancer*. 4:781-792.
- Gibbs, J.W. 1873. A method of geometrical representation of the thermodynamic properties of substances by means of surfaces, New Haven.
- Gilmore, R., G. Blobel, and P. Walter. 1982. Protein translocation across the endoplasmic reticulum. Detection in the microsomal membrane of a receptor for the signal recognition particle. *The Journal of Cell Biology*. 95:463-469.
- Gingras, A.-C., B. Raught, S.P. Gygi, A. Niedzwiecka, M. Miron, S.K. Burley, R.D. Polakiewicz, A. Wyslouch-Cieszynska, R. Aebersold, and N. Sonenberg. 2001. Hierarchical phosphorylation of the translation inhibitor 4E-BP1. *Genes & Development*. 15:2852-2864.
- Gingras, A.-C., B. Raught, and N. Sonenberg. 1999. eIF4 Initiation Factors: Effectors of mRNA Recruitment to Ribosomes and Regulators of Translation. *Annual Review of Biochemistry*. 68:913-963.
- Giorgi, C., G.W. Yeo, M.E. Stone, D.B. Katz, C. Burge, G. Turrigiano, and M.J. Moore. 2007. The EJC factor eIF4AIII modulates synaptic strength and neuronal protein expression. *Cell*. 130:179-191.
- Godemann, R., J. Madden, J. Krämer, M. Smith, U. Fritz, T. Hesterkamp, J. Barker, S. Höppner, D. Hallett, A. Cesura, A. Ebnet, and J. Kemp. 2009. Fragment-Based Discovery of BACE1 Inhibitors Using Functional Assays. *Biochemistry*. 48:10743-10751.
- Goedert, M., C.M. Wischik, R.A. Crowther, J.E. Walker, and A. Klug. 1988. Cloning and sequencing of the cDNA encoding a core protein of the paired helical filament of Alzheimer disease: identification as the microtubule-associated protein tau. *Proceedings of the National Academy of Sciences*. 85:4051-4055.
- Goke, A., R. Goke, A. Knolle, H. Trusheim, H. Schmidt, A. Wilmen, R. Carmody, B. Goke, and Y.H. Chen. 2002. DUG is a novel homologue of translation initiation factor 4G that binds eIF4A. *Biochemical and Biophysical Research Communication*. 297:78-82.
- Goldstein, L. 1970. A radioautographic investigation of the relation between transcription and translation in a eukaryotic cell. *Experimental Cell Research*. 61:218-222.
- Gomez, E., S.S. Mohammad, and G.D. Pavitt. 2002. Characterization of the minimal catalytic domain within eIF2B: the guanine-nucleotide exchange factor for translation initiation. *EMBO Journal*. 21:5292-5301.
- Gorbalenya, A.E., and E.V. Koonin. 1993. Helicases: amino acid sequence comparisons and structure-function relationships. *Current Opinion in Structural Biology*. 3:419-429.
- Graff, J.R., B.W. Konicek, J.H. Carter, and E.G. Marcusson. 2008. Targeting the Eukaryotic Translation Initiation Factor 4E for Cancer Therapy. *Cancer Research*. 68:631-634.
- Graff, J.R., B.W. Konicek, T.M. Vincent, R.L. Lynch, D. Monteith, S.N. Weir, P. Schvier, A. Capen, R.L. Goode, M.S. Dowless, Y. Chen, H. Zhang, S. Sissons, K. Cox, A.M. McNulty, S.H. Parsons, T. Wang, L. Sams, S. Geeganage, L.E. Douglass, B.L. Neubauer, N.M. Dean, K. Blanchard, J. Shou, L.F. Stancato, J.H. Carter, and E.G. Marcusson. 2007. Therapeutic suppression of translation initiation factor eIF4E expression reduces tumor growth without toxicity. *The Journal of Clinical Investigation*. 117:2638-2648.
- Gray, N.K., and M. Wickens. 1998. Control of translation initiation in animals. *Annual Review of Cell Developmental Biology*. 14:399-458.
- Greganova, E., M. Altmann, and P. Bütikofer. 2011. Unique modifications of translation elongation factors. *Federation of European Biochemical Societies Journal*. 278:2613-2624.
- Grens, A., and I.E. Scheffler. 1990. The 5'- and 3'-untranslated regions of ornithine decarboxylase mRNA affect the translational efficiency. *Journal of Biological Chemistry*. 265:11810-11816.

- Grifo, J.A., R.D. Abramson, C.A. Satler, and W.C. Merrick. 1984. RNA-stimulated ATPase activity of eukaryotic initiation factors. *Journal of Biological Chemistry*. 259:8648-8654.
- Grifo, J.A., S.M. Tahara, J.P. Leis, M.A. Morgan, A.J. Shatkin, and W.C. Merrick. 1982. Characterization of eukaryotic initiation factor 4A, a protein involved in ATP-dependent binding of globin mRNA. *Journal of Biological Chemistry*. 257:5246-5252.
- Grosjean, H., S. Auxilien, F. Constantinesco, C. Simon, Y. Corda, H.F. Becker, D. Foiret, A. Morin, Y.X. Jin, M. Fournier, and J.L. Fourrey. 1996. Enzymatic conversion of adenosine to inosine and to N1-methylinosine in transfer RNAs: A review. *Biochimie*. 78:488-501.
- Haass, C., C.A. Lemere, A. Capell, M. Citron, P. Seubert, D. Schenk, L. Lannfelt, and D.J. Selkoe. 1995. The Swedish mutation causes early-onset Alzheimer's disease by beta-secretase cleavage within the secretory pathway. *Nature Medicine*. 1:1291-1296.
- Haghighat, A., S. Mader, A. Pause, and N. Sonenberg. 1995. Repression of cap-dependent translation by 4E-binding protein competition with p220 for binding to eukaryotic initiation factor-4E. *EMBO Journal*. 14:5701-5709.
- Haley, J.D., and M.D. Waterfield. 1991. Contributory effects of de novo transcription and premature transcript termination in the regulation of human epidermal growth factor receptor proto-oncogene RNA synthesis. *Journal of Biological Chemistry*. 266:1746-1753.
- Hall, C.N., A.F. Badawi, P.J. O'Connor, and S. R. 1991. The detection of alkylation damage in the DNA of human gastrointestinal tissues. *British Journal of Cancer*. 64:59-63.
- Hampel, H., K. Blennow, L.M. Shaw, Y.C. Hoessler, H. Zetterberg, and J.Q. Trojanowski. 2010. Total and phosphorylated tau protein as biological markers of Alzheimer's disease. *Experimental Gerontology*. 45:30-40.
- Hanahan, D., and R.A. Weinberg. 2000. The Hallmarks of Cancer. *Cell*. 100:57-70.
- Hanahan, D., and R.A. Weinberg. 2011. Hallmarks of Cancer: The Next Generation. *Cell*. 144:646-674.
- Hancock, J.M., D. Tautz, and G.A. Dover. 1988. Evolution of the secondary structures and compensatory mutations of the ribosomal RNAs of *Drosophila melanogaster*. *Molecular Biology and Evolution*. 5:393-414.
- Hanson, A.J. 1992. The rolling ball. In *Graphics Gems III*. Academic Press Professional, Inc. 51-60.
- Harding, H.P., I. Novoa, Y. Zhang, H. Zeng, R. Wek, M. Schapira, and D. Ron. 2000. Regulated Translation Initiation Controls Stress-Induced Gene Expression in Mammalian Cells. *Molecular Cell*. 6:1099-1108.
- Hardy, J. 1997. Amyloid, the presenilins and Alzheimer's disease. *Trends in Neurosciences*. 20:154-159.
- Harembaki, T., J. Sridharan, S. Dvora, and D.C. Weinstein. 2010. Regulation of vertebrate embryogenesis by the exon junction complex core component Eif4a3. *Developmental Dynamics*. 239:1977-1987.
- Hartwell, L.H., and M.B. Kastan. 1994. Cell cycle control and cancer. *Science*. 266:1821-1828.
- Hasselmo, M.E. 2006. The role of acetylcholine in learning and memory. *Current Opinion in Neurobiology*. 16:710-715.
- Hay, N., and N. Sonenberg. 2004. Upstream and downstream of mTOR. *Genes and Development*. 18:1926-1945.
- Hellen, C.U., and P. Sarnow. 2001. Internal ribosome entry sites in eukaryotic mRNA molecules. *Genes and Development*. 15:1593-1612.
- Hensley, K., N. Hall, R. Subramaniam, P. Cole, M. Harris, M. Aksenov, M. Aksenova, S.P. Gabbita, J.F. Wu, J.M. Carney, M. Lovell, W.R. Markesbery, and D.A. Butterfield. 1995. Brain Regional Correspondence Between Alzheimer's Disease Histopathology and Biomarkers of Protein Oxidation. *Journal of Neurochemistry*. 65:2146-2156.
- Hentze, M.W. 1995. Translational regulation: versatile mechanisms for metabolic and developmental control. *Current Opinion in Cell Biology*. 7:393-398.

- Hentze, M.W., S.W. Caughman, T.A. Rouault, J.G. Barriocanal, A. Dancis, J.B. Harford, and R.D. Klausner. 1987. Identification of the iron-responsive element for the translational regulation of human ferritin mRNA. *Science*. 238:1570-1573.
- Hentze, M.W., and L.C. Kuhn. 1996. Molecular control of vertebrate iron metabolism: mRNA-based regulatory circuits operated by iron, nitric oxide, and oxidative stress. *Proceedings of the National Academy of Sciences of the United States of America*. 93:8175-8182.
- Herbst, R.S. 2004. Review of epidermal growth factor receptor biology. *International journal of radiation oncology, biology, physics*. 59:S21-S26.
- Hernández, G. 2008. Was the initiation of translation in early eukaryotes IRES-driven? *Trends in Biochemical Sciences*. 33:58-64.
- Hershey, J.W.B., and W.C. Merrick. 2000. Translational Control of Gene Expression. Cold Spring Harbor Laboratory Press, Cold Spring Harbor.
- Heyman, A., W.E. Wilkinson, J.A. Stafford, M.J. Helms, A.H. Sigmon, and T. Weinberg. 1984. Alzheimer's disease: A study of epidemiological aspects. *Annals of Neurology*. 15:335-341.
- Higgs, P.G. 2000. RNA secondary structure: physical and computational aspects. *Quarterly Reviews of Biophysics*. 33:199-253.
- Hinnebusch, A.G. 2000. Translational control of gene expression. Cold Spring Harbor Laboratory Press, Cold Spring Harbor.
- Hinnebusch, A.G. 2011. Molecular Mechanism of Scanning and Start Codon Selection in Eukaryotes. *Microbiology and Molecular Biology Reviews*. 75:434-467.
- Hiremath, L.S., N.R. Webb, and R.E. Rhoads. 1985. Immunological detection of the messenger RNA cap-binding protein. *Journal of Biological Chemistry*. 260:7843-7849.
- Hollams, E.M., K.M. Giles, A.M. Thomson, and P.J. Leedman. 2002. mRNA Stability and the Control of Gene Expression: Implications for Human Disease. *Journal of Neurochemical Research*. 27:1573-6903.
- Hollstein, M., D. Sidransky, B. Vogelstein, and C.C. Harris. 1991. p53 mutations in human cancers. *Science*. 253:49-53.
- Holzmann, K., C. Gerner, A. Pörtl, R. Schäfer, P. Obrist, C. Ensinger, R. Grimm, and G. Saueremann. 2000. A Human Common Nuclear Matrix Protein Homologous to Eukaryotic Translation Initiation Factor 4A. *Biochemical and Biophysical Research Communications*. 267:339-344.
- Homann, N., F. Stickel, I.R. König, A. Jacobs, K. Junghanns, M. Benesova, D. Schuppan, S. Himsel, I. Zuber-Jerger, C. Hellerbrand, D. Ludwig, W.H. Caselmann, and H.K. Seitz. 2006. Alcohol dehydrogenase 1C allele is a genetic marker for alcohol-associated cancer in heavy drinkers. *International Journal of Cancer*. 118:1998-2002.
- Hoogsteen, K. 1963. The crystal and molecular structure of a hydrogen-bonded complex between 1-methylthymine and 9-methyladenine. *Acta Crystallographica*. 16:907-916.
- Hooper, C., R. Killick, and S. Lovestone. 2008. The GSK3 hypothesis of Alzheimer's disease. *Journal of Neurochemistry*. 104:1433-1439.
- Hooper, C., V. Markevich, F. Plattner, R. Killick, E. Schofield, T. Engel, F. Hernandez, B. Anderton, K. Rosenblum, T. Bliss, S.F. Cooke, J. Avila, J.J. Lucas, K.P. Giese, J. Stephenson, and S. Lovestone. 2007. Glycogen synthase kinase-3 inhibition is integral to long-term potentiation. *European Journal of Neuroscience*. 25:81-86.
- Huang, J., and R.J. Schneider. 1991. Adenovirus inhibition of cellular protein synthesis involves inactivation of cap-binding protein. *Cell*. 65:271-280.
- Huez, I., L. Creancier, S. Audigier, M.-C. Gensac, A.-C. Prats, and H. Prats. 1998. Two Independent Internal Ribosome Entry Sites Are Involved in Translation Initiation of Vascular Endothelial Growth Factor mRNA. *Molecular and Cellular Biology*. 18:6178-6190.
- Humphrey, P.A., A.J. Wong, B. Vogelstein, M.R. Zalutsky, G.N. Fuller, G.E. Archer, H.S. Friedman, M.M. Kwatra, S.H. Bigner, and D.D. Bigner. 1990. Anti-synthetic peptide antibody reacting at the fusion junction of deletion-mutant epidermal growth factor receptors in human glioblastoma. *Proceedings of the National Academy of Sciences*. 87:4207-4211.

- Hussain, I., D. Powell, D.R. Howlett, D.G. Tew, T.D. Meek, C. Chapman, I.S. Gloger, K.E. Murphy, C.D. Southan, D.M. Ryan, T.S. Smith, D.L. Simmons, F.S. Walsh, C. Dingwall, and G. Christie. 1999. Identification of a Novel Aspartic Protease (Asp 2) as beta-Secretase. *Molecular and Cellular Neuroscience*. 14:419-427.
- Hwang, B.Y., B. Su, H. Chai, Q. Mi, L.B.S. Kardono, J.J. Afriastini, S. Riswan, B.D. Santarsiero, A.D. Mesecar, R. Wild, C.R. Fairchild, G.D. Vite, W.C. Rose, N.R. Farnsworth, G.A. Cordell, J.M. Pezzuto, S.M. Swanson, and A.D. Kinghorn. 2004. Silvestrol and Episilvestrol, Potential Anticancer Rocaglate Derivatives from *Aglaia silvestris*. *Journal of Biological Chemistry*. 69:3350-3358.
- Iborra, F.J., D.A. Jackson, and P.R. Cook. 2004. The case for nuclear translation. *Journal of Cell Science*. 117:5713-5720.
- Ill-Raga, G., E. Palomer, M.A. Wozniak, E. Ramos-Fernández, M. Bosch-Morató, M. Tajés, F.X. Guix, J.J. Galán, J. Clarimón, C. Antúnez, L.M. Real, M. Boada, R.F. Itzhaki, C. Fandos, and F.J. Muñoz. 2011. Activation of PKR Causes Amyloid beta-Peptide Accumulation via De-Repression of BACE1 Expression. *PLoS ONE*. 6:e21456.
- Itoh, N., and H. Okamoto. 1980. Translational control of proinsulin synthesis by glucose. *Nature*. 283:100-102.
- J., W.H., G.R. Adami, N. Wei, K. Keyomarsi, and S.J. Elledge. 1993. The p21 Cdk-interacting protein Cip1 is a potent inhibitor of G1 cyclin-dependent kinases. *Cell*. 75:805-816.
- Jackson, R.J. 1988. Picornaviruses break the rules. *Nature*. 334:292-293.
- Jackson, R.J., C.U.T. Hellen, and T.V. Pestova. 2010. The mechanism of eukaryotic translation initiation and principles of its regulation. *Nat Rev Mol Cell Biol*. 11:113-127.
- Jackson, R.J., M.T. Howell, and A. Kaminski. 1990. The novel mechanism of initiation of picornavirus RNA translation. *Trends in Biochemical Sciences*. 15:477-483.
- Jain, A.K., N. Tewari-Singh, M. Gu, S. Inturi, C.W. White, and R. Agarwal. 2011. Sulfur mustard analog, 2-chloroethyl ethyl sulfide-induced skin injury involves DNA damage and induction of inflammatory mediators, in part via oxidative stress, in SKH-1 hairless mouse skin. *Toxicology Letters*. 205:293-301.
- Jang, S.K., H.G. Krausslich, M.J. Nicklin, G.M. Duke, A.C. Palmenberg, and E. Wimmer. 1988. A segment of the 5' nontranslated region of encephalomyocarditis virus RNA directs internal entry of ribosomes during in vitro translation. *Journal of Virology*. 62:2636-2643.
- Johannes, G., M.S. Carter, M.B. Eisen, P.O. Brown, and P. Sarnow. 1999. Identification of eukaryotic mRNAs that are translated at reduced cap binding complex eIF4F concentrations using a cDNA microarray. *Proceedings of the National Academy of Science USA*. 96:13118-13123.
- Jopling, C.L., K.A. Spriggs, S.A. Mitchell, M. Stoneley, and A.E. Willis. 2004. L-Myc protein synthesis is initiated by internal ribosome entry. *RNA*. 10:287-298.
- Jopling, C.L., and A.E. Willis. 2001. N-myc translation is initiated via an internal ribosome entry segment that displays enhanced activity in neuronal cells. *Oncogene*. 20:2664-2670.
- Kaether, C., C. Haass, and H. Steiner. 2006. Assembly, Trafficking and Function of  $\gamma$ -Secretase. *Neurodegenerative Diseases*. 3:275-283.
- Kalaria, R.N. 2000. The role of cerebral ischemia in Alzheimer's disease. *Neurobiology of aging*. 21:321-330.
- Kaminski, A., S.L. Hunt, J.G. Patton, and R.J. Jackson. 1995. Direct evidence that polypyrimidine tract binding protein (PTB) is essential for internal initiation of translation of encephalomyocarditis virus RNA. *RNA*. 1:924-938.
- Kapp, L.D., and J.R. Lorsch. 2004. The Molecular Mechanics of Eukaryotic Translation. *Annual Review of Biochemistry*. 73:657-704.
- Kataoka, N., M. Ohno, K. Kangawa, Y. Tokoro, and Y. Shimura. 1994. Cloning of a complementary DNA encoding an 80 kilodalton nuclear cap binding protein. *Nucleic Acids Research*. 19:3861-3865.
- Kato, A., S. Fujita, and Y. Komeda. 2001. Identification and Characterization of Two Genes Encoding the Eukaryotic Initiation Factor 4A in Rice. *Mitochondrial DNA*. 12:295-303.

- Kaufman, R.J. 2004. Regulation of mRNA translation by protein folding in the endoplasmic reticulum. *Trends in Biochemical Sciences*. 29:152-158.
- Keenan, R.J., D.M. Freymann, R.M. Stroud, and P. Walter. 2001. The Signal Recognition Particle. *Annual Review of Biochemistry*. 70:755-775.
- Kersting, C., N. Tidow, H. Schmidt, C. Liedtke, J. Neumann, W. Boecker, P.J.v. Diest, B. Brandt, and H. Buerger. 2004. Gene dosage PCR and fluorescence in situ hybridization reveal low frequency of egfr amplifications despite protein overexpression in invasive breast carcinoma. *Laboratory Investigation*. 84:582-587.
- Khaleghpour, K., Y.V. Svitkin, A.W. Craig, C.T. DeMaria, R.C. Deo, S.K. Burley, and N. Sonenberg. 2001. Translational Repression by a Novel Partner of Human Poly(A) Binding Protein, Paip2. *Molecular Cell*. 7:205-216.
- Kibbe, W.A. 2007. OligoCalc: an online oligonucleotide properties calculator. *Nucleic Acids Research*. 35:W43-W46.
- Kieft, J.S., K. Zhou, A. Grech, R. Jubin, and J.A. Doudna. 2002. Crystal structure of an RNA tertiary domain essential to HCV IRES-mediated translation initiation. *Nature Structural & Molecular Biology*. 9:370-374.
- Kim, S., A.A. Salim, S.M. Swanson, and A. Douglas Kinghorn. 2006. Potential of Cyclopentabenzofurans from Aglaia Species in Cancer Chemotherapy. *Anti-Cancer Agents in Medicinal Chemistry*.
- Kim, W.J., S.H. Back, V. Kim, I. Ryu, and S.K. Jang. 2005. Sequestration of TRAF2 into Stress Granules Interrupts Tumor Necrosis Factor Signaling under Stress Conditions. *Molecular and Cellular Biology*. 25:2450-2462.
- Kim, W.J., J.H. Kim, and S.K. Jang. 2007. Anti-inflammatory lipid mediator 15d-PGJ2 inhibits translation through inactivation of eIF4A. *EMBO Journal*. 26:5020-5032.
- Kimball, S.R. 1999. Eukaryotic initiation factor eIF2. *The International Journal of Biochemistry & Cell Biology*. 31:25-29.
- Kimball, S.R., R.L. Horetsky, and L.S. Jefferson. 1998. Implication of eIF2B Rather Than eIF4E in the Regulation of Global Protein Synthesis by Amino Acids in L6 Myoblasts. *Journal of Biological Chemistry*. 273:30945-30953.
- King, M.C., and A.C. Wilson. 1975. Evolution at two levels in humans and chimpanzees. *Science*. 188:107-116.
- Kisselev, L., M. Ehrenberg, and L. Frolova. 2003. Termination of translation: interplay of mRNA, rRNAs and release factors? *EMBO Journal*. 22:175-182.
- Knudson, A.G. 1971. Mutation and Cancer: Statistical Study of Retinoblastoma. *Proceedings of the National Academy of Sciences*. 68:820-823.
- Kolupaeva, V.G., I.B. Lomakin, T.V. Pestova, and C.U.T. Hellen. 2003. Eukaryotic Initiation Factors 4G and 4A Mediate Conformational Changes Downstream of the Initiation Codon of the Encephalomyocarditis Virus Internal Ribosomal Entry Site. *Molecular and Cellular Biology*. 23:687-698.
- Kolupaeva, V.G., T.V. Pestova, C.U.T. Hellen, and I.N. Shatsky. 1998. Translation Eukaryotic Initiation Factor 4G Recognizes a Specific Structural Element within the Internal Ribosome Entry Site of Encephalomyocarditis Virus RNA. *Journal of Biological Chemistry*. 273:18599-18604.
- Komar, A.A., and M. Hatzoglou. 2011. Cellular IRES-mediated translation: The war of ITAFs in pathophysiological states. *Cell Cycle*. 10:229-240.
- Koritzinsky, M., M.G. Magagnin, T. van den Beucken, R. Seigneuric, K. Savelkouls, J. Dostie, S. Pyronnet, R.J. Kaufman, S.A. Wepler, J.W. Voncken, P. Lambin, C. Koumenis, N. Sonenberg, and B.G. Wouters. 2006. Gene expression during acute and prolonged hypoxia is regulated by distinct mechanisms of translational control. *EMBO Journal*. 25:1114-1125.
- Koritzinsky, M., K.M.A. Rouschop, T. van den Beucken, M.G. Magagnin, K. Savelkouls, P. Lambin, and B.G. Wouters. 2007. Phosphorylation of eIF2 $\alpha$  is required for mRNA translation inhibition and survival during moderate hypoxia. *Radiotherapy and Oncology*. 83:353-361.
- Koumenis, C., C. Naczki, M. Koritzinsky, S. Rastani, A. Diehl, N. Sonenberg, A. Koromilas, and B.G. Wouters. 2002. Regulation of Protein Synthesis by Hypoxia via Activation of the Endoplasmic Reticulum Kinase PERK and Phosphorylation of the Translation Initiation Factor eIF2 $\alpha$ . *Molecular and Cellular Biology*. 22:7405-7416.

- Kozak, M. 1980. Influence of mRNA secondary structure on binding and migration of 40S ribosomal subunits. *Cell*. 19:79-90.
- Kozak, M. 1984a. Compilation and analysis of sequences upstream from the translational start site in eukaryotic mRNAs. *Nucleic Acids Research*. 12:857-872.
- Kozak, M. 1984b. Point mutations close to the AUG initiator codon affect the efficiency of translation of rat preproinsulin in vivo. *Nature*. 308:241-246.
- Kozak, M. 1987. An analysis of 5'-noncoding sequences from 699 vertebrate messenger RNAs. *Nucleic Acids Research*. 15:8125-8148.
- Kozak, M. 1989. The scanning model for translation: an update. *The Journal of Cell Biology*. 108:229-241.
- Kozak, M. 1991a. An analysis of vertebrate mRNA sequences: intimations of translational control. *Journal of Cellular Biology*. 115:887-903.
- Kozak, M. 1991b. Structural features in eukaryotic mRNAs that modulate the initiation of translation. *Journal of Biological Chemistry*. 266:19867-19870.
- Kozak, M. 1999. Initiation of translation in prokaryotes and eukaryotes. *Gene*. 234:187-208.
- Kramer, A. 1996. The Structure and Function of Proteins Involved in Mammalian Pre-mRNA Splicing. *Annual Review of Biochemistry*. 65:367-409.
- Kurzrock, R., H.M. Kantarjian, B.J. Druker, and M. Talpaz. 2003. Philadelphia Chromosome Positive Leukemias: From Basic Mechanisms to Molecular Therapeutics. *Annals of Internal Medicine*. 138:819-830.
- Kwee, W.S., R.W. Veldhuizen, R.P. Golding, H. Mullink, J. Stam, R. Donner, and M.E. Boon. 1982. Histologic distinction between malignant mesothelioma, benign pleural lesion and carcinoma metastasis. *Virchows Archive*. 397:287-299.
- Kyrpides, N.C., and C.R. Woese. 1998. Universally conserved translation initiation factors. *Proceedings of the National Academy of Sciences*. 95:224-228.
- Laderoute, K.R., T.D. Grant, B.J. Murphy, and R.M. Sutherland. 1992. Enhanced epidermal growth factor receptor synthesis in human squamous carcinoma cells exposed to low levels of oxygen. *International Journal of Cancer*. 52:428-432.
- Lai, E.C. 2002. Micro RNAs are complementary to 3 prime UTR sequence motifs that mediate negative post-transcriptional regulation. *Nature Genetics*. 30:363-364.
- Lambert, B.O., and S.-M. He. 1988. DNA and Chromosome Damage Induced by Acetaldehyde in Human Lymphocytes in Vitro. *Annals of the New York Academy of Sciences*. 534:369-376.
- Lambert, J.-C., S. Heath, G. Even, D. Champion, K. Slegers, M. Hiltunen, O. Combarros, D. Zelenika, M.J. Bullido, B. Tavernier, L. Letenneur, K. Bettens, C. Berr, F. Pasquier, N. Fievet, P. Barberger-Gateau, S. Engelborghs, P. De Deyn, I. Mateo, A. Franck, S. Helisalimi, E. Porcellini, O. Hanon, M.M. de Pancorbo, C. Lendon, C. Dufouil, C. Jaillard, T. Leveillard, V. Alvarez, P. Bosco, M. Mancuso, F. Panza, B. Nacmias, P. Bossu, P. Piccardi, G. Annoni, D. Seripa, D. Galimberti, D. Hannequin, F. Licastro, H. Soininen, K. Ritchie, H. Blanche, J.-F. Dartigues, C. Tzourio, I. Gut, C. Van Broeckhoven, A. Alperovitch, M. Lathrop, and P. Amouyel. 2009. Genome-wide association study identifies variants at CLU and CR1 associated with Alzheimer's disease. *Nature Genetics*. 41:1094-1099.
- Lammich, S., D. Buell, S. Zilow, A.-K. Ludwig, B. Nuscher, S.F. Lichtenthaler, C. Prinzen, F. Fahrenholz, and C. Haass. 2010. Expression of the Anti-amyloidogenic Secretase ADAM10 Is Suppressed by Its 5' Untranslated Region. *Journal of Biological Chemistry*. 285:15753-15760.
- Lammich, S., E. Kojro, R. Postina, S. Gilbert, R. Pfeiffer, M. Jasionowski, C. Haass, and F. Fahrenholz. 1999. Constitutive and regulated  $\alpha$ -secretase cleavage of Alzheimer's amyloid precursor protein by a disintegrin metalloprotease. *Proceedings of the National Academy of Sciences*. 96:3922-3927.
- Lammich, S., S. Schobel, A.-K. Zimmer, S.F. Lichtenthaler, and C. Haass. 2004. Expression of the Alzheimer protease BACE1 is suppressed via its 5'-untranslated region. *EMBO Reports*. 5:620-625.
- Lamphear, B.J., R. Kirchweger, T. Skern, and R.E. Rhoads. 1995. Mapping of Functional Domains in Eukaryotic Protein Synthesis Initiation Factor 4G (eIF4G) with Picornaviral Proteases. *Journal of Biological Chemistry*. 270:21975-21983.

- Larkin, M.A., G. Blackshields, N.P. Brown, R. Chenna, P.A. McGettigan, H. McWilliam, F. Valentin, I.M. Wallace, A. Wilm, R. Lopez, J.D. Thompson, T.J. Gibson, and D.G. Higgins. 2007. Clustal W and Clustal X version 2.0. *Bioinformatics*. 23:2947-2948.
- Lawrence, T., D.A. Willoughby, and D.W. Gilroy. 2002. Anti-inflammatory lipid mediators and insights into the resolution of inflammation. *Nature Reviews Immunology*. 2:787-795.
- Lazaris-Karatzas, A., K.S. Montine, and N. Sonenberg. 1990. Malignant transformation by a eukaryotic initiation factor subunit that binds to mRNA 5' cap. *Nature*. 345:544-547.
- Le, S.-Y., and J.V. Maizel. 1997. A common RNA structural motif involved in the internal initiation of translation of cellular mRNAs. *Nucleic Acids Research*. 25:362-369.
- Lee, H.C., H. Cho, and Y.K. Kim. 2008. Ectopic expression of eIF4E-transporter triggers the movement of eIF4E into P-bodies, inhibiting steady-state translation but not the pioneer round of translation. *Biochemical and Biophysical Research Communications*. 369:1160-1165.
- LeFebvre, A.K., N.J. Korneeva, M. Trutschl, U. Cvek, R.D. Duzan, C.A. Bradley, J.W.B. Hershey, and R.E. Rhoads. 2006. Translation Initiation Factor eIF4G-1 Binds to eIF3 through the eIF3e Subunit. *Journal of Biological Chemistry*. 281:22917-22932.
- Leontis, N.B., J. Stombaugh, and E. Westhof. 2002. The non Watson-Crick base pairs and their associated isostericity matrices. *Nucleic Acids Research*. 30:3497-3531.
- Lerner, R.S., and C.V. Nicchitta. 2006. mRNA translation is compartmentalized to the endoplasmic reticulum following physiological inhibition of cap-dependent translation. *RNA*. 12:775-789.
- Levkau, B., H. Koyama, E.W. Raines, B.E. Clurman, B. Herren, K. Orth, J.M. Roberts, and R. Ross. 1998. Cleavage of p21Cip1/Waf1 and p27Kip1 Mediates Apoptosis in Endothelial Cells through Activation of Cdk2: Role of a Caspase Cascade. *Molecular Cell*. 1:553-563.
- Levy, A.P., N.S. Levy, and M.A. Goldberg. 1996. Hypoxia-inducible Protein Binding to Vascular Endothelial Growth Factor mRNA and Its Modulation by the von Hippel-Lindau Protein. *Journal of Biological Chemistry*. 271:25492-25497.
- Lewis, J.D., E. Izaurralde, A. Jarmolowski, C. McGuigan, and I.W. Mattaj. 1996. A nuclear cap-binding complex facilitates association of U1 snRNP with the cap-proximal 5' splice site. *Genes & Development*. 10:1699-1708.
- Lewis, S.M., and M. Holcik. 2007. For IRES trans-acting factors, it is all about location. *Oncogene*. 27:1033-1035.
- Li, F.P., and J.F. Fraumeni. 1969. Soft-Tissue Sarcomas, Breast Cancer, and Other Neoplasms. *Annals of Internal Medicine*. 71:747-752.
- Li, Q., H. Imataka, S. Morino, G.W. Rogers, Jr., N.J. Richter-Cook, W.C. Merrick, and N. Sonenberg. 1999. Eukaryotic translation initiation factor 4AIII (eIF4AIII) is functionally distinct from eIF4AI and eIF4AII. *Molecular and Cellular Biology*. 19:7336-7346.
- Li, W., N. Ross-Smith, C.G. Proud, and G.J. Belsham. 2001. Cleavage of translation initiation factor 4AI (eIF4AI) but not eIF4AII by foot-and-mouth disease virus 3C protease: identification of the eIF4AI cleavage site. *FEBS Letters*. 507:1-5.
- Li, W., X. Wang, M.S. van der Knaap, and C.G. Proud. 2004. Mutations Linked to Leukoencephalopathy with Vanishing White Matter Impair the Function of the Eukaryotic Initiation Factor 2B Complex in Diverse Ways. *Molecular and Cellular Biology*. 24:3295-3306.
- Lichtenstein, P., N.V. Holm, P.K. Verkasalo, A. Iliadou, J. Kaprio, M. Koskenvuo, E. Pukkala, A. Skytthe, and K. Hemminki. 2000. Environmental and Heritable Factors in the Causation of Cancer - Analyses of Cohorts of Twins from Sweden, Denmark, and Finland. *New England Journal of Medicine*. 343:78-85.
- Lin, D., T.V. Pestova, C.U.T. Hellen, and H. Tiedge. 2008. Translational Control by a small RNA: Dendritic BC1 RNA Targets eIF4A Helicase Mechanism. *Molecular Cell Biology*. 10:1128-1134.
- Lin, T.A., X. Kong, T.A. Haystead, A. Pause, G. Belsham, N. Sonenberg, and J.C. Lawrence, Jr. 1994. PHAS-I as a link between mitogen-activated protein kinase and translation initiation. *Science*. 266:653-656.

- Lin, X., G. Koelsch, S. Wu, D. Downs, A. Dashti, and J. Tang. 2000. Human aspartic protease memapsin 2 cleaves the  $\beta$ -secretase site of  $\beta$ -amyloid precursor protein. *Proceedings of the National Academy of Sciences*. 97:1456-1460.
- Linder, P., P.F. Lasko, M. Ashburner, P. Leroy, P.J. Nielsen, K. Nishi, J. Schnier, and P.P. Slonimski. 1989. Birth of the D-E-A-D box. *Nature*. 337:121-122.
- Lingelbach, K., and B. Dobberstein. 1988. An extended RNA/RNA duplex structure within the coding region of mRNA does not block translational elongation. *Nucleic Acids Research*. 16:3405-3414.
- Liotta, L.A., P.S. Steeg, and W.G. Stetler. 1991. Cancer metastasis and angiogenesis : an imbalance of positive and negative regulation. Cell Press, Cambridge, MA, ETATS-UNIS. 10 pp.
- Liu, L., T.P. Cash, R.G. Jones, B. Keith, C.B. Thompson, and M.C. Simon. 2006. Hypoxia-Induced Energy Stress Regulates mRNA Translation and Cell Growth. *Molecular Cell*. 21:521-531.
- Lobert, S., B. Vulevic, and J.J. Correia. 1996. Interaction of Vinca Alkaloids with Tubulin: A Comparison of Vinblastine, Vincristine, and Vinorelbine. *Biochemistry*. 35:6806-6814.
- Loetscher, P., G. Pratt, and M. Rechsteiner. 1991. The C terminus of mouse ornithine decarboxylase confers rapid degradation on dihydrofolate reductase. Support for the pest hypothesis. *Journal of Biological Chemistry*. 266:11213-11220.
- Lomakin, I.B., C.U.T. Hellen, and T.V. Pestova. 2000. Physical Association of Eukaryotic Initiation Factor 4G (eIF4G) with eIF4A Strongly Enhances Binding of eIF4G to the Internal Ribosomal Entry Site of Encephalomyocarditis Virus and Is Required for Internal Initiation of Translation. *Molecular and Cellular Biology*. 20:6019-6029.
- Lomakin, I.B., V.G. Kolupaeva, A. Marintchev, G. Wagner, and T.V. Pestova. 2003. Position of eukaryotic initiation factor eIF1 on the 40S ribosomal subunit determined by directed hydroxyl radical probing. *Genes and Development*. 17:2786-2797.
- Lovell, M.A., J.D. Robertson, W.J. Teesdale, J.L. Campbell, and W.R. Markesbery. 1998. Copper, iron and zinc in Alzheimer's disease senile plaques. *Journal of the neurological sciences*. 158:47-52.
- Lovell, M.A., C. Xie, S.P. Gabbita, and W.R. Markesbery. 2000. Decreased thioredoxin and increased thioredoxin reductase levels in alzheimer's disease brain. *Free Radical Biology and Medicine*. 28:418-427.
- Low, W.K., Y. Dang, T. Schneider-Poetsch, Z. Shi, N.S. Choi, W.C. Merrick, D. Romo, and J.O. Liu. 2005. Inhibition of eukaryotic translation initiation by the marine natural product pateamine A. *Molecular Cell*. 20:709-722.
- Ma, Y., and L.M. Hendershot. 2003. Delineation of a Negative Feedback Regulatory Loop That Controls Protein Translation during Endoplasmic Reticulum Stress. *Journal of Biological Chemistry*. 278:34864-34873.
- Maekawa, T., F. Imamoto, G.T. Merlino, I. Pastan, and S. Ishii. 1989. Cooperative function of two separate enhancers of the human epidermal growth factor receptor proto-oncogene. *Journal of Biological Chemistry*. 264:5488-5494.
- Makkinje, A., H. Xiong, M. Li, and Z. Damuni. 1995. Phosphorylation of Eukaryotic Protein Synthesis Initiation Factor 4E by Insulin-stimulated Protamine Kinase. *Journal of Biological Chemistry*. 270:14824-14828.
- Malkin, D. 2011. Li-Fraumeni Syndrome. *Genes & Cancer*. 2:475-484.
- Mancuso, C., T.E. Bates, D.A. Butterfield, S. Calafato, C. Cornelius, A.D. Lorenzo, A.T. Dinkova Kostova, and V. Calabrese. 2007. Natural antioxidants in Alzheimer's disease. *Expert Opinion on Investigational Drugs*. 16:1921-1931.
- Mann, D.M.A., P.O. Yates, and B. Marcyniuk. 1984. Alzheimer's presenile dementia, senile dementia of Alzheimer type and Down's syndrome in middle age form an age related continuum of pathological changes. *Neuropathology and Applied Neurobiology*. 10:185-207.
- Marcinkiewicz, M., and N.G. Seidah. 2000. Coordinated expression of beta-amyloid precursor protein and the putative beta-secretase BACE and alpha-secretase ADAM10 in mouse and human brain. *Journal of Neurochemistry*. 75:2133-2143.
- Markesbery, W.R. 1997. Oxidative Stress Hypothesis in Alzheimer's Disease. *Free Radical Biology and Medicine*. 23:134-147.

- Martineau, C., L.G. Whyte, and C.W. Greer. 2008. Development of a SYBR safe™ technique for the sensitive detection of DNA in cesium chloride density gradients for stable isotope probing assays. *Journal of Microbiological Methods*. 73:199-202.
- Martinez-Salas, E., R. Ramos, E. Lafuente, and S. Lopez de Quinto. 2001. Functional interactions in internal translation initiation directed by viral and cellular IRES elements. *Journal of General Virology*. 82:973-984.
- Masimirembwa, C.M., R. Thompson, and T.B. Andersson. 2001. In Vitro High Throughput Screening of Compounds for Favorable Metabolic Properties in Drug Discovery. *Combinatorial Chemistry & High Throughput Screening*. 4:245-263.
- Mathews, D. 2006a. Predicting RNA secondary structure by free energy minimization. *Theoretical Chemistry Accounts*. 116:160-168.
- Mathews, D.H. 2006b. Revolutions in RNA Secondary Structure Prediction. *Journal of Molecular Biology*. 359:526-532.
- Mathews, M., N. Sonenberg, and J.W.B. Hershey. 2007. Translational control in biology and medicine. Cold Spring Harbor Laboratory, New York.
- Mathews, M.B., N. Sonenberg, and J.W.B. Hershey. 2000. Origins and principles of translation control. *In* Translational control of gene expression. N.S.e. al., editor. Cold Spring Harbor Laboratory Press, NY. 1-32.
- Mazumder, B., V. Seshadri, and P.L. Fox. 2003. Translational control by the 3'-UTR: the ends specify the means. *Trends in Biochemical Sciences*. 28:91-98.
- Mazumder, B., V. Seshadri, H. Imataka, N. Sonenberg, and P.L. Fox. 2001. Translational Silencing of Ceruloplasmin Requires the Essential Elements of mRNA Circularization: Poly(A) Tail, Poly(A)-Binding Protein, and Eukaryotic Translation Initiation Factor 4G. *Molecular and Cellular Biology*. 21:6440-6449.
- McCarthy, J.E.G. 1998. Posttranscriptional Control of Gene Expression in Yeast. *Microbiology and Molecular Biology Reviews*. 62:1492-1553.
- McDermott, F.A. 1911. LUCIFERESCEINE,2 THE FLUORESCENT MATERIAL PRESENT IN CERTAIN LUMINOUS INSECTS. *Journal of the American Chemical Society*. 33:410-416.
- Mecocci, P., U. MacGarvey, and M.F. Beal. 1994. Oxidative damage to mitochondrial DNA is increased in Alzheimer's disease. *Annals of Neurology*. 36:747-751.
- Mehta, A., C.R. Trotta, and S.W. Peltz. 2006. Derepression of the Her-2 uORF is mediated by a novel post-transcriptional control mechanism in cancer cells. *Genes & Development*. 20:939-953.
- Meier, W., A. du Bois, A. Reuss, W. Kuhn, S. Olbricht, M. Gropp, B. Richter, H.-J. Lück, R. Kimmig, and J. Pfisterer. 2009. Topotecan versus treosulfan, an alkylating agent, in patients with epithelial ovarian cancer and relapse within 12 months following 1st-line platinum/paclitaxel chemotherapy. A prospectively randomized phase III trial by the Arbeitsgemeinschaft Gynaekologische Onkologie Ovarian Cancer Study Group (AGO-OVAR). *Gynecologic Oncology*. 114:199-205.
- Meng, Z., N.L. Jackson, H. Choi, P.H. King, P.D. Emanuel, and S.W. Blume. 2008. Alterations in RNA-binding activities of IRES-regulatory proteins as a mechanism for physiological variability and pathological dysregulation of IGF-IR translational control in human breast tumor cells. *Journal of Cellular Physiology*. 217:172-183.
- Methot, N., M.S. Song, and N. Sonenberg. 1996. A region rich in aspartic acid, arginine, tyrosine, and glycine (DRYG) mediates eukaryotic initiation factor 4B (eIF4B) self-association and interaction with eIF3. *Molecular and Cellular Biology*. 16:5328-5334.
- Mihailovich, M., R. Thermann, F. Grohovaz, M.W. Hentze, and D. Zaccchetti. 2007. Complex translational regulation of BACE1 involves upstream AUGs and stimulatory elements within the 5' untranslated region. *Nucleic Acids Research*. 35:2975-2985.
- Miller, P.F., and A.G. Hinnebusch. 1990. cis-Acting sequences involved in the translational control of GCN4 expression. *Biochimica et Biophysica Acta*. 1050:151-154.
- Milton J, C. 1960. Studies of the bioluminescence of *Renilla reniformis*: I. Requirements for luminescence in extracts and characteristics of the system. *Biochimica et Biophysica Acta*. 42:333-343.
- Minich, W.B., M.L. Balasta, D.J. Goss, and R.E. Rhoads. 1994. Chromatographic resolution of in vivo phosphorylated and nonphosphorylated eukaryotic translation initiation factor

- eIF-4E: increased cap affinity of the phosphorylated form. *Proceedings of the National Academy of Sciences of the USA*. 91:7668-7672.
- Mironov, A.S., I. Gusarov, R. Rafikov, L.E. Lopez, K. Shatalin, R.A. Kreneva, D.A. Perumov, and E. Nudler. 2002. Sensing Small Molecules by Nascent RNA: A Mechanism to Control Transcription in Bacteria. *Cell*. 111:747-756.
- Mitchell, S.A., K.A. Spriggs, M. Bushell, J.R. Evans, M. Stoneley, J.P. Le Quesne, R.V. Spriggs, and A.E. Willis. 2005. Identification of a motif that mediates polypyrimidine tract-binding protein-dependent internal ribosome entry. *Genes & Development*. 19:1556-1571.
- Modrek, B., and C. Lee. 2002. A genomic view of alternative splicing. *Nature Genetics*. 30:13-19.
- Morris, D.R., and A.P. Geballe. 2000. Upstream Open Reading Frames as Regulators of mRNA Translation. *Molecular and Cellular Biology*. 20:8635-8642.
- Muir, J.L. 1997. Acetylcholine, Aging, and Alzheimer's Disease. *Pharmacology Biochemistry and Behavior*. 56:687-696.
- Munger, K., M. Scheffner, J.M. Huibregtse, and P.M. Howley. 1992. Interactions of HPV E6 and E7 oncoproteins with tumour suppressor gene products. *Cancer Surveys*. 12:197-217.
- Munoz, N., F.X. Bosch, S. de Sanjose, L. Tafur, I. Izarzugaza, M. Gili, P. Viladiu, C. Navarro, C. Martos, N. Ascunce, L.C. Gonzalez, J.M. Kaldor, E. Guerrero, A. Lorincz, M. Santamaria, P.A. De Ruiz, N. Aristizabal, and K. Shah. 1992. The causal link between human papillomavirus and invasive cervical cancer: A population-based case-control study in colombia and spain. *International Journal of Cancer*. 52:743-749.
- Munro, S., S.M. Carr, and N.B. La Thangue. 2012. Diversity within the pRb pathway: is there a code of conduct. *Oncogene*.
- Munroe, D., and A. Jacobson. 1990. mRNA poly(A) tail, a 3' enhancer of translational initiation. *Molecular and Cellular Biology*. 10:3441-3455.
- Myasnikov, A.G., A. Simonetti, S. Marzi, and B.P. Klaholz. 2009. Structure–function insights into prokaryotic and eukaryotic translation initiation. *Current Opinion in Structural Biology*. 19:300-309.
- Nakazawa, K., Y. Dobashi, S. Suzuki, H. Fujii, Y. Takeda, and A. Ooi. 2005. Amplification and overexpression of c-erbB-2, epidermal growth factor receptor, and c-met in biliary tract cancers. *The Journal of Pathology*. 206:356-365.
- Nicholson, R.I., J.M.W. Gee, and M.E. Harper. 2001. EGFR and cancer prognosis. *European Journal of Cancer*. 37:9-15.
- Nielsen, K.H., M.A. Behrens, Y. He, C.L.P. Oliveira, L. Sottrup Jensen, S.V. Hoffmann, J.S. Pedersen, and G.R. Andersen. 2011. Synergistic activation of eIF4A by eIF4B and eIF4G. *Nucleic Acids Research*. 39:2678-2689.
- Nielsen, P.J., and H. Trachsel. 1988. The mouse protein synthesis initiation factor 4A gene family includes two related functional genes which are differentially expressed. *EMBO Journal*. 7:2097-2105.
- Nikolov, D.B., and S.K. Burley. 1997. RNA polymerase II transcription initiation: A structural view. *Proceedings of the National Academy of Sciences*. 94:15-22.
- Nikolova, E.N., E. Kim, A.A. Wise, P.J. O'Brien, I. Andricioaei, and H.M. Al-Hashimi. 2011. Transient Hoogsteen base pairs in canonical duplex DNA. *Nature*. 470:498-502.
- Nishi, H., K.H. Nishi, and A.C. Johnson. 2002. Early Growth Response-1 Gene Mediates Up-Regulation of Epidermal Growth Factor Receptor Expression during Hypoxia. *Cancer Research*. 62:827-834.
- Noble, C.G., and H. Song. 2007. MLN51 Stimulates the RNA-Helicase Activity of eIF4AIII. *PLoS ONE*. 2:e303.
- Noller, H.F. 2004. The driving force for molecular evolution of translation. *RNA*. 10:1833-1837.
- Novac, O., A.S. Guenier, and J. Pelletier. 2004. Inhibitors of protein synthesis identified by a high throughput multiplexed translation screen. *Nucleic Acids Research*. 32:902-915.
- Nunan, J., and D.H. Small. 2000. Regulation of APP cleavage by  $\alpha$ -,  $\beta$ - and  $\gamma$ -secretases. *FEBS Letters*. 483:6-10.
- O'Reilly, K.E., M. Warycha, M.A. Davies, V. Rodrik, X.K. Zhou, H. Yee, D. Polsky, A.C. Pavlick, N. Rosen, N. Bhardwaj, G. Mills, and I. Osman. 2009. Phosphorylated 4E-

- BP1 Is Associated with Poor Survival in Melanoma. *Clinical Cancer Research*. 15:2872-2878.
- Oda, K., Y. Matsuoka, A. Funahashi, and H. Kitano. 2005. A comprehensive pathway map of epidermal growth factor receptor signaling. *Molecular Systems Biology*. 1.
- Ohshima, H., and H. Bartsch. 1994. Chronic infections and inflammatory processes as cancer risk factors: possible role of nitric oxide in carcinogenesis. *Mutation Research*. 305:253-264.
- Onishi, Y., S. Hashimoto, and H. Kizaki. 1998. Cloning of the TIS gene suppressed by topoisomerase inhibitors. *Gene*. 215:453-459.
- Ooi, A., T. Takehana, X. Li, S. Suzuki, K. Kunitomo, H. Iino, H. Fujii, Y. Takeda, and Y. Dobashi. 2004. Protein overexpression and gene amplification of HER-2 and EGFR in colorectal cancers: an immunohistochemical and fluorescent in situ hybridization study. *Modern Pathology*. 17:895-904.
- Otto, G.A., and J.D. Puglisi. 2004. The Pathway of HCV IRES-Mediated Translation Initiation. *Cell*. 119:369-380.
- Pacheco, A., and E. Martinez-Salas. 2010. Insights into the Biology of IRES Elements through Riboproteomic Approaches. *Journal of Biomedicine and Biotechnology*. 2010.
- Pahl, J.H.W., S.E.N. Ruslan, E.P. Buddingh, S.J. Santos, K. Szuhai, M. Serra, H. Gelderblom, P.C.W. Hogendoorn, R.M. Egeler, M.W. Schilham, and A.C. Lankester. 2012. Anti-EGFR Antibody Cetuximab Enhances the Cytolytic Activity of Natural Killer Cells toward Osteosarcoma. *Clinical Cancer Research*. 18:432-441.
- Palacios, I.M., D. Gatfield, D. St Johnston, and E. Izaurralde. 2004. An eIF4AIII-containing complex required for mRNA localization and nonsense-mediated mRNA decay. *Nature*. 427:753-757.
- Palmer, A.M., and M.A. Burns. 1994. Selective increase in lipid peroxidation in the inferior temporal cortex in Alzheimer's disease. *Brain Research*. 645:338-342.
- Pappolla, M.A., R.A. Omar, K.S. Kim, and N.K. Robakis. 1992. Immunohistochemical evidence of oxidative stress in Alzheimer's disease. *The American Journal of Pathology*. 3:621-628.
- Passmore, L.A., T.M. Schmeing, D. Maag, D.J. Applefield, M.G. Acker, M.A. Algire, J.R. Lorsch, and V. Ramakrishnan. 2007. The Eukaryotic Translation Initiation Factors eIF1 and eIF1A Induce an Open Conformation of the 40S Ribosome. *Molecular Cell*. 26:41-50.
- Patton, J.G., S.A. Mayer, P. Tempst, and B. Nadal-Ginard. 1991. Characterization and molecular cloning of polypyrimidine tract-binding protein: a component of a complex necessary for pre-mRNA splicing. *Genes & Development*. 5:1237-1251.
- Paul, M.S., and B.L. Bass. 1998. Inosine exists in mRNA at tissue-specific levels and is most abundant in brain mRNA. *EMBO Journal*. 17:1120-1127.
- Pause, A., G.J. Belsham, A.C. Gingras, O. Donze, T.A. Lin, J.C. Lawrence, and N. Sonenberg. 1994a. Insulin-dependent stimulation of protein synthesis by phosphorylation of a regulator of 5'-cap function. *Nature*. 371:762-767.
- Pause, A., N. Methot, and N. Sonenberg. 1993. The HRIGRXXR region of the DEAD box RNA helicase eukaryotic translation initiation factor 4A is required for RNA binding and ATP hydrolysis. *Molecular and Cellular Biology*. 13:6789-6798.
- Pause, A., N. Methot, Y. Svitkin, W.C. Merrick, and N. Sonenberg. 1994b. Dominant negative mutants of mammalian translation initiation factor eIF-4A define a critical role for eIF-4F in cap-dependent and cap-independent initiation of translation. *EMBO Journal*. 13:1205-1215.
- Pelletier, J., and N. Sonenberg. 1988. Internal initiation of translation of eukaryotic mRNA directed by a sequence derived from poliovirus RNA. *Nature*. 334:320-325.
- Perry, E.K., B.E. Tomlinson, G. Blessed, K. Bergmann, P.H. Gibson, and R.H. Perry. 1978. Correlation of cholinergic abnormalities with senile plaques and mental test scores in senile dementia. *British Medical Journal*. 2:1457-1459.
- Perry, R.P., and D.E. Kelley. 1974. Existence of methylated messenger RNA in mouse L cells. *Cell*. 1:37-42.
- Perz, J.F., G.L. Armstrong, L.A. Farrington, Y.J.F. Hutin, and B.P. Bell. 2006. The contributions of hepatitis B virus and hepatitis C virus infections to cirrhosis and primary liver cancer worldwide. *Journal of Hepatology*. 45:529-538.

- Pesole, G., G. Grillo, A. Larizza, and S. Liuni. 2000. The untranslated regions of eukaryotic mRNAs: structure, function, evolution and bioinformatic tools for their analysis. *Brief Bioinform.* 1:236-249.
- Pestka, S. 1974. Antibiotics as Probes of Ribosome Structure: Binding of Chloramphenicol and Erythromycin to Polyribosomes; Effect of Other Antibiotics. *Antimicrobial Agents and Chemotherapy.* 5:255-267.
- Pestova, T.V., C.U. Hellen, and I.N. Shatsky. 1996a. Canonical eukaryotic initiation factors determine initiation of translation by internal ribosomal entry. *Molecular and Cellular Biology.* 16:6859-6869.
- Pestova, T.V., V.G. Kolupaeva, I.B. Lomakin, E.V. Pilipenko, I.N. Shatsky, V.I. Agol, and C.U.T. Hellen. 2001. Molecular mechanisms of translation initiation in eukaryotes. *Proceedings of the National Academy of Sciences.* 98:7029-7036.
- Pestova, T.V., I.B. Lomakin, J.H. Lee, S.K. Choi, T.E. Dever, and C.U.T. Hellen. 2000. The joining of ribosomal subunits in eukaryotes requires eIF5B. *Nature.* 403:332-335.
- Pestova, T.V., I.N. Shatsky, and C.U. Hellen. 1996b. Functional dissection of eukaryotic initiation factor 4F: the 4A subunit and the central domain of the 4G subunit are sufficient to mediate internal entry of 43S preinitiation complexes. *Molecular and Cellular Biology.* 16:6870-6878.
- Pettersen, E.O., N.O. Juul, and Ø.W. Rønning. 1986. Regulation of Protein Metabolism of Human Cells during and after Acute Hypoxia. *Cancer Research.* 46:4346-4351.
- Pettersson, F., C. Yau, M.C. Dobocan, B. Culjkovic-Kraljacic, H. Retrouvay, R. Puckett, L.M. Flores, I.E. Krop, C. Rousseau, E. Cocolakis, K.L.B. Borden, C.C. Benz, and W.H. Miller. 2011. Ribavirin Treatment Effects on Breast Cancers Overexpressing eIF4E, a Biomarker with Prognostic Specificity for Luminal B-Type Breast Cancer. *Clinical Cancer Research.* 17:2874-2884.
- Piccinelli, P., and T. Samuelsson. 2007. Evolution of the iron-responsive element. *RNA.* 13:952-966.
- Pickering, B.M., and A.E. Willis. 2005. The implications of structured 5' untranslated regions on translation and disease. *Seminars in Cell & Developmental Biology.* 16:39-47.
- Pischon, T., U. Nöthlings, and H. Boeing. 2008. Obesity and cancer. *Proceedings of the Nutrition Society.* 67:128-145.
- Plate, K.H., G. Breier, H.A. Weich, and W. Risau. 1992. Vascular endothelial growth factor is a potential tumour angiogenesis factor in human gliomas in vivo. *Nature.* 359:845-848.
- Plouët, J., J. Schilling, and D. Gospodarowicz. 1989. Isolation and characterization of a newly identified endothelial cell mitogen produced by AtT-20 cells. *EMBO Journal.* 8:3801-3806.
- Powell, W.S. 2003. 15-deoxy- $\Delta$ 12,14-PGJ2: endogenous PPAR $\gamma$  ligand or minor eicosanoid degradation product? *The Journal of Clinical Investigation.* 112:828-830.
- Prall, F. 2007. Tumour budding in colorectal carcinoma. *Histopathology.* 50:151-162.
- Pratt, A.J., and I.J. MacRae. 2009. The RNA-induced Silencing Complex: A Versatile Gene-silencing Machine. *Journal of Biological Chemistry.* 284:17897-17901.
- Preece, P., D.J. Virley, M. Costandi, R. Coombes, S.J. Moss, A.W. Mudge, E. Jazin, and N.J. Cairns. 2003. Beta-secretase (BACE) and GSK-3 mRNA levels in Alzheimer's disease. *Brain research. Molecular brain research.* 116:155-158.
- Prevot, D., J.L. Darlix, and T. Ohlmann. 2003. Conducting the initiation of protein synthesis: the role of eIF4G. *Biology of the Cell.* 95:141-156.
- Priller, C., T. Bauer, G. Mitteregger, B. Krebs, H.A. Kretzschmar, and J. Herms. 2006. Synapse Formation and Function Is Modulated by the Amyloid Precursor Protein *The Journal of Neuroscience.* 26:7212-7221.
- Proud, C.G. 2011. Vanishing white matter: the next 10 years. *Future Neurology.* 7:81-92.
- Pyronnet, S., H. Imataka, A.-C. Gingras, R. Fukunaga, T. Hunter, and N. Sonenberg. 1999. Human eukaryotic translation initiation factor 4G (eIF4G) recruits Mnk1 to phosphorylate eIF4E. *EMBO Journal.* 18:270-279.
- Pyronnet, S., L. Pradayrol, and N. Sonenberg. 2000. A cell cycle-dependent internal ribosome entry site. *Molecular Cell.* 5:607-616.
- Ramakrishnan, V. 2002. Ribosome Structure and the Mechanism of Translation. *Cell.* 108:557-572.

- Rasheedi, S., S. Ghosh, M. Suragani, N. Tuteja, S.K. Sopory, S.E. Hasnain, and N.Z. Ehtesham. 2007. Pisum sativum contains a factor with strong homology to eIF5B. *Gene*. 399:144-151.
- Raught, B., and A.-C. Gingras. 1999. eIF4E activity is regulated at multiple levels. *The International Journal of Biochemistry & Cell Biology*. 31:43-57.
- Ray, B.K., T.G. Lawson, J.C. Kramer, M.H. Cladaras, J.A. Grifo, R.D. Abramson, W.C. Merrick, and R.E. Thach. 1985. ATP-dependent unwinding of messenger RNA structure by eukaryotic initiation factors. *Journal of Biological Chemistry*. 260:7651-7658.
- Reddy, R., T.S. Ro-Choi, D. Henning, and H. Busch. 1974. Primary Sequence of U-1 Nuclear Ribonucleic Acid of Novikoff Hepatoma Ascites Cells. *Journal of Biological Chemistry*. 249:6486-6494.
- Reiche, E.M.V., S.O.V. Nunes, and H.K. Morimoto. 2004. Stress, depression, the immune system, and cancer. *The Lancet Oncology*. 5:617-625.
- Rezvanfar, M.A., R.A. Sadrkhanlou, A. Ahmadi, H. Shojaei-Sadee, A. Mohammadirad, A. Salehnia, and M. Abdollahi. 2008. Protection of cyclophosphamide-induced toxicity in reproductive tract histology, sperm characteristics, and DNA damage by an herbal source; evidence for role of free-radical toxic stress. *Human & Experimental Toxicology*. 27:901-910.
- Rhoads, R.E. 2009. eIF4E: New Family Members, New Binding Partners, New Roles. *Journal of Biological Chemistry*. 284:16711-16715.
- Richter-Cook, N.J., T.E. Dever, J.O. Hensold, and W.C. Merrick. 1998. Purification and Characterization of a New Eukaryotic Protein Translation Factor eukaryotic initiation factor 4H. *Journal of Biological Chemistry*. 273:7579-7587.
- Richter, J.D., and N. Sonenberg. 2005. Regulation of cap-dependent translation by eIF4E inhibitory proteins. *Nature*. 433:477-480.
- Richter, N.J., G.W. Rogers, J.O. Hensold, and W.C. Merrick. 1999. Further biochemical and kinetic characterization of human eukaryotic initiation factor 4H. *Journal of Biological Chemistry*. 274:35415-35424.
- Riis, B., S.I.S. Rattan, B.F.C. Clark, and W.C. Merrick. 1990. Eukaryotic protein elongation factors. *Trends in Biochemical Sciences*. 15:420-424.
- Robin, R. 1996. Initial splice-site recognition and pairing during pre-mRNA splicing. *Current Opinion in Genetics and Development*. 6:215-220.
- Rocak, S., and P. Linder. 2004. DEAD-box proteins: the driving forces behind RNA metabolism. *Nature Reviews Molecular Cell Biology*. 5:232-241.
- Rocha, S., K. Campbell, K. Roche, and N. Perkins. 2003. The p53-inhibitor Pifithrin-alpha inhibits Firefly Luciferase activity in vivo and in vitro. *Biomedcentral Molecular Biology*. 4:9.
- Rogers, G.W., A.A. Komar, and W.C. Merrick. 2002a. eIF4A: The godfather of the DEAD box helicases. *In Progress in Nucleic Acid Research and Molecular Biology*. Vol. Volume 72. Academic Press. 307-331.
- Rogers, G.W., W.F. Lima, and W.C. Merrick. 2001a. Further characterization of the helicase activity of eIF4A. Substrate specificity. *Journal of Biological Chemistry*. 276:12598-12608.
- Rogers, G.W., N.J. Richter, W.F. Lima, and W.C. Merrick. 2001b. Modulation of the helicase activity of eIF4A by eIF4B, eIF4H, and eIF4F. *Journal of Biological Chemistry*. 276:30914-30922.
- Rogers, G.W., N.J. Richter, and W.C. Merrick. 1999a. Biochemical and kinetic characterization of the RNA helicase activity of eukaryotic initiation factor 4A. *Journal of Biological Chemistry*. 274:12236-12244.
- Rogers, J.T., L.M. Leiter, J. McPhee, C.M. Cahill, S.S. Zhan, H. Potter, and L.N. Nilsson. 1999b. Translation of the Alzheimer amyloid precursor protein mRNA is up-regulated by interleukin-1 through 5'-untranslated region sequences. *Journal of Biological Chemistry*. 274:6421-6431.
- Rogers, J.T., J.D. Randall, C.M. Cahill, P.S. Eder, X. Huang, H. Gunshin, L. Leiter, J. McPhee, S.S. Sarang, T. Utsuki, N.H. Greig, D.K. Lahiri, R.E. Tanzi, A.I. Bush, T. Giordano, and S.R. Gullans. 2002b. An iron-responsive element type II in the 5'-

- untranslated region of the Alzheimer's amyloid precursor protein transcript. *Journal of Biological Chemistry*. 277:45518-45528.
- Romo, D., R.M. Rzasa, H.A. Shea, K. Park, J.M. Langenhan, L. Sun, A. Akhiezer, and J.O. Liu. 1998. Total Synthesis and Immunosuppressive Activity of Pateamine A and Related Compounds: Implementation of Lactam-Based Macrocyclization. *Journal of the American Chemical Society*. 120:12237-12254.
- Rosenbaum-Dekel, Y., A. Fuchs, E. Yakirevich, A. Azriel, S. Mazareb, M.B. Resnick, and B.-Z. Levi. 2005. Nuclear localization of long-VEGF is associated with hypoxia and tumor angiogenesis. *Biochemical and Biophysical Research Communications*. 332:271-278.
- Rosenthal, S., and S. Kaufman. 1974. Vincristine Neurotoxicity. *Annals of Internal Medicine*. 80:733-737.
- Rouault, T.A. 2012. Regulation of Iron Metabolism in Mammalian Cells Iron Physiology and Pathophysiology in Humans. In *Regulation of Iron Metabolism in Mammalian Cells Iron Physiology and Pathophysiology in Humans*. G.J.a.M. Anderson, Gordon D., editor. Humana Press. 51-62.
- Roy, G., G. De Crescenzo, K. Khaleghpour, A. Kahvejian, M. O'Connor-McCourt, and N. Sonenberg. 2002. Paip1 Interacts with Poly(A) Binding Protein through Two Independent Binding Motifs. *Molecular and Cellular Biology*. 22:3769-3782.
- Roy S, H. 2004. Review of epidermal growth factor receptor biology. *International Journal of Radiation Oncology\*Biophysics\*Physic*. 59:S21-S26.
- Roza, L., F.R. De Grujil, J.B.A. Bergen Henegouwen, K. Guikers, H. Van Weelden, G.P. Van Der Schans, and R.A. Baan. 1991. Detection of Photorepair of UV-Induced Thymine Dimers in Human Epidermis by Immunofluorescence Microscopy. *Journal of Investigative Dermatology*. 96:903-907.
- Rozen, F., I. Edery, K. Meerovitch, T.E. Dever, W.C. Merrick, and N. Sonenberg. 1990. Bidirectional RNA helicase activity of eucaryotic translation initiation factors 4A and 4F. *Molecular and Cellular Biology*. 10:1134-1144.
- Rozovsky, N., A.C. Butterworth, and M.J. Moore. 2008. Interactions between eIF4AI and its accessory factors eIF4B and eIF4H. *RNA*. 14:2136-2148.
- Russell, D., and S.H. Snyder. 1968. Amine synthesis in rapidly growing tissues: ornithine decarboxylase activity in regenerating rat liver, chick embryo, and various tumors. *Proceedings of the National Academy of Sciences*. 60:1420-1427.
- Russell, E.S. 1940. A comparison of benign and "malignant" tumors in *Drosophila melanogaster*. *Journal of Experimental Zoology*. 84:363-385.
- Sachs, A.B., M.W. Bond, and R.D. Kornberg. 1986. A single gene from yeast for both nuclear and cytoplasmic polyadenylate-binding proteins: domain structure and expression. *Cell*. 45:827-835.
- Sanerkin, N.G. 1962. Transdural spread of glioblastoma multiforme. *The Journal of Pathology and Bacteriology*. 84:228-233.
- Sarnow, P. 1989. Translation of glucose-regulated protein 78/ immunoglobulin heavy-chain binding protein mRNA is increased in poliovirus-infected cells at a time when cap-dependent translation of cellular mRNAs is inhibited. *Proceedings of the National Academy of Sciences of the USA*. 86:5795-5799.
- Sawyers, C. 2004. Targeted cancer therapy. *Nature*. 432:294-297.
- Schiavi, S.C., J.G. Belasco, and M.E. Greenberg. 1992. Regulation of proto-oncogene mRNA stability. *Biochimica et Biophysica Acta*. 1114:95-106.
- Schlegel, J., A. Merdes, G. Stumm, F.K. Albert, M. Forsting, N. Hynes, and M. Kiessling. 1994. Amplification of the epidermal-growth-factor-receptor gene correlates with different growth behaviour in human glioblastoma. *International Journal of Cancer*. 56:72-77.
- Schneider, A., R.H. Younis, and J.S. Gutkind. 2008. Hypoxia-Induced Energy Stress Inhibits the mTOR Pathway by Activating an AMPK/REDD1 Signaling Axis in Head and Neck Squamous Cell Carcinoma. *Neoplasia*. 10:1295-1302.
- Schrijvers, E.M.C., P.J. Koudstaal, A. Hofman, and M.M.B. Breteler. 2011. Plasma Clusterin and the Risk of Alzheimer Disease. *The Journal of the American Medical Association*. 305:1322-1326.

- Schwechheimer, K., S. Huang, and W.K. Cavenee. 1995. EGFR gene amplification - rearrangement in human glioblastomas. *International Journal of Cancer*. 62:145-148.
- Searfoss, A., T.E. Dever, and R. Wickner. 2001. Linking the 3' poly(A) tail to the subunit joining step of translation initiation: Relations of Pab1p, eukaryotic translation initiation factor 5b (Fun12p), and Ski2p-Slh1p. *Molecular and Cellular Biology*. 21:4900-4908.
- Sergeevich Spirin, A. 1999. Ribosomes. Springer, New York.
- Shahbazian, D., A. Parsyan, E. Petroulakis, J.W.B. Hershey, and N. Sonenberg. 2010. eIF4B controls survival and proliferation and is regulated by proto-oncogenic signaling pathways. *Cell Cycle*. 9:4106-4109.
- Shahbazian, D., P.P. Roux, V. Mieulet, M.S. Cohen, B. Raught, J. Taunton, J.W. Hershey, J. Blenis, M. Pende, and N. Sonenberg. 2006. The mTOR/PI3K and MAPK pathways converge on eIF4B to control its phosphorylation and activity. *EMBO Journal*. 25:2781-2791.
- Shen, T., K. Tai, R.H. Henchman, and J.A. McCammon. 2002. Molecular Dynamics of Acetylcholinesterase. *Accounts of Chemical Research*. 35:332-340.
- Sherrington, R., E.I. Rogaevev, Y. Liang, E.A. Rogaeveva, G. Levesque, M. Ikeda, H. Chi, C. Lin, G. Li, K. Holman, T. Tsuda, L. Mar, J.F. Foncin, A.C. Bruni, M.P. Montesi, S. Sorbi, I. Rainero, L. Pinessi, L. Nee, I. Chumakov, D. Pollen, A. Brookes, P. Sanseau, R.J. Polinsky, W. Wasco, H.A.R. Da Silva, J.L. Haines, M.A. Pericak-Vance, R.E. Tanzi, A.D. Roses, P.E. Fraser, J.M. Rommens, and P.H. George-Hyslop. 1995. Cloning of a gene bearing missense mutations in early-onset familial Alzheimer's disease. *Nature*. 375:754-760.
- Shibahara, K., M. Asano, Y. Ishida, T. Aoki, T. Koike, and T. Honjo. 1995. Isolation of a novel mouse gene MA-3 that is induced upon programmed cell death. *Gene*. 166:297-301.
- Shibuya, T., T.O. Tange, N. Sonenberg, and M.J. Moore. 2004. eIF4AIII binds spliced mRNA in the exon junction complex and is essential for nonsense-mediated decay. *Nature Structural & Molecular Biology*. 11:346-351.
- Shimohama, S. 2000. Apoptosis in Alzheimer's disease - an update. *Apoptosis*. 5:9-16.
- Shuda, M., N. Kondoh, K. Tanaka, A. Ryo, T. Wakatsuki, A. Hada, N. Goseki, T. Igari, K. Hatsuse, T. Aihara, S. Horiuchi, M. Shichita, N. Yamamoto, and M. Yamamoto. 2000. Enhanced expression of translation factor mRNAs in hepatocellular carcinoma. *Anticancer Research*. 20.
- Shweiki, D., A. Itin, D. Soffer, and E. Keshet. 1992. Vascular endothelial growth factor induced by hypoxia may mediate hypoxia-initiated angiogenesis. *Nature*. 359:843-845.
- Signori, E., C. Bagni, S. Papa, B. Primerano, M. Rinaldi, F. Amaldi, and V.M. Fazio. 2001. A somatic mutation in the 5'UTR of BRCA1 gene in sporadic breast cancer causes down-modulation of translation efficiency. *Oncogene*. 20:4596-4600.
- Silvera, D., S.C. Formenti, and R.J. Schneider. 2010. Translational control in cancer. *Nature Reviews Cancer*. 10:254-266.
- Singh, P., R. Marikkannu, N. Bitomsky, and K.H. Klempnauer. 2009. Disruption of the Pcd4 tumor suppressor gene in chicken DT40 cells reveals its role in the DNA-damage response. *Oncogene*. 28:3758-3764.
- Sinha, R.P., and D.P. Hader. 2002. UV-induced DNA damage and repair: a review. *Photochemical & Photobiological Sciences*. 1:225-236.
- Sinha, S., J.P. Anderson, R. Barbour, G.S. Basi, R. Caccavello, D. Davis, M. Doan, H.F. Dovey, N. Frigon, J. Hong, K. Jacobson-Croak, N. Jewett, P. Keim, J. Knops, I. Lieberburg, M. Power, H. Tan, G. Tatsuno, J. Tung, D. Schenk, P. Seubert, S.M. Suomensari, S. Wang, D. Walker, J. Zhao, L. McConlogue, and V. John. 1999. Purification and cloning of amyloid precursor protein beta-secretase from human brain. *Nature*. 402:537-540.
- Sisodia, S.S. 1992. Beta-amyloid precursor protein cleavage by a membrane-bound protease. *Proc Natl Acad Sci U S A*. 89:6075-6079.
- Small, S.A., and K. Duff. 2008. Linking Abeta and tau in late-onset Alzheimer's disease: a dual pathway hypothesis. *Neuron*. 60:534-542.

- Smith, C.W.J., E.B. Porro, J.G. Patton, and B. Nadal-Ginard. 1989. Scanning from an independently specified branch point defines the 3 prime splice site of mammalian introns. *Nature*. 342:243-247.
- Smith, M.A., K. Hirai, K. Hsiao, M.A. Pappolla, P.L.R. Harris, S.L. Siedlak, M. Tabaton, and G. Perry. 1998. Amyloid- $\beta$  Deposition in Alzheimer Transgenic Mice Is Associated with Oxidative Stress. *Journal of Neurochemistry*. 70:2212-2215.
- Sonenberg, N., and A.G. Hinnebusch. 2009. Regulation of translation initiation in eukaryotes: mechanisms and biological targets. *Cell*. 136:731-745.
- Sonenberg, N., E.C. Waldo, and M. Kivie. 1988. Cap-Binding Proteins of Eukaryotic Messenger RNA: Functions in Initiation and Control of Translation. *In Progress in Nucleic Acid Research and Molecular Biology*. Vol. Volume 35. Academic Press. 173-207.
- Šponer, J., J. Leszczyński, and P. Hobza. 1996. Nature of Nucleic Acid–Base Stacking: Nonempirical ab Initio and Empirical Potential Characterization of 10 Stacked Base Dimers. Comparison of Stacked and H-Bonded Base Pairs. *The Journal of Physical Chemistry*. 100:5590-5596.
- Spriggs, K.A., M. Bushell, S.A. Mitchell, and A.E. Willis. 2005. Internal ribosome entry segment-mediated translation during apoptosis: the role of IRES-trans-acting factors. *Cell Death & Differentiation*. 12:585-591.
- Spriggs, K.A., L.C. Cobbold, C.L. Jopling, R.E. Cooper, L.A. Wilson, M. Stoneley, M.J. Coldwell, D. Poncet, Y.C. Shen, S.J. Morley, M. Bushell, and A.E. Willis. 2009. Canonical initiation factor requirements of the Myc family of internal ribosome entry segments. *Molecular and Cellular Biology*. 29:1565-1574.
- Srai, S.K., and P. Sharp. 2012. Proteins of Iron Homeostasis Iron Physiology and Pathophysiology in Humans. G.J.a.M. Anderson, Gordon D., editor. Humana Press. 3-25.
- Stewart, E.A. 2001. Uterine fibroids. *The Lancet*. 357:293-298.
- Stoneley, M., F.E. Paulin, J.P. Le Quesne, S.A. Chappell, and A.E. Willis. 1998. C-Myc 5' untranslated region contains an internal ribosome entry segment. *Oncogene*. 16:423-428.
- Stoneley, M., and A.E. Willis. 2004. Cellular internal ribosome entry segments: structures, trans-acting factors and regulation of gene expression. *Oncogene*. 23:3200-3207.
- Storkebaum, E., D. Lambrechts, and P. Carmeliet. 2004. VEGF: once regarded as a specific angiogenic factor, now implicated in neuroprotection. *BioEssays*. 26:943-954.
- Straus, D.S., and C.K. Glass. 2001. Cyclopentenone prostaglandins: New insights on biological activities and cellular targets. *Medicinal Research Reviews*. 21:185-210.
- Straus, D.S., G. Pascual, M. Li, J.S. Welch, M. Ricote, C.-H. Hsiang, L.L. Sengchanthalangsy, G. Ghosh, and C.K. Glass. 2000. 15-Deoxy-12,14-prostaglandin J2 inhibits multiple steps in the NF- $\kappa$ B signaling pathway. *Proceedings of the National Academy of Sciences*. 97:4844-4849.
- Stürzenbaum, S.R., and P. Kille. 2001. Control genes in quantitative molecular biological techniques: the variability of invariance. *Comparative Biochemistry and Physiology Part B: Biochemistry and Molecular Biology*. 130:281-289.
- Su, Y., J. Ryder, and B. Ni. 2003. Inhibition of A $\beta$  production and APP maturation by a specific PKA inhibitor. *FEBS Letters*. 546:407-410.
- Suchowersky, O., and M. Hayden. 1984. Down's syndrome and Alzheimer's disease. *Annals of Neurology*. 16:263-263.
- Sugiharas, H., V. Andrisani, and P.M. Salvaterra. 1990. Drosophila Choline Acetyltransferase Uses a Non-AUG Initiation Codon and Full Length RNA Is Inefficiently Translated. *Journal of Biological Chemistry*. 265:21714-21719.
- Sugimoto, N., R. Kierzek, S.M. Freier, and D.H. Turner. 1986. Energetics of internal GU mismatches in ribooligonucleotide helices. *Biochemistry*. 25:5755-5759.
- Sun, X., G. He, H. Qing, W. Zhou, F. Dobie, F. Cai, M. Staufenbiel, L.E. Huang, and W. Song. 2006. Hypoxia facilitates Alzheimer's disease pathogenesis by up-regulating BACE1 gene expression. *Proceedings of the National Academy of Sciences*. 103:18727-18732.
- Svitkin, Y.V., A. Pause, A. Haghighat, S. Pyronnet, G. Witherell, G.J. Belsham, and N. Sonenberg. 2001. The requirement for eukaryotic initiation factor 4A (eIF4A) in

- translation is in direct proportion to the degree of mRNA 5' secondary structure. *RNA*. 7:382-394.
- Swinson, D.E.B., and K.J. O'Byrne. 2006. Interactions Between Hypoxia and Epidermal Growth Factor Receptor in Non-Small-Cell Lung Cancer. *Clinical Lung Cancer*. 7:250-256.
- Tabor, C.W., and H. Tabor. 1984. Polyamines. *Annual Review of Biochemistry*. 53:749-790.
- Takimoto, Y., and A. Kuramoto. 1994. Gene regulation by the 5'-untranslated region of the platelet-derived growth factor A-chain. *Biochimica et Biophysica Acta*. 1222:511-514.
- Takyar, S., R.P. Hickerson, and H.F. Noller. 2005. mRNA Helicase Activity of the Ribosome. *Cell*. 120:49-58.
- Tanner, N.K., O. Cordin, J. Banroques, M. Doere, and P. Linder. 2003. The Q motif: a newly identified motif in DEAD box helicases may regulate ATP binding and hydrolysis. *Molecular Cell*. 11:127-138.
- Tarun, S.Z., and A.B. Sachs. 1996. Association of the yeast poly(A) tail binding protein with translation initiation factor eIF4G. *EMBO Journal*. 15.
- Teitell, M.A., and P.P. Pandolfi. 2009. Molecular Genetics of Acute Lymphoblastic Leukemia. *Annual Review of Pathology: Mechanisms of Disease*. 4:175-198.
- Testa, U., L. Kühn, M. Petrini, M.T. Quaranta, E. Pelosi, and C. Peschle. 1991. Differential regulation of iron regulatory element-binding protein(s) in cell extracts of activated lymphocytes versus monocytes-macrophages. *Journal of Biological Chemistry*. 266:13925-13930.
- Testa, U., E. Pelosi, and C. Peschle. 1993. The transferrin receptor. *Critical Reviews In Oncogenesis*. 4:241-276.
- Thach, R.E. 1991. Translationally regulated genes in higher eukaryotes. Karger, Basel; München; Paris; London; New York; New Delhi; Bangkok; Singapore; Tokyo; Sydney.
- Thambisetty, M., A. Simmons, L. Velayudhan, A. Hye, J. Campbell, Y. Zhang, L.-O. Wahlund, E. Westman, A. Kinsey, A. Guntert, P. Proitsi, J. Powell, M. Causevic, R. Killick, K. Lunnon, S. Lynham, M. Broadstock, F. Choudhry, D.R. Howlett, R.J. Williams, S.I. Sharp, C. Mitchelmore, C. Tunnard, R. Leung, C. Foy, D. O'Brien, G. Breen, S.J. Furney, M. Ward, I. Kloszewska, P. Mecocci, H. Soininen, M. Tsolaki, B. Vellas, A. Hodges, D.G.M. Murphy, S. Parkins, J.C. Richardson, S.M. Resnick, L. Ferrucci, D.F. Wong, Y. Zhou, S. Muehlboeck, A. Evans, P.T. Francis, C. Spenger, and S. Lovestone. 2010. Association of Plasma Clusterin Concentration With Severity, Pathology, and Progression in Alzheimer Disease. *Archives of General Psychiatry*. 67:739-748.
- Theil, E.C. 1990. Regulation of ferritin and transferrin receptor mRNAs. *Journal of Biological Chemistry*. 265:4771-4774.
- Thoma, C., G. Bergamini, B. Galy, P. Hundsdoerfer, and M.W. Hentze. 2004. Enhancement of IRES-mediated translation of the c-myc and BiP mRNAs by the poly(A) tail is independent of intact eIF4G and PABP. *Molecular Cell*. 15:925-935.
- Thomas, M., P. Massimi, and L. Banks. 1996. HPV-18 E6 inhibits p53 DNA binding activity regardless of the oligomeric state of p53 or the exact p53 recognition sequence. *Oncogene*. 13:471-480.
- Tikole, S., and R. Sankararamkrishnan. 2006. A survey of mRNA sequences with a non-AUG start codon in RefSeq database. *Journal of Biomolecular Structure and Dynamics*. 34:33-42.
- Tolnay, and Probst. 1999. REVIEW: tau protein pathology in Alzheimer's disease and related disorders. *Neuropathology and Applied Neurobiology*. 25:171-187.
- Torti, F.M., and S.V. Torti. 2002. Regulation of ferritin genes and protein. *Blood*. 99:3505-3516.
- Tsuchihashi, Z., S. Khambata-Ford, N. Hanna, and P.A. Jänne. 2005. Responsiveness to Cetuximab without Mutations in EGFR. *New England Journal of Medicine*. 353:208-209.
- Tsukiyama-Kohara, K., N. Iizuka, M. Kohara, and A. Nomoto. 1992. Internal ribosome entry site within hepatitis C virus RNA. *Journal of Virology*. 66:1476-1483.

- Tucker, B.J., and R.R. Breaker. 2005. Riboswitches as versatile gene control elements. *Current Opinion in Structural Biology*. 15:342-348.
- Tucker, M., and R. Parker. 2003. Mechanisms and control of mRNA decapping in *Saccharomyces cerevisiae*. *Annual Review of Biochemistry*. 69:571-595.
- Turner, P.R., K. O'Connor, W.P. Tate, and W.C. Abraham. 2003. Roles of amyloid precursor protein and its fragments in regulating neural activity, plasticity and memory. *Progress in Neurobiology*. 70:1-32.
- Ubeda, M., and J.F. Habener. 2000. CHOP gene expression in response to endoplasmic-reticular stress requires NFY interaction with different domains of a conserved DNA-binding element. *Nucleic Acids Research*. 28:4987-4997.
- Unbehaun, A., S.I. Borukhov, C.U. Hellen, and T.V. Pestova. 2004. Release of initiation factors from 48S complexes during ribosomal subunit joining and the link between establishment of codon-anticodon base-pairing and hydrolysis of eIF2-bound GTP. *Genes and Development*. 18:3078-3093.
- Valencia-Sanchez, M.A., J. Liu, G.J. Hannon, and R. Parker. 2006. Control of translation and mRNA degradation by miRNAs and siRNAs. *Genes & Development*. 20:515-524.
- van Oosterom, A.T., I. Judson, J. Verweij, S. Stroobants, E.D. di Paola, S. Dimitrijevic, M. Martens, A. Webb, R. Sciot, M. Van Glabbeke, S. Silberman, and O.S. Nielsen. 2001. Safety and efficacy of imatinib (STI571) in metastatic gastrointestinal stromal tumours: a phase I study. *The Lancet*. 358:1421-1423.
- Vikhreva, P., M. Shepelev, E. Korobko, and I. Korobko. 2010. Pcd4 tumor suppressor: Properties, functions, and possible applications in oncology. *Molecular Genetics, Microbiology and Virology*. 25:47-55.
- Vincent, L., and P. Soille. 1991. Watersheds in Digital Spaces: An Efficient Algorithm Based on Immersion Simulations. *IEEE Transactions on Pattern Analysis and Machine Intelligence*. 13:583-598.
- Wachter, A. 2010. Riboswitch-mediated control of gene expression in eukaryotes. *RNA Biology*. 7:67-76.
- Wakiyama, M., H. Imataka, and N. Sonenberg. 2000. Interaction of eIF4G with poly(A)-binding protein stimulates translation and is critical for *Xenopus* oocyte maturation. *Current Biology*. 10:1147-1150.
- Walter, P., and G. Blobel. 1983. Subcellular distribution of signal recognition particle and 7SL-RNA determined with polypeptide-specific antibodies and complementary DNA probe. *The Journal of Cell Biology*. 97:1693-1699.
- Walther, T.N., T.H. Wittop Koning, and D. Schümperli. 1998. A 5'-3' exonuclease activity involved in forming the 3' products of histone pre-mRNA processing in vitro. *RNA*. 4:1034-1046.
- Wang, L., M.S. Lewis, and A.W. Johnson. 2005. Domain interactions within the Ski2/3/8 complex and between the Ski complex and Ski7p. *RNA*. 11:1291-1302.
- Wang, X., P. Yue, C.-B. Chan, K. Ye, T. Ueda, R. Watanabe-Fukunaga, R. Fukunaga, H. Fu, F.R. Khuri, and S.-Y. Sun. 2007. Inhibition of Mammalian Target of Rapamycin Induces Phosphatidylinositol 3-Kinase-Dependent and Mnk-Mediated Eukaryotic Translation Initiation Factor 4E Phosphorylation. *Molecular and Cellular Biology*. 27:7405-7413.
- Warburton, C., W.H. Dragowska, K. Gelmon, S. Chia, H. Yan, D. Masin, T. Denyssevych, A.E. Wallis, and M.B. Bally. 2004. Treatment of HER-2/neu Overexpressing Breast Cancer Xenograft Models with Trastuzumab (Herceptin) and Gefitinib (ZD1839): Drug Combination Effects on Tumor Growth, HER-2/neu and Epidermal Growth Factor Receptor Expression, and Viable Hypoxic Cell Fraction. *Clinical Cancer Research*. 10:2512-2524.
- Warmuth, M., M. Bergmann, A. Priey, K. Hausmann, B. Emmerich, and M. Hallek. 1997. The Src Family Kinase Hck Interacts with Bcr-Abl by a Kinase-independent Mechanism and Phosphorylates the Grb2-binding Site of Bcr. *Journal of Biological Chemistry*. 272:33260-33270.
- Warner, J.R., P.M. Knopf, and A. Rich. 1963. A multiple ribosomal structure in protein synthesis. *Proceedings of the National Academy of Sciences of the USA*. 49:122-129.
- Watson, J.D., and F.H.C. Crick. 1953. Molecular Structure of Nucleic Acids: A Structure for Deoxyribose Nucleic Acid. *Nature*. 171:737-738.

- Webb, B.L., and C.G. Proud. 1997. Eukaryotic initiation factor 2B (eIF2B). *International Journal of Biochemical Cell Biology*. 10:1127-1131.
- Wek, R.C., K.A. Staschke, and J. Narasimhan. 2004. Nutrient-induced responses in eukaryotic cells. Springer-Verlag, Berlin.
- Wells, S.E., P.E. Hillner, R.D. Vale, and A.B. Sachs. 1998. Circularization of mRNA by Eukaryotic Translation Initiation Factors. *Molecular Cell*. 2:135-140.
- Welsh, M., N. Scherberg, R. Gilmore, and D.F. Steiner. 1986. Translational control of insulin biosynthesis. Evidence for regulation of elongation, initiation and signal-recognition-particle-mediated translational arrest by glucose. *Biochemical Journal*. 235:459-467.
- Westhof, E., and P. Auffinger. 2006. RNA Tertiary Structure. In *Encyclopedia of Analytical Chemistry*. John Wiley & Sons, Ltd.
- White, R.E. 2000. High-Throughput Screening in Drug Metabolism and Pharmacokinetic Support of Drug Discovery. *Annual Review of Pharmacology and Toxicology*. 40:133-157.
- Wickens, M. 1990. How the messenger got its tail: Addition of poly(A) in the nucleus. *Trends in Biochemical Science*. 15:277-281.
- Wiedmann, M., T.V. Kurzchalia, E. Hartmann, and T.A. Rapoport. 1987. A signal sequence receptor in the endoplasmic reticulum membrane. *Nature*. 328:830-833.
- Wikstrand, C.J., C.J. Reist, G.E. Archer, M.R. Zalutsky, and D.D. Bigner. 1998. The class III variant of the epidermal growth factor receptor (EGFRvIII): characterization and utilization as an immunotherapeutic target. *Journal of Neurovirology*. 4:148-158.
- Wilkinson, M.F., and A.-B. Shyu. 2002. RNA surveillance by nuclear scanning? *Nature Cell Biology*. 4:E144-E147.
- Williams-Hill, D.M., R.F. Duncan, P.J. Nielsen, and S.M. Tahara. 1997. Differential expression of the murine eukaryotic translation initiation factor isogenes eIF4A(I) and eIF4A(II) is dependent upon cellular growth status. *Archives of Biochemistry and Biophysics*. 338:111-120.
- Williams, D.D., N.T. Price, A.J. Loughlin, and C.G. Proud. 2001. Characterization of the mammalian initiation factor eIF2B complex as a GDP dissociation stimulator protein. *Journal of Biological Chemistry* 276:24697-24703.
- Williams, K.P., and J.E. Scott. 2009. Enzyme Assay Design for High-Throughput Screening High Throughput Screening. Vol. 565. W.P. Janzen and P. Bernasconi, editors. Humana Press. 107-126.
- Willis, A.E. 1999. Translational control of growth factor and proto-oncogene expression. *The International Journal of Biochemistry & Cell Biology*. 31:73-86.
- Wilusz, C.J., M. Wormington, and S.W. Peltz. 2001. The cap-to-tail guide to mRNA turnover. *Nature Reviews Molecular Cell Biology*. 2:237-246.
- Woese, C.R. 2002. On the evolution of cells. *Proceedings of the National Academy of Sciences of the USA*. 99:8742-8747.
- Wollman, E.E., L. d'Auriol, L. Rimsky, A. Shaw, J.P. Jacquot, P. Wingfield, P. Graber, F. Dessarps, P. Robin, and F. Galibert. 1988. Cloning and expression of a cDNA for human thioredoxin. *Journal of Biological Chemistry*. 263:15506-15512.
- Woodcock, J., D. Moazed, M. Cannon, J. Davies, and H.F. Noller. 1991. Interaction of antibiotics with A- and P-site-specific bases in 16S ribosomal RNA. *EMBO Journal*. 10:3099-3103.
- Xia, X., and M. Holcik. 2009. Strong Eukaryotic IRESs Have Weak Secondary Structure. *PLoS ONE*. 4:e4136.
- Xu, J., H. Wu, C. Zhang, Y. Cao, L. Wang, L. Zeng, X. Ye, Q. Wu, J. Dai, Y. Xie, and Y. Mao. 2002. Identification of a novel human DDX40 gene, a new member of the DEAH-box protein family. *The American Journal of Human Genetics*. 47:681-683.
- Yamada-Okabe, T., T. Mio, Y. Kashima, M. Matsui, M. Arisawa, and H. Yamada-Okabe. 1999. The *Candida albicans* gene for mRNA 5'-cap methyltransferase: identification of additional residues essential for catalysis. *Microbiology*. 145:3023-3033.
- Yaman, I., J. Fernandez, H. Liu, M. Caprara, A.A. Komar, A.E. Koromilas, L. Zhou, M.D. Snider, D. Scheuner, R.J. Kaufman, and M. Hatzoglou. 2003. The Zipper Model of Translational Control: A Small Upstream ORF Is the Switch that Controls Structural Remodeling of an mRNA Leader. *Cell*. 113:519-531.

- Yamazaki, H., Y. Ohba, N. Tamaoki, and M. Shibuya. 1990. A Deletion Mutation within the Ligand Binding Domain Is Responsible for Activation of Epidermal Growth Factor Receptor Gene in Human Brain Tumors. *Cancer Science*. 81:773-779.
- Yan, R., M.J. Bienkowski, M.E. Shuck, H. Miao, M.C. Tory, A.M. Pauley, J.R. Brashler, N.C. Stratman, W.R. Mathews, A.E. Buhl, D.B. Carter, A.G. Tomasselli, L.A. Parodi, R.L. Henrikson, and M.E. Gurney. 1999. Membrane-anchored aspartyl protease with Alzheimer's disease beta-secretase activity. *Nature*. 402:533-537.
- Yang, H.S., A.P. Jansen, A.A. Komar, X. Zheng, W.C. Merrick, S. Costes, S.J. Lockett, N. Sonenberg, and N.H. Colburn. 2003. The transformation suppressor Pdc4 is a novel eukaryotic translation initiation factor 4A binding protein that inhibits translation. *Molecular and Cellular Biology*. 23:26-37.
- Yang, H.S., A.P. Jansen, R. Nair, K. Shibahara, A.K. Verma, J.L. Cmarik, and N.H. Colburn. 2001. A novel transformation suppressor, Pdc4, inhibits AP-1 transactivation but not NF-kB or ODC transactivation. *Oncogene*. 20:669-676.
- Yankner, B.A., L.K. Duffy, and D.A. Kirschner. 1990. Neurotrophic and neurotoxic effects of amyloid beta protein: reversal by tachykinin neuropeptides. *Science*. 250:279-282.
- Yarosh, D., A.Y.V. Lori Green, A. Oberyszyn, K.J. Tsimis, R.R. Mitchell, and C.M. Spinowitz. 1992. Pyrimidine dimer removal enhanced by DNA repair liposomes reduces the incidence of UV skin cancer in mice. American Association for Cancer Research, Philadelphia, PA, ETATS-UNIS.
- Yazaki, K., T. Yoshida, M. Wakiyama, and K. -i. Miura. 2000. Polysomes of eukaryotic cells observed by electron microscopy. *Journal of Electron Microscopy*. 49:663-668.
- Yoder-Hill, J., A. Pause, N. Sonenberg, and W.C. Merrick. 1993. The p46 subunit of eukaryotic initiation factor (eIF)-4F exchanges with eIF-4A. *The Journal of Biological Chemistry*. 268:5566-5573.
- Yokoi, K., and I.J. Fidler. 2004. Hypoxia Increases Resistance of Human Pancreatic Cancer Cells to Apoptosis Induced by Gemcitabine. *Clinical Cancer Research*. 10:2299-2306.
- Yoon, E.J., H.-J. Park, G.-Y. Kim, H. Cho, J.-H. Choi, H.-Y. Park, J.-Y. Jang, H. Rhim, and S. Kang. 2009. Intracellular amyloid beta interacts with SOD1 and impairs the enzymatic activity of SOD1: implications for the pathogenesis of amyotrophic lateral sclerosis. *Experimental & Molecular Medicine*. 41:611-617.
- Yoshida, M., H. Hayashi, M. Taira, and K. Isono. 1992. Elevated Expression of the Ornithine Decarboxylase Gene in Human Esophageal Cancer. *Cancer Research*. 52:6671-6675.
- Yoshida, M., K. Yoshida, G. Kozlov, N.S. Lim, G. De Crescenzo, Z. Pang, J.J. Berlanga, A. Kahvejian, K. Gehring, S.S. Wing, and N. Sonenberg. 2006. Poly(A) binding protein (PABP) homeostasis is mediated by the stability of its inhibitor, Paip2. *EMBO Journal*. 25:1934-1944.
- Yoshinaga, H., S. Matsushashi, C. Fujiyama, and Z. Masaki. 1999. Novel human PDCD4 (H731) gene expressed in proliferative cells is expressed in the small duct epithelial cells of the breast as revealed by an anti-H731 antibody. *Pathology International*. 49:1067-1077.
- Zhang, R.D., J.E. Price, T. Fujimaki, C.D. Bucana, and I.J. Fidler. 1992. Differential permeability of the blood-brain barrier in experimental brain metastases produced by human neoplasms implanted into nude mice. *American Journal of Pathology*. 141:1115-1124.
- Zhou, W., and W. Song. 2006. Leaky scanning and reinitiation regulate BACE1 gene expression. *Molecular and Cellular Biology*. 26:3353-3364.
- Zhou, Z., L.J. Licklider, S.P. Gygi, and R. Reed. 2002. Comprehensive proteomic analysis of the human spliceosome. *Nature*. 419:182-185.
- Zuker, M. 2003. Mfold web server for nucleic acid folding and hybridization prediction. *Nucleic Acids Research*. 31:3406-3415.
- Zurawel, R.H., C. Allen, R. Wechsler-Reya, M.P. Scott, and C. Raffel. 2000. Evidence that haploinsufficiency of Ptch leads to medulloblastoma in mice. *Genes, Chromosomes and Cancer*. 28:77-81.



# Website References

---

**Website Reference 1.**

<http://www.internetchemie.info/news/2009/nov09/pateamine-a.html> 2012

**Website Reference 2.**

<http://upload.wikimedia.org/wikipedia/commons/b/be/Hippuristanol.svg> 2012

**Website Reference 3.**

<http://ccc.chem.pitt.edu/wipf/MOMs.html> 2012

**Website Reference 4.**

<http://www.nia.nih.gov/Alzheimers/Resources/HighRes.htm> 2011

**Website Reference 5.**

<http://www.rcpsych.ac.uk/mentalhealthinfo/alzheimersanddementia/drugtreatmentofalzheimers.aspx> 2011

**Website Reference 6.**

[http://www.nytimes.com/2010/01/19/health/19brod.html?\\_r=1](http://www.nytimes.com/2010/01/19/health/19brod.html?_r=1) 2011

**Website Reference 7.**

[http://alzheimers.org.uk/site/scripts/documents\\_info.php?documentID=147](http://alzheimers.org.uk/site/scripts/documents_info.php?documentID=147) 2011

**Website Reference 8.**

[http://alzheimers.org.uk/site/scripts/documents\\_info.php?documentID=341](http://alzheimers.org.uk/site/scripts/documents_info.php?documentID=341) 2011

**Website Reference 9.**

<http://www.affibody.com/upload/Research%20Reagents/Application%20notes/egfr%20ip%202006-06-07.pdf> 2011

**Website Reference 10.**

<http://www.abcam.com/Anti-EGFR-Affibody-Molecule-Agarose-Immobilized-ab36039.html>

**Website Reference 11.**

<http://www.sigmaaldrich.com/etc/medialib/sigmaaldrich/migrationresource3/mission-pathways-large.Par.0001.Image.-1.-1.1.gif>

**Website Reference 12.**

[http://upload.wikimedia.org/wikipedia/commons/f/fb/Protein\\_PDCD4\\_PDB\\_2ggf.png](http://upload.wikimedia.org/wikipedia/commons/f/fb/Protein_PDCD4_PDB_2ggf.png)

**Website Reference 13.**

<http://www.chemicalbook.com/CAS%5CGIF%5C87893-55-8.gif>